



UNIVERSIDADE DE LISBOA
INSTITUTO SUPERIOR TÉCNICO

**REMOVAL OF GENOTOXIC IMPURITIES FROM ACTIVE
PHARMACEUTICAL INGREDIENTS: adsorption and membrane approaches**

FLÁVIO ALVES FERREIRA

Supervisor: Doctor Frederico Castelo Alves Ferreira

Co-supervisor: Doctor Teresa Sofia Araújo Esteves

Thesis approved in public session to obtain the PhD Degree in Chemical Engineering

Jury final classification: Pass with Distinction

2019



UNIVERSIDADE DE LISBOA

INSTITUTO SUPERIOR TÉCNICO

**REMOVAL OF GENOTOXIC IMPURITIES FROM ACTIVE
PHARMACEUTICAL INGREDIENTS: adsorption and membrane approaches**

FLÁVIO ALVES FERREIRA

Supervisor: Doctor Frederico Castelo Alves Ferreira

Co-supervisor: Doctor Teresa Sofia Araújo Esteves

Thesis approved in public session to obtain the PhD Degree in Chemical Engineering

Jury final classification: Pass with Distinction

Jury

Chairperson: Doctor Francisco Manuel da Silva Lemos, Instituto Superior Técnico, Universidade de Lisboa.

Members of the Committee:

Doctor Carlos Alberto Mateus Afonso, Faculdade de Farmácia, Universidade de Lisboa;

Doctor Francisco Manuel da Silva Lemos, Instituto Superior Técnico, Universidade de Lisboa;

Doctor Vitor Manuel Geraledes Fernandes, Instituto Superior Técnico, Universidade de Lisboa;

Doctor Frederico Castelo Alves Ferreira, Instituto Superior Técnico, Universidade de Lisboa;

Doctor Ludmila Georgieva Peeva, Faculty of Engineering, Imperial College London, UK;

Doctor Carla Maria Carvalho Gil Brazinha de Barros Ferreira, Faculdade de Ciências e Tecnologia, Universidade Nova de Lisboa.

FUNDING INSTITUTIONS

Conselho Nacional de Desenvolvimento Científico e Tecnológico (CNPq-Brasil),
funding 205201/2014-8.

2019

Resumo

No ramo da engenharia química é comum a busca pelo desenvolvimento de novos materiais ou processos para a otimização de uma ou mais fases de uma produção industrial. Processos de separação são trivialmente utilizados para garantir a pureza do produto final, mas implicam diminuição no rendimento decorrentes das perdas envolvidas, ocasionando redução do lucro e ao mesmo tempo aumentando o custo do produto para o consumidor.

No caso das indústrias farmacêuticas, o elevado grau de pureza exigido pelas agências reguladoras para assegurar que a saúde dos utilizadores não seja comprometida, acompanhado do meio orgânico no qual o produto é sintetizado, tornam a purificação um grande desafio. Processos de separação são utilizados para garantir a pureza do ingrediente farmacêutico ativo (IFA), mas implicam a diminuição nos rendimentos devido a perdas associadas ao produto e intermediários, levando assim, à redução do lucro. Portanto, há uma necessidade do desenvolvimento e implementação de estágios de purificação capazes de abordar a remoção quase total de impurezas, com perdas mínimas de produto, utilizando agentes seletivos, como adsorventes ou membranas, compatíveis com solventes orgânicos.

Esta tese tem por objetivo minimizar as perdas de produtos farmacêuticos provenientes do processo de purificação, contando com o desenvolvimento de novos materiais adsorventes compatíveis com solventes orgânicos, por meio de alterações físico-químicas ou através de funcionalizações com bases de ADN (por exemplo, adenina ou timina) ou ácidos carboxílicos no polímero polibenzimidazolo (PBI), explorando afinidades específicas para remoção de impurezas potencialmente genotóxicas. Dois processos híbridos, isto é, combinando duas operações unitárias através de recirculação, foram

testados para mitigar as perdas de IFA. O primeiro considera a purificação final por recristalização e a posterior recuperação do IFA das águas-mães utilizando resinas comerciais. O segundo processo híbrido combina a purificação final por nanofiltração de solvente orgânico (OSN) acoplada a adsorção, utilizando um dos PBIs desenvolvidos. Adicionalmente, um modelo matemático foi desenvolvido para auxiliar na escolha do processo de purificação mais adequado: apenas adsorção, apenas OSN ou OSN combinada com adsorção, baseado em parâmetros como constantes de adsorção e rejeições dos compostos por membranas. O modelo apresenta como objectivo perdas de IFA inferiores a 10% respeitando os limites máximos de impurezas estipulados pelas agências reguladoras.

Palavras-chave: Polímeros Resistentes a Solventes, Funcionalização de Polímeros, Biomimetismo, Adsorção, Nanofiltração de Solventes Orgânicos, Impureza Genotóxica.

Abstract

In the field of chemical engineering, it is common to search for the development of new materials or processes for the optimization of one or more phases of an industrial operation.

In pharmaceutical industries, a high degree of purity is required by regulatory agencies, to ensure that users' health is not compromised. Such requirements, together with the use of solvents as reaction and processing media, makes purification a major challenge. Separation processes are used to ensure the purity of the final active pharmaceutical ingredient (API), but imply a decrease in yield associated with product and intermediates losses involved, thus leading to a reduction of profit. Therefore, there is a call for development and implementation of purification stages able to address almost total removal of impurities, with minimal product losses, using selective agents, such as adsorbents or membranes, compatible with organic solvents.

This thesis aims to minimize the losses of pharmaceutical products from purification processes, relying on the development of new adsorbent materials compatible with organic solvents. The thesis reports the development of new enhanced adsorbents through physicochemical alteration, functionalisation with DNA bases (e.g. adenine or thymine) or carboxylic acids of the solvent stable polybenzimidazole (PBI) polymer, introducing specific affinity moieties for the removal of potentially genotoxic impurities. Two hybrid processes, i.e. combining in feedback loops two different unit operations, were assessed to mitigate API losses. One considers a final purification by re-recrystallization and further API recovery from methanolic mother liquors using commercial resins. The second hybrid process combines a final purification by organic solvent nanofiltration (OSN) coupled with adsorption, using one modified PBI. For the later case, a mathematical model is

developed to aid in the choice of the most suitable purification process: adsorption alone, OSN alone or OSN combined with adsorption, based on parameters such as adsorption constants and membrane rejections of the products. The model targets API losses below 10 %, respecting impurity limits imposed by regulatory authorities.

Key-words: Solvent Stable Polymers, Polymer Functionalization, Biomimetism, Adsorption, Organic Solvent Nanofiltration, Genotoxic Impurity.

Acknowledgments

Em primeiro lugar, devo agradecer a Deus pela grande oportunidade e por todas as pessoas fantásticas que foram colocadas na minha vida durante este percurso.

São tantas as pessoas as quais gostaria de expressar minha gratidão pelo contributo seja na parte técnica, acadêmica ou com apoio emocional, e mesmo que não apareçam aqui devidamente nomeadas, foram e serão muito importantes para mim.

Agradeço imensamente ao meu orientador Frederico Ferreira por ter aceite a difícil missão de orientar esta tese, pelos desafios aos quais superamos juntos nesta longa jornada e principalmente pela confiança depositada em mim.

Teresa Esteves, realmente a pessoa que esteve ao meu lado em quase todos os momentos, meu ponto principal de apoio, te agradeço por tudo, desde as “chapadas” até a força extra que me motivou a seguir sempre em frente. Obrigado por todo o tempo que tens dedicado para mim. Saibas que sempre serás meu exemplo de conduta profissional.

Professor Carlos Afonso e Ana Vicente, meu profundo obrigado pelo acolhimento durante o período que estive na Faculdade de Farmácia, pelo conhecimento transmitido e o mais importante, pelas discussões e apoio contínuo.

João Bandarra e Hoviove Farmaciência S/A, pelo material e conhecimentos.

Ana Rosa, Rui Carvalho, Marisa Santos, Sofia Duarte, Teresa Cesário, Carla Carvalho e Filipe Carvalho, pela amizade e companheirismo durante todos estes anos.

A todos os meus companheiros do iBB-BERG (7º e 8º piso da Torre Sul-IST), colegas do Tagus Park e estimados amigos da Faculdade de Farmácia pelo agradável convívio cotidiano e pela ajuda mútua.

A todos os membros do enorme grupo do professor Frederico, em especial meus amigos do laboratório 7 e Fábio Garrudo do Tagus Park.

A todos os alunos de mestrado e bolsiros em que de alguma forma contribuíram na execução deste trabalho.

Isabel Nogueira – Microlab IST, pelas belas eletromicrografias e Nuno Costa – Requimte Nova, pelas análises BET.

A tutti i miei “fratelli d’Italia”, un ringraziamento speciale per essere stati come una famiglia nel corso di quest’anni che sono stato lontano dalla mia vera famiglia, vi voglio un sacco di bene! Giulia, Guido, Laura, Silvia e Serena, ogni attimo insieme a voi è stato un piacere. Lucca ed Alessandro, tesori miei, grazie di cuore per avermi fatto sentire che anche se siete lontani, ci sarete sempre per me.

Драгана Поповић и Петар Кековић, хвала вам не само за друштво и за разговоре у лабораторији, већ и за отварање врата ваших кућа и ваших срца за мене, да ме мало подучавате овом предивном језику и култури. Драгана, немам речи да ти се захвалим што си ме увек укључивала у своје традиционалне прославе и чинила да се осећам као део породице и да сам "ујак" Олге. Кека, хвала ти што си више од пријатеља, моја дубока захвалност теби и твојој мајци за топлину и гостопримство.

Jon Kepa, lagun maitea, sin duda una de las personas más importantes de mi vida, agradezco por todos los momentos que pasamos juntos, por la motivación y el cariño, te adoro txispi!

Melhyssa e Edilene, obrigado por serem como uma família e cuidarem de mim.

Dona Rosa, sempre tão querida e prestativa, agradeço pelo ânimo que me tens dado todos os dias com sua boa disposição.

Ao projecto SelectHost (PTDC/QEQ-PRS/4157/2014).

Conselho Nacional de Desenvolvimento Científico e Tecnológico (CNPq-Brasil), pelo financiamento (205201/2014-8), sem o qual tudo isto não seria possível.

Adriana Gonçalves, minha querida amiga, e a minha família que mesmo do outro lado do Atlântico continuam sempre ao meu lado.

Index

RESUMO.....	I
ABSTRACT	III
ACKNOWLEDGMENTS.....	V
GENERAL ABBREVIATIONS AND MATHEMATICAL SYMBOLS	XV
FIGURE INDEX.....	XIX
TABLE INDEX.....	XXV
SCHEME INDEX.....	XXVII
CHAPTER I: <i>OBJECTIVE AND OVERVIEW</i>	1
1.1. WORK SCOPE AND GOALS	2
1.2. RESEARCH QUESTIONS.....	3
1.3. RESEACH STRATEGY: THE MODEL CASE STUDY.....	4
1.4. THESIS OUTLINE	7
1.5. RESEARCH CONTRIBUTIONS IN PUBLICATIONS	8
1.6. REFERENCES	10
CHAPTER II: <i>BACKGROUND</i>	11
2.1. GENOTOXIC IMPURITIES	12
2.1.1. REGULAMENTATION	12
2.1.2. DRUG RECALL	14
2.1.3. REACTION BETWEEN GTI AND DNA AND STRUCTURAL ALERTS.....	15
2.2. PURIFICATION PROCESS	18
2.2.1 RECRISTALLIZATION	19
2.2.2 ORGANIC SOLVENT NANOFILTRATION (OSN)	20
2.2.3 ADSORPTION	22
2.2.4 BIOMIMETICS IN ADSORPTION	26
2.3. REFERENCES	28
CHAPTER III: <i>POLYBENZIMIDAZOLE PHYSICOCHEMICAL TREATMENTS FOR ENHANCED GENOTOXIC IMPURITIES REMOVAL FROM ACTIVE PHARMACEUTICAL INGREDIENTS STREAMS: BEADS AND ELECTROSPUN FIBERS</i>	33
3.1 OUTLINE	34
3.2. INTRODUCTION	35
3.3. MATERIALS AND METHODS	36

3.3.1. MATERIALS	36
3.3.2. APPARATUS AND ANALYSIS.....	37
3.3.3. PBI THERMAL TREATMENT	37
3.3.4. PBI pH CONDITIONING	38
3.3.5. GTI BINDING EXPERIMENTS	38
3.3.6. BINDING ADSORPTION ISOTHERM EXPERIMENTS	39
3.3.7. API RECOVERY EXPERIMENTS.....	40
3.3.8. ELECTROSPINNING SETUP.....	41
3.4. RESULTS AND DISCUSSION.....	41
3.4.1. SCREENING PBI ADSORBERS FOR GTI REMOVAL	42
3.4.2. ADSORBERS CHARACTERIZATION.....	45
3.4.3. BINDING ISOTHERM AND KINETIC STUDIES	47
3.4.4. API PURIFICATION STUDIES.....	48
3.4.4.1. <i>GTI removal and API losses</i>	48
3.4.4.2. <i>Development of a post binding protocol: API recovery and GTI elution</i> ..	52
3.5. CONCLUSIONS.....	54
3.6. REFERENCES	54
CHAPTER IV: POLYBENZIMIDAZOLE MODIFIED WITH CARBOXYLIC ACID GROUPS FOR AROMATIC AMINE IMPURITIES SCAVENGING.....	59
4.1. OUTLINE.....	60
4.2. INTRODUCTION	61
4.3. EXPERIMENTAL SECTION	62
4.3.1. MATERIALS	62
4.3.2. PREPARATION OF THE MODIFIED PBI POLYMERS	62
4.3.2.1. <i>Reaction with 3-bromopropionic acid</i>	62
4.3.2.2. <i>Reaction with 5-bromovaleric acid</i>	63
4.3.2.3. <i>Reaction with 11-bromoundecanoic acid</i>	63
4.3.3. APPARATUS AND ANALYSIS	63
4.3.4. BATCH BINDING EXPERIMENTS.....	65
4.3.5. BINDING ISOTHERM AND KINETIC EXPERIMENTS.....	66
4.4. RESULTS AND DISCUSSION.....	68
4.4.1. POLYMER SYNTHESIS	68
4.4.2. BINDING STUDIES: EFFECT OF MOLAR REACTION RATIO OF BROMO ALKYL CARBOXYL ACID TO PBI AND SIZE OF ALKYL SPACER CHAIN	72
4.4.3. POLYMER CHARACTERIZATION	73
4.4.4. KINETIC AND BINDING ISOTHERM STUDIES.....	75
4.4.5. BINDING TOWARDS SEVERAL IMPURITIES.....	77
4.5. CONCLUSIONS.....	78

4.6. REFERENCES	79
CHAPTER V: MIMICKING DNA ALKYLATION: REMOVING GENOTOXIN IMPURITIES FROM API STREAMS WITH A SOLVENT STABLE POLYBENZIMIDAZOLE-ADENINE POLYMER	
5.1. OUTLINE.....	84
5.2. INTRODUCTION	85
5.3. EXPERIMENTAL	88
5.3.1. MATERIALS	88
5.3.2. APPARATUS AND ANALYSIS.....	88
5.3.3. BINDING EXPERIMENTS	90
5.3.4. API RECOVERY EXPERIMENTS.....	91
5.3.5. KINETIC STUDIES.....	91
5.3.6. ADSORPTION ISOTHERM STUDIES	92
5.4. RESULTS AND DISCUSSION.....	93
5.4.1. GTI BINDING EXPERIMENTS	93
5.4.1.1. <i>Temperature effect on GTI binding</i>	98
5.4.1.2. <i>Adsorption isotherm characterization</i>	101
5.4.2. API BINDING EXPERIMENTS	102
5.4.3. PROCESS DESIGN FOR API PURIFICATION	106
5.5. CONCLUSIONS.....	110
5.6. REFERENCES	111
CHAPTER VI: SCREENING COMMERCIAL AVAILABLE RESINS FOR SIMULTANEOUS REMOVAL OF TWO POTENTIAL GENOTOXINS FROM API METHANOLIC STREAMS.....	
6.1 OUTLINE.....	116
6.2 INTRODUCTION	117
6.3 MATERIALS AND METHODS.....	119
6.3.1 <i>MODEL COMPOUNDS AND SOLVENTS</i>	119
6.3.2 <i>RESINS AND ADSORBENTS</i>	119
6.3.3 <i>HPLC ANALYSES</i>	121
6.3.4 <i>RECRYSTALLIZATION PROCESS</i>	121
6.3.5 <i>RESIN ASSESSMENT FOR SOLUTE ADSORPTION</i>	122
6.3.6 <i>MOTHER LIQUOR PURIFICATION</i>	124
6.4 RESULTS AND DISCUSSION.....	124
6.4.1 <i>RECRYSTALLIZATION</i>	124
6.4.2 <i>SCREENING SCAVENGERS FOR DMAP ADSORPTION</i>	126
6.4.3 <i>SCREENING SCAVENGERS FOR MPTS ADSORPTION</i>	130

6.4.4 SCREENING SCAVENGERS FOR LOW META ADSORPTION	131
6.4.5 MOTHER LIQUOR PURIFICATION USING RESINS: ASSESSING STRATEGIES TO COMBINE DIFFERENT RESINS.....	133
6.4.5.1 ML purification with AG 50W-X2 and IRA68 resins in MeOH	133
6.4.5.2. ML purification with AGW-X2 and IRA68 resins in MeOH in presence of secondary species.....	134
6.4.6 API RECLAIMING: ASSESSMENT OF DIFFERENT PROCESS APPROACHES.....	137
6.4.7 ECONOMIC ASSESSMENT.....	141
6.5. CONCLUSIONS.....	144
6.6. REFERENCES	145
CHAPTER VII: OPTIMIZATION OF ORGANIC DIA(NANO)FILTRATION WITH ADSORPTION RECYCLE LOOP FOR PRODUCT RECLAIMING: APPLICATION TO GENOTOXICS REMOVAL FROM ACTIVE PHARMACEUTICAL COMPOUNDS.....	
7.1. OUTLINE.....	148
7.2. INTRODUCTION	149
7.3. MATHEMATICAL APPROACH: MODELING SECTION	151
7.3.1. SET-UP AND BOUNDARIES	151
7.3.2. ORGANIC SOLVENT NANO DIAFILTRATIONS (OSND).....	152
7.3.3. ADSORPTION	155
7.3.4 HYBRID PROCESS	160
7.4. MATERIALS AND METHODS: EXPERIMENTAL SECTION.....	165
7.4.1. MATERIALS.....	166
7.4.2. APPARATUS AND ANALYSIS.....	166
7.4.3. ORGANIC SOLVENT NANOFILTRATION (OSN) EXPERIMENTS.....	167
7.3.3. ADSORPTION EXPERIMENTS	167
7.3.4. BINDING ADSORPTION ISOTHERM EXPERIMENTS	168
7.5. RESULTS AND DISCUSSION.....	169
7.5.1 MODEL RESULTS: DECISION MAKING FRAMEWORK	169
7.5.2 OSN DIAFILTRATION: THRESHOLDS	169
7.5.3 ADSORPTION: THRESHOLDS	171
7.5.3.1 Langmuir's Isotherm behavior.....	172
7.5.3.2 Freundlich's Isotherm behavior.....	176
7.5.4 HYBRID PROCESS CALCULATIONS	179
7.5.4.1 Calculation of performance over several separation cycles.....	179
7.5.4.2 Effect of recirculation to feed stream ratio, V_{Rec}/V_F	182
7.5.4.3 Effect of adsorber amount.....	183
7.5.5. EXPERIMENTAL VALIDATION	185
7.5.5.1 OSN Diafiltration.....	185

7.5.5.2 Adsorption.....	186
7.5.5.3 Hybrid Process.....	188
7.5.6. ECONOMIC AND ENVIRONMENTAL ANALYSIS OF PROCESS SCALE-UP	189
7.5.6.1. Process design and scale-up factors	190
7.5.6.2. Economic analysis.....	193
7.5.3.3. Environmental analysis	199
7.6. CONCLUSIONS.....	201
7.7. REFERENCES	202
CHAPTER VIII: CONCLUSIONS AND FUTURE PERSPECTIVES	203
8.2 WORK SUMMARY.....	204
8.3 FUTURE PERSPECTIVES	207
APPENDIX	209
APPENDIX A - SUPPORTING INFORMATION FOR CHAPTER V.....	210
APPENDIX B - SUPPORTING INFORMATION FOR CHAPTER VI	213
APPENDIX C - SUPPORTING INFORMATION FOR CHAPTER VII.....	217

General abbreviations and mathematical symbols

API – Active pharmaceutical ingredient

Beta – Betamethasone acetate

BPA – 3-bromopropionic acid

BPTS – Butyl *p*-toluenesulfonate

BUA – 11-bromoundecanoic acid

BVA – 5-bromovaleric acid

DBB – 1,4-dibromobutane

DBE – 1,2-dibromoethane

DBP – 1,3-dibromopropane

DCM – Dichloromethane

DDC – Dodecane

DMAc – Dimethylacetamide

DMAP – 4-Dimethylaminopyridine

DMAP-Me – methylated 4- Dimethylaminopyridine

DMF – Dimethylformamide

DMS – Dimethyl sulfate

DMSO – Dimethylsulfoxide

DNA – Deoxyribonucleic acid

∈ – Belongs to

EPI - Epichlorohydrin

EPTS – Ethyl *p*-toluenesulfonate

EtMS – Ethyl methanesulfonate

F – Feed stream

F' – Feed stream in recirculation

FDA – Food and Drugs Administration

GCD –Glycidol

GTI – Genotoxic impurity

H₂O – Water

HCl – Hydrochloric acid

HPLC – High-performance liquid chromatography

iBB – Institute for bioengineering and biosciences (Instituto Superior Técnico)

IFA – Ingrediente farmacêutico ativo

iMed – Research Institute for Medicine (Faculty of Pharmacy)

ICH – International conference for harmonization

K₂CO₃ – Potassium carbonate

MeCN – Acetonitrile

MeOH – Methanol

Meta – Mometasone furoate

MIP – Molecularly imprinted polymer

ML – Mother liquor

MMS – Methyl methanesulfonate

MPTS – Methyl *p*-toluenesulfonate

MsCl – Methanesulfonyl chloride

NaOH – Sodium hydroxide

OSN – Organic solvent nanofiltration

OSNd – Organic solvent nano(dia)filtration

P – Permeate

P' – Permeate after distillation

PBI – Polybenzimidazole

PBI-A – Acidified polybenzimidazole

PBI-Adenine – Polybenzimidazole functionalized with adenine

PBI-B – Basified polybenzimidazole

PBI-BPA – Polybenzimidazole functionalized with 3-bromopropionic acid

PBI-BUA – Polybenzimidazole functionalized with 11-bromoundecanoic acid

PBI-BVA – Polybenzimidazole functionalized with 5-bromovaleric acid

PBI-COOH – Polybenzimidazole functionalized with carboxylic acid

PBI-T – Thermally treated polybenzimidazole

PBI-TA – Thermally treated and acidified polybenzimidazole

PBI-TB – Thermally treated and basified polybenzimidazole

PGTI – Potential Genotoxic impurity

pH – Negative decadic logarithm of the free hydrogen ion concentration

PhRMA – Pharmaceutical Research and Manufacturers of America

PTSA – *p*-toluene sulfonic acid

\mathbb{R}_+^* – positive real number not null

R – Retentate

Rej – Rejection

SEM – Scanning electron microscopy

TTC – Threshold of toxicological concern

Figure index

Chapter I

FIGURE 1.1. REACTION OF SULFONYLATION OF MOMETASONE CATALYZED BY DMAP.... 4

Chapter II

FIGURE 2.1. NUMBER OF DRUG RECALLS BETWEEN 2012 AND 2017[6].	15
FIGURE 2.2. ATTACK ON THE DNA BY GENOTOXINS, WHERE THE ARROWS INDICATE THE TARGETED NUCLEOPHILIC SITES OF THE DNA BASES (BASED ON MADELEINE PRICE BALL'S FIGURE, GNU FREE DOCUMENTATION LICENSE).	16
FIGURE 2.3. DNA BASES.....	16
FIGURE 2.4. SCHEMATIC REPRESENTATION OF DIAFILTRATION.....	21
FIGURE 2.5. MIMETISM OF GTI BINDING TO ADENINE.	28

Chapter III

FIGURE 3.1. TOP: DMAP BINDING FOR 100 PPM, 1,000 PPM AND 5,000 PPM SOLUTIONS IN DCM FOR DIFFERENT PBI ADSORBERS. BOTTOM: MPTS BINDING FOR 100 PPM, 1,000 PPM AND 5,000 PPM SOLUTIONS IN DCM FOR DIFFERENT PBI ADSORBERS.	42
FIGURE 3.2. SEM IMAGES OF PBI POLYMER PARTICLES AND FIBERS. TOP PANELS: BEADS OBTAINED WITHOUT THERMAL TREATMENT. MIDDLE PANEL: BEADS OBTAINED AFTER THERMAL TREATMENT. BOTTOM PANEL: ELECTROSPUN FIBERS OBTAINED FROM THERMAL TREATED PBI.	46
FIGURE 3.3. TOP: BINDING ISOTHERM FITTING MODELS FOR DMAP (RIGHT) AND META (LEFT) FOR PBI-TA AT ROOM TEMPERATURE. MIDDLE: BINDING ISOTHERM FITTING MODELS FOR MPTS (RIGHT) AND META (LEFT) FOR PBI-TB AT ROOM TEMPERATURE. BOTTOM: KINETIC FITTING MODELS FOR DMAP AND PBI-TA AT ROOM TEMPERATURE (LEFT) AND MPTS AND PBI-TB AT 50 °C (RIGHT).	47
FIGURE 3.4. TOP: COMPARISON OF ADSORPTION OF SOLUTIONS OF ISOLATED API, ISOLATED DMAP AND API+DMAP WITH PBI-TA AT ROOM TEMPERATURE. BOTTOM: COMPARISON OF ADSORPTION OF SOLUTIONS OF ISOLATED API, ISOLATED MPTS AND API+MPTS WITH PBI-TB AT ROOM TEMPERATURE AND AT 50 °C.....	50
FIGURE 3.5. COMPARISON BETWEEN BINDING PERFORMANCE OF BEADS AND FIBERS. TOP: PBI-TA FOR DMAP AND META AT ROOM TEMPERATURE. BOTTOM: PBI-TB FOR MPTS AND META AT 50°C.....	51

Chapter IV

FIGURE 4.1. ¹ H NMR SPECTRUM OF PBI-COOH, PREPARED WITH BPA, IN DMSO-D ₆ . LEFT: FULL SPECTRUM. RIGHT: COMPARISON BETWEEN DIFFERENT AMOUNTS OF CARBOXYLIC ACID EQUIVALENTS INSERTED.	69
FIGURE 4.2. ¹ H NMR OF PBI-BPA, IN DMSO-D ₆ , FROM 6.5 TO 9.5 PPM WITH SIGNALS INTEGRATION	70
FIGURE 4.3. DMAP REMOVAL FOR THE SEVERAL POLYMERS OBTAINED WITH BPA. 1 mL OF A 100 PPM OR 1000 PPM SOLUTION OF DMAP IN DCM WAS LOADED ON 50 MG OF RAW AND MODIFIED PBI POLYMERS.	72
FIGURE 4.4. SEM PICTURES OF PBI (LEFT) AND PBI OBTAINED IN THE PRESENCE OF 1.00 EQ OF BPA (RIGHT).	74
FIGURE 4.5. ADSORPTION ISOTHERM MODELS (LEFT) AND KINETIC MODELS (RIGHT) FOR PBI MODIFIED BY ADDITION OF 1.00 EQ OF BPA.	75
FIGURE 4.6. STRUCTURE OF SEVERAL AROMATIC AMINES ASSESSED.	77

Chapter V

FIGURE 5.1. EXAMPLE OF PBI-ADENINE-GTI ADDUCT FORMATION.	87
FIGURE 5.2. GTI BINDING TO PBI AND PBI-ADENINE SCAVENGERS, FOR 50 MG OF POLYMER IN 1 mL OF A 100 PPM SOLUTION IN DCM OF EACH GTI AFTER 24 HOURS OR 2 WEEKS AT ROOM TEMPERATURE.	94
FIGURE 5.3. GTI BINDING TO PBI-ADENINE SCAVENGER, FOR 50 MG OF POLYMER IN 1 mL OF A 100 PPM SOLUTION IN DCM OF EACH GTI AFTER 24 HOURS AT ROOM TEMPERATURE. GTIS WITHIN THE SAME FAMILY ARE ORDERED BY INCREASING MOLECULAR WEIGHT FROM LEFT TO RIGHT.	97
FIGURE 5.4. GTI BINDING TO PBI-ADENINE SCAVENGER, FOR 50 MG OF POLYMER IN 1 mL OF A 100 PPM SOLUTION IN DCM OR MEOH OF EACH GTI AFTER 24 HOURS OR 2 WEEKS AT ROOM TEMPERATURE.	98
FIGURE 5.5. MPTS, MMS, EPTS AND EtMS BINDING TO PBI AND PBI-ADENINE AT 25 °C AND 55 °C IN DCM, FOR 50 MG OF POLYMER IN 1 mL OF A 100 PPM SOLUTION OF EACH GTI FOR 2 HOURS OR 24 HOURS IN CONTACT WITH THE POLYMER.	99
FIGURE 5.6. KINETIC MODELS FOR MPTS AND MMS AT 25 °C AND 55 °C IN DCM.	100
FIGURE 5.7. ISOTHERM ADSORPTION MODELS FOR MPTS AND MMS AT 25 °C AND 55 °C IN DCM.	101
FIGURE 5.8. CHEMICAL STRUCTURES OF THE APIs STUDIED IN THIS WORK: MOMETASONE FUROATE (META) AND BETAMETHASONE ACETATE (BETA).	102
FIGURE 5.9. MPTS AND META BINDING TO PBI-ADENINE WHEN PRESENT ALONE OR TOGETHER IN SOLUTIONS AT 25 °C AND 55 °C IN DCM. META RECOVERY IN WASHING STEPS AFTER BINDING.	103
FIGURE 5.10. MPTS AND BETA BINDING TO PBI-ADENINE WHEN PRESENT ALONE OR TOGETHER IN SOLUTIONS AT 25 °C AND 55 °C IN DCM. BETA RECOVERY IN WASHING STEPS AFTER BINDING.	103

Chapter VI

- FIGURE 6.1.** STRUCTURES OF META, DMAP AND MPTS. 117
- FIGURE 6.2.** DMAP BINDING FOR DIFFERENT RESINS TESTED: A) WITHOUT pH ADJUSTMENT FOR DIFFERENT SOLVENT MATRICES; B) INFLUENCE OF pH ON DMAP ADSORPTION IN MeOH. AC – ACTIVATED CHARCOAL. 127
- FIGURE 6.3.** LEFT: TEMPERATURE INFLUENCE IN DMAP ADSORPTION FROM MeOH. RIGHT: DMAP BINDING CAPACITY IN AG 50W-X2 RESIN FOR A 1 g/L SOLUTION IN MeOH ALONG TIME AT 25 °C. 128
- FIGURE 6.4.** ADSORPTION ISOTHERM MODELS FOR DMAP IN MeOH FOR SEVERAL RESINS AT 25 °C: A) AG 50W-X2; B) IRC50; C) IRC86. A GOOD CORRELATION OF THE LANGMUIR FITTING WITH AG 50W-X2 RESIN COULD NOT BE DETERMINED..... 129
- FIGURE 6.5.** A) MPTS EQUILIBRIUM BINDING PERCENTAGE FOR SEVERAL SCAVENGERS FROM A 1 g/L SOLUTION IN MeOH AT DIFFERENT pH VALUES AT 25 °C; B) MPTS EQUILIBRIUM BINDING PERCENTAGE TO IRA68 RESIN FOR A 1 g/L SOLUTION IN MeOH AT DIFFERENT TEMPERATURES; C) MPTS BINDING CAPACITY IN IRA68 RESIN FOR A 1 g/L SOLUTION IN MeOH ALONG TIME; FITTING TRENDS TO PSEUDO 1ST AND 2ND ORDER KINETIC MODELS AND RESPECTIVE PARAMETERS; D) MPTS EQUILIBRIA ISOTHERM IN IRA68 RESIN AND FITTING TRENDS TO LANGMUIR AND FREUNDLICH MODELS AND RESPECTIVE PARAMETERS AT 25 °C. AC – ACTIVATED CHARCOAL... 131
- FIGURE 6.6.** AMOUNT OF API AND GTI REMOVED IN MeOH FOR META AND DMAP MIXTURE WITH AG 50W-X2 AND IRC50 RESINS, AND FOR META AND MPTS MIXTURE WITH IRA68 RESIN. 132
- FIGURE 6.7.** PROPOSED FORMATION OF DMAP-Me AND PTSA IN RECRYSTALLIZATION MOTHER LIQUOR. 135
- FIGURE 6.8.** SCHEMATIC ILLUSTRATION OF THE ROLE OF A RESIN BASED STEP, IN TWO DIFFERENT APPROACHES, TO: (i) REMOVE GTI FROM RECRYSTALLIZATION MOTHER LIQUOR TO AN ULTRA-LOW LEVEL, ALLOWING DIRECT RECLAIM OF API FROM MOTHER LIQUOR; OR (ii) REMOVE GTI FROM RECRYSTALLIZATION MOTHER LIQUOR TO AN INTERMEDIATE LOW LEVEL, DECREASING THE GTI/API RATIO ALLOWING MOTHER LIQUOR RECYCLING TO INITIAL POST-SYNTHETIC API CRUDE STREAM FED INTO RECRYSTALLIZATION. GREY FILLED BOXES AND SOLID BLACK LINES REPRESENT RECRYSTALLIZATION PROCESS ALONE; BLACK DOTTED LINES AND EMPTY BOXES REPRESENT STEPS FOR MOTHER LIQUOR SUBJECTED TO RESIN TREATMENT FOR API LOSS MITIGATION. 138
- FIGURE 6.9.** POTENTIAL TO IMPROVE API YIELDS IN RECRYSTALLIZATION/ACTIVATED CHARCOAL PROCESS BY API RECLAIMING DIRECTLY FROM THE MOTHER LIQUOR OR RECYCLING FEEDBACK LOOP OF MOTHER LIQUOR AFTER RESIN TREATMENT: A) CALCULATIONS FOR POTENTIAL DIRECT API RECLAIM AS FUNCTION OF API LOSSES IN RECRYSTALLIZATION/ACTIVATED CHARCOAL PROCESS (ASSUMING A 20% API BINDING TO THE RESINS), OR AFTER STEADY STATE IS REACHED THROUGH SUCCESSIVE RECYCLING OF RESIN TREATED MOTHER LIQUOR; B) TRANSIENT PROFILE OF API ISOLATED AS CRYSTALS WHEN RESIN TREATED MOTHER LIQUOR STREAMS ARE

RECYCLED INTO NEXT BATCH RECRYSTALLIZATION/ACTIVATED CHARCOAL CYCLE (ASSUMING A CASE OF AN INITIAL RECRYSTALLIZATION/ACTIVATED CHARCOAL PROCESS WITH 15% API LOSSES AND SEVERAL PERCENTAGES OF API BIDDING TO THE RESINS).....	139
FIGURE 6.10. COSTS ASSOCIATED TO API RESIN ADSORPTION STEP FOR: TOP - API RECLAIMING DIRECTLY FROM MOTHER LIQUOR; BOTTOM - RECYCLING FEEDBACK LOOP OF MOTHER LIQUOR AFTER RESIN TREATMENT. ASSUMPTIONS: THE RESIN IS NOT RECYCLED; NO FRESH SOLVENT IS ADDED; SOLVENT DISPOSAL IS NOT CONSIDERED; ADDITIONAL EQUIPMENT CONCERNS PUMPS, FLUIDIZED BED REACTORS FOR ADSORPTION AND EXTENDED PERIOD OF HOVEN AND DRYER USAGE, WITH THE LATER TWO ALREADY INCLUDED IN THE RECRYSTALLIZATION PROCESS.	142
FIGURE 6.11. POTENTIAL GAIN IN API RECLAIMING DIRECTLY FROM THE MOTHER LIQUOR WITH A RESIN ADSORPTION STEP FOR SEVERAL PERCENTAGES (10 – 25)% OF API LOSS IN MOTHER LIQUOR (ASSUMING A NON-OPTIMIZED CASE SCENARIO CONSIDERING THE USE OF 50 KG OF SELECTIVE AGENT PER 1 M ³ OF MOTHER LIQUOR AND A CONSTANT RECOVERY OF 80% OF API) AND CONSIDERING SEVERAL SCENARIOS FOR API PRICE IN €/KG.	143

Chapter VII

FIGURE 7.1. SCHEMATIC REPRESENTATION OF HYBRID PROCESS OSN-ADSORPTION, THE DASHED LINE INDICATES THE VOLUME OF CONTROL FOR MASS BALLANCE.....	160
FIGURE 7.2. COMPARISON OF EFFECT OF RECIRCULATION VOLUME ON API LOSS AND DIAVOLUMES FOR HYBRID PROCESS USING LANGMUIR OR FREUNDLICH ADSORBER.	182
FIGURE 7.3. HYBRID PROCESS RESULTS BY CYCLE COMPARATIVE FOR 20G/L AND 40G/L. LANGMUIR BEHAVIOUR, COMBINATION B4CI, USING OSN MEMBRANE WITH REJECTIONS OF API 90% GTI 10%,).	184
FIGURE 7.4. HYBRID PROCESS RESULTS BY CYCLE COMPARATIVE FOR 20G/L AND 76G/L OF PBI-TB (FREUNDLICH BEHAVIOUR USING OSN MEMBRANE WITH REJECTIONS OF API 90% GTI 10%,).	184
FIGURE 7.5. GTI REJECTION ISOLATED AND IN PRESENCE OF META OR BETA. TOP: DMAP REJECTION BOTTOM: MPTS REJECTION.	185
FIGURE 7.6. TOP: COMPARISON OF ADSORPTION OF SOLUTIONS OF ISOLATED APIS, DMAP AND API+DMAP IN PBI-TA. BOTTOM: COMPARISON OF ADSORPTION OF SOLUTIONS OF ISOLATED APIS, MPTS AND API+MPTS IN PBI-TB.....	187
FIGURE 7.7. PROCESS FLOW DIAGRAMS FOR THE TWO PROCESSES CONSIDERED FOR THE CASE STUDIES. PROCESSES: LEFT) ORGANIC SOLVENT (DIA)NANOFILTRATION PROCESS; RIGHT) HYBRID PROCESS USING BOTH ORGANIC SOLVENT (DIA)NANOFILTRATION AND COLUMN CHROMATOGRAPHY STEPS.....	192
FIGURE 7.8. ANNUAL COST DISTRIBUTION FEATURING THE MOST SIGNIFICANT CONTRIBUTIONS FOR THE TWO PROCESSES: OSN (A) AND HYBRID (B).	195

FIGURE 7.9. COMPARISON OF SOLVENT AND SELECTIVE AGENT (ADSORBER) REQUIREMENTS FOR OSN AND HYBRID PROCESSES, IN A BATCH BASIS.	197
FIGURE 7.10. COMPARISON OF ENERGY REQUIREMENTS PER BATCH IN TERMS OF STEAM, COOLING AND PUMPING, FOR ADSORPTION, OSN AND HYBRID PROCESSES.	197
FIGURE 7.11. COMPARISON ON PERCENTAGE OF REVENUE LOSS IN TERMS OF COST OF PURIFICATION TREATMENT AND COST OF API LOSS IN EACH PURIFICATION PROCESS (OSN AND HYBRID).....	199
FIGURE 7.12. TOP: MASS INTENSITY AND ENERGY INTENSITY METRICS. BOTTOM: ENVIRONMENTAL (E) FACTOR AND CARBON DIOXIDE INTENSITY METRICS.	200

Table index

Chapter II

TABLE 2.1: PROPOSED ALLOWABLE DAILY INTAKE (UG/DAY) FOR GTIS OF UNKNOWN CARCINOGENIC POTENTIAL DURING CLINICAL DEVELOPMENT, A STAGGED TTC DEPENDING ON DURATION OF EXPOSURE.	13
--	----

Chapter III

TABLE 3.1. PBI ADSORBERS PREPARED AND EVALUATED, AS WELL AS RESPECTIVE LABELLING USED IN THIS CHAPTER.	38
TABLE 3.2. PHYSICAL PROPERTIES OF PRISTINE PBI AND THE SEVERAL PBI DERIVED ADSORBERS OBTAINED BY MULTIPOINT BET METHOD.	46
TABLE 3.3. BINDING ISOTHERM PHYSICAL PARAMETERS OBTAINED FOR DMAP, MPTS AND META FOR PBI-TA AND PBI-TB AT ROOM TEMPERATURE.....	48
TABLE 3.4. API LOSS AND MGGTI/GAPI USING PBI-TA FOR DMAP REMOVAL IN A META SOLUTION.	53
TABLE 3.5. API LOSS AND MGGTI/GAPI USING PBI-TB FOR MPTS REMOVAL IN A META SOLUTION.	53

Chapter IV

TABLE 4.1. REAL EQUIVALENTS INSERTED AND YIELDS FOR PBI-BPA.....	71
TABLE 4.2. BINDING OF DMAP (1,000 PPM) AND META (10,000 PPM) IN DCM TOWARDS PBI-COOH POLYMERS WITH DIFFERENT SPACER CHAINS AND THEIR RESPECTIVE RATIO MG GTI/G API.	73
TABLE 4.3. PHYSICAL PROPERTIES OF PBI AND PBI MODIFIED POLYMERS WITH BPA, OBTAINED BY MULTIPOINT BET METHOD.	74
TABLE 4.4. BINDING ISOTHERM PHYSICAL PARAMETERS OBTAINED FOR DMAP, FOR PBI-PBA AT ROOM TEMPERATURE.	76
TABLE 4.5. KINETIC PHYSICAL PARAMETERS OBTAINED FOR DMAP AND PBI-BPA AT ROOM TEMPERATURE.	76
TABLE 4.6. BINDING VALUES FOR 1,000 PPM SOLUTIONS IN DCM FOR SEVERAL AROMATIC AMINES TOWARDS PBI-BPA, PBI-BVA AND PBI-BUA.	78

Chapter V

TABLE 5.1. PROPOSED PBI-ADENINE POLYMER ADDUCT FORMATION WITH SEVERAL DNA ALKYLATING AGENTS. THE INTERACTION BETWEEN PBI-ADENINE POLYMER AND MPTS WAS STUDIED IN DETAIL USING ^1H NMR IN A PREVIOUS STUDY. [28]....	95
TABLE 5.2. MPTS VS API BINDING DATA IN BATCH EXPERIMENTS, FOR PREVIOUSLY REPORTED CASES AND CURRENT WORK.	106

Chapter VI

TABLE 6.1. CHEMICAL NATURE OF THE RESINS USED IN THIS STUDY.....	120
TABLE 6.2. STRATEGIES FOR ML PURIFICATION WITH AG 50W-X2 AND IRA68 RESINS IN MEOH.....	133
TABLE 6.3. STRATEGIES FOR ML PURIFICATION WITH AG 50W-X2 AND IRA68 RESINS IN MEOH IN THE PRESENCE OF SECONDARY SPECIES.....	136

Chapter VII

TABLE 7.1. DIAVOLUME REQUIRED FOR DIFFERENT COMBINATION OF API AND GTI REJECTIONS.	170
TABLE 7.2. API LOSS IN DIAFILTRATION MODE FOR DIFFERENT COMBINATIONS OF API AND GTI REJECTIONS.	170
TABLE 7.3. SELECTED LANGMUIR'S CONSTANTS FOR API AND GTI.	173
TABLE 7.4. REQUIRED MASS CALCULATED FOR EACH LANGMUIR ADSORBER.	174
TABLE 7.5. API LOSS RELATED EACH LANGMUIR ADSORBER.....	175
TABLE 7.6. REQUIRED MASS CALCULATED FOR FREUNDLICH N=1.....	176
TABLE 7.7. API LOSS RELATED FOR FREUNDLICH N=1 ADSORBER.....	177
TABLE 7.8. REQUIRED MASS CALCULATED FOR FREUNDLICH N=2.....	177
TABLE 7.9. API LOSS RELATED FOR FREUNDLICH N=2 ADSORBER.....	178
TABLE 7.10. REQUIRED MASS CALCULATED FOR FREUNDLICH N=3.....	178
TABLE 7.11. API LOSS RELATED FOR FREUNDLICH N=3 ADSORBER.....	179
TABLE 7.12. VALUES OF CONTAMINATION IN PERMATE FOR DIFFERENT API/GTI REJECTIONS.	181
TABLE 7.13. COMPARISON BETWEEN PREDICTED AND EXPERIMENTAL VALUES OF HYBRID PROCESS.	189

Scheme index

Chapter II

SCHEME 2.1. REACTION SCHEME TO OBTAIN ALKYLATED ADENINE.	27
SCHEME 2.2. REACTION SCHEME OF THE SYNTHESIS OF PBI MODIFIED WITH ALKYLATED ADENINE.	27

Chapter III

SCHEME 3.1. PROPOSED INTERACTION MECHANISMS BETWEEN PBI-TA AND DMAP (TOP) AND PBI-TB AND MPTS (BOTTOM).	44
--	----

Chapter IV

SCHEME 4.1. SYNTHESIS OF THE MODIFIED PBI POLYMER WITH A FREE CARBOXYLIC ACID FUNCTION (PBI-COOH).	68
---	----

Chapter I
Objective and overview

1.1. Work scope and goals

According to the World Health Organization (WHO), cancer is the second most common cause of death in Western countries, reported to be responsible for 9.6 million of deaths in 2018, and by 2020 it is projected that there will be 16 million new cancer cases and 10 million deaths every year [1].

Commercially available drugs are synthesized using highly reactive reactants in organic solvent media, generally in the presence of catalysts, originating not only the active ingredients used in the preparation of the drug, also generating by-products or impurities which may cause adverse effects such as mutagenicity or carcinogenicity. Therefore, related active pharmaceutical ingredients (API) administration risks for patient's health have become an increasing concern of pharmaceutical companies, regulatory authorities, patients and doctors.

In this scenario, it is crucial that existing purification processes ensure the complete removal of compounds that could endanger the health of the patient, or at least reduce them to the maximum limit allowed by regulatory agencies.

However, reaching ultra low limits of impurities, that may be present in the final product, also means a reduction in production yield due to losses arising during purification, implying a loss to pharmaceutical industries, that may be reflected in the market price of the drug, in particular for generic drugs. Therefore, the development of purification processes able to manage genotoxic impurity (GTI) content in API production with minimal API losses to maintain economic competitiveness is crucial for pharmaceutical industries.

The main goal of this work is the development of cost efficient and sustainable strategies for API purification, with API losses below 10%, achieving GTI removal to values below the limits imposed by regulatory agencies, decreasing risk to patients' health.

To achieve this objective, two strategies were developed, the first one being related to new adsorbent materials, obtained through the structural (functionalization) or physicochemical alteration of a starting polymer, and the second, related to the development/improvement of the purification process mitigating API losses with recovery steps, whether in isolated unit operations or combining unit operations through stream recirculation, generating a hybrid process.

1.2. Research questions

Specifically, this thesis aims to answer the following research questions:

1. Can the change in the protonation state of polybenzimidazole polymer increase its affinity in the removal of genotoxic compounds?
2. Is a polybenzimidazole polymer modified with carboxyl groups a good scavenger for aromatic amines?
3. A polymer containing a DNA base in its structure is capable of providing enhanced removal of genotoxic compounds through a biomimetic approach, i.e., mimicking the mechanism in which DNA bases are attacked by genotoxic compounds?
4. Is it economically viable to add an adsorption step to recover API lost in the mother liquor of a recrystallization?
5. Can a hybrid process, comprising nanofiltration and adsorption, mitigate the API lost in a nanofiltration operation, using an adsorption recycling loop?

1.3. Research Strategy: the model case study

To accomplish the objectives presented in section 1.1, several compounds were assessed as example of genotoxic impurities, compounds with structural alerts or APIs.

The main case study is the purification of mometasone furoate (Meta). This API is a glucocorticoid used in inflammatory diseases treatment [2].

During the synthesis of Meta, the reactant methanesulfonyl chloride (MsCl), an alkylating agent, is used to obtain an intermediate product, and 4-dimethylaminopyridine [3] (compound with a structural alert) is used as catalyst in this reaction as illustrated in Figure 1.1.

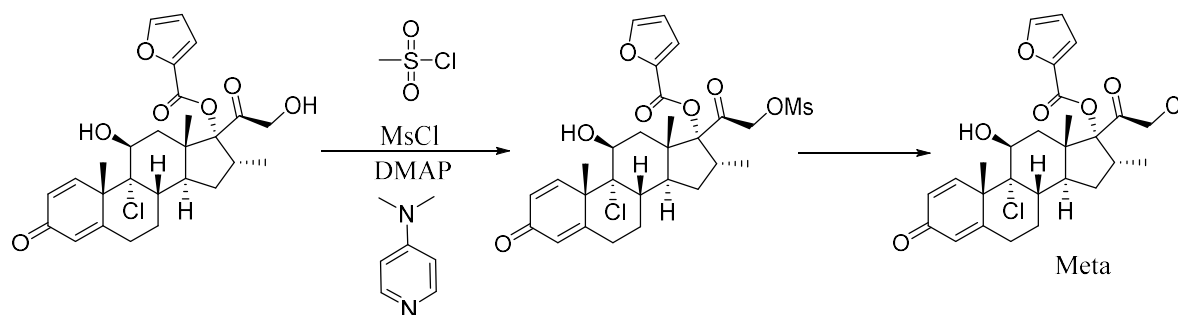


Figure 1.1. Reaction of sulfonylation of mometasone catalyzed by DMAP.

In this thesis, *p*-toluenesulfonate (MPTS) was used as surrogate of MsCl, to facilitate quantification by HPLC-UV.

Although not considered a green solvent and its effects on human health lead to a search for alternatives to its use, dichloromethane (DCM) still continues to be widely used in the chemical industry. Due to the high volatility of this solvent and its ability to dissolve a wide range of organic compounds, DCM is still the ideal solvent for many chemical synthesis, including the synthesis of APIs, (e.g. Meta). For this reason, this solvent has been kept for most of the studies carried out in this thesis.

The limit of GTI content allowed in an API formulation is determined by the Threshold of Toxicological Concern (TTC) value and the API maximum daily dose (g/day) [4]. For example, for a maximum daily dosage of 500 $\mu\text{g}/\text{day}$ of Meta, the 1.5 $\mu\text{g}/\text{day}$ TTC value corresponds to a GTI limit of 3 mgGTI/gAPI. In such case, considering a final Meta crude solution comprised by 10 g/L of Meta, 1 g/L of DMAP and 1 g/L of MPTS, for an ideal purification system, where no Meta is lost, 97% of GTIs would need to be removed to comply with the TTC. Meta is a corticoid, which daily dosage administered varies with inflammatory conditions targeted: typical maximum Meta dosages of 200 $\mu\text{g}/\text{day}$ or 2 mg/day are established for airways (e.g. allergic rhinitis and asthma) or skin (e.g. eczema and psoriasis) administration, corresponding to GTI limits of 7.5 and 0.75 mgGTI/gAPI, respectively. Considering case scenarios for GTI/API target limits, the previously mentioned Meta crude composition and no Meta losses during purification, GTI removals of 92.5% and 99.2% for airways or skin administration would be required. However, as a fraction of API is lost during purification steps, higher removal efficiencies are needed to reach the target GTI/API ratio.

Therefore, its control to TTC levels is suggested following ICH Guidelines.[5] Although primary and secondary aromatic amines are generally not inherently genotoxic, their metabolic activation *in vivo* generates electrophilic species, which are considered the proximate mutagen/carcinogen that binds to DNA.[6]

In the development of new adsorbent materials for the removal of genotoxic impurities from API, polybenzimidazole (PBI) was chosen as the polymer to be functionalized due to its chemical, thermal and mechanical stabilities. Furthermore, PBI is soluble in only a few polar aprotic solvents, such as dimethylacetamide and

dimethylsulphoxide, being a promising material to be explored in organic solvents such as DCM.

In Chapter III, thermal and pH conditioning was explored in order to verify if different protonation states have influence in adsorption behaviour of genotoxic compounds, and another approach based on polymer functionalization was explored in Chapter IV and V.

The rationale to functionalize PBI is to insert functional groups in the polymer backbone in order to increase its GTI removal capacity.

The strategy used to synthesize those new adsorbers was through the reaction of electrophilic substitution of the hydrogen of the secondary amines present in the imidazole ring of PBI's monomers by compounds that contain a good leaving group, as halogens. Those secondary amines react readily with the brominated compounds used in Chapters IV and V, being able to originate the functionalized polymers explored in those chapters.

Especially in Chapter V, the insertion of adenine in the PBI backbone provides a specific recognition site for compounds that react with the DNA, as the different alkylating agents studied, mimicking the mechanism that GTI would perform *in vivo* being a novel approach for GTI removal.

In the case of improvement of the existing processes, in Chapter VI, the recovery of API lost in the mother liquor of recrystallization was sought because it is an industrial effluent stream containing API in considerable quantity due to the losses caused during purification.

In Chapter VII, the recovery of API lost in the OSN permeate was target, since to reach a high degree of purity an increased number of diavolumes is used, and consequently, more API is dragged in this stream.

1.4. Thesis outline

This thesis is organized in eight chapters, written to allow an independent reading of different chapters. For that reason, some redundance can be found in some sections, such as “introduction” and “materials and methods”.

In this first chapter, the main goal, the research questions and strategies are presented.

In the second chapter a literature review is presented, providing the reader the legislation context concerning GTI content in medicines and the main topics covered in this thesis.

From the third to the fifth chapter, this thesis describes the experimental work carried out, where novel adsorbent materials were obtained from the PBI, by physicochemical alterations (Chapter III) or by functionalization with different chemical groups (Chapter IV and V), as well as their performance evaluated in the purification of APIs.

In the sixth and seventh chapters, the mitigation of API losses in purification processes is addressed. The insertion of an adsorption step to recover API lost in the mother liquor of a recrystallization is presented in Chapter VI, and a model which assists in decision making between purification by OSN, adsorption or by a hybrid approach combining both strategies is presented in Chapter VII.

The eighth chapter closes this thesis by presenting a general conclusion and future work.

1.5. Research contributions in publications

The experimental chapters of this thesis are composed of original work already published and in a final phase of submission for peer review.

Each of the authors mentioned in the following chapters had their contribution to the conception of the manuscript, with those appearing as first authors who led the research and made the greatest contribution either, by the original idea explored, written document, execution experimental or discussion of results.

At Chapter III, the manuscript was **submitted to Industrial and Engineering Chemistry Research** by Flávio Alves Ferreira, Teresa Esteves, Marta Carrasco, João Bandarra, Carlos A. M. Afonso, Frederico Castelo Ferreira with the title: “Polybenzimidazole for active pharmaceutical ingredient purification: beads and electrospun fibers”, with the leadership of Flávio Ferreira in collaboration with PhD supervisors.

In this work, my contributions were: original idea, experimental work and writing. The others authors contributed with some experimental work, helping with analytical techniques, discussion of results and writing.

At Chapter IV, an original material, yet to be **submitted for peer revision**, by Teresa Esteves, Flávio Ferreira, Ana I. Vicente, Carlos A. M. Afonso and Frederico Castelo Ferreira has the provisory title: “Polybenzimidazole modified with carboxylic acid groups for aromatic amine impurities scavenging, with leadership of Teresa Esteves.

In this work, my contributions cover the experimental work comprising the synthesis of polymeric compounds to the analytic techniques, having also contributions in discussion and writing.

The others authors contributed with the idea to be explored, discussion and writing.

At Chapter V, the work was **published in Reactive and Functional Polymers**, 131, (2018), 258-265 by Teresa Esteves, Ana I. Vicente, Flávio A. Ferreira, Carlos A. M. Afonso, Frederico Castelo Ferreira, with the title “Mimicking DNA alkylation: Removing genotoxin impurities from API streams with a solvent stable polybenzimidazole-adenine polymer”, with leadership of Teresa Esteves.

In this work, my contributions cover the experimental work comprising the synthesis of compounds to the analytic techniques, having also contributions in discussion and writing.

The other authors contributed with the idea to be explored, discussion and writing.

At Chapter VI, the work was **published in Separation Science and Technology** · December 2018, DOI: 10.1080/01496395.2018.1556304 by Teresa Esteves, Flávio A. Ferreira, Mariana Pina, João Bandarra, and Frederico Castelo Ferreira, with the title “Screening commercial available resins for simultaneous removal of two potential genotoxins from API methanolic streams”, with leadership of Teresa Esteves.

In this work, my contributions cover the experimental work comprising recrystallization and adsorption processes, the analytic techniques, having also contributions in discussion and writing.

The other authors contributed with the idea to be explored, experimental work, economic analysis, discussion and writing.

At Chapter VII, the manuscript will be **submitted to Journal of Membrane Science** by Flávio Alves Ferreira, Teresa Esteves, Maria Leonor Resina and Frederico Castelo Ferreira with the title: “Optimization of organic dia(nano)filtration with adsorption

recycle loop for product reclaiming: application to genotoxics removal from active pharmaceutical compounds”, with the leadership of Flávio Ferreira in collaboration with PhD supervisors.

In this work, my contributions were: original idea, experimental work, mathematical modelling and writing.

The other authors contributed in helping with mathematical modelling, economic analysis, discussion of results and writing.

1.6. References

- [1] World Health Organization, <https://www.who.int/cancer/en/> (assessed in September 2018).
- [2] Bousquet, J., Mometasone furoate: an effective anti-inflammatory with a well-defined safety and tolerability profile in the treatment of asthma, *Int. J. Clinical Practice*, 63, 2009, 806-819.
- [3] Draper, W. R. et al, Unusual hydroxy- γ -sultone byproducts on steroid 21-methanesulfonylation. An efficient synthesis of mometasone 17-furoate (Sch32088), *Tetrahedron*, 55, (1999), 3355-3364.
- [4] EMEA Guidelines on the “Limits on Genotoxic Impurities”, EMEA/CHMP/QWP/251344/2006, 2006.
- [5] Snodin D. ICH Guideline M7 on mutagenic impurities in pharmaceuticals, 14, 3, (2017).
- [6] Snodin, D. J. Genotoxic impurities: From structural alerts to qualification. *Org. Process Res. Dev.*, 14, (2010) 960-976.

Chapter II

Background

2.1. Genotoxic impurities

2.1.1. Regulamentation

The need to minimize the differences in the requirements for drug development regulations from country to country, motivate Japan, Europe and the United States to organize the International Conference on Harmonization (ICH) for technical requirements for the registration of pharmaceutical products for human use in 1990 at a World Health Organization conference on Drug Regulatory, with several guidelines emerging from this initiative.

Since then, several guidelines were published in ICH [1]. In ICH's, Q3 referred to compounds with "unusual toxicity", which was a clear reference to genotoxic impurities, and mentioned the need to set tighter limits for these impurities. The ICH Q3A guideline, that regulates impurities on new active substances, presents limits for reporting, identifying and qualifying impurities. The ICH Q3B is similar to ICH QA but refers to new drugs. The ICH Q3C directive controls residual solvents, being the first time that ICH applies specific limits to these substances. Accordingly, residual solvents were divided in three classes. Class I solvents should be avoided, Class II solvents should have a daily allowable exposure limit and Class III solvents should have no defined exposure limit provided that the daily exposure is less than 50 mg/day. The ICH Q3D guideline establishes limits of heavy metals in drugs.

The published ICH standards are not appropriate for most genotoxic impurities. Typically, drug synthesis involves the use of reactive materials that have the ability to interact with human DNA causing mutations and cancer, even though they are present in rather low concentrations. Thus, genotoxic impurities should be avoided or, if this is not possible, reduced to a level below a threshold.

In 2004, Pharmaceutical Research and Manufacturers of America (PhRMA) formed a working group to discuss genotoxic impurities, resulting in the publication of an article [2] that introduced two very important new concepts:

1. A classification system for genotoxic impurities in 5 classes. Class 1: Impurities known to be both genotoxic (mutagenic) and carcinogenic. Class 2: Impurities known to be genotoxic (mutagenic), but with unknown carcinogenic potential. Class 3: Alerting structure, unrelated to the structure of API and of unknown genotoxic (mutagenic) potential. Class 4: Alerting structure related to API. Class 5: No alerting structure or sufficient evidence for absence of genotoxicity.

2. Implementation of a staged TTC in clinical trials. For the calculation of this parameter, the dose and duration of the clinical trials are taken into account, resulting in a lower TTC for higher doses and a higher TTC for shorter exposure times [3], as presented in table 2.1. The estimated values for staged TTC should apply at all stages of development and for each individual compound in cases where several genotoxic impurities are present.

Table 2.1: Proposed allowable daily intake (ug/day) for GTIs of unknown carcinogenic potential during clinical development, a staged TTC depending on duration of exposure.

	Time of exposure (months)				
	> 1	1 < t < 3	3 < t < 6	6 < t < 12	> 12
Allowable daily intake (µg/day)	120	40	20	10	1.5

For the case of genotoxic impurities for which limit-based mechanisms cannot be defined, the use of the As Low As Reasonably Practicable (ALARP) principle is suggested; this approach specifies that every effort should be made to prevent the

formation of these impurities during drug synthesis and, if this is not possible, post-synthesis efforts should be made to reduce their levels.

In cases where genotoxic impurities cannot be avoided, the guideline recommends the implementation of a risk assessment. The standard proposes the use of a "toxicological risk threshold" (TTC) for genotoxic impurities. This approach had already been mentioned in the report of the PhRMA working group. It was estimated that the numerical value of TTC would be 1.5 µg/day, which corresponds to a cancer risk of 1 in 1,000,000. [4]

2.1.2. Drug recall

When defects are detected or identified in a product that already went to the market and it causes risks to consumer safety, the industries promote the withdrawal of this product from the market, such initiative is called recall.

Recall of medicines can occur for several reasons, from defective labeling to side effects and contamination problems, being the latter the most serious case.

In 2007, the Viracept retroviral was withdrawn from the market due to the presence of the alkylating agent ethyl mesylate [5].

Despite the efforts and measures used by the pharmaceutical industries to ensure the quality of medicines, 7670 recalls were registered by the Food and Drugs Administration (FDA) between 2012 and 2017 [6] as can be seen in figure 2.1.

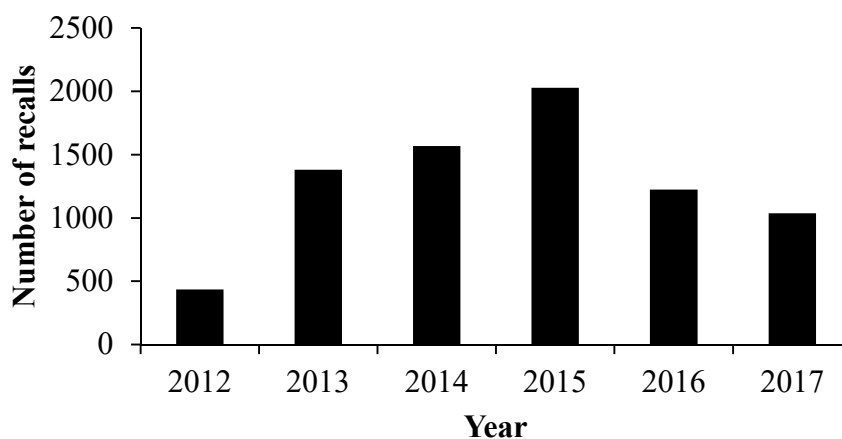


Figure 2.1. Number of drug recalls between 2012 and 2017[6].

In 2018, detection of undisclosed impurities has led to Apotex Corporation recalling 36 lots of Piperacillin and Tazobactam for Injection [7], and more recently, cases related to hydrochlorothiazide [8] and nitrosodimethylamine at off-limits in drugs for hypertension such as Valsartan [9,10,11] were also registered by the FDA.

2.1.3. Reaction between GTI and DNA and structural alerts

For a compound to have carcinogenic or mutagenic effects it must react with the DNA, which may have an immediate action or be activated by one of the metabolic pathways. According to the theory of James and Elizabeth Miller, electrophilic attacks are more susceptible in the nucleophilic centers of DNA, occurring in the nitrogen and oxygen atoms of the purine bases (Adenine and Guanine) and pyrimidine (Cytosine and Thymine) and phosphodiester skeleton [12]. This electrophilic attack produces a covalent bond between the compound and the DNA forming adducts. Fig. 2.2. illustrates the DNA with the targets in their bases and Fig. 2.3. illustrates each DNA base, with a numeration that indicates the atom position showing where the reaction mechanism occurs.

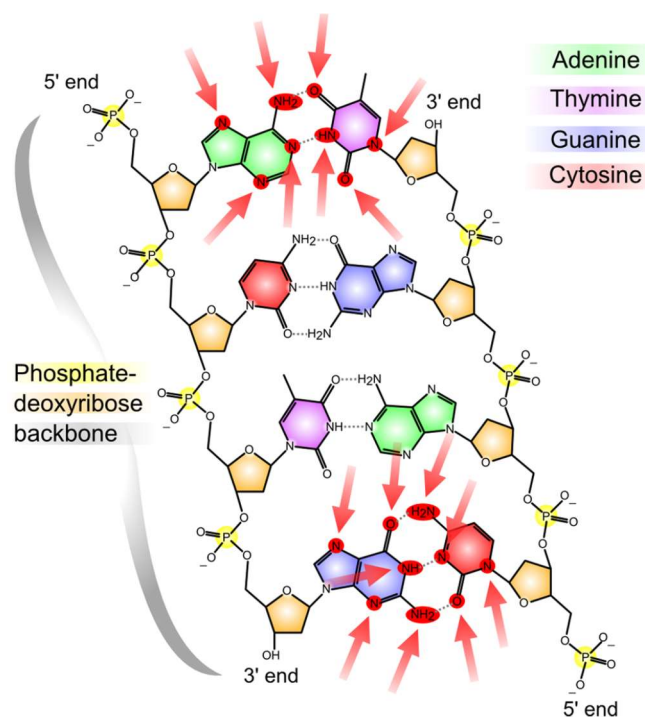


Figure 2.2. Attack on the DNA by genotoxins, where the arrows indicate the targeted nucleophilic sites of the DNA bases (based on Madeleine Price Ball's figure, GNU Free Documentation License).

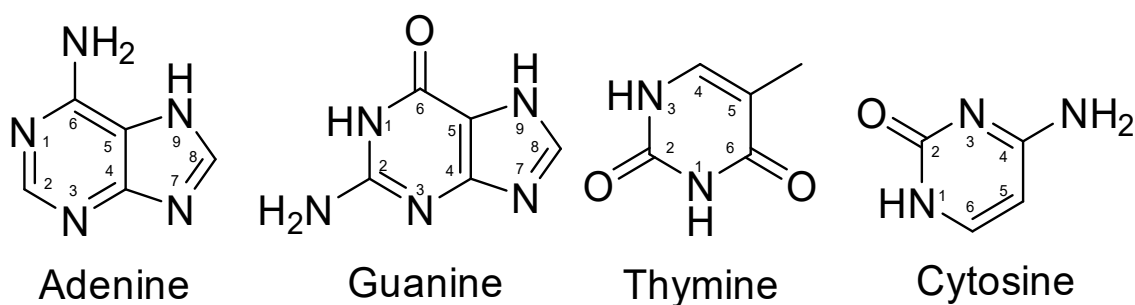


Figure 2.3. DNA bases.

Another factor that influences the reaction site, besides reactivity, is the steric hindrance that makes access to the nucleophile difficult, as for example the N3 and N7 sites in guanine and adenine are the most nucleophiles, however the N7 of guanine is exposed in the major groove of the normal DNA helix nucleus, being more accessible and

consequently has greater availability to the reaction than adenine N3, oriented to the minor groove. Analogously very electrophilic sites such as adenine N1 and cytosine N3 may not react due to steric hindrance. Low nucleophilic sites may also form adducts at the C8 position of guanine (for example in the case of reactions with reactive metabolites of aromatic amines). However, evidence indicates that this type of adduct is formed by rearrangement after initial attack at position N7 [12].

There are several chemical structures and families that can react with DNA. Some molecules have known genotoxic effects and others are reported as dangerous due to their association with reactive groups classified as structural alerts [13].

The presence of genotoxic compounds in API may occur due to the introduction of these species as reagents, catalysts or solvents and may also originate as by-products of the reaction. Among the compounds designated as having structural alerts, the most common ones used in API syntheses are alkylating agents (donor of alkyl radical), acylating agents (donors of acyl group, IUPAC name alkanoyl) and aromatic amines.

Alkylating agents are electrophilic species that react directly with DNA substituting a hydrogen atom for an alkyl group or can transfer alkyl residues to the DNA after activation by the metabolic pathway, being more common the attack in the N7 position of the guanine, however preferences by other sites can occur due to weak or strong reactivity.

Acylating agents react by transferring the acyl group to the DNA bases, forming adducts at the O6 position of guanine and the exocyclic amine groups of cytosine, adenine and guanine.

Arylamines can be activated in highly electrophilic species by reacting with the DNA to give arylamines derivatives at the N2 and C8 positions of guanine.

In addition to adducts formation, the DNA can be attacked by compounds that can bind at the same time in adjacent base pairs and as a consequence of this intercalation, structural DNA alterations or even chain breakdowns may occur [12].

2.2. Purification process

Chemical processes for manufacturing include several unit operations for synthesis and isolation of APIs or their intermediates, which can contribute to mitigate the GTI presence, for example removal by distillation or extraction according to its volatility or solubility. However, the last step must consider a purification process of an API in order to ensure not only quality but also safety.

Purification processes always have as consequence product loss, and losses getting higher as the degree of purity desired becomes higher, being crucial the search for new materials or the improvement of existing processes to reduce the losses.

Considering the significant losses of expensive API, the competitive purification/separation of API processes is still a challenge. Székely et al [14] reviews GTI sources over API syntheses, and overviews on conventional separation techniques used in API purification (crystallization, adsorbents), while Marchetti et al [15] critically reviews molecular separation by OSN. Székely et al [16] also compared economic and environmentally three API purification processes (crystallization, flash chromatography, OSN) and showed that conventional separation techniques are suitable for GTI removal, but ultra-low GTI levels could only be achieved at the expense of high API losses, which means a significant impact in industry profitability.

Molecularly imprinted polymers also have been recently developed targeting specific GTI [17-20].

2.2.1 Recrystallization

Recrystallization is one of the most used processes in the pharmaceutical industry for the purification of APIs, as it allows to obtain API in the desired crystallographic form, besides allowing the careful control of the particle size.

The recrystallization process is based on the difference of solubility between API and GTI which may occur through a single solvent or by solvent exchange.

Purification by recrystallization ideally requires a solvent matrix in which the API is very soluble at higher temperatures and less soluble at lower temperatures, while the GTI is very soluble both in hot and cold solutions, so that during the slow cooling the API can recrystallize while the GTI remains soluble in the mother liquor.

When API and GTI are very soluble in the same solvent over a wide temperature range, recrystallization can be done by gradual solvent exchange from a solubilization solvent (where the API is less soluble than the GTI) to a second solvent, the recrystallization solvent, (in which the API has low solubility while GTI remains soluble) allowing the precipitation of the API by volume reduction by evaporation of the solubilization solvent and gradually addition of recrystallization solvent, allowing the API to recrystallize during cooling [21]. After cooling, the solid API is subsequently separated through filtration, washed with cold solvent and dried.

Recrystallization usually leads to isolation of APIs with a higher grade of purity but the major drawback is related to API loss in the mother liquor and washing solutions.

2.2.2 Organic Solvent Nanofiltration (OSN)

A membrane is defined as a thin film structure that acts as a selective barrier for the separation of two fluids (gases or liquids), allowing the passage of some solutes and solvents, but not others, when exposed to the action of a driving force (concentration, pressure, temperature gradients, electrical potential).

The membrane filtration process is a physical-chemical process that aims to remove contaminants present in the liquid phase. When operated on the concentration mode, the phase that cannot pass through the membrane becomes more concentrated and is called retentate and the phase passing through the membrane becomes less concentrated and is called the permeate. Depending on the characteristics of the membrane to be used, the resistance of passage of specific particles, molecules, substances and even biological agents such as viruses and bacteria can be offered [22,23].

Organic Solvent Nanofiltration (OSN) is a controlled pressure membrane process where it is possible to separate solutes ranging from 200-2000 g/mol and has enormous potential for industries using processes of production or purification involving organic solvents, such as the pharmaceutical industries [24].

OSN can be used as an independent or combined unit operation to potentiate the efficiency of conventional operations, such as distillation, crystallization, and furthermore offer the advantage of promoting solvent exchanges *in situ* and can be used for the recycling of solvents [25].

OSN can be used by the pharmaceutical industry as a unitary operation in the API purification process to retain a target molecule in the retentate or to allow passage into the permeate. Generally, API molecular weight is higher than the one of the GTI, which

means that the API is retained while GTI permeates through the membrane. However, OSN is not perfectly effective, as a small amount of API can permeate the membrane and a small fraction of GTI can be retained. The amount of API present in permeate should be as small as possible in order to avoid yield losses.

OSN can be performed in different modes, including concentration mode to concentrate the solution by solvent removal or in diafiltration mode to allow separation of compounds pushing impurities through the permeate.

In an attempt to reach ultra-low levels of GTI, OSN can be operated in diafiltration mode, where fresh solvent is added at the same rate of permeation to keep the upstream at constant volume, washing GTI through the permeate. A diavolume corresponds to a volume of fresh solvent added, equal to the volume of initial feed solution, and can be calculated by Eq. 2.1, where D is the number of diavolume required, C_R is the concentration of retentate and Re_j is the percentage of rejection of the specie to be permeated.

$$D = \frac{\ln \frac{C_R}{C_F}}{1 - Re_j} \quad (2.1)$$

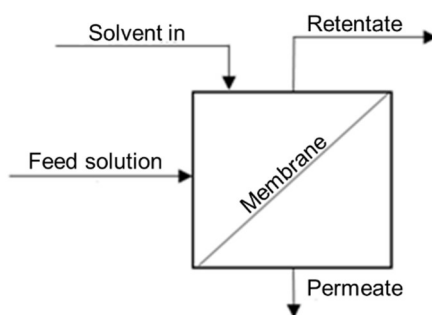


Figure 2.4. Schematic representation of diafiltration.

Depending on membrane rejections for API and GTI, a certain number of diavolumes is required to reach the targeted level of GTI content. In consequence, as lower the level of GTI, the higher the number of diavolumes, potentially making the solvent consumption very high for OSN diafiltrations. Ideally, to reach minimal API loss during diafiltration, the rejection for API and GTI must be near to 100% and 0%, respectively, , otherwise API losses will necessarily increase with the increase of diavolumes used.

2.2.3 Adsorption

Adsorption is a phenomenon in which molecules of a component are transferred from a fluid phase to the surface of an adsorbent solid, to which they adhere.

The process originates from the attractive forces between the adsorbate and the adsorbent. The adsorption forces involved depend on the nature of both the adsorbent and the adsorbate and can be of the Van der Waals type, electrostatic attraction or adsorbate-adsorbate interaction.

Depending on the forces involved, adsorption may be physical (physisorption) involving a relatively weak interaction that can be attributed to Van der Waals forces, usually occurs rapidly and is reversible. Chemical adsorption (chemisorption) involves the exchange or sharing of electrons resulting in a chemical reaction, its speed being dependent on the activation energy, it will be fast if it is null or low and slow if it is high.

The adsorption phenomena are the result of a combination of the forces involved in the physical and chemical adsorption.

The adsorption equilibrium is generally an essential requirement for obtaining relevant information on design and analysis of an adsorption separation process. Adsorption occurs when an adsorbent solid comes into contact with a volume of fluid containing the adsorbate, the adsorption equilibrium occurs when the solute concentration in the fluid phase remains constant over time and the adsorptive capacity of the adsorbent can be determined.

Adsorption kinetics is expressed as the rate of removal of the adsorbate in the fluid phase as a function of time.

Several linear kinetic models are used to examine the controlling mechanism of the adsorption process, such as chemical reaction, diffusion control and mass transfer, however the most commonly used models are the pseudo first order and pseudo second order.

The pseudo first order model is based on the solid capacity and is given by the Lagergren equation (Eq. 2.2) [26].

$$\frac{dq_t}{dt} = k_1(q_e - q_t) \quad (2.2)$$

where k_1 is the adsorption rate constant (min^{-1}) and q_e and q_t are the adsorbed quantities at equilibrium and at time t (mg /g).

After the integration of Eq. 2.2, and applying the boundary conditions $q_t = 0$ and $t = 0$, when $q_t = q_t$ and $t = t$, we get Eq. 2.3, where we can determine the value of k_1 through the slope of the curve obtained from the graph of $\ln(q_e - q_t)$ as a function of t .

$$\ln(q_e - q_t) = \ln q_e - k_1 t \quad (2.3)$$

In most adsorption processes the pseudo first order model does not fit well for the entire length of the contact time and is generally applicable in the initial 20-30 minutes of adsorption.

The pseudo second order model is also based on the capacity of the solid and can be expressed according to Eq. 2.4.

$$\frac{dq_t}{dt} = k_2(q_e - q_t)^2 \quad (2.4)$$

where k_2 is the adsorption rate constant of pseudo second order (g/mg.min) and q_e and q_t are the adsorbed quantities at equilibrium and time t (mg/g).

Integrating Eq. 2.4 and applying the boundary conditions $q_t = 0$ and $t = 0$, when $q_t = q_t$ and $t = t$, we get Eq. 2.5

$$\frac{1}{(q_e - q_t)} = \frac{1}{q_e} + k_2 t \quad (2.5)$$

Eq. 2.5 can be linearized, giving rise to Eq. 2.6 from which the value of k_2 can be obtained through the slope of the curve obtained from the graph of (t/q_t) as a function of t [27].

$$\frac{t}{q_t} = \frac{1}{k_2 q_e^2} + \frac{t}{q_e} \quad (2.6)$$

Isotherms are diagrams showing the variation of equilibrium concentration in the adsorbent solid as a function of the partial pressure or concentration of the liquid phase at a given temperature.

The most widely used models for adjusting the experimental data of isotherms are the Langmuir and the Freundlich models [28].

The Langmuir model assumes that the surface of the adsorbent is formed by perfect planes, so that the probability of adsorption is the same for all sites. In addition, the adsorbate is considered ideal so that the interactions between its particles are negligible and that the occupation of a site by a particle does not affect adsorption at the adjacent site. This model indicates that the adsorption is homogeneous and occurs in a monolayer that covers the entire surface of the adsorbent.

The Langmuir isotherm is represented by Eq. 2.7.

$$q_e = \frac{q_0 K_L C_e}{1 + K_L C_e} \quad (2.7)$$

where q is the adsorption capacity at equilibrium, q_0 is the maximum adsorption capacity, C_e is the concentration of adsorbate in the equilibrium solution, and K_L is the ratio of adsorption and desorption constants. The linearized form of the isotherm is shown in Eq. 2.8.

$$\frac{C_e}{q} = \frac{1}{q_0 K_L} + \frac{1}{q_0} C_e \quad (2.8)$$

The Freundlich model assumes that the surface of the adsorbent is heterogeneous, where the interactions between the adsorbent particles are not disregarded, which leads to a heterogeneous distribution of adsorption probability for the different sites of the material surface. This model indicates that adsorption can take place in multilayers. The Freundlich isotherm is represented by Eq. 2.9.

$$q = K_F C_e^{1/n} \quad (2.9)$$

where K_F is the Freundlich constant and the parameter $1/n$ provides information on the isotherm, indicating whether the adsorption is favorable (values between 0 and 1) or unfavorable. As in the Langmuir isotherm, the parameters can be obtained through the graphical representation of $(\ln q)$ as a function of $(\ln C_e)$, whose intercept gives $(\ln K_F)$ and the slope is equal to $1/n$, as shown in Eq. 2.10.

$$\ln q = \ln K_F + \frac{1}{n} \ln C_e \quad (2.10)$$

2.2.4 Biomimetics in adsorption

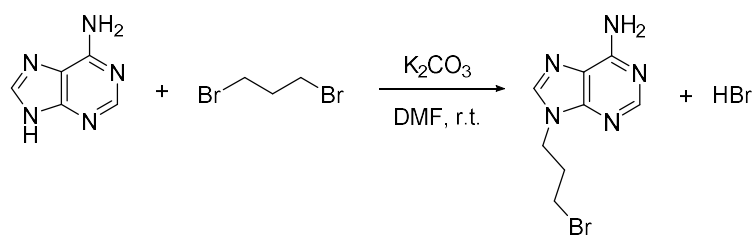
Biomimetics is an approach to solve problems based on the imitation of the models and elements of nature. In that context, for genotoxics removal, the main idea explored in this thesis is to mimic the way that GTI molecules attack DNA. This approach was tried for the first time by iBB/iMed teams reported by Vicente et al. through a functionalized polybenzimidazole (PBI) polymer with adenine aiming API degenotoxification [29] (Scheme 2.2). In this study, the developed polymer was able to efficiently remove methyl *p*-toluenesulfonate from a solution of an API, mometasone furoate, in organic media, being a promising scavenger for alkylating agents.

The PBI combines the ideal characteristics for a working material to be used in organic media, since it is an amorphous thermoplastic polymer, which has high thermal stability (glass transition around 425-436 ° C), with excellent chemical and mechanical resistance, soluble in only some aprotic polar solvents such as dimethylsulfoxide and dimethylacetamide [30].

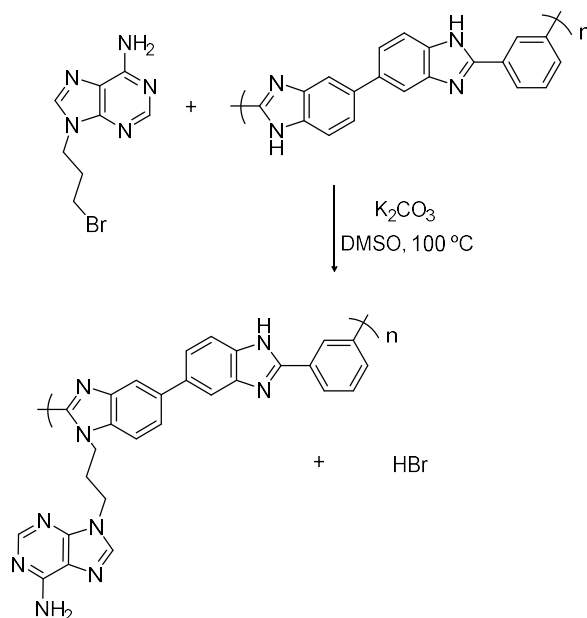
To obtain the PBI functionalized with adenine, the DNA base was previously alkylated with 1,3-dibromopropane to have a good leaving group (Br) to react with PBI

through covalent bond of N9 adenine nitrogen, the same position in which this base is bound to the deoxyribose, remaining the other position free to interaction with GTIs (Scheme 2.1).

The alkyl chain between PBI and adenine was included as a spacer to avoid stereochemical limitations (Fig. 2.5).



Scheme 2.1. Reaction Scheme to obtain alkylated adenine.



Scheme 2.2. Reaction scheme of the synthesis of PBI modified with alkylated adenine.

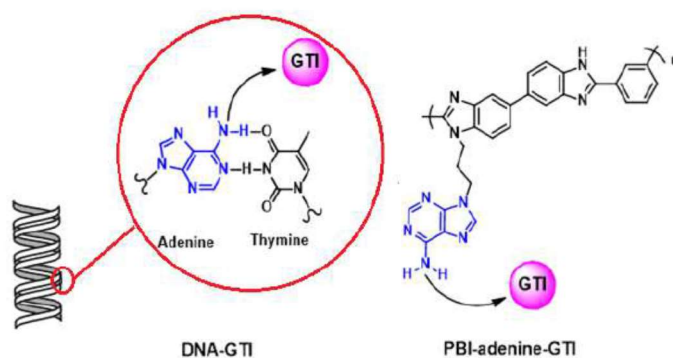


Figure 2.5. Mimetism of GTI binding to adenine.

2.3. References

- [1] www.ich.org/products/guidelines/quality/article/quality-guidelines.html (assessed in March 2019)
- [2] MÜLLER, L., et al., A rationale for determining, testing, and controlling specific impurities in pharmaceuticals that possess potential for genotoxicity. *Regulatory Toxicology and Pharmacology*, 44, 3, 2006, 198-211.
- [3] HUMFREY, C.D.N., Recent Developments in the Risk Assessment of Potentially Genotoxic Impurities in Pharmaceutical Drug Substances. *Toxicological Sciences*, 100,1, 2007, 24-28.
- [4] EMEA Guidelines on the “Limits on Genotoxic Impurities”, EMEA/CHMP/QWP/251344/2006, 2006.

- [5] www.ema.europa.eu/en/news/european-medicines-agency-announces-recall-viracept (assessed in March 2019)
- [6] www.statista.com/statistics/618383/total-fda-drug-enforcement-reports/ (assessed in March 2019)
- [7] www.fda.gov/Safety/Recalls/ucm607653.htm (assessed in March 2019)
- [8] www.fda.gov/Safety/Recalls/ucm632509.htm (assessed in March 2019)
- [9] www.fda.gov/Safety/Recalls/ucm626802.htm (assessed in March 2019)
- [10] www.fda.gov/Safety/Recalls/ucm632442.htm (assessed in March 2019)
- [11] www.fda.gov/Safety/Recalls/ucm629627.htm (assessed in March 2019)
- [12] BENIGNI, R.; BOSSA, C. Mechanisms of Chemical Carcinogenicity and Mutagenicity: A Review with Implications for Predictive Toxicology. *Chemical Reviews*. 111, 4, 2011, 2507-2536.
- [13] PLOSNIK, A., et al., Mutagenic and carcinogenic structural alerts and their mechanism of action, *Arh Hig Rada Toksikol*, 67, 2016, 169-182.
- [14] SZÉKELY, G., et al, Sources of genotoxic impurities in drug synthesis: a systematic review. *Chem. Rev.*, 2015, 115, 8182 - 8229.
- [15] MARCHETTI, P., et al, Molecular separation with organic nanofiltration: a critical review, *Chem. Rev.*, 114, 2014, 10735 - 10806.
- [16] SZÉKELY, G., et al, Environmental and economic analysis for selection and engineering sustainable API degenotoxification processes. *Green Chem.*, 15, 2013, 210 - 225.

- [17] KECILI, R. et al, Fast identification of selective resins for removal of genotoxic aminopyridine impurities via screening of molecularly imprinted polymer libraries, *Journal of chromatography A*, 1339, 2014, 65-72
- [18] SZÉKELY, G., et al, Design, preparation and characterization of novel molecularly imprinted polymers for removal of potentially genotoxic 1,3-diisopropylurea from API solutions *Separation and Purification Technology*, 85, 2012, 190-198.
- [19] HASHEMI-MOGHADDAM H. and SHAKERI M., Removal of potentially genotoxic impurity from fluroxamine maleate crude drug by molecularly imprinted polymer *Korean J. Chem. Eng.*, 31,10, 2014, 1898-1902.
- [20] ESTEVES, T., et al, Molecularly imprinted polymer strategies for removal of a genotoxic impurity, 4-dimethylaminopyridine, from an active pharmaceutical ingredient post-reaction stream, *Separation and Purification Technology*, 163, 2016, 206-214.
- [21] SZÉKELY, G., et al, Environmental and economics analysis for selection and engineering sustainable API degenotoxification process, *Green Chem.*, (2013), 15, 210-225
- [22] VANDEZANDE, P., et al, Solvent resistant nanofiltration: separating on a molecular level, *Chem. Soc. Rev.* 37, 2, 2008, 365–405.
- [23] HABERT, A.C., et al, *Processos de Separação por Membranas*, Epapers, Rio de Janeiro, 2006.
- [24] SZÉKELY, G. et al, Organic solvent nanofiltration: A platform for removal of genotoxins from active pharmaceutical ingredients, *J. Membr. Sci.* 381, 2011 21-33.

- [25] SZÉKELY, G. et al, “A hybrid approach to reach stringent low genotoxic impurity contents in active pharmaceutical ingredients: combining molecularly imprinted polymers and organic solvent nanofiltration for removal of 1,3-diisopropylurea”. *Sep. Purif. Technol.* 86, 2012, 79–87.
- [26] HO, Y.S. and MCKAY, G., Sorption of dye from aqueous solution by peat, *Chem. Eng. J.*, 70, 1998, 115-124.
- [27] HO, Y.S. and MCKAY, G., Pseudo-second order model for sorption process, *Process Biochemistry*, 34, 5, 1999, 451-465.
- [28] Qiu, H.; et al, Critical Review in Adsorption Kinetic Models, *J. Zhejiang Univ. Sci. A*, 10, 2009, 716-724.
- [29] VICENTE, A. I, et al, “Solvent compatible polymer functionalization with adenine, a DNA base, for API degenotoxification: Preparation and characterization”, *Sep. Pur. Technol.*,179, 2017, 438-448.
- [30] CHUNG,T-S, A critical review of polybenzimidazoles: historical development and future R&D, *J. of Mol. Sci., Part C, Polymer reviews*, 37, 2, 1997, 273-301.

Chapter III

Polybenzimidazole physicochemical treatments for enhanced
genotoxic impurities removal from active pharmaceutical
ingredients streams: beads and electrospun fibers

*Paper submitted to Industrial and Engineering Chemistry Research by Flávio Alves
Ferreira, Teresa Esteves, Marta Carrasco, João Bandarra, Carlos Afonso, Frederico
Castelo Ferreira with the title: “Polybenzimidazole for active pharmaceutical ingredient
purification: beads and electrospun fibers.”*

3.1 Outline

This study reports for the first time, a new approach to improve the performance of polybenzimidazole (PBI), a solvent stable polymer, to efficient GTI removal. Two families of GTIs, alkylating agents and aromatic amines are considered, using methyl *p*-toluenesulfonate and 4-dimethylaminopyridine as their representatives. It is reported the discovery that the use of specific thermal (i.e. redissolution of PBI in DMSO at 163 °C) and pH conditioning of PBI adsorber (i.e. after formation of beads or fibers, there is a treatment with HCl or NaOH) improves GTI removal efficiency. The results section starts with the study of the effect of the different PBI treatments for each of the GTIs alone at different concentrations or in combination with API (section 3.4.1). Adsorbers prepared are then characterized by Nitrogen adsorption isotherm and scanning electron microscopy to have some insights about their structure (section 3.4.2). A dedicated study of the adsorption of GTIs and the model API used, Meta, reporting the kinetics and isothermics of such solutes from DCM solutions, the model solvent used, is presented (section 3.4.3). Finally, a set of studies of API purification presented section 3.4.4 illustrates the use of the enhanced PBI adsorbers in the context of removal of GTIs from an API stream, including strategies to recover non-specifically bound API and, when possible, to recycle the adsorber. Electrospun fibers are explored, aiming at process versatility. Similar removals of GTI, more than 97%, are achieved with virtually no API loss.

KEYWORDS: Polybenzimidazole adsorber; Polybenzimidazole fibers; genotoxic impurity; Active pharmaceutical ingredient purification.

3.2. Introduction

The presence of genotoxic impurities (GTIs) in active pharmaceutical ingredients (APIs) is an issue of permanent concern for pharmaceutical companies and patients' wellbeing [1,2]. Synthetic API production is mainly performed in organic solvent matrices using highly reactive species (e.g. reagents, catalysts) that may persist in the final formulations [3]. Strict regulatory measures impose a Threshold of Toxicological Concern (TTC) limiting the presence of GTIs in APIs to a maximum of 1.5 $\mu\text{g}/\text{day}$ [4,5]. To address this challenging low limit, several purification strategies have been extensively explored [6] including distillation, solvent exchange, recrystallization, organic solvent nanofiltration (OSN) platforms [7-9] or the use of conventional [10] or tailor made imprinted adsorbers [11,12]. However, since APIs are mainly obtained in organic solvent streams, the use of existing simple and efficient adsorbers is sometimes impaired or even impossible. Here, we addressed the purification of a corticosteroid API, mometasone furoate (Meta), and removal of two potential GTIs (4-dimethylaminopyridine, DMAP, and methyl *p*-toluenesulfonate, MPTS). Meta is used in the treatment of several inflammatory disorders[13] being possible to establish examples with administrations of 200 $\mu\text{g}/\text{day}$ for airways treatment (e.g. allergic rhinitis and asthma) or 2 mg/day for topic use (e.g. eczema and psoriasis), corresponding to limits imposed by the TTC of 7.5 and 0.75 mgGTI/gAPI, respectively. API synthesis usually includes the use of harsher chemical conditions and the development of robust and versatile adsorbers able to be used on such conditions still remains challenging. Polybenzimidazole (PBI) is an organic solvent compatible polymer that has been explored in the manufacturing of OSN membranes for API purification [14-17]. Recently, this polymer has been modified to bear adenine motifs in appending chains and has been

assessed for the removal of several families of DNA alkylating GTI agents in dichloromethane (DCM) solutions with good results [18].

In such previous reports, PBI was dissolved in dimethylsulfoxide (DMSO) at high temperatures (>160 °C), ensuring its complete dissolution or/and mixing of reagents [18,19], which led us to question if such heating step could have an effect on GTI adsorption, through induction of some structural or configurational features on PBI. Also, considering the chemical structure of unmodified PBI (Scheme 3.1), we decided to investigate in this work whether PBI adsorbers for GTIs could be developed using adequate thermal and/or pH conditioning. Therefore, this study provides a systematic assessment of such conditioned PBIs on their performance for GTI removal from API mixtures in an organic solvent. Moreover, in this report, a model system is considered comprising Meta as API, and DMAP and MPTS as model GTIs.

3.3. Materials and methods

3.3.1. Materials

4-Dimethylaminopyridine (DMAP) and methyl *p*-toluenesulfonate (MPTS) and *p*-toluenesulfonic acid monohydrate (PTSA) were purchased from Acros (Belgium). Pristine polybenzimidazole (PBI) polymer 100 mesh powder was purchased from PBI Performance Products Inc. (USA). All these reagents were used as supplied without further purification. Dichloromethane (DCM), methanol (MeOH) and acetonitrile (MeCN) HPLC grade solvents, hydrochloric acid (HCl) 37% solution and sodium hydroxide (NaOH) pellets were purchased from Fisher Chemicals (USA). Dimethylsulfoxide (DMSO) was purchased from Carlo Erba (Spain). Formic acid (FA) and dimethylacetamide (DMAc) were purchased from Panreac (Spain). Mometasone furoate (Meta) and betamethasone acetate (Beta) were kindly provided by Hovione PharmaScience Ltd (Portugal).

3.3.2. Apparatus and analysis

The experiments at 50 °C were controlled in an incubation chamber from J. P. Selecta (Spain). Nitrogen adsorption isotherms were obtained at 77 K in adsorption apparatus (ASAP 2010 Micromeritics) and the samples were degasified at 80 °C for 16 h. HPLC measurements were performed on a Merck Hitachi pump coupled to a L-2400 tunable UV detector using an analytic Macherey-Nagel C18 reversed-phase column Nucleosil 100-10, 250 x 4.6 mm, an injection volume of 10 μL and the eluents, A: aqueous 0.1% FA solution, B: MeCN 0.1% FA solution. For MPTS, a flow rate of 2 $\text{mL}\cdot\text{min}^{-1}$ and UV detection at 230 nm was used; method: 0-15 min, 70%A-30%B. For PTSA, a flow rate of 1.5 $\text{mL}\cdot\text{min}^{-1}$ and UV detection at 230 nm was used with the method: 0-10 min, 90%A-10%B. For DMAP, Meta and Beta, UV detection at 280 nm and a flow rate of 1 $\text{mL}\cdot\text{min}^{-1}$ was used with the method: 0-3 min, 60%-20% A; 3-4 min, 20% A; 4-8 min, 20%-60% A; 8-15 min 60% A. SEM experiments were performed on a FEG-SEM (Field Emission Gun Scanning Electron Microscope) from JEOL, model JSM-7001F, with an accelerating voltage set to 15 kV. Samples were mounted on aluminum stubs using carbon tape and were gold/palladium coated on a Southbay Technologies, model Polaron E-5100.

3.3.3. PBI thermal treatment

Pristine PBI polymer was dissolved in DMSO (15% w/w) by heating, under air, at 163 °C for 3 h with magnetic stirring. The solution was then cooled to 50 °C and precipitated with water. The resulting solid was crushed, filtered and successively washed with water (40 mL/g polymer), MeOH (20 mL/g polymer) and DCM (20 mL/g polymer) for 3 min each with magnetic stirring (3 times for each solvent). The solid obtained (Table 3.1) was then dried under vacuum.

Table 3.1. PBI adsorbers prepared and evaluated, as well as respective labelling used in this chapter.

Adsorber	Treatment
PBI-T	pristine PBI with thermal treatment
PBI-A	pristine PBI with acidic pH conditioning
PBI-B	pristine PBI with basic pH conditioning
PBI-TA	pristine PBI with thermal treatment and acidic pH conditioning
PBI-TB	pristine PBI with thermal treatment and basic pH conditioning;

3.3.4. PBI pH conditioning

Pristine PBI polymer with and without thermal treatment was pH conditioned with HCl 0.25 M or NaOH 0.1 M solutions by washing. The polymer was immersed for 3 min in 20 mL of acidic or basic solution per g of polymer with magnetic stirring. After this, the polymer was successively washed by magnetically stirring for 3 min in solutions of water (40 mL/g polymer), MeOH (20 mL/g polymer) and DCM (20 mL/g polymer) (3 times for each solvent) and dried under vacuum overnight (Table 3.1). The polymer was removed from each solution by simple filtration and transferred to the next solvent.

3.3.5. GTI binding experiments

Batch binding experiments were performed by placing 50 mg of each polymer in 2 ml Eppendorf vials or in a 7.5 mL borosilicate threaded test tube with Teflon-lined phenolic screw cap (Pyrex®) for experiments at 50 °C, and addition of 1 mL of a solution of each GTI (DMAP, MPTS) alone or in combination with each API (Meta, Beta) prepared in DCM at concentrations of 100 ppm, 1,000 ppm and 5,000 ppm for the GTIs or 10,000 ppm for the APIs. The suspensions were stirred for 24 h at 200 rpm. After this time the

samples were centrifuged for 3 min at 10,000 rpm, and the supernatant filtered and analyzed by HPLC for GTI and API quantification. These assays were performed with duplicate samples against controls. The same procedure was performed using 10 mg of fibers, instead of 50 mg, in 1 mL sample volume, with API and GTI mixtures in DCM.

The percentage of GTI or API bound to the polymers was calculated from Eq. (3.1) where C_0 (mg/L) is the initial GTI or API concentration and C_f (mg/L) is the final GTI or API concentration in solution.

$$\text{Binding (\%)} = \frac{[C_0 - C_f]}{C_0} \times 100 \quad (3.1)$$

The amount of GTI or API bound to the polymers was calculated from Eq. (3.2), where Q (mg/g) is the amount of GTI or API bound to the polymer, C_0 (mg/L) is the initial GTI or API concentration, C_f (mg/L) is the final concentration of GTI or API in solution, V (L) is the volume of solution used and M (g) is the polymer mass.

$$Q = \frac{V \times [C_0 - C_f]}{M} \quad (3.2)$$

3.3.6. Binding adsorption isotherm experiments

For the adsorption isotherm experiments at room temperature, 1 mL of DMAP, MPTS or Meta solutions prepared in DCM, with different initial concentrations, from 100 ppm to 10,000 ppm, were added to 50 mg of the polymers. The mixtures were stirred at 200 rpm for 24 h. After that time, the suspensions were centrifuged, and the supernatants were filtered and analyzed by HPLC. All experiments were carried out in duplicate. The percentage and the amount of GTI or API bound to the polymers was calculated from Eq. (3.1) and (3.2). The experimental data were fitted to the Langmuir and Freundlich isotherm models [20] according to Eq. (3.3) and (3.4), respectively, where q_m (mg/g) is the maximum amount of GTI bound to the resin in a monolayer for the Langmuir model, whereas K_L and K_F are equilibrium constants (L/mg) for the Langmuir and Freundlich

models, respectively, and are related with the energy taken for adsorption, n is a parameter related with the surface layer heterogeneity.

$$\frac{q_f}{q_m} = \frac{K_L C_f}{1 + K_L C_f} \quad (3.3)$$

$$q_f = K_F C_f^{\frac{1}{n}} \quad (3.4)$$

To compare the validity of each model, chi square (χ^2) was assessed, according to Eq. (3.5), since correlation coefficient (R^2) may not justify the selection of the most suited adsorption model because it only translates the fit between linear forms of the model equations and experimental data, while the suitability between experimental and predicted values of the adsorption capacity is described by chi square (χ^2). The lower the χ^2 value, the better the fit [21].

$$\chi^2 = \sum \frac{(\text{predicted data} - \text{experimental data})^2}{\text{predicted data}} \quad (3.5)$$

3.3.7. API recovery experiments

For Meta recovery, after binding experiments, the adsorbers, **PBI-TA** and **PBI-TB**, were washed with 1 mL of DCM for 24 h at 200 rpm, centrifuged and the supernatant was analyzed by HPLC. After that, for GTI removal from **PBI-TA** or **PBI-TB**, the polymers were washed with 1 mL of MeOH for 24 h at 200 rpm, centrifuged and the supernatants were analyzed by HPLC. Meta recovery and GTI removal were calculated by simple percentage.

3.3.8. Electrospinning setup

Fibers were prepared for a 13 wt% PBI solution in DMAc. The electrospinning process was carried out at 30 kV with a steady flow of 0.3 mL·h⁻¹ in a home-made set up previously described [22]. A needle with 0.51 mm of internal diameter was used and the electrospun fibers were collected on an aluminum target at a distance of 16 cm from the needle. The fibers obtained were subjected to pH conditioning by immersion in HCl 0.25 M or NaOH 0.1 M solutions for 3 min (20 mL of solution per g of polymer, with occasional stirring). After this, the fibers were successively washed, for 3 min, in water (40 mL/g polymer), MeOH (20 mL/g polymer) and DCM (20 mL/g polymer) (3 times for each solvent) and dried under vacuum overnight. The fibers were removed from each solution by decantation and transferred to the next solvent.

3.4. Results and discussion

In this report we study whether a dissolution step, at high temperature, and different ionic states of PBI polymer, similarly to ionic exchange resins, could be explored to confer improved adsorption properties to PBI. PBI can be found in different protonation states according to its pKa (5.23) [23,24]. The imidazole ring present in PBI structure can act either as an electron acceptor or donor and be present in different protonation states depending on the pH. Therefore, the initial pristine PBI was subjected to a thermal treatment (**PBI-T**) or/and acidic (**PBI-A/PBI-TA**) and basic (**PBI-B/PBI-TB**) pH conditioning to verify the optimal properties that could improve impurity removal, from solution, at the expense of the lowest API losses.

3.4.1. Screening PBI adsorbers for GTI removal

The performance of the new adsorbers, **PBI-T**, **PBI-A**, **PBI-B**, **PBI-TA** and **PBI-TB**, was assessed against solutions of GTIs (DMAP or MPTS) in DCM. From the results presented in Figure 3.1, it was possible to observe that **PBI-T**, with thermal treatment, induces a better performance for GTI removal (40% - 99%) comparing with pristine PBI polymer (2% - 14%). Moreover, coupling this feature to specific pH conditioning improves, according with GTI nature, even further this performance for highly concentrated GTI solutions, above 1,000 ppm. For this reason, **PBI-TA** and **PBI-TB** were the adsorbers selected to be further explored in the remaining studies reported in this work.

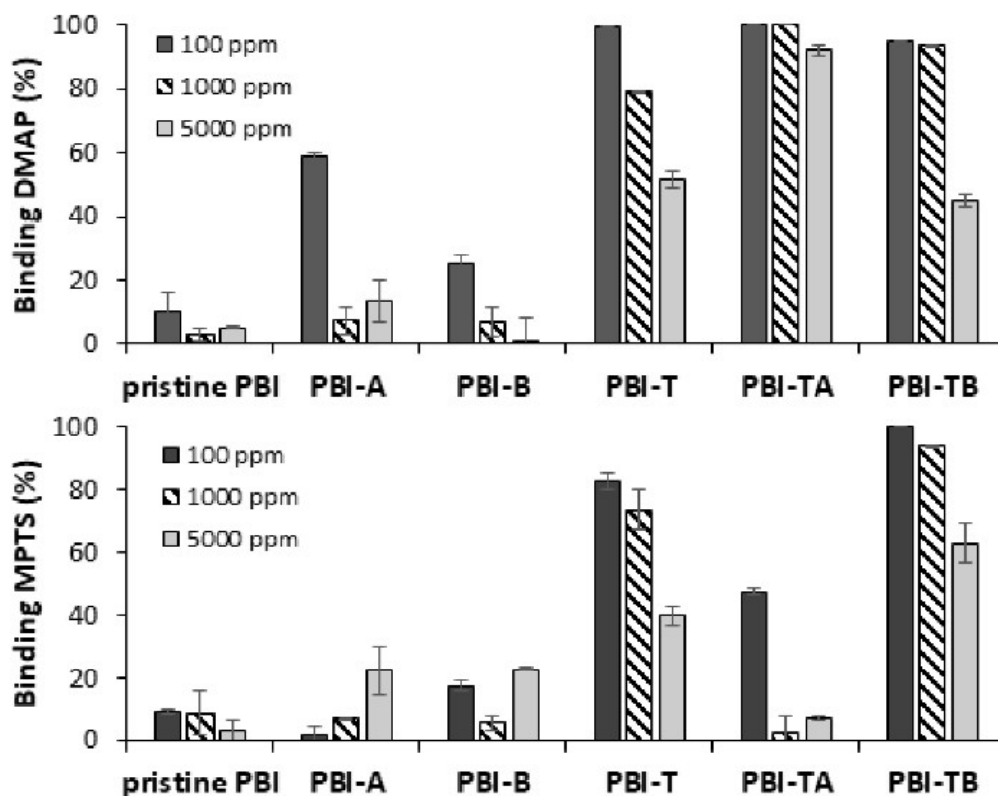
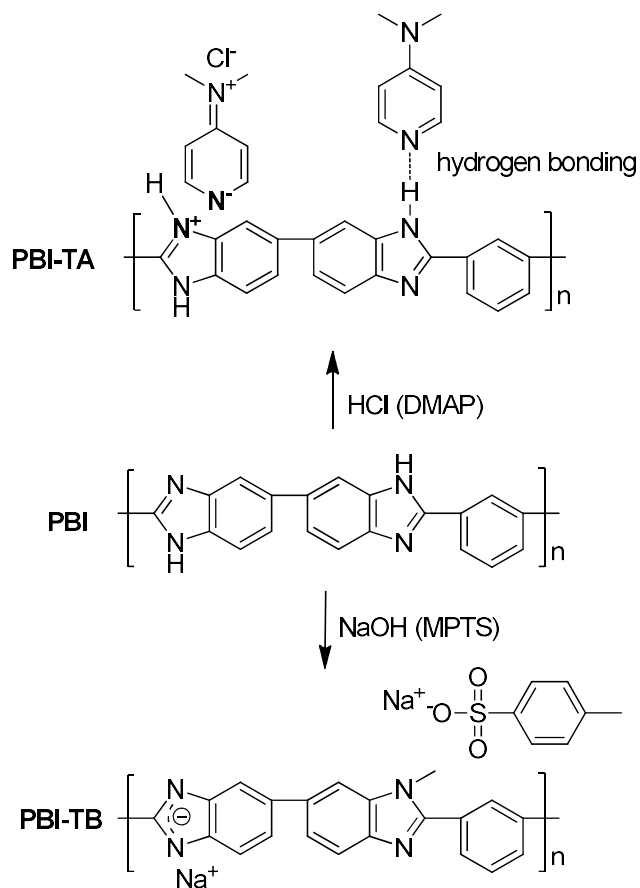


Figure 3.1. Top: DMAP binding for 100 ppm, 1,000 ppm and 5,000 ppm solutions in DCM for different PBI adsorbers. Bottom: MPTS binding for 100 ppm, 1,000 ppm and 5,000 ppm solutions in DCM for different PBI adsorbers.

In the specific case of DMAP, for a solution concentration of 1,000 ppm, both **PBI-TA** and **PBI-TB** are effective with removals higher than 93%. However, when the concentration is increased to 5,000 ppm, only **PBI-TA** remains effective (92%) while **PBI-TB** removal decreases by half (45%), remaining at the same level of DMAP removal achieved by **PBI-T**, at this concentration. For this reason, **PBI-TA** polymer was selected to address DMAP scavenging. DMAP can interact with pristine PBI through hydrogen bonding between the nitrogen of the aromatic ring and the amine groups present in benzimidazole rings of PBI. However, DMAP also presents a dipolar resonance allocating the negative charge on the nitrogen of the aromatic ring [25], which can favor an ionic interaction with the protonated groups of **PBI-TA** (Scheme 3.1). Synergistically, both these interactions may improve DMAP binding for **PBI-TA** for concentrations higher than 1,000 ppm as was observed.



Scheme 3.1. Proposed interaction mechanisms between **PBI-TA** and DMAP (top) and **PBI-TB** and MPTS (bottom).

In the case of MPTS, **PBI-TB** always presented a higher performance (63% - 97%) in removing this impurity when compared to **PBI-TA** (7% - 47%). A significant improvement of the basic treatment was obtained with higher MPTS removals for **PBI-TB** when compared with **PBI-T**, however the acid treatment resulted in lower MPTS removals by **PBI-TA**. For this reason, **PBI-TB** polymer was considered the more suited adsorber to treat solutions containing this GTI. In the case of this impurity, the interaction with PBI is expected to follow a methylation reaction of the amine groups of the imidazole rings of the adsorber, as will be further discussed on Chapter V, binding with a **PBI-adenine** modified polymer [18]. However, further deprotonation of PBI in the presence

of NaOH, originating **PBI-TB**, favors this reaction, with the sodium ions stabilizing the anion of MPTS, as represented in Scheme 3.1.

3.4.2. Adsorbers characterization

Nitrogen gas adsorption was used to estimate BET surface area, the total pore volume and the pore size for the different adsorbers (Table 3.2). Only for the polymers subjected to thermal treatment (**PBI-T**, **PBI-TA**, **PBI-TB**), it was possible to record the different parameters, with all polymers showing similar properties. For the remaining polymers, due to the lower surface area, the isotherms showed an irregular behavior, not allowing to calculate BET parameters for these samples. This can be due to surface modification of the particles that occurs during polymer precipitation in water, acting as a co-solvent, in a process similar to phase inversion that is used in the casting of PBI membranes [26]. This observation is supported by SEM images showing the presence of a smooth surface for pristine PBI, **PBI-A** and **PBI-B** particles, contrasting to a rough porous surface for **PBI-T**, **PBI-TA** and **PBI-TB** particles (Figure 3.2).

From the SEM images it is clear the formation of a more opened and porous structure for beads obtained after thermal treatment that involves the dissolution of PBI at high temperatures in DMSO, than for pristine PBI beads. Although **PBI-TA** and **PBI-TB** presented a good binding towards the GTIs, each adsorber targets only one of the species preferentially (**PBI-TA** for DMAP and **PBI-TB** for MPTS). This result indicates that the interaction behind GTI recognition is not only governed by the surface area of the polymeric particles, relying instead in specific ionic or covalent interactions established between the adsorbers, in a specific ionic state, and the GTI molecules, as discussed in section 3.4.1. Furthermore, SEM images (Figure 3.2) show that the electrospun fibers

obtained are randomly deposited, have an approximate diameter of 100 nm to 200 nm, and their morphology is not affected after pH conditioning, maintaining their integrity.

Table 3.2. Physical properties of pristine PBI and the several PBI derived adsorbers obtained by multipoint BET method.

	BET surface area ($\text{m}^2 \cdot \text{g}^{-1}$)	Pore volume ($\text{cm}^3 \cdot \text{g}^{-1}$)	Pore diameter (\AA)
Pristine PBI	n.d.	n.d.	n.d.
PBI-T	28.31	0.19	299.55
PBI-A	n.d.	n.d.	n.d.
PBI-B	n.d.	n.d.	n.d.
PBI-TA	27.77	0.18	309.35
PBI-TB	33.26	0.21	308.90

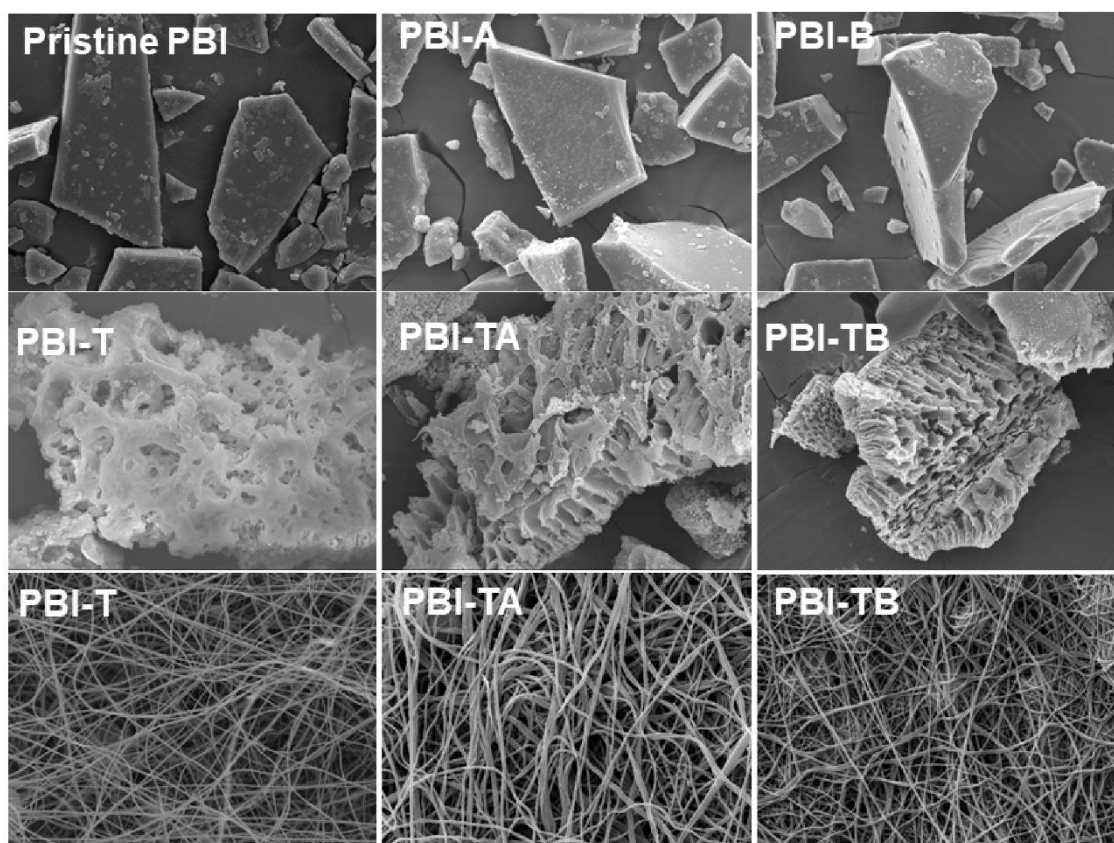


Figure 3.2. SEM images of PBI polymer particles and fibers (magnification 1000x). Top Panels: Beads obtained without thermal treatment. Middle panel: Beads obtained after thermal treatment. Bottom panel: electrospun fibers obtained from thermal treated PBI.

3.4.3. Binding isotherm and kinetic studies

The adsorption binding experiments show that DMAP and Meta follow the Langmuir model on **PBI-TA** (Figure 3.3) with the formation of a monolayer with maximum adsorption of 100 mg of DMAP (and 8.22 mg of Meta) per gram of polymer. Whereas MPTS and Meta follow the Freundlich model on **PBI-TB** (Figure 3.3) following adsorption on multilayers. Physical parameters determined for both adsorbers, **PBI-TA** and **PBI-TB**, are presented in Table 3.3.

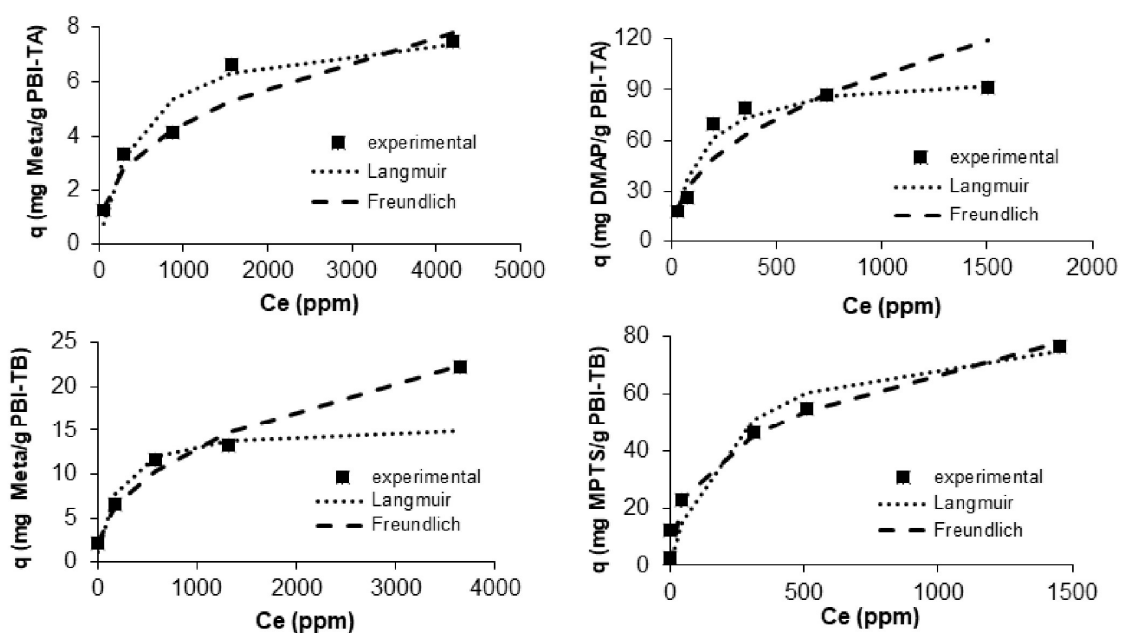


Figure 3.3. Top: Binding isotherm fitting models for DMAP (right) and Meta (left) for **PBI-TA** at room temperature. Bottom: Binding isotherm fitting models for MPTS (right) and Meta (left) for **PBI-TB** at room temperature.

Table 3. 3. Binding isotherm physical parameters obtained for DMAP, MPTS and Meta for PBI-TA and PBI-TB at room temperature.

		PBI-TA		PBI-TB	
		DMAP	Meta	MPTS	Meta
Langmuir	$K_L \times 10^{-3}$ (L/mg)	8.1 ± 1.8	2.1 ± 0.7	4.6 ± 1.5	5.5 ± 6.6
	q_m (mg/g)	100.00 ± 0.01	8.22 ± 0.01	86.21 ± 0.01	15.60 ± 0.01
	R^2	0.9940	0.9810	0.9847	0.9714
	χ^2	4.7860	0.2960	5.2252	4.6595
Freundlich	K_F (L/mg)	4.94 ± 2.25	0.30 ± 0.01	6.06 ± 0.35	0.71 ± 0.10
	1/n	0.43 ± 0.08	0.39 ± 0.04	0.35 ± 0.01	0.42 ± 0.02
	R^2	0.8776	0.9657	0.9984	0.9922
	χ^2	20.7816	0.4525	4.5119	0.3001

3.4.4. API purification studies.

3.4.4.1. GTI removal and API losses

In Sections 3.4.1. and 3.4.2., adsorption for single solute solutions, containing API or GTIs alone, were evaluated. However, for solutions containing both API and GTI, a possible competition between the species for available binding sites of adsorber may take place, possibly affecting the binding of different species. In order to assess this, solutions simulating an API post reaction stream in DCM, with 10,000 ppm of API and 1,000 ppm of GTI, were assessed with **PBI-TA** and **PBI-TB** polymers (Figure 3.4).

For DMAP and **PBI-TA**, no difference was observed for GTI removals (around 99%), using single solute solutions or mixtures of GTI and API. For the APIs, Meta adsorption on **PBI-TA** remained lower than 10%, and for Beta the adsorption remained around 20%, showing that this adsorber performance was not affected by the presence of both species in solution.

However, for MPTS in **PBI-TB** at room temperature, there was a significant reduction of GTI removal, from 94% to 50%, followed by an increase in APIs adsorption, from around 9% to around 25% when both compounds were mixed in solution.

Betamethasone acetate (Beta), also a glucocorticoid like Meta, was tested to verify if the results obtained for **PBI-TB** were only due to the presence of Meta. These APIs, although presenting the same general structure, contain different chemical functionalities that may impair or not the interaction with the adsorbers. Both APIs present halogen atoms at 9 α position, with a chlorine for Meta and a fluorine for Beta. Moreover, at position 21 Meta has an additional chlorine atom and at position 17 it has a furoate group, whereas Beta presents an ester group at position 21 and a hydroxyl group at position 17. Despite these structural differences, for **PBI-TB**, the same trend was observed for both glucocorticoids, with a lower efficiency in GTI removal and an increment in API loss for mixtures of MPTS and APIs than for single solute assays. At this point, following the same reasoning of the binding kinetic studies, and in order to solve this drawback, these experiments were also performed at 50 °C (Figure 3.4). The use of borosilicate test tube with screw cap allows to the experiment run without DCM losses due to evaporation, one time the system was closed, the pressure inside the tube contributes in the change in DCM's boiling point. With the increase in temperature, it was possible to observe that GTI removal was reestablished to previous values above 96% with API binding to the adsorber of only around 9%.

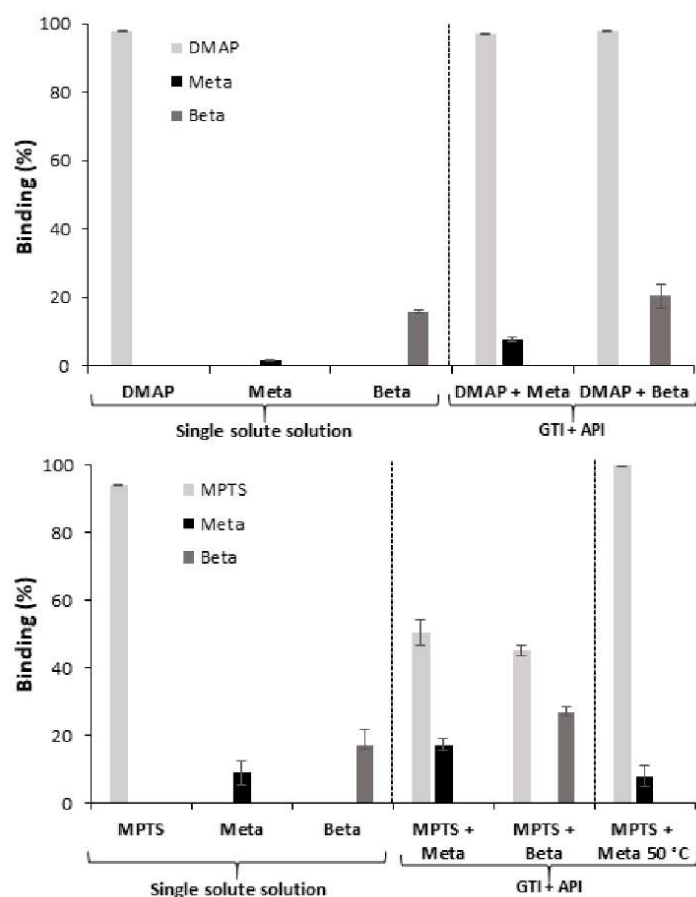


Figure 3.4. Top: Comparison of adsorption of solutions of isolated API, isolated DMAP and API+DMAP with **PBI-TA** at room temperature. Bottom: Comparison of adsorption of solutions of isolated API, isolated MPTS and API+MPTS with **PBI-TB** at room temperature and at 50 °C.

The use of PBI electrospun fibers is well established in literature for applications in proton conductive membranes [27,28]. Moreover, the use of fiber meshes allows for diverse process configurations, such as membrane contactors and adsorbers [29,30]. As illustrated on SEM images, when PBI is electrospun, uniform and regular structures are obtained. Adsorption of GTIs and API were assessed for GTI and API mixtures using 10 mg of **PBI-TA** beads or fibers at room temperature and **PBI-TB** beads or fibers at 50 °C in 1 ml of DCM. Note that, sub-optimal amounts of 10 mg/ml of adsorber were used to perform experiments in conditions below the 100% GTI removal observed when using 50 mg/ml of beads. The reasoning for this is, the use of 10 mg/ml of polymer (instead of

50 mg/ml) avoids fiber compaction in the 1 ml test solution and allows for experimental detection of potential differences between fiber and beads adsorption performance.

DMAP removal in **PBI-TA** was slightly higher for the fibers, although not statistically significant ($p = 0.12$), than for beads (Figure 3.5). Concerning API loss, it was similar and around 20%. In the case of MPTS with **PBI-TB**, the API loss followed the same trend (around 10%) with a similar MPTS removal ($p = 0.40$) of around 50%. These preliminary experiments suggest that, independently of the morphology of the adsorber, the physico-chemical characteristics conferred to the material remained similar. This fact is important in applications requiring the use of electrospun fiber meshes such as in membrane separation processes to perform purification of APIs in organic solvent matrices.

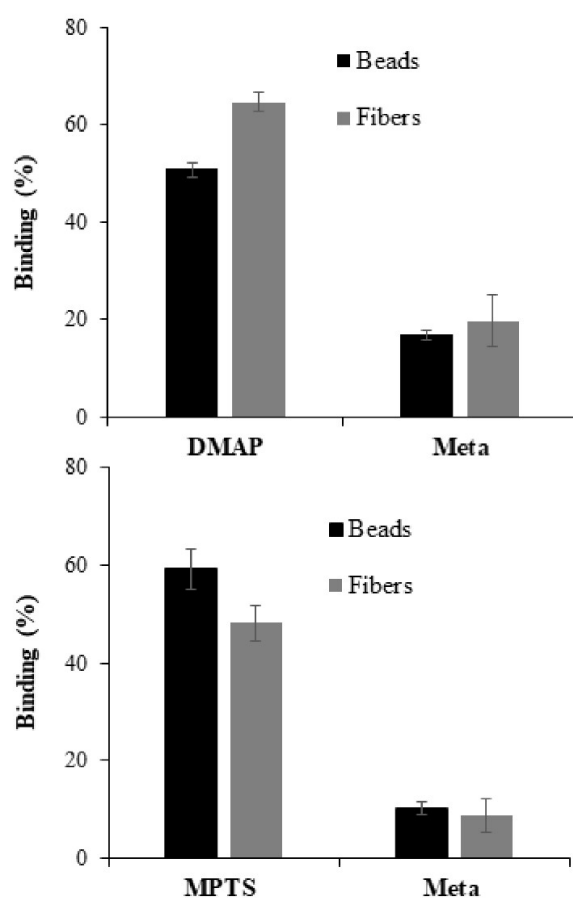


Figure 3.5. Comparison between binding performance of beads and fibers. Top: **PBI-TA** for DMAP and Meta at room temperature. Bottom: **PBI-TB** for MPTS and Meta at 50°C.

3.4.4.2. Development of a post binding protocol: API recovery and GTI elution

Since the PBI beads and fibers showed a similar behavior in solution, the recovery of the API that remained bound to the adsorbers was only assessed for the beads. In order to reduce API loss, a recovery step was performed by assessing Meta desorption from the adsorbers using DCM or MeOH. Virtually, all the API was recovered from both polymers, **PBI-TA** and **PBI-TB**, after a simple first DCM washing (2 mL DCM per gram of polymer) (Table 3.4 and Table 3.5); in the case of **PBI-TA**, a minimum DMAP back contamination (around 1% of adsorbed GTI) was observed. When, alternatively, the polymer was first washed with MeOH, the API could also be fully recovered but with 80% of DMAP contamination (Table 3.4). Therefore, it is here suggested to use a first DCM washing for API recovery, followed by a MeOH washing step for DMAP removal. When such strategy was followed around (80-90%) of DMAP was removed from **PBI-TA**.

In the case of **PBI-TB**, in the first DCM washing, only Meta was recovered (Table 3.6). The resulting salt of MPTS shows a poor solubility in this solvent, and therefore most probably remains precipitated with the adsorber, probably contributing to less than 1% of GTI contamination. The suggestion that the interaction between the GTI and **PBI-TB** comprises a chemical modification of the adsorber, with hydrolysis of MPTS, is coherent with the detection of GTI anion (*p*-toluenesulfonate) on MeOH washing solution, since this solvent is able to solubilize this compound. This observation was validated by co-elution with a sample of *p*-toluenesulfonic acid (PTSA), presenting the same *p*-toluenesulfonate anion (see Chapter VI, Figure 6.7 for more informations).

Table 3.4. API loss and mgGTI/gAPI using PBI-TA for DMAP removal in a Meta solution.

Recovery (%)							
DCM		MeOH		After adsorption		After DCM washing	
Meta	DMAP	Meta	DMAP	mgGTI/gAPI	API loss (%)	mgGTI/gAPI	API loss (%)
100	1.03	100	80.39	2.95	1.62	3.90	0

Table 3.5. API loss and mgGTI/gAPI using PBI-TB for MPTS removal in a Meta solution.

Recovery (%)							
DCM		MeOH		After adsorption		After DCM washing	
Meta	MPTS	Meta	MPTS	mgGTI/gAPI	API loss (%)	mgGTI/gAPI	API loss (%)
100	< 0.5	100	< 0.65	< 0.27	7.93	< 0.25	0

Since the API recovery steps are able to mitigate its loss without exceeding a target value of 7.5 mgGTI/gAPI, a possible API purification strategy can be sought with each adsorber targeting each impurity. Using **PBI-TA**, it is possible to remove DMAP and recover the API with a simple DCM washing step and to remove the bound impurity with a simple MeOH washing. Further regeneration of the adsorber could be performed with a HCl solution. In the case of **PBI-TB**, the adsorption step must take place at 50°C to improve impurity removal. However, a simple DCM washing is enough to recover the API that was bound to the adsorber and reach the targeted values of 7.5 or 0.75 mgGTI/gAPI. For this polymer, a MeOH washing is able to remove the salt of the impurity, but its regeneration is impaired by the nature of the reaction between MPTS and the amine groups of the imidazole rings of the adsorber.

3.5. Conclusions

PBI based adsorbers were obtained for the removal of impurities from API solutions in DCM. The polymer subjected to thermal treatment and acidic conditioning, **PBI-TA**, showed the best performance for the removal of an aromatic amine, DMAP, with API losses lower than 10%. When the PBI is subjected to a basic treatment, the resulting adsorber, **PBI-TB**, shows improved performance to remove a sulfonate alkylating agent from solution with low API losses. However, in this case, the process requires improvement with temperature. The same adsorbers formulated as fibers showed a similar performance in API purification strategies, opening the way to several possibilities for separation processes based on filtration in organic solvent matrices using the fibers. In the case of both types of impurities, the final ratios of mgGTI/gAPI obtained were within the limits imposed by the TTC in the case of the API studied, Meta.

3.6. REFERENCES

- [1] Zhou, L., et al, Impurity Profile Tracking for Active Pharmaceutical Ingredients: Case Reports. *J. Pharm. Biomed. Anal.*, 44, 2007, 421-429.
- [2] Chang, S. J., et al, Risk Assessment of Genotoxic Impurities in New Chemical Entities: Strategies to Demonstrate Control. *Org. Process Res. Dev.*, 17, 2013, 221–230.
- [3] Székely, et al, Genotoxic Impurities in Pharmaceutical Manufacturing: Sources, Regulations, and Mitigation. *Chem. Rev.*, 16, 2015, 8182-8229.
- [4] EMEA Guidelines on “Limits on Genotoxic Impurities”, EMEA/CHMP/QWP/251344/2006, 2006.

[5] Guidance for Industry Genotoxic and Carcinogenic Impurities in Drug Substances and Products: Recommended Approaches; U.S. Department of Health and Human Services; Food and Drug Administration; Center for Drug Evaluation and Research (CDER); December 2008.

[6] Teasdale, A. Genotoxic Impurities: Strategies for Identification and Control; John Wiley & Sons: New Jersey, 2010.

[7] Buonomenna, M. G.; Bae, J. Organic Solvent Nanofiltration in Pharmaceutical Industry. *Sep. Purif. Rev.*, 44, 2015, 157-182.

[8] Székely, G., et al, Environmental and Economic Analysis for Selection and Engineering Sustainable API Degenotoxification Processes. *Green Chem.*, 15, 2013, 210-225.

[9] Székely, G., et al, Organic Solvent Nanofiltration: a Platform for Removal of Genotoxins from Active Pharmaceutical Ingredients. *J. Membrane Sci.*, 381, 2011, 21-33.

[10] Esteves, T.; et al, Screening Commercial Available Resins for Simultaneous Removal of Two Potential Genotoxins from API Methanolic Streams. *Sep. Sci. Technol.* 2018, DOI: 10.1080/01496395.2018.1556304.

[11] Esteves, T, et al, Molecularly Imprinted Polymer Strategies for Removal of a Genotoxic Impurity, 4-dimethylaminopyridine, from an Active Pharmaceutical Ingredient Post-reaction Stream. *Sep. Purif. Technol.*, 163, 2016, 206-214.

[12] Székely, G.; et al, Design, Preparation and Characterization of Novel Molecularly Imprinted Polymers for Removal of Potentially Genotoxic 1,3-diisopropylurea from API Solutions. *Sep. Purif. Technol.*, 86, 2012, 190-198.

[13] Heggie, W. Process for the Preparation of Mometasone Furoate, US 6177560 B1, 2001.

[14] Peeva, L., et al, Continuous Purification of Active Pharmaceutical Ingredients Using Multistage Organic Solvent Nanofiltration Membrane Cascade. *Chem. Eng. Sci.*, 116, 2014, 183-194.

[15] Székely, G., et al, Molecularly Imprinted Organic Solvent Nanofiltration Membranes – Revealing Molecular Recognition and Solute Rejection Behavior. *React. Funct. Polym.*, 86, 2015, 215-224.

[16] Kim, J. F, et al, Increasing the Sustainability of Membrane Processes Through Cascade Approach and Solvent Recovery – Pharmaceutical Purification Case Study. *Green Chem.*, 16, 2014, 133-145.

[17] Valtcheva, I. B., et al, Beyond Polyimide: Crosslinked Polybenzimidazole Membranes for Organic Solvent Nanofiltration (OSN) in Harsh Environments. *J. Membrane Sci.*, 457, 2014, 62–72.

[18] Vicente, A. I., et al, Solvent Compatible Polymer Functionalized with Adenine, a DNA Base, for API Degenotoxification: Preparation and Characterization. *Sep. Purif. Technol.*, 179, 2017, 438-448.

[19] Dominguez, P. H, et al, Nanostructured Poly(benzimidazole) Membranes by N-alkylation. *eXPRESS Polym. Lett.*, 8, 2014,30-38.

[20] Rahimi, M.; Vadi, M.; Langmuir, Freundlich and Temkin Adsorption Isotherms of Propranolol on Multi-Wall Carbon Nanotube. *J. Modern Drug Discovery and Drug Delivery Res.* 2014, DOI: 10.5281/zenodo.893491.

[21] Ho Y. Selection of Optimum Sorption Isotherm. *Carbon*, 42, 2002, 2115-2116.

[22] Canadas R. F., et al, Polyhydroxyalkanoates: Waste Glycerol Upgrade Into Electrospun Fibrous Scaffolds for Stem Cells Culture. *Int. J. Biol. Macromol.*, 71, 2014, 131-140.

[23] Pu, H. *Polymers for PEM Fuel Cells*; John Wiley and Sons: Hoboken, New Jersey, 2014.

[24] Li, Q.; Jensen, J. O. *Membranes for Energy Conversion, Volume 2*; Wiley-VCH: Weinheim, 2008.

[25] Scudder, P.H. *Electron Flow in Organic Chemistry: A Decision-Based Guide to Organic Mechanisms*; John Wiley & Sons: New Jersey, 2013.

[26] Valtcheva, I. B, et al, Crosslinked Polybenzimidazole Membranes for Organic Solvent Nanofiltration (OSN): Analysis of Crosslinking Reaction Mechanism and Effects of Reaction Parameters. *J. Membrane Sci.*, 493, 2015, 568-579.

[27] Li H.; Liu Y. Polyelectrolyte Composite Membranes of Polybenzimidazole and Crosslinked Polybenzimidazole-polybenzoxazine Electrospun Nanofibers for Proton Exchange Membrane Fuel Cells. *J. Mater. Chem. A*, 1, 2013, 1171–1178.

[28] Jahangiri S., et al, Fabrication and Optimization of Proton Conductive Polybenzimidazole Electrospun Nanofiber Membranes. *Polym. Adv. Technol.*, 29, 2018, 594-602.

[29] Ki C. S., et al, Nanofibrous Membrane of Wool Keratose/Silk Fibroin Blend for Heavy Metal Ion Adsorption. *J. Membrane Sci.*, 302, 2007, 20–26.

[30] Park M. J., et al, Mixed Matrix Nanofiber as a Flow-Through Membrane Adsorber for Continuous Li⁺ Recovery from Seawater. *J. Membrane Sci.*, 510, 2016, 141–154.

Chapter IV

Polybenzimidazole modified with carboxylic acid groups for aromatic amine impurities scavenging

Original material: yet to be submitted as a manuscript for peer revision

4.1. Outline

This study reports the application of a novel polybenzimidazole (PBI) polymer modified with different carboxylic acids as scavenger for aromatic amines. This chapter reports the synthesis of PBI with alkyl carboxyl groups with different length of the alkyl chain (2, 4, 10 carbon atoms) being used as spacer between the carboxyl group and the polymer backbone. PBI functionalized with carboxylic acids, prepared using equivalent molar reaction ratios between 0.25 to 1.0 of mol equivalents to mols of reactive secondary amines in the PBI backbone, were assessed using 4-dimethylaminopyridine (DMAP) as model of potential GTI in section 4.4.2. Such polymers were preliminary characterized by BET (Section 4.4.3) and for a reaction ratio of 1.0 eq. it is also presented SEM (Section 4.4.3) and kinetic and isothermic profiles using DMAP dissolved in DCM as model solution (Section 4.4.44). DMAP and Meta dissolved in DCM were used together as model compounds to study the effect of alkyl chain length using PBI prepared at reaction ratios of 1 mol eq. of 3-bromopropionic acid, 5-bromovaleric acid or 11-bromoundecanoic acid to reactive secondary PBI amines (Section 4.4.2),. Removal of ten different compounds were assessed, although some of them showed no affinity. A removal higher than 95 % was observed for DMAP, and the pKa value of the adsorbates seem to be a determinant factor for the removal, maybe due to the electrostatic repulsion of both protonated species. API purification was addressed, and an efficient purification was achieved with losses lower than 8%, reaching values between 2 and 5 mgGTI/gAPI respecting the Threshold of Toxicological Concern (TTC) value.

Keywords: Polybenzimidazole adsorber; carboxylic acid; aromatic amine; Active pharmaceutical ingredient; purification.

4.2. Introduction

Impurities from chemical synthesis of API can react readily with DNA, being genotoxic by their very nature, or producing genotoxic compounds after being metabolized *in vivo*. Such impurities may arise either by the formation of by-products or even be introduced intentionally, due to their reactivity as in the case of substances such as 4-dimethylaminopyridine (DMAP), commonly used as a catalyst [1,2], including in API synthesis as in the case of Mometasone furoate (Meta) [3] .

DMAP is an aromatic amine, such compounds are classified as potentially genotoxic due to the association of the arylamine groups present in their structure, which after being metabolized can be covalently bound to DNA [4,5,6].

Although it is desirable to avoid the use of GTIs in the manufacture of APIs, this is not always possible, and therefore, it is mandatory to produce APIs with low GTI content, controlled below the Threshold of Toxicological Concern (TTC) established by regulatory authorities (1.5 µg/day). Such regulatory framework is also valid for amines with structural alert [7,8].

The use of molecularly imprinted polymers (MIP) has demonstrated high efficiency in genotoxic removal [9,10], however, such adsorbents have the limitation of being exclusive to the removal of the molecule used as a template.

The development of materials that are able to selectively remove a wide range of genotoxic compounds is a major challenge, since they have different structures and cover different chemical families.

In this chapter, a polymeric adsorbent, functionalized with carboxylic acids, proposed as scavenger for aromatic amines is presented.

4.3. Experimental section

4.3.1. Materials

4-Dimethylaminopyridine (DMAP), 3-nitroaniline, 4-methyl-3-nitroaniline, 4-methyl-2-nitroaniline, 4-chloroaniline, 2,6-dichloroaniline and 2,6-dimethylaniline were purchased from Acros (Belgium). Potassium carbonate (K_2CO_3), 3-bromopropionic acid (BPA), 5-bromovaleric acid (BVA), pyridine and 3-pyridinecarboxaldehyde were purchased from Sigma Aldrich (Switzerland). 4-Aminobiphenyl was purchased from Alpha Aesar. 11-Bromoundecanoic acid (BUA) was purchased from TCI (Belgium). Polybenzimidazole (PBI) polymer 100 mesh powder was purchased from PBI Performance Products Inc. (USA). All chemicals were of reagent grade or higher and were used as received. The 1H spectra were recorded using $DMSO-d_6$ (99.9%) purchased from CIL (USA). Dichloromethane (DCM) and acetonitrile (MeCN) HPLC grade, methanol (MeOH), dimethylsulfoxide (DMSO) and hydrochloric acid (HCl) were purchased from Fisher Chemicals (USA). Formic acid (FA) was purchased from Panreac (Spain). All solvents were used without further purification. Lupanine was provided by Faculty of Pharmacy, University of Lisbon. Mometasone furoate was kindly provided by Hovione PharmaScience Ltd, Portugal.

4.3.2. Preparation of the Modified PBI Polymers

4.3.2.1. Reaction with 3-bromopropionic acid.

A solution of PBI (2.00 g, 12.8 mmol) in DMSO (13 mL) was left stirring for 3 h at 160 °C, approximately. The solution was cooled to 50 °C and 1.00 eq of K_2CO_3 (1.74 g, 12.6 mmol) was added followed by 1.00 eq of BPA (1.00 g, 12.6 mmol). The reaction temperature was raised to 100 °C for 24 h. After this time, the reaction was allowed to

come to 50 °C and the polymer precipitated after the addition of 40 mL of water. The resulting solid was crushed, filtered and then successively washed with 40 mL MeOH and 40 mL of DCM. The polymeric particles were washed with an aqueous 0.25 M HCl solution for 3 min. After this time, the polymers were washed with 80 mL of water, 40 mL of MeOH and 40 mL of DCM (three times each) and dried overnight under vacuum. The final polymer was obtained as a brown solid. ^1H NMR (300 MHz, DMSO- d_6): δ 2.87 (d, 2H), 4.72 (d, 2H) 8.01-7.59 (m, 7H), 9.1 (sl, 1H), 8.3 and 8.7 (sl, 1H). The polymers obtained in the presence of different equivalents of BPA were synthesized by following the previous protocol only changing the mol equivalents of carboxylic acid, (note that, for equivalent molar calculations, each PBI monomer has two available atoms for insertion). Similarly, the polymers with different spacer chains were obtained by following the above described procedure, by replacing BPA for BVA or BUA.

4.3.2.2. Reaction with 5-bromovaleric acid.

^1H NMR (300 MHz, DMSO- d_6): δ 1.54 (m, 4H), 1.94 (d, 2H), 2.3 (d, 2H), 8.01-7.59 (m, 7H), 9.1 and 8.3 (sl, 1H).

4.3.2.3. Reaction with 11-bromoundecanoic acid.

^1H NMR (300 MHz, DMSO- d_6): δ 1.6-0.8 (m, 12H), 2.3-1.85 (m, 4H), 3.85 (m, 2H), 8.01-7.59 (m, 7H), 9.1 and 8.3 (sl, 1H).

4.3.3. Apparatus and Analysis

^1H NMR spectra were obtained on a Bruker spectrometer MX300 operating at 300 MHz.

Visualization of the morphology of the polymeric particles was performed using scanning electron microscopy (SEM) on a FEG-SEM (Field Emission Gun Scanning Electron Microscope) from JEOL, model JSM-7001F, with an accelerating voltage set to 15 kV. The samples were mounted on aluminum stubs using carbon tape and were gold/palladium coated on a Southbay Technologies, model Polaron E-5100. HPLC measurements were performed at room temperature with 10 μ L injection volume on a Merck Hitachi pump coupled to a L-2400 tunable UV detector using an analytic Macherey-Nagel C18 reversed-phase column Nucleosil 100-10, 250 x 4.6 mm and eluents, A: aqueous 0.1% formic acid solution, B: MeCN 0.1% formic acid solution. For DMAP and Meta a flow rate of 1 mL \cdot min⁻¹ was used with UV detection at 280 nm: 0-3 min, 60%-20% A; 3-4 min, 20% A; 4-8 min, 20%-60% A; 8-15 min 60% A. For pyridine a flow rate of 1 mL \cdot min⁻¹ was used with UV detection at 260 nm: 0-15 min, 70%A-30%B. For pyridine-3-carboxaldehyde a flow rate of 1 mL \cdot min⁻¹ was used with UV detection at 280 nm: 0-15 min, 40%A-60%B. For nitroanilines a flow rate of 0.8 mL \cdot min⁻¹ was used with UV detection at 254 nm: 0-10 min, 35%A-65%B. For 4-aminobiphenyl a flow rate of 1 mL \cdot min⁻¹ was used with UV detection at 275 nm, and 60% MeCN / 40% water: for 15 min.

A Luna C18 reversed phase column (100-10, 250 x 4.6 mm) from Phenomenex was used for 6-dimethylaniline, 4-chloroaniline and 2,6-dichloroaniline with UV detection at 254 nm and the eluents A: aqueous 0.1% FA solution, B: MeCN 0.1% FA solution with an injection volume of 10 μ L. For 6-dimethylaniline and 4-chloroaniline a flow rate of 1 mL \cdot min⁻¹ was used: 0-10 min, 80%A-20%B. For 2,6-dichloroaniline a flow rate of 1.5 mL \cdot min⁻¹ was used: 0-15 min, 50%A-50%B.

Specific surface area and pore diameter of the polymeric particles were determined by nitrogen adsorption according to the BET method. An accelerated surface area and porosimetry system (ASAP 2010 Micromeritics) was used under nitrogen flow. pH was measured using a 702 MS Titrino from Metrohm (Switzerland).

4.3.4. Batch Binding Experiments

Batch scavenging experiments were performed with 50 mg of polymer in 2 ml Eppendorf tubes and addition of 1 mL of a DMAP solution prepared in DCM at 100 ppm or 1,000 ppm. The suspensions were stirred for 24 h at 200 rpm at room temperature. After this time, the samples were centrifuged at 10,000 rpm for 20 min, the supernatant was filtered and analysed by HPLC. The amount of DMAP or Meta bound to the polymers was calculated from equation (4.1), where, C_0 (mg/L) is the initial analyte concentration, C_e (mg/L) is the equilibrium concentration of the analyte in solution.

The assays were all carried out in duplicates against controls.

$$\text{Binding (\%)} = \frac{[C_0 - C_f] \times 100}{C_0} \quad (4.1)$$

The amount of analyte bound to the polymers was calculated from Eq. (4.2), where Q (mg/g) is the amount of analyte bound to the polymer, C_0 (mg/L) is the initial analyte concentration, C_f (mg/L) is the final concentration of analyte in solution, V (L) is the volume of solution used and M (g) is the polymer mass.

$$Q = \frac{V \times [C_0 - C_f]}{M} \quad (4.2)$$

4.3.5. Binding Isotherm and Kinetic Experiments

Binding isotherm experiment was performed as described above, placing 50 mg of the polymer in Eppendorf tubes with 1 mL of DMAP solutions with concentrations ranging from 5 ppm to 1,000 ppm. After 24 h at 200 rpm and room temperature the solutions were centrifuged, the supernatant was filtered and analyzed by HPLC for DMAP quantification.

The percentage and the amount of DMAP bound to the polymers was calculated from Eq. (4.1) and (4.2). The experimental data were fitted to the Langmuir and Freundlich isotherm models [11] according to Eq. (4.3) and (4.4), respectively, where q_m (mg/g) is the maximum amount of DMAP bound to the resin in a monolayer for the Langmuir model, whereas K_L and K_F are equilibrium constants (L/mg) for the Langmuir and Freundlich models, respectively, and are related with the energy taken for adsorption, n is a parameter related with the surface layer heterogeneity.

$$\frac{q_f}{q_m} = \frac{K_L C_f}{1 + K_L C_f} \quad (4.3)$$

$$q_f = K_F C_f^{\frac{1}{n}} \quad (4.4)$$

The kinetic study was performed at room temperature with a 100 ppm DMAP solution. 50 mg of the polymer was placed in contact with 1 mL of this solution and sacrificial samples were treated, as previously described for the binding isotherm studies, and analyzed by HPLC at 5 min, 15 min, 30 min and 1, 2, 4, 6, 8, 24 and 27 h. The assays were all carried out in duplicates against controls. The percentage and the amount of DMAP bound to the polymer was calculated from Eq. (4.1) and (4.2). The experimental data were fitted to pseudo-first and pseudo-second order kinetic models [12] according to

Eq. (4.5) and (4.6) respectively, where q_f and q_t (mg/g) are the adsorption capacities at the final and time t (min) respectively, and k_1 (min^{-1}) and k_2 ($\text{g}/(\text{mg}\cdot\text{min})$) are the pseudo-first and second order rate constants for the models.

$$\ln(q_f - q_t) = \ln(q_f) - k_1 \cdot t \quad (4.5)$$

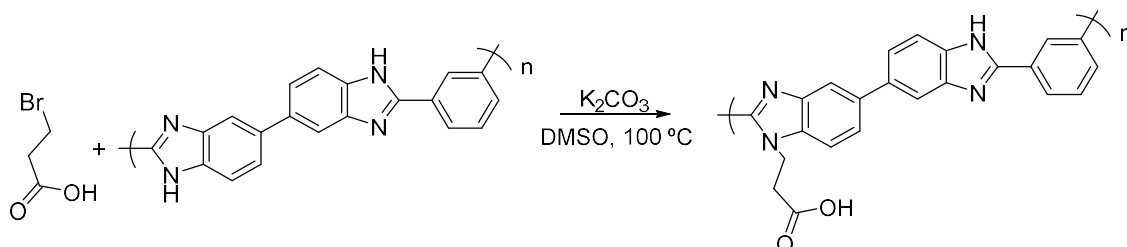
$$\frac{t}{q_t} = \frac{1}{k_2 \cdot q_f^2} + \frac{t}{q_f} \quad (4.6)$$

To compare the validity of each model, chi square (χ^2) was assessed since correlation coefficient (R^2) may not justify the selection of the most suited model because it only translates the fit between linear forms of the model equations and experimental data, while the suitability between experimental and predicted values is described by chi square (χ^2). The lower the χ^2 value, the better the fit.

4.4. Results and discussion

4.4.1. Polymer Synthesis

The synthetic strategy followed was based on a recently published protocol developed in our group to obtain a PBI polymer modified with a DNA base [13]. This procedure comprises the dissolution of PBI in DMSO for 3 h at 160 °C followed by the addition of K_2CO_3 and a bromo alkylated DNA base. Similarly, the synthesis of the modified PBI polymers bearing a free carboxylic acid function, consisted in the reaction of the bromo alkyl carboxylic acid with PBI in DMSO in the presence of K_2CO_3 as depicted in Scheme 4.1, 1 for BPA. The resulting solution was then precipitated with water, the resulting solid was crushed, washed with MeOH, DCM and HCl and dried to obtain the desired product as a brown solid.



Scheme 4.1. Synthesis of the modified PBI polymer with a free carboxylic acid function (PBI-COOH).

In these reactions a replacement of a hydrogen that was attached to a secondary amine takes place, generating a deviation of the signal located at 9.1 ppm in the 1H NMR spectrum (indicated by 7 in Fig. 4.1) to 8.7 ppm (indicated by 7' in Fig. 4.1), caused by the difference in chemical environment, and the intensity of the signal emitted to 8.7 ppm increases with the amount equivalents of carboxylic acid inserted (Fig 4.1).

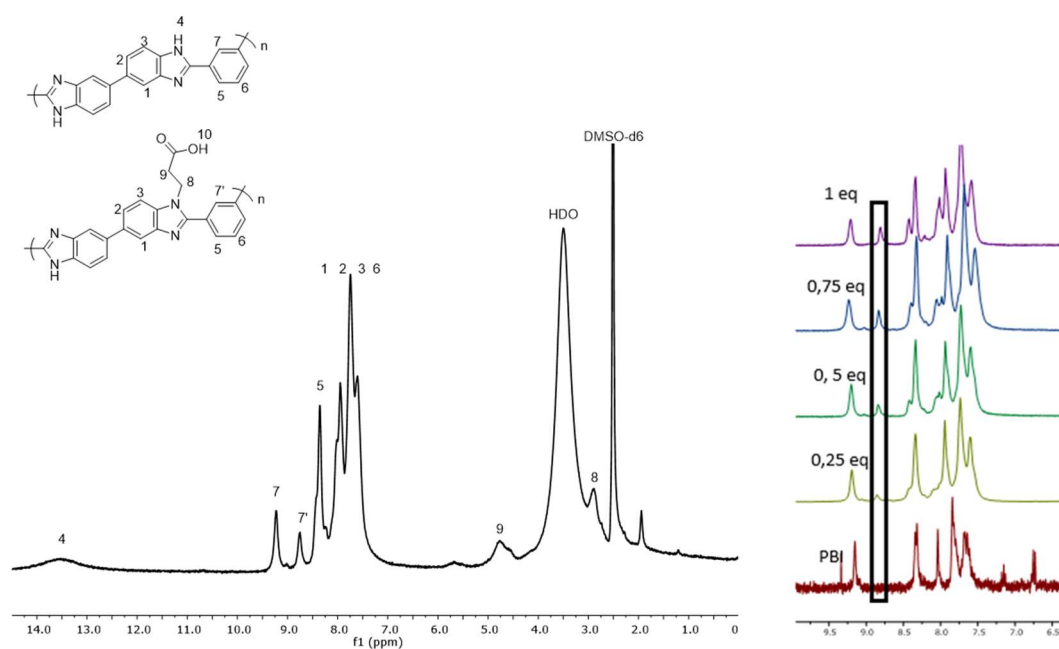


Figure 4.1. ^1H NMR spectrum of PBI-COOH, prepared with BPA, in DMSO- d_6 . Left: full spectrum. Right: comparison between different amounts of carboxylic acid equivalents inserted.

Stoichiometrically, 2 equivalents of propionic acid are required for total replacement of the hydrogen atoms per monomer of the polymer. As the maximum equivalents used for the modification has reached 1 equivalent, it was not enough to replace all the hydrogens, so there are both signals corresponding to $-\text{NH}$ not substituted (9.1 ppm) and $-\text{NH}$ substituted (8.7 ppm) in all samples of the modified polymers. As an example, Fig. 4.2 illustrates the region from 6.5 to 9.5 of the ^1H NMR spectrum obtained for PBI-BPA with 1 equivalent of BPA. It is possible to observe that the signal at 9.1 ppm integrates to 0.58 while the signal situated at 8.7 ppm, corresponding to the chemical modification, integrates to 0.42. Since these two signals belong to the unfolding of 1 proton of the molecule, the sum of the integration of both signals corresponds to that proton.

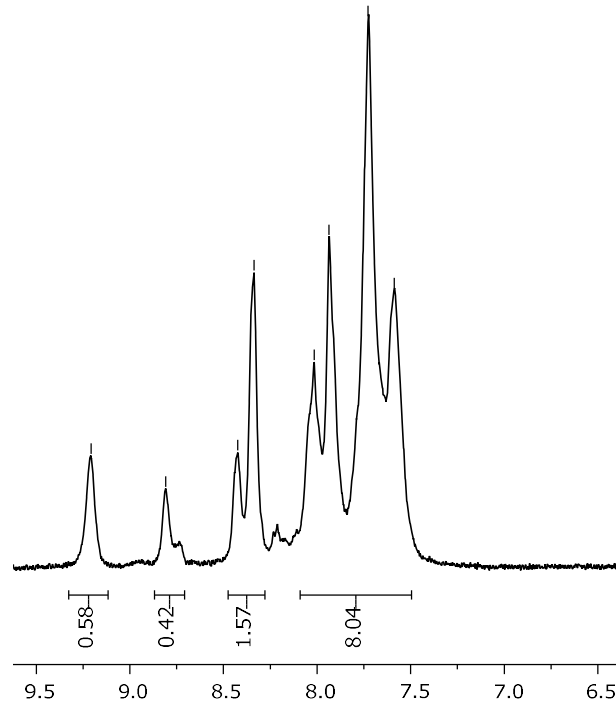


Figure 4.2. ^1H NMR of PBI-BPA, in DMSO-d_6 , from 6.5 to 9.5 ppm with signals integration

It is expected that a chemical reaction does not reach 100% yield, therefore, the real amount of inserted equivalent can be calculated by Eq. 4.7, in which the factor 2, relates to 2 equivalents of PBI, since the ratio between the areas include the entire monomer.

$$Eq_{real} = 2 \frac{A_{8,7 \text{ ppm}}}{A_{8,7 \text{ ppm}} + A_{9,1 \text{ ppm}}} \quad (4.7)$$

where, $A_{8,7 \text{ ppm}}$ is the area of the signal at 8,7 ppm and $A_{9,1 \text{ ppm}}$ is the area of the signal at 9,1 ppm.

By applying Eq.4.7, in the case presented in Fig. 4.2, the real equivalent of BPA is obtained (0.84), allowing to calculate the yield for this reaction of 84% by Eq. 4.8, the real equivalent and yield of all BPA synthesized are presented in Table 4.1.

$$\eta = \frac{\text{real equivalents}}{\text{theoretica equivalent}} \cdot 100\% \quad (4.8)$$

In the polymer obtained from the reaction between PBI and BPA the spacer chain between the polymer backbone and the terminal acid group has a length of only 2 carbon atoms. If we consider the interaction of this polymer with a bulkier amine this may pose some steric hindrance and impair the desired interaction. To overcome this aspect, PBI-COOH polymers with a longer spacer chain were also synthesized by the reaction of PBI with BVA and BUA, as previously described for BPA, originating polymers with spacer chains with 4 and 10 carbon atoms, respectively. Their characterization was performed as explained above by ¹H NMR (Table 4.1.).

Table 4.1. Real equivalents inserted and yields for PBI-BPA.

	Theoretical	Real	Yield (%)
BPA equivalents	0.25	0.24	96.00
	0.5	0.49	98.00
	0.75	0.65	86.67
	1	0.84	84.00

The values presented in table 4.1 show the effective insertion of carboxylic acid groups in PBI backbone with yields higher than 80% for all mol equivalents tested. The real molar equivalents give very important information about the polymer obtained. If the polymers synthesized with different molar equivalents have similar real equivalents, this indicates that we obtain a similar polymer, for example, if a polymer synthesized with 0.5 equivalents and another one with 1 equivalent present equivalents molars of 0.49 and 0.51, respectively, this result indicates that both are similar, and that in fact, there is no polymer synthesized with 1 equivalent, but two polymers with 0.5 equivalent.

None of the synthesized PBI-BPAs reached a real equivalent similar to any other, this fact indicates that each PBI-BPA obtained has different degrees of insertions and that the results presented for each molar equivalent in Section 4 of this chapter, do not represent a duplicate of another synthesized polymer.

4.4.2. Binding Studies: effect of molar reaction ratio of bromo alkyl carboxyl acid to PBI and size of alkyl spacer chain

Several polymers were obtained by changing the ratio of PBI to BPA. The ability of these polymers to remove DMAP from a DCM solution was assessed and the results were compared with the starting material (PBI). According to Figure 4.3, the polymer obtained in the presence of 1.00 eq of BPA showed the best removal (92%) of the aromatic amine from solutions with concentrations as high as 1,000 ppm. In these experiments, the PBI starting material revealed the lowest affinity for DMAP with binding values between 6% and 10%. Based on these results, the synthesis of the polymers with longer spacer chains was only attempted in the presence of 1.00 eq of the respective bromoalkyl carboxylic acid.

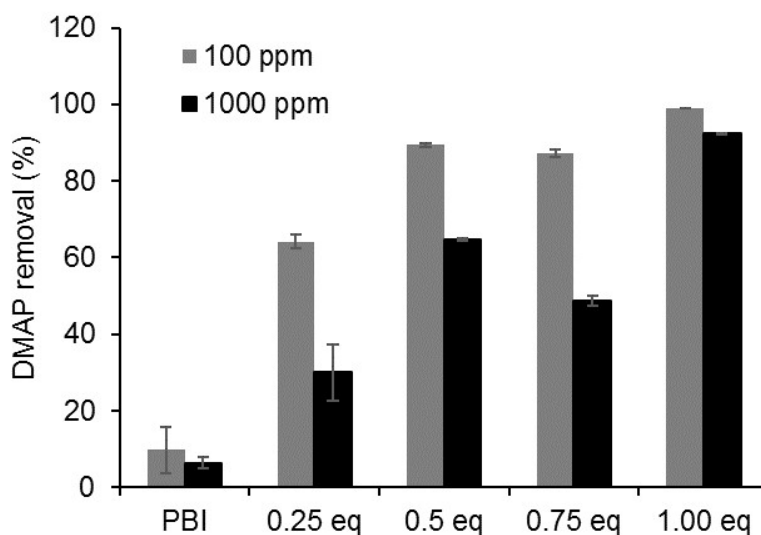


Figure 4.3. DMAP removal for the several polymers obtained with BPA. 1 mL of a 100 ppm or 1000 ppm solution of DMAP in DCM was loaded on 50 mg of raw and modified PBI polymers.

The binding performance for DMAP, for the polymers with different spacer chains, was also assessed in the presence of Meta in solution. From Table 4.2 it is possible to observe that all polymers present similar DMAP removals, showing that for the particular binding of DMAP it seems that a steric hindrance effect is not present, with all polymers reaching ratios of DMAP/Meta lower than 7.5 mg /g needed to respect the TTC value imposed, proving that these polymers are able to perform the purification of Meta, removing more than 95% of DMAP. However, the PBI-COOH polymer with the shortest spacer chain presented the lowest adsorption for the API (4.98%), making this the chosen polymer to be further characterized in the following studies.

Table 4.2. Binding of DMAP (1,000 ppm) and Meta (10,000 ppm) in DCM towards PBI-COOH polymers with different spacer chains and their respective ratio mg GTI/g API.

	Binding (%)		Ratio GTI/API
	DMAP	Meta	(mg GTI/g API)
PBI raw	2.88 ± 0.06	4.16 ± 0.37	101,34 ± 0,16
Spacer	BPA	95.14 ± 0.05	4.98 ± 2.65
	BVA	98.17 ± 0.19	7.63 ± 2.80
	BUA	96.70 ± 0.28	6.08 ± 0.66

4.4.3. Polymer characterization

The polymers obtained with BPA at different reaction molar ratios were characterized by the BET method and compared with the PBI starting material. The isotherms for both PBI and the polymer obtained in the presence of 0.25 eq of BPA revealed an irregular behaviour, with a low nitrogen adsorption and the different parameters could not be determined. For the remaining samples, the data in Table 4.3 showed that the polymer

obtained in the presence of 1.00 eq of BPA had the highest surface area which also corresponded to the best performing polymer for DMAP adsorption.

Table 4.3. Physical properties of PBI and PBI modified polymers with BPA, obtained by multipoint BET method.

	BET surface area ($\text{m}^2 \cdot \text{g}^{-1}$)	Pore volume ($\text{cm}^3 \cdot \text{g}^{-1}$)	Pore size (nm)
Raw PBI	n.d.	n.d.	n.d.
PBI-0.25 eq	n.d.	n.d.	n.d.
PBI-0.5 eq	12.79	0.11	41.0
PBI-0.75 eq	7.10	0.44	30.6
PBI-1.00 eq	60.06	0.22	20.9

n.d.=not determined

The remaining characterization was performed for the polymer that showed the highest removal of DMAP from solution. SEM pictures (Figure 4.4) showed that PBI has non-porous smooth surface particles contrasting with the modified polymer. The reaction conditions and the insertion of the new functionality in the PBI chains induce roughness in the particles surface.

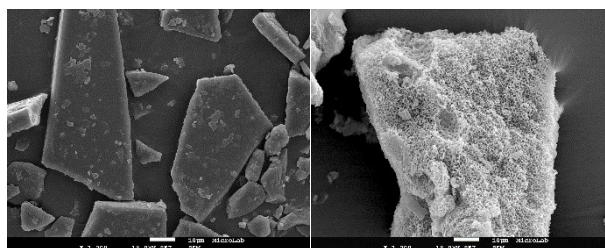


Figure 4.4. SEM pictures (magnification: 1000x) of PBI (left) and PBI obtained in the presence of 1.00 eq of BPA (right).

4.4.4. Kinetic and binding isotherm studies

The kinetic and binding isotherm profiles were assessed for PBI-COOH obtained in the presence of 1.00 eq. of BPA. From Figure 4.5 it is possible to observe that the adsorption process at 25°C is fast, reaching equilibrium after only 30 min with more than 95% binding of DMAP, following a second order kinetics and its adsorption behavior is best described by the Langmuir model with the formation of a monolayer with maximum adsorption of 13 mg of DMAP per gram of polymer. Physical parameters determined for isotherm and kinetics are presented in Tables 4.3 and 4.4.

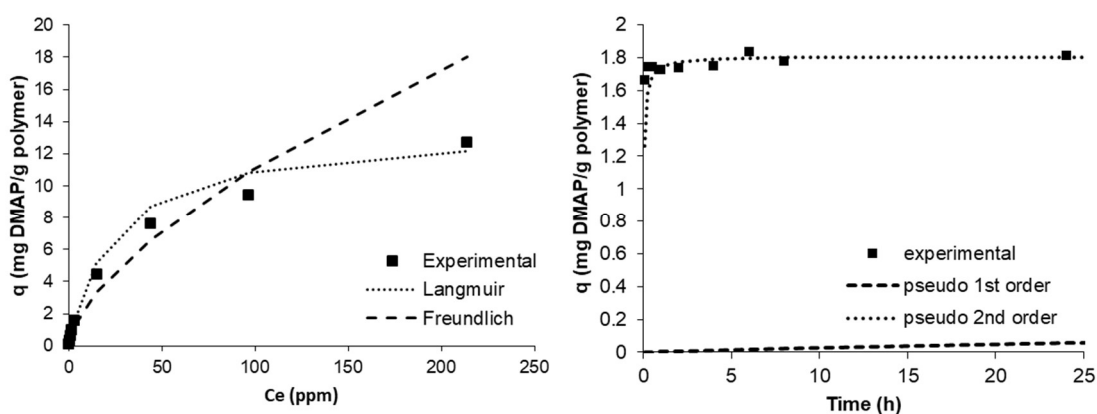


Figure 4.5. Adsorption isotherm models (left) and kinetic models (right) for PBI modified by addition of 1.00 eq of BPA.

Table 4.4. Binding isotherm physical parameters obtained for DMAP, for PBI-PBA at room temperature.

		PBI-BPA	
		DMAP	
Langmuir	$K_L \times 10^{-3}$ (L/mg)	0.04 ± 0.01	
	q_m (mg/g)	13.59 ± 0.01	
	R^2	0.9844	
	χ^2	0.5476	
Freundlich	K_F (L/mg)	0.59 ± 0.08	
	1/n	0.64 ± 0.04	
	R^2	0.9667	
	χ^2	3.6535	

Table 4.5. Kinetic physical parameters obtained for DMAP and **PBI-BPA** at room temperature.

		1st order	2nd order
DMAP	k_1 (h^{-1})	0.05 ± 0.03	-
	k_2 ($g \cdot mg^{-1} \cdot h^{-1}$)	-	15.31 ± 0.02
	q_e ($mg \cdot g^{-1}$)	0.08 ± 0.03	1.81 ± 0.01
	R^2	0.1990	0.9999
	χ^2	30967.92	0.4408

4.4.5. Binding towards several impurities

The potential use of the PBI-BPA scavenger was assessed for a wide range of aromatic amines, represented in Figure 4.6.

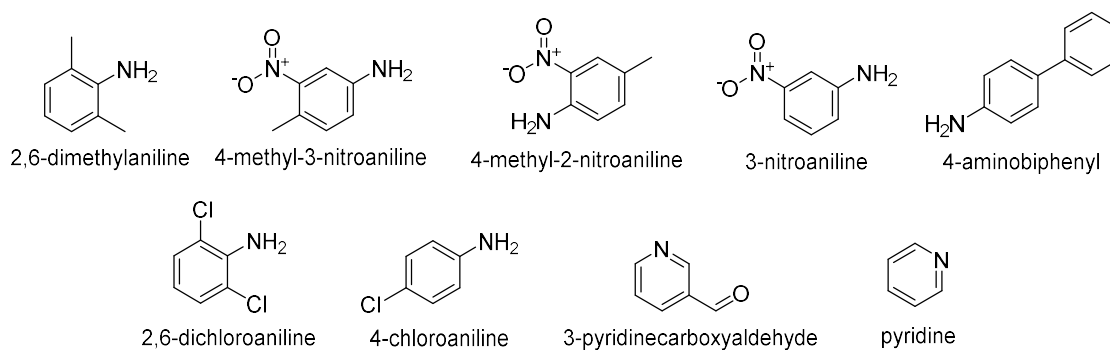


Figure 4.6. Structure of several aromatic amines assessed.

From the results presented in Table 4.6, it is possible to observe that there is no binding for the chloroanilines and 2,6-dimethylaniline. The remaining compounds showed bindings much lower (8.13% – 24.36%) than the obtained for DMAP (92%). After the synthesis the polymer presents a pH of about 2.10, which is inferior to the pKa of the several amines assessed, which means that these compounds will probably be in their protonated form. At this pH, the polymer will also probably be protonated and therefore the interaction between the adsorber and these compounds is not favoured. In order to assess this assumption, we evaluated the binding of PBI-BPA towards lupanine, an alkaloid with a pKa of 9.1 [14]. For this compound the binding, was higher (49.21%) than the obtained for the remaining compounds, reinforcing this hypothesis.

Table 4.6. Binding values for 1,000 ppm solutions in DCM for several aromatic amines towards PBI-BPA, PBI-BVA and PBI-BUA.

	Binding (%)			pka
	BPA	BVA	BUA	
2,6-dimethylaniline	0	0	0	3.98 ¹⁵
4-methyl-3-nitroaniline	8.13 ± 1.21	3.86 ± 0.11	5.14 ± 0.16	2.90 ¹⁶
4-methyl-2-nitroaniline	15.76 ± 2.02	11.04 ± 0.06	2.84 ± 0.80	0.45 ¹⁶
3-nitroaniline	20.60 ± 0.15	22.99 ± 3.10	17.72 ± 0.32	2.50 ¹⁶
2,6-dichloroaniline	0	0	0	0.42 ¹⁷
4-chloroaniline	0	0	0	4.0 ¹⁸
3-pyridinecarboxaldehyde	17.23 ± 3.28	24.35 ± 2.02	15.82 ± 2.15	3.8 ¹⁹
pyridine	24.36 ± 0.49	23.95 ± 1.82	21.12 ± 2.84	5.23 ¹⁷
4-aminobiphenyl	14.29 ± 3.64	10.39 ± 0.89	5.98 ± 0.40	4.35 ²⁰

4.5. Conclusions

The development of new PBI adsorbers containing carboxylic groups, with spacer chains of different length (2, 4 or 10 C atoms), was successfully obtained. In all cases, DMAP removal from solution was achieved originating final API solutions with DMAP contamination under the TTC established for Meta.

The ability to scavenge a broad range of aromatic amines from organic solvent based solutions was investigated, but an efficient removal was only observed for DMAP among the several compounds assessed.

The potential of removal may be limited to the pKa of the adsorbate, maybe due to the electrostatic repulsion of both protonated species in solution. Further studies are needed to assess aromatic amines with high pKa values, probably exploring different solvents and different protonation states of the polymer and the solutes.

4.6. References

- 1 – Xu, S.; et al, The DMAP-catalyzed acetylation of alcohols-A mechanistic study (DMAP=4-(dimethylamino)pyridine), *Chem. Eur. J.*, 11, 2005, 4751-4757.
- 2 – Sakakura A. et al, Widely Useful DMAP-Catalyzed Esterification under Auxiliary Base- and Solvent-Free Conditions, *J. Am. Chem. Soc.*, 129, 2007, 14775-14779.
- 3 – Draper, W. R. et al, Unusual hydroxy- γ -sultone byproducts on steroid 21-methanesulfonylation. An efficient synthesis of mometasone 17-furoate (Sch32088), *Tetrahedron*, 55, 1999, 3355-3364.
- 4 – Benigni, R. et al, Quantitative Structure-Activity relationship of mutagenic and carcinogenic aromatic amines, *Chem. Rev.*, 100, 10, 2000, 3697–3714.
- 5 – Aßmann N., et al, Genotoxic activity of important nitrobenzenes and nitroanilines in the Ames test and their structure-activity relationship, *Mutation Research*, 395, 1997, 139–144.
- 6 – Sawatari, K., et al, Relationships between chemical structures and mutagenicity: a preliminary survey for a database of mutagenicity test results of new work place chemicals. *Ind Health*, 39, 4, 2001, 341-345.
- 7 – Teasdale A.; Elder D.; Chang S. J.; Wang S.; Thompson R.; Benz N.; Flores I. H. S., *Org. Process Res. Dev.* 17, 2013, 221-230.
- 8 – EMEA Guidelines on the “Limits on Genotoxic Impurities”, EMEA/CHMP/QWP/251344/2006, 2006.
- 9 – Esteves, T. et al, Molecularly imprinted polymer strategies for removal of a genotoxic impurity, 4-dimethylaminopyridine, from an active pharmaceutical ingredient post-reaction stream, *Sep. Purif. Technol.*, 163, 2016, 206-214.

- 10 – Székely, G. et al, Design, Preparation and Characterization of Novel Molecularly Imprinted Polymers for Removal of Potentially Genotoxic 1,3-diisopropylurea from API Solutions, *Sep. Purif. Technol*, 86, 2012, 190-198.
- 11 – Rahimi, M.; Vadi, M.; Langmuir, Freundlich and Temkin Adsorption Isotherms of Propranolol on Multi-Wall Carbon Nanotube. *J. Modern Drug Discovery and Drug Delivery Res.* 2014, DOI: 10.5281/zenodo.893491.
- 12 – Qiu, H., et al, Q. Critical Review in Adsorption Kinetic Models. *J. Zhejiang Univ. Sci. A*, 10, 2009, 716-724.
- 13 – Vicente I. A. et al., Solvent compatible polymer functionalization with adenine, a DNA base, for API degenotoxification: Preparation and characterization, *Sep. Purif. Technol*, 179, 2017, 438-448.
- 14 – Mende P. et al., Uptake of the quinolizidine alkaloid lupanine by protoplasts and isolated vacuoles of suspension-cultured *Lupinus polyphyllus* cells, Diffusion or carrier-mediated Transport?, *J. Plant Physiol.*, 129, 1987, 229–242.
- 15 – Clark J. et al., Prediction of the strengths of organic bases, *Q. Rev. Chem. Soc.*, 18, 1964, 295-320.
- 16 – Mohammad A. et al., Quantitative aspects of Lewis acidity. Part VII. Equilibria between gallium trihalides and aniline bases in ether solution, *J. Chem. Soc. (B)*, 1967, 403-406.
- 17 – Tehan B. G. et al., Estimation of pKa Using semiempirical molecular orbital methods. Part 2: Application to amines, anilines and various nitrogen containing heterocyclic compounds, *Quant. Struct.-Act. Relat.*, 21, 2002, 473-485.
- 18 – Brillas E. et al., Electrochemical destruction of aniline and 4-chloroaniline for wastewater treatment using carbon-PTFE O₂-Fed cathode, *J. Electrochem. Soc.*, 142, 1995, 1733-1741.

19 – Naik D. B. et al., Pulse radiolysis of 3-pyridine methanol and 3-pyridine carboxaldehyde in aqueous solution, *Res. Chem. Intermed.*, 30, 2004, 287-297.

20 – Perrin D. D., *Dissociation constants of organic basis in aqueous solution*, IUPAC Publications, Butterworth & Co Publishers Ltd, 1965, ISBN-13: 978-0408891714.

Chapter V

Mimicking DNA alkylation: Removing genotoxin impurities from API streams with a solvent stable polybenzimidazole-adenine polymer

Article *in* Reactive and Functional Polymers, 131, (2018), 258-265 by Teresa Esteves, Ana I. Vicente, Flávio A. Ferreira, Carlos A.M. Afonso, Frederico Castelo Ferreira, with the title “Mimicking DNA alkylation: Removing genotoxin impurities from API streams with a solvent stable polybenzimidazole-adenine polymer”

5.1. Outline

This study reports the application of a novel polybenzimidazole (PBI) polymer modified with an alkylated DNA base - adenine - as an effective scavenger for several families of DNA alkylating agents. This new material addresses an important issue in active pharmaceutical ingredients (APIs) manufacture, the removal of genotoxic impurities (GTIs) to strictly low regulated limits. Instead of targeting individual GTIs removal, **PBI-adenine** scavenger mimics the concept of DNA-GTI adduct formation that takes place *in vivo*, but in this case, in an organic solvent matrix where APIs are chemically synthesized. The result section (section 5.1.1) presents a study in which the removal of eleven GTIs from five different chemical families is assessed with more than 80 % removal. Slow binding kinetics for some GTIs at room temperature was identified as one of the limitations of the **PBI-adenine** polymer. Then, in section 5.4.2 is presented a study in which API purification is addressed and an efficient process is presented for two APIs studied, mometasone furoate and betamethasone acetate, using MPTS as a model GTI, affording high impurity removals (more than 96%) and high API recovery with low API loss (3.5 %) for these case studies. Finally, in section 5.4.2 it is explored the possible application of this straightforward strategy in API post-reaction stream purification. In this study is shown that it is possible to attain GTI imposed limits as low as 0.6 mg GTI/g API respecting the Threshold of Toxicological Concern (TTC) value.

Keywords: Polybenzimidazole-adenine; Genotoxic impurity; DNA alkylating agent; Active pharmaceutical ingredient purification.

5.2. Introduction

Pharmaceutical regulatory authorities have shown increased concern about impurities - especially genotoxic impurities (GTIs) – in active pharmaceutical ingredients (APIs) due to their adverse effects on human health [1,2]. Sources for organic impurities in APIs include unreacted starting materials and reagents, intermediary products, catalysts, by-products formed, and degradation and storage products [3,4]. The best route to prevent GTI presence in the final formulations is their elimination from synthetic pathways. However, when the formation of GTIs in APIs production cannot be prevented, purification of the API must be performed until the GTI is removed to satisfying levels: a Threshold of Toxicological Concern (TTC) value of 1.5 $\mu\text{g}/\text{day}$ imposed by strict regulatory guidelines [1,2].

Conventional separation techniques used in API purification include crystallization, filtration, distillation, the use of adsorbents, resins and column chromatography [4-6]. However, since these operation units are not dedicated to GTI removal, to achieve the required low GTI concentration, significant amounts of API can be lost with great economic impact for pharmaceutical companies [5]. More recently, the use of organic solvent nanofiltration (OSN) [5-9], molecular imprinting techniques [10-12] and combinations thereof [13-15] have been suggested to address this challenge, based on size discrimination and specific interactions to target molecules.

Reactive resins as adsorbents, bearing specific functional groups, are versatile and robust materials with vast application in aqueous systems [16-21]. Those will be also explored on Chapter VI, for methanolic solvent matrices, as swelling data of many polymers by alcohols is limited in the literature. Nevertheless, API manufacturing synthetic processes often take place in organic solvent media, rendering their application

challenging. For this reason, the development of a versatile organic solvent compatible material, for DNA alkylating agents scavenging, is a huge achievement with promising successful applications in pharmaceutical industry, ultimately contributing for API patients' wellbeing.

Several authors have been pursuing the aim of finding good performing organic solvent compatible adsorbers useful in the context of API purification [10-13,22,23]. For sulfonate GTIs, scavenging nucleophilic resins [22-23] or molecular imprinted polymers (MIPs) [10] have been explored, taking advantage of specific interactions established between the polymers functional groups and the target sulfonate molecules. The amount of adsorber varies between 50 – 200 mg per 1 mL of solution to be treated [10,22,23] and generally, when GTI removal is around 100 % there is still a considerable API loss in some cases [23]. Therefore, the challenge remains to find a platform suitable to perform in organic solvents, able to remove the highest amount of GTI with the lowest API loss possible.

GTIs cover a wide range of compounds from different chemical families including electrophilic reagents such as sulfonates, alkyl halides or epoxides, which are genotoxins that act as DNA alkylating agents. These species alkylate DNA through a nucleophilic attack by the nitrogen or oxygen of the pyrimidine and purine bases present in DNA to the electrophilic carbon of the GTIs [4,24-27]. In order to mimic the process that takes place *in vivo*, herein we explore the potential of a recent material developed within our group, based on polybenzimidazole (PBI) polymer with an appending adenine moiety (**PBI-adenine**, Fig. 5.1) for API purification [28]. PBI is a versatile organic solvent compatible polymer that contains heterocyclic amine groups that can be modified with adequate chemical functionalities. In this case, PBI was modified to present as side group a DNA base, namely adenine, originating a new powder porous material suitable to

interact with a wide range of DNA alkylating agents. The modification of PBI with adenine had been attempted in order to mimic what happens in biologic systems, where alkylating GTIs interact with DNA originating DNA-GTI adducts [24], as exemplified in Figure 5.1.

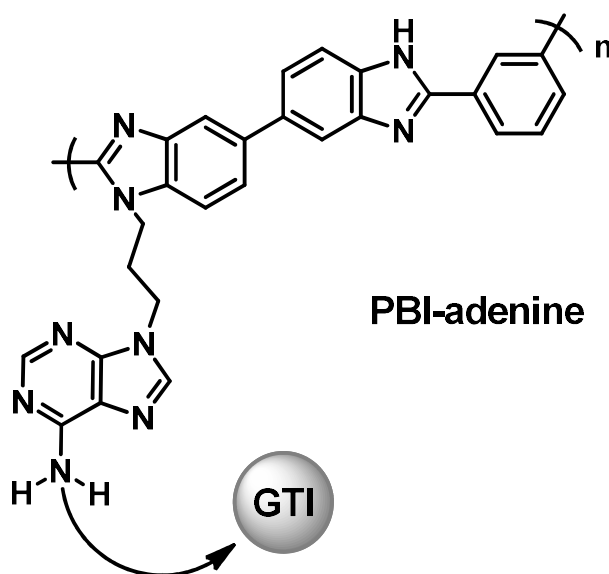


Figure 5.1. Example of **PBI-adenine**-GTI adduct formation.

The synthesis of modified polymer (**PBI-adenine**) is presented elsewhere [28] and the current study is focused on exploring the capability of this innovative material to remove a broad range of DNA alkylating agents from API organic solvent solutions, identify limitations for the use of **PBI-adenine** for API degenotoxification and, to define strategies and operation conditions at which **PBI-adenine** can successfully remove GTIs down to TTC values, with minimal API losses.

5.3. Experimental

5.3.1. Materials

All chemicals were of reagent grade or higher and used as received. Methyl *p*-toluenesulfonate (MPTS), methyl methanesulfonate (MMS), ethyl methanesulfonate (EtMS), 1,3-dibromopropane (DBP), dimethyl sulfate (DMS) and dodecane (DDC) were purchased from Acros (Belgium). Ethyl *p*-toluenesulfonate (EPTS), 1,4-dibromobutane (DBB) and epichlorohydrin (EPI) were purchased from Alfa Aesar (United Kingdom). Butyl *p*-toluenesulfonate (BPTS) was purchased from TCI (Japan). 1,2-Dibromoethane (DBE) and glycidol (GCD) were purchased from Aldrich (USA). Mometasone furoate (Meta) and betamethasone acetate (Beta) were kindly provided by Hovione PharmaScience Ltd (Portugal). Dichloromethane (DCM) and acetonitrile (MeCN) HPLC grade solvents were purchased from Fisher Chemicals (USA). Formic acid (FA) was purchased from Panreac (Spain). The synthesis and full characterization of **PBI-adenine** was performed previously [28].

5.3.2. Apparatus and analysis

The experiments at 55 °C were controlled in an incubation chamber from J. P. Selecta (Spain). HPLC measurements for MPTS, EPTS, BPTS, Meta and Beta were performed on a Merck Hitachi pump coupled to a L-2400 tunable UV detector using an analytic Macherey-Nagel C18 reversed-phase column Nucleosil 100-10, 250 x 4.6 mm with 10 µL injection volume and eluents, A: aqueous 0.1 % FA solution, B: MeCN 0.1 % FA solution. For MPTS, EPTS and BPTS a flow rate of 2 mL·min⁻¹ and UV detection

at 230 nm was used with the following methods: MPTS: 12 min, 70 % A, $t_R = 7.80$ min; EPTS: 10 min, 60 % A, $t_R = 5.38$ min; BPTS: 6 min, 40 % A, $t_R = 3.12$ min. For Meta and Beta a flow rate of $1 \text{ mL} \cdot \text{min}^{-1}$ and UV detection at 280 nm was used; method: 0-3 min, (60-20) % A; 3-4 min, 20 % A; 4-8 min, (20-60) % A; 8-15 min 60 % A, t_R (Meta) = 7.25 min, t_R (Beta) = 6.12 min. GC measurements for MMS, EtMS, DBE, DBP, DBB, GCD, EPI and DMS were performed on a GC-2010 Plus by Shimadzu (Japan) equipped with a TRB-5 column ($30.0 \text{ m} \times 0.25 \text{ mm}$, $0.12 \text{ } \mu\text{m}$ film thickness) from Teknokroma (Spain) using an injection volume of $1.0 \text{ } \mu\text{L}$, a 1:2 split ratio and DDC as internal standard. Ultra-high purity helium was used as carrier gas and column flow was kept constant throughout the runs at $1 \text{ mL} \cdot \text{min}^{-1}$. Both injector and detector were set at $250 \text{ }^\circ\text{C}$. MMS: oven at $50 \text{ }^\circ\text{C}$ for 9 min, ramp $30 \text{ }^\circ\text{C}/\text{min}$ to $120 \text{ }^\circ\text{C}$, 4 min at $120 \text{ }^\circ\text{C}$ and ramp $25 \text{ }^\circ\text{C}/\text{min}$ to $180 \text{ }^\circ\text{C}$, t_R (MMS) = 6.62 min, t_R (DDC) = 15.53 min. EtMS: oven at $60 \text{ }^\circ\text{C}$ for 9 min, ramp $25 \text{ }^\circ\text{C}/\text{min}$ to $120 \text{ }^\circ\text{C}$, 4 min at $120 \text{ }^\circ\text{C}$ and ramp $25 \text{ }^\circ\text{C}/\text{min}$ to $150 \text{ }^\circ\text{C}$, t_R (EtMS) = 7.47 min, t_R (DDC) = 15.75 min. DBE: oven at $40 \text{ }^\circ\text{C}$ for 8 min, ramp $40 \text{ }^\circ\text{C}/\text{min}$ to $120 \text{ }^\circ\text{C}$, 4 min at $120 \text{ }^\circ\text{C}$ and ramp $30 \text{ }^\circ\text{C}/\text{min}$ to $150 \text{ }^\circ\text{C}$, t_R (DBE) = 6.04 min, t_R (DDC) = 14.63 min. DBP: oven at $60 \text{ }^\circ\text{C}$ for 9 min, ramp $30 \text{ }^\circ\text{C}/\text{min}$ to $120 \text{ }^\circ\text{C}$, 4 min at $120 \text{ }^\circ\text{C}$ and ramp $30 \text{ }^\circ\text{C}/\text{min}$ to $150 \text{ }^\circ\text{C}$, t_R (DBP) = 7.77 min, t_R (DDC) = 14.75 min. DBB: oven at $80 \text{ }^\circ\text{C}$ for 9 min, ramp $40 \text{ }^\circ\text{C}/\text{min}$ to $120 \text{ }^\circ\text{C}$, 4 min at $120 \text{ }^\circ\text{C}$ and ramp $30 \text{ }^\circ\text{C}/\text{min}$ to $150 \text{ }^\circ\text{C}$, t_R (DBB) = 8.58 min, t_R (DDC) = 12.30 min. GCD and EPI: oven at $40 \text{ }^\circ\text{C}$ for 5 min, ramp $50 \text{ }^\circ\text{C}/\text{min}$ to $120 \text{ }^\circ\text{C}$, 2 min at $120 \text{ }^\circ\text{C}$, ramp $30 \text{ }^\circ\text{C}/\text{min}$ to $180 \text{ }^\circ\text{C}$, and $180 \text{ }^\circ\text{C}$ for 2 min, t_R (GCD) = 4.00 min, t_R (EPI) = 3.89 min, t_R (DDC) = 10.69 min. DMS: oven at $40 \text{ }^\circ\text{C}$ for 9 min, ramp $40 \text{ }^\circ\text{C}/\text{min}$ to $120 \text{ }^\circ\text{C}$, 4 min at $120 \text{ }^\circ\text{C}$ and ramp $30 \text{ }^\circ\text{C}/\text{min}$ to $180 \text{ }^\circ\text{C}$, t_R (DMS) = 9.03 min, t_R (DDC) = 15.61 min.

5.3.3. Binding experiments

For each GTI, 50 mg of polymer (**PBI-adenine**) were placed in 2 mL round bottom tubes and 1 mL of a 100 ppm solution of GTI, prepared in DCM, was added. The suspension mixtures were magnetically stirred at 200 rpm for 24 hours or 2 weeks at room temperature. After this time the suspensions were centrifuged at 13,000 rpm for 20 min and the supernatants were filtered and analysed by HPLC or GC. All experiments were carried out in duplicate. The percentage of GTI bound to the polymer was calculated from equation (5.1) where C_0 (mg/L) is the initial GTI concentration and C_f (mg/L) is the final GTI concentration in solution.

$$\% = \frac{[C_0 - C_f]}{C_0} \times 100 \quad (5.1)$$

The amount of GTI bound to the polymer was calculated from equation (5.2) where q (mg/g) is the amount of GTI bound to the polymer, C_0 (mg/L) is the initial GTI concentration, C_f (mg/L) is the final GTI concentration in solution, V (L) is the volume of solution used and M (g) is the polymer mass.

$$q = \frac{V \times [C_0 - C_f]}{M} \quad (5.2)$$

For experiments at 55 °C, the suspension mixtures were stirred at 200 rpm for 2-8 hours at 55 °C in glass test tubes with screw caps. Afterwards, the suspensions were centrifuged and processed as described above. These experiments were carried out in duplicate. The percentage of GTI bound to the polymer was calculated from equation (5.1).

The binding experiments performed for the APIs and GTI/API mixtures followed the procedures described above at room temperature for 24 hours and at 55 °C for 2-8 hours. In these experiments, the GTIs were present at a concentration of 100 ppm and the APIs were present at a concentration of 10 g/L. The percentage of API bound to the polymer was calculated from equation (1) where, in this case, C_0 (g/L) is the initial API concentration and C_f (g/L) is the final API concentration in solution. All experiments were carried out in duplicate and compared to blank samples.

5.3.4. API recovery experiments

1 mL of DCM was added to 50 mg of polymer used in API batch binding experiments. The suspension mixtures were stirred at 200 rpm for 24 hours at room temperature. After this time, the suspensions were centrifuged and the supernatants were filtered and analysed by HPLC for API quantification. All experiments were carried out in duplicate.

5.3.5. Kinetic studies

Several solutions were prepared with 50 mg of polymer and 1 mL of a 100 ppm solution of MPTS or MMS prepared in DCM. The suspension mixtures were stirred at 200 rpm at room temperature or 55 °C. At certain time intervals of 5, 15 and 30 minutes and 1, 2, 4, 6, 8, 24 and 27 hours, the suspensions were centrifuged and the supernatants were filtered and analysed by HPLC or GC. All experiments were carried out in duplicate. The percentage and amount of GTI bound to the polymer was calculated from equations (5.1) and (5.2). Experimental data were fitted to pseudo-first and pseudo-second order kinetic models [29] according to equations (5.3) and (5.4) respectively, where q_f and q_t

(mg/g) are the adsorption capacities at the final and time t (min) respectively, and k_1 (min^{-1}) and k_2 ($\text{g}/(\text{mg} \cdot \text{min})$) are the pseudo- first and second order rate constants for the models.

$$\ln(q_f - q_t) = \ln(q_f) - k_1 \cdot t \quad (5.3)$$

$$\frac{t}{q_t} = \frac{1}{k_2 \cdot q_f^2} + \frac{t}{q_f} \quad (5.4)$$

5.3.6. Adsorption isotherm studies

For adsorption isotherm experiments, 1 mL of MPTS or MMS solutions prepared in DCM, with different initial concentrations (5 – 1,000 ppm), were added to 50 mg of **PBI-adenine**. The mixtures were stirred at 200 rpm for 24 hours at room temperature, or for 3 - 8 hours at 55 °C. After that, the suspensions were centrifuged and the supernatants were filtered and analysed by HPLC or GC. All experiments were carried out in duplicate. The percentage and amount of GTI bound to the polymer was calculated from equations (5.1) and (5.2). Experimental data were fitted to the Langmuir and Freundlich isotherm models [30] according to equations (5.5) and (5.6) respectively, where q_m (mg/g) is the maximum amount of GTI bound to the polymer in a monolayer for the Langmuir model, whereas K_L and K_F are equilibrium constants (L/mg) for the Langmuir and Freundlich models, respectively, and are related with the energy taken for adsorption, n is a parameter related with the surface layer heterogeneity.

$$\frac{q_f}{q_m} = \frac{K_L C_f}{1 + K_L C_f} \quad (5.5)$$

$$q_f = K_F C_f^{\frac{1}{n}} \quad (5.6)$$

5.4. Results and Discussion

5.4.1. GTI binding experiments

The first objective of this study was to develop a versatile material, compatible with organic solvents, able to scavenge a broad range of DNA alkylating molecules presenting different chemical functionalities. In order to assess the versatility of **PBI-adenine** polymer, batch binding experiments in dichloromethane (DCM) were performed for several GTIs belonging to the following different five chemical families: (i) alkyl tosylates (MPTS, EPTS, BPTS); (ii) alkyl mesylates (MMS, EtMS), (iii) di-halo alkanes (DBE, DBP, DBB), (iv) epoxides (GCD, EPI), and (v) dimethyl sulfate (DMS). For all GTIs assessed in this report, the expected alkylation interactions with the scavenger are represented in Table 5.1. After alkylation, is expected that ionic interaction may also occur, as well as some pi-pi interaction between the aromatic heterocycle and the tosyl group. In case of the other tested genotoxic impurities the molecule is covalently bonded to the adenine.

For all cases, we obtained a GTI removal higher than 80 % for the same initial concentration of 100 ppm, at room temperature (Fig. 5.2). For performance comparison, in blank experiments, performed with, PBI raw polymer we obtained GTI removals lower than 40%, under the same operation conditions. These results show the efficiency obtained after chemical modification of PBI with adenine side chains that should derive mainly from nucleophilic substitution by adenine unit on the electrophilic carbon present in the tested genotoxic impurities (Table 5.1). DCM was selected as solvent for the different experiments as it is a solvent with high solvability properties and low boiling point. Therefore, in spite of the environmental issues raised, it is still a solvent broadly used in synthesis in the pharmaceutical industry, allowing reagents ready dissolution,

product isolation and low energy intensive solvent recycling. Specifically, for the synthesis of steroids, the model APIs selected for this study, DCM is typically used as solvent on the final synthetic reaction steps.

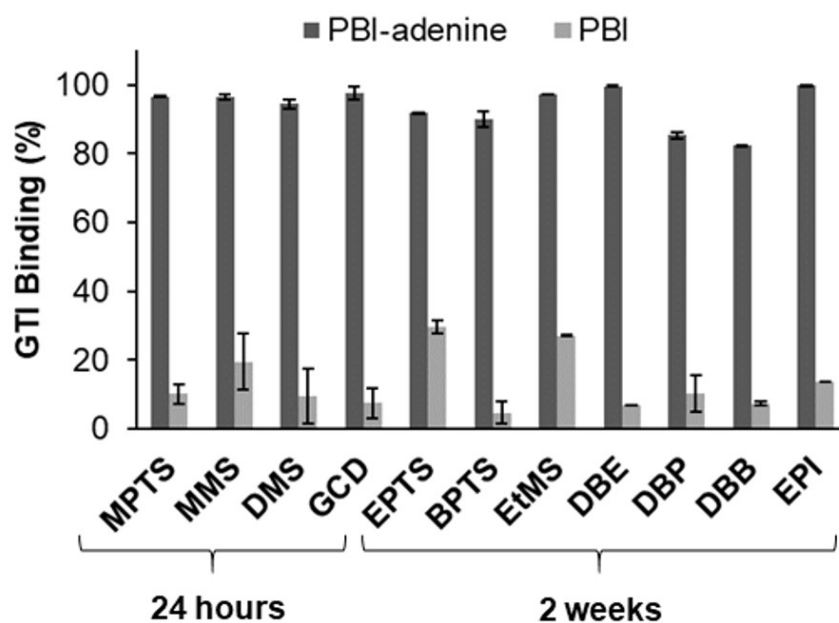
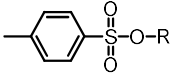
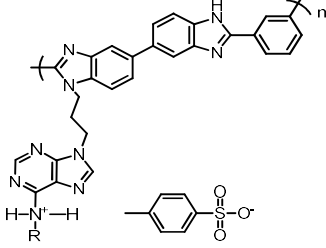
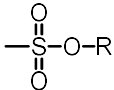
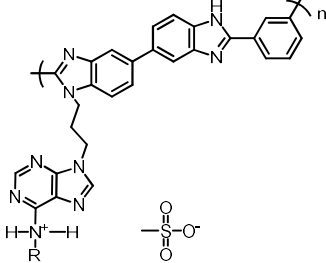
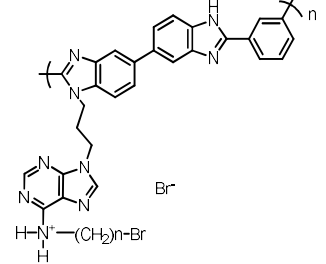
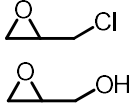
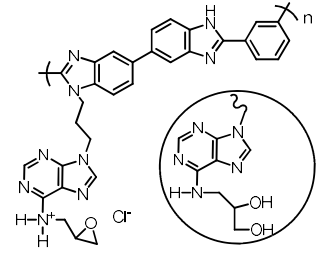
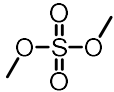
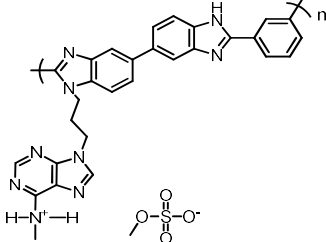


Figure 5.2. GTI binding to PBI and **PBI-adenine** scavengers, for 50 mg of polymer in 1 mL of a 100 ppm solution in DCM of each GTI after 24 hours or 2 weeks at room temperature.

Table 5.1. Proposed **PBI-adenine** polymer adduct formation with several DNA alkylating agents. The interaction between **PBI-adenine** polymer and MPTS was studied in detail using ^1H NMR in a previous study. [28]

GTI family	Polymer-GTI adduct
Alkyl tosylate (MPTS, EPTS, BPTS) 	
Alkyl mesylate (MMS, EtMS) 	
Dihalo alkane (DBE, DBP, DBB) $\text{Br}-(\text{CH}_2)_n-\text{Br}$	
Epoxide (GCD, EPI) 	
Dimethyl sulfate (DMS) 	

However, MPTS, MMS, DMS and GCD needed 24 hours to achieve removals higher than 94 %, while the remaining GTIs required an extended period of about 2 weeks to reach higher removals. The slower kinetics observed at room temperature represent the first identified limitation for the novel **PBI-adenine** polymer and can probably be attributed to structural constraints presented by the GTIs. For example, the alkyl side chains present in the structures of EPTS, BPTS and EtMS, may cause some steric hindrance, not allowing a good proximity or interaction between adenine side chains of the polymer and GTI molecules.

A similar observation was reported by Lee et al. [23] in which several nucleophilic resins were screened for sulfonate esters removal from solutions prepared in methanol (MeOH). The authors assigned this behaviour to the increased steric bulkiness of EPTS and EtMS, for example, compared to MPTS or MMS. This tendency can be easily observed in Figure 5.3 where, within the same GTI family, the binding percentage is represented as function of increasing molecular weight of GTIs. On the other hand, the presence of electron withdrawing elements such as -Cl or -Br in EPI, DBE, DBP and DBB, seems to also have some negative influence in the interaction between these GTIs and the polymer, leading to an extended incubation time to achieve GTI removals comparable to GCD, for example.

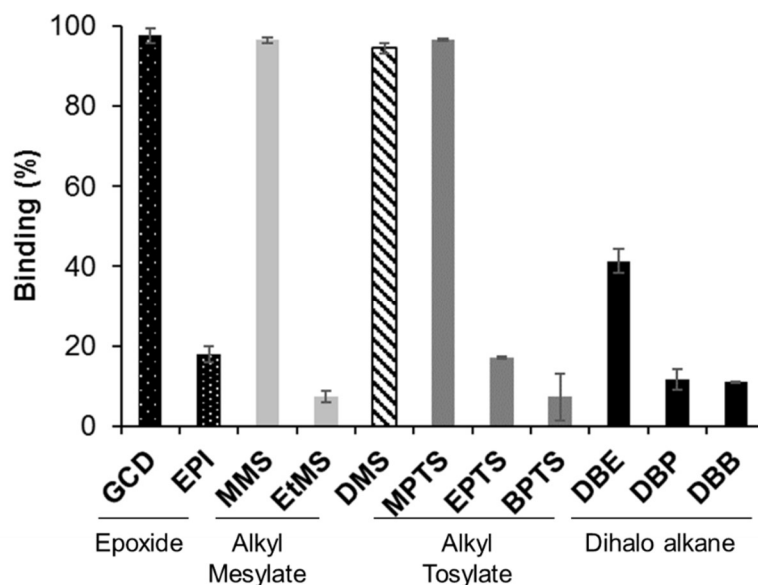


Figure 5.3. GTI binding to **PBI-adenine** scavenger, for 50 mg of polymer in 1 mL of a 100 ppm solution in DCM of each GTI after 24 hours at room temperature. GTIs within the same family are ordered by increasing molecular weight from left to right.

We also assessed solvent compatibility of **PBI-adenine** polymer in MeOH and performed binding studies in this solvent. We observed a good solvent resistance of the material but the results in Figure 5.4 show that in MeOH, the binding is less favoured than in DCM. This may be explained by a possible competition between the solvent and GTIs towards recognition sites, since -OH groups of MeOH may interact with adenine -NH₂ groups by hydrogen bonding. Additionally, the different swelling of the polymer in these solvents can also have different impacts on GTI binding (see Appendix A)

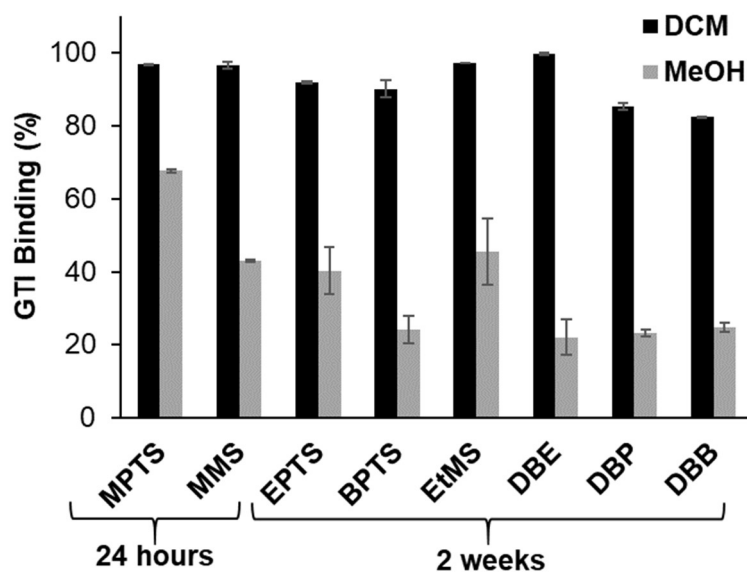


Figure 5.4. GTI binding to **PBI-adenine** scavenger, for 50 mg of polymer in 1 mL of a 100 ppm solution in DCM or MeOH of each GTI after 24 hours or 2 weeks at room temperature.

5.4.1.1. Temperature effect on GTI binding

Decreasing operation times is crucial to make the use of **PBI-adenine** a viable alternative for removal of GTIs. Therefore, we explored the influence of temperature in GTI binding in order to increase kinetics and improve GTI removal by assessing binding experiments performed at 55 °C. For these experiments, the same temperature and contact time with the polymer were used to assess the binding of two GTIs with low binding rate, EPTS and EtMS, and compared against two other GTIs with faster binding rates, MPTS and MMS (which reached more than 95 % GTI removal at room temperature within 24 hours).

From Figure 5.5 we observe a positive effect of temperature in MPTS, MMS and EtMS binding. However, EPTS gain in binding from 17 % at 25 °C to 25 % at 55 °C is not statistically significant (p value > 0.05) and the EtMS nine-fold increase improvement

in binding from 7% at 25 °C to 67 % at 55 °C does not reach the high desirable binding values superior to 95 % obtained for MPTS or MMS at the GTI/scavenger ratios used and in a single binding step. For PBI raw polymer, we did not observe a positive effect in binding with temperature, indicating that the PBI itself is not contributing to binding to the GTIs and the adenine functionalization is promoting the interaction with the solutes.

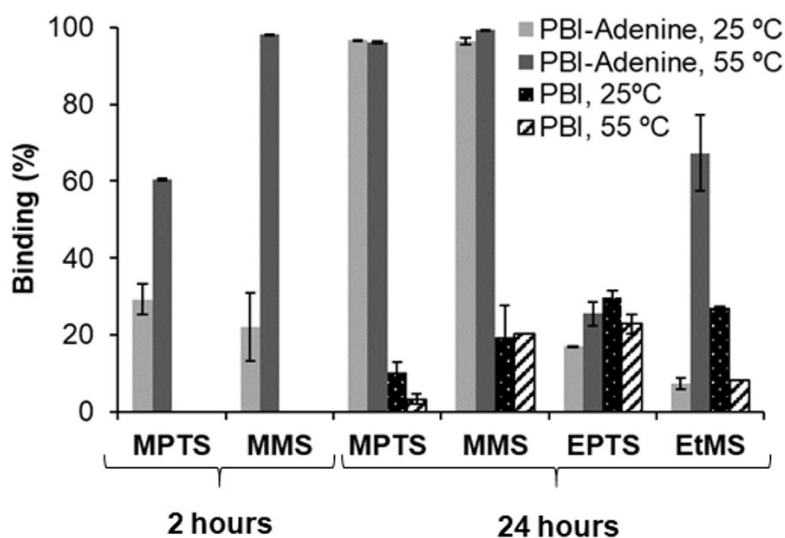


Figure 5.5. MPTS, MMS, EPTS and EtMS binding to PBI and **PBI-adenine** at 25 °C and 55 °C in DCM, for 50 mg of polymer in 1 mL of a 100 ppm solution of each GTI for 2 hours or 24 hours in contact with the polymer.

In the case of MPTS and MMS at 55 °C, after only 2 hours, MPTS registered a two-fold increase in binding to the polymer (from 29 % to 60 %), whereas for MMS there is a four-fold increase (from 22 % to 98 %). We also observed that, at 25 °C for both GTIs, a pseudo first order kinetic model is followed, while at 55 °C a pseudo second order kinetic model is followed instead (Fig. 5.6). Moreover, for MMS at 55 °C around 60 % of the GTI is removed after only 30 minutes, while MPTS requires a longer time period,

since 60 % of this GTI is removed only after 2 hours. These data were obtained from the binding kinetic studies at 25 °C and 55 °C in DCM for both GTIs which mathematical parameters are presented in Supporting Information. The results support the hypothesis that bulkier side chains may pose some steric hindrance in the interaction between the polymer and the GTIs as discussed above. In this case, the aromatic moiety of MPTS may impair the close proximity to adenine moieties, requiring a longer time period to interact, compared to MMS. Moreover, at a higher temperature, the polymer side chains may move more freely in solution, favouring accessibility between GTIs and -NH₂ adenine groups, making the binding process to reach equilibrium faster.

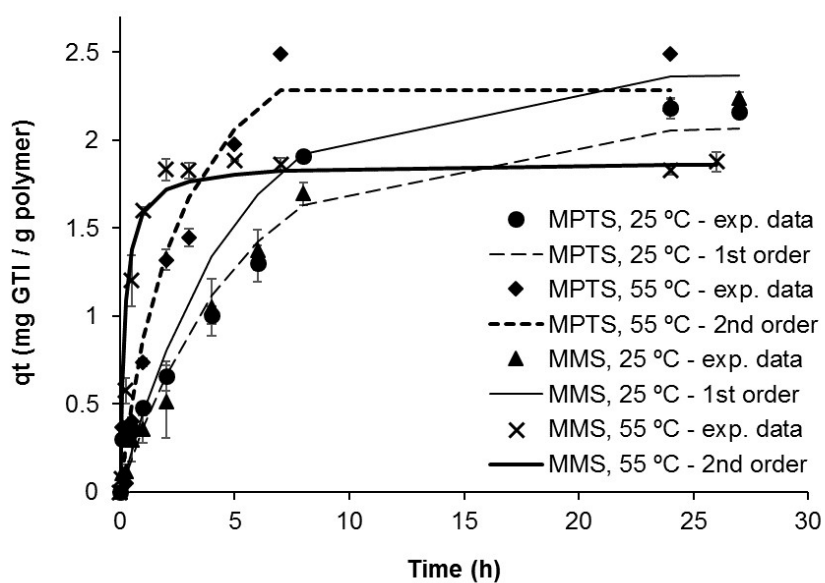


Figure 5.6. Kinetic models for MPTS and MMS at 25 °C and 55 °C in DCM.

5.4.1.2. Adsorption isotherm characterization

Adsorption isotherm studies were performed for MPTS and MMS in DCM at 25 °C and 55 °C. The experimental data were fitted to different mathematical models and the parameters determined are presented in Supporting Information. Both GTIs presented the same behaviour. At 25 °C, the binding of MPTS and MMS follows the Freundlich model (Fig. 5.7). This model assumes that the adsorber presents a heterogeneous binding site distribution and that as the GTI concentration increases, its concentration on the polymer will also increase with the amount bound being the sum on all sites [30]; the $1/n$ values of 0.55 and 0.69 estimated for the Freundlich model suggest that the binding sites available are saturated resulting in relatively lower binding. However, at 55 °C for both GTIs the Langmuir model is followed, assuming a monolayer adsorption taking place at definite localized sites with no interaction or steric hindrance between the GTI bound molecules [30]. This behaviour may be explained by the polymer chains being less constrained at a higher temperature and the proximity and interaction with the GTIs being favoured that way.

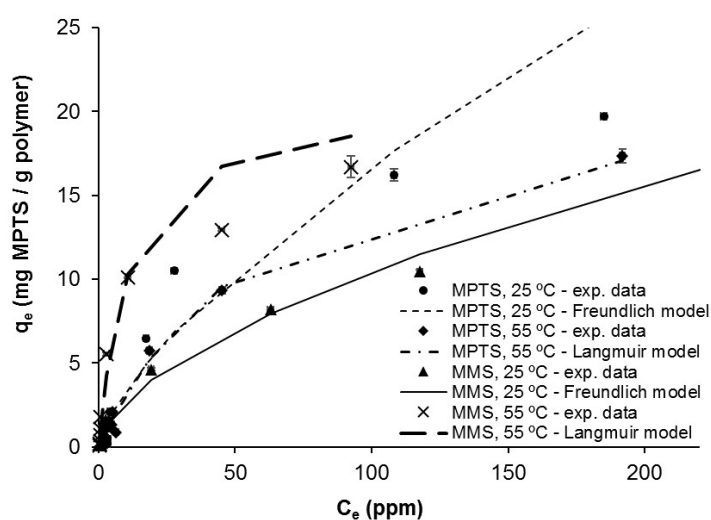


Figure 5.7. Isotherm adsorption models for MPTS and MMS at 25 °C and 55 °C in DCM.

While **PBI-adenine** proved to be already extremely efficient for removal of smaller GTIs, the results obtained suggest a slow performance for larger GTIs, which has still room for binding rates improvement by increasing temperature or surface area.

5.4.2. API binding experiments

Considering the GTI removal efficiencies, the next step was to assess **PBI-adenine** binding ability towards the APIs, to quantify possible losses and recoveries. This was performed for two glucocorticoid steroids readily soluble in DCM: mometasone furoate (Meta) and betamethasone acetate (Beta), both represented in Figure 5.8. Meta is used topically to reduce inflammation on skin (eczema, psoriasis) or airways (allergic rhinitis, some asthma patients) pathologies [5,31], while Beta is used as an oral suspension to treat arthritis, allergic or inflammatory conditions or reactive airways diseases [32].

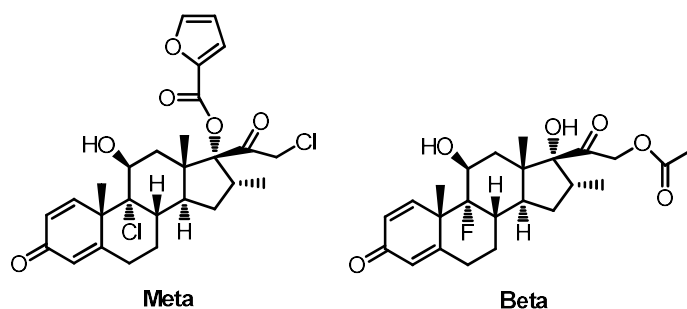


Figure 5.8. Chemical structures of the APIs studied in this work: mometasone furoate (Meta) and betamethasone acetate (Beta).

A solution of each API was prepared in DCM at a concentration of 10 g/L and assessed alone or in the presence of 100 ppm of MPTS. After 24 hours in contact with the polymer at room temperature, or 8 hours at 55 °C, the amount of API present in solution was quantified. For both APIs there was no influence in binding towards the polymer

caused by temperature change or the presence of the GTI (p value > 0.05) with an average binding value around 8 % for Meta (Fig. 5.9) and 17 % for Beta (Fig. 5.10). The relatively high percentage of API binding to **PBI-adenine** may be identified as the second limitation of this new material.

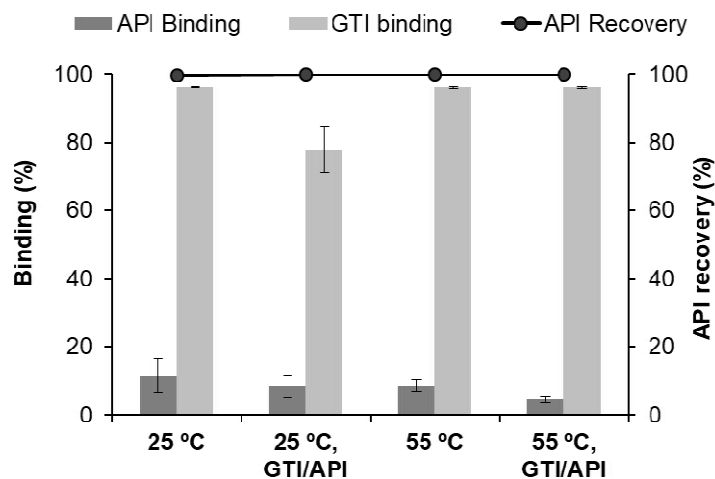


Figure 5.9. MPTS and Meta binding to **PBI-adenine** when present alone or together in solutions at 25 °C and 55 °C in DCM. Meta recovery in washing steps after binding.

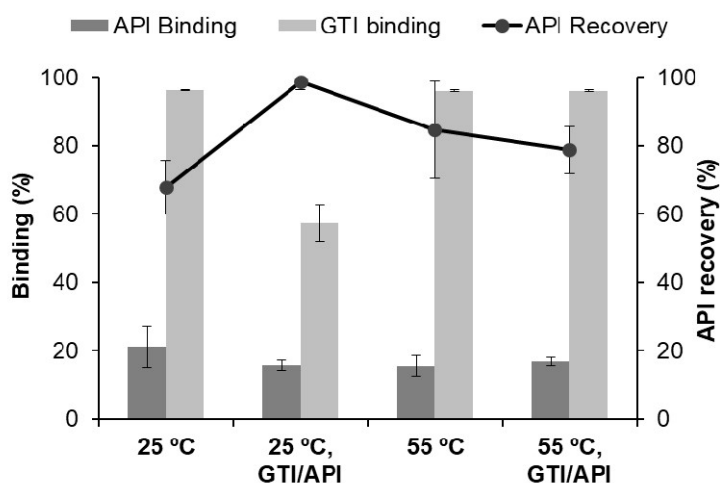


Figure 5.10. MPTS and Beta binding to **PBI-adenine** when present alone or together in solutions at 25 °C and 55 °C in DCM. Beta recovery in washing steps after binding.

GTI removals were similar at a value around 96% when the GTI is alone or in the API mixtures at 55 °C with no significant differences (p value > 0.05) found. However, at 25 °C there is a considerable impairment in GTI binding to the polymer with Meta and Beta presence leading to GTI removals decrease to values as low as 78 % and 57 %, respectively. Therefore, the use of a higher temperature (e.g. 55 °C) seems to be beneficial not only to increase binding rate, but also to prevent API inhibition of GTI binding.

In a previous study [28] it was shown that **PBI-adenine** washing with DCM or MeOH alone was inefficient to remove MPTS bound to this polymer, since the adsorption takes place through a covalent interaction between this GTI and adenine moieties of the polymer. Release and recovery of *p*-toluenesulfonic acid (PTSA) formed was only possible using methanolic solutions of triethylamine or sodium methoxide (see Table 5.1 for alkyl tosylates), as **PBI-adenine** polymer scavenges MPTS by adenine alkylation and then, behaves as an ionic exchanger, in the presence of an organic base, for PTSA formed during this reaction. Therefore, considering that the GTI is not easily removed from the polymer, we envisaged the possibility to decrease API losses (8-17%) by straightforward recovery of the API, eventually trapped in **PBI-adenine**, by a simple solvent washing procedure, potentially without any GTI back extraction. The implementation of such washing step using DCM allowed full Meta recovery, with virtually no API loss, whereas for Beta an average recovery of about 83 % was achieved leading to a loss around 3 % of this API. No PTSA, formed during binding, was detected in API recovered solutions, proving that APIs are recovered without any GTI back contamination.

Beta recovery from **PBI-adenine**, using DCM at room temperature, is significantly higher when the polymer is used in the previous binding step, with Beta/GTI mixtures (around 98 %) than when Beta individual solutions were used. The impossibility

to have a full recovery of this API suggests that some covalent interaction may be taking place with the polymer. The ester functional group present in Beta may be forming amide bonds with -NH_2 groups of the polymer. In this way, some API remains bound to the polymer and is not fully recovered. Nevertheless, for both APIs, HPLC chromatograms did not reveal the presence of other impurities that could be originated from polymer treatment.

Due to sulfonates intrinsic genotoxicity, several authors explored different adsorbers for the removal of MPTS from API solutions, employing different procedures (Table 5.2). For example, Székely et al. reported a low GTI removal of (15-45) % with a considerable API loss of (10-15) % using a MIP specifically designed for this GTI [10]. Lee et al. reported 100 % removal of MPTS but also a high API loss, around 10 % [23]. Furthermore, Kecili et al. also reported a 100 % removal of this GTI with full recovery of the API. However, the authors needed 150 mg of adsorber per 1 mL of solution to achieve this result [22]. With **PBI-adenine** polymer we are able to remove more than 96 % of the same GTI with full API recovery with only one third of that amount of adsorber (50 mg/mL). These results illustrate the high efficiency and improved performance of the developed PBI modified polymer comparing with other adsorbing systems.

Table 5.2. MPTS vs API binding data in batch experiments, for previously reported cases and current work.

Reference	[10]	[22]	[23]	Current work
Adsorber	MIP	Nucleophilic resin		PBI-adenine
Solvent	DCM	2-propanol	MeCN, MeOH	DCM
[GTI] (ppm)	1,000	5	100	100
[API] (ppm)	10,000	500	100	10,000
GTI:API	1:10	1:100	1:1	1:100
Time / Temperature	24 h / RT	2 h / RT	1 h / 40 °C	8 h / 55 °C
Adsorber amount	50 mg /mL	150 mg/mL	200 mg /mL	50 mg/mL
API loss	(10–15)%	100%recovery	< 10%	3.5%
GTI removal	(15-45)%	100%	100%	96%

5.4.3. Process design for API purification

Considering the results presented in Figures 5.9 and 5.10, we envisaged a binding step process at 55 °C with the potential to eliminate a GTI from an API solution. In these conditions, the **PBI-adenine** polymer is able of 96 % GTI removal with a total recovery of Meta and only 3.5 % loss of Beta.

For Meta degenotoxification, we consider two case scenarios for the therapeutic use of this corticosteroid: nebulization for the treatment of airways diseases or topical application in the treatment of eczema, with administered daily dose of 200 µg or 2 mg

of API, respectively. The amount of GTI allowed is determined considering a TTC value of 1.5 μg GTI/day and the maximum daily dose in g API/day at the values of 7.5 or 0.75 mg GTI/g API for the airways or the skin treatment, respectively.

For Beta, we consider a case scenario in which the patient is administered an initial high dose of 2.5 mg/day for the treatment of rheumatoid arthritis. For the imposed TTC value of 1.5 μg GTI/day, this case implies the need to reach a limit of 0.6 mg GTI/g API.

For both cases, we considered a post-reaction stream to be treated, with an API load of 10 g/L and a GTI contamination at a concentration of 100 ppm, simulating an industrial batch production in which the API is found in a higher concentration compared to the GTI with a ratio of 10 mg GTI/g API. We performed bindings at 25 °C and 55 °C and compared results for both strategies.

For Meta, the API is totally recovered for both operational temperatures (Fig. 5.11). However, at 25 °C about 22 % of the GTI remains in solution, reaching a final ratio of 2.2 mg GTI/g Meta, which is an acceptable value for the airways treatment case (target limit set at 7.5 mgGTI/gAPI), but not for the skin treatment (target limit of 0.75 mgGTI/gAPI). Nevertheless, when the process takes place at 55 °C only about 4 % of GTI remains in solution, reaching a final ratio of 0.39 mg GTI/g Meta, which is suited for both case scenarios.

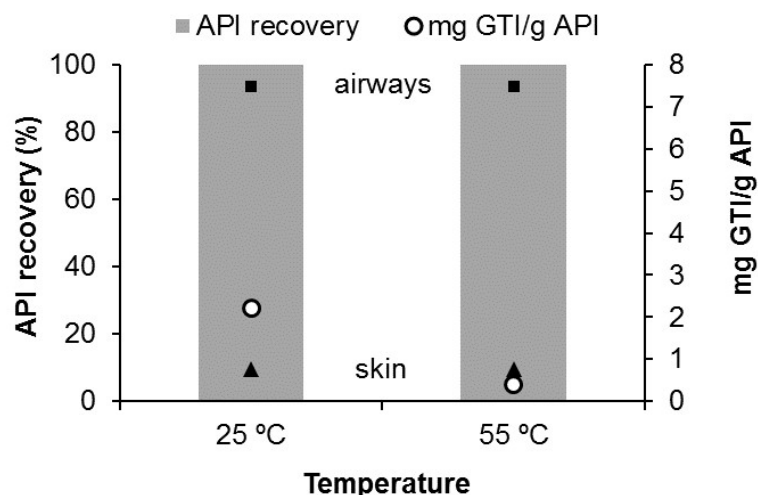


Fig. 5.11. Performance of a single step process concerning API recovery and level of degenotoxification of MPTS to Meta as a function of temperature (white dots). Squares represent the limit for airways treatment of 7.5 mg GTI/g API. Triangles represent the limit for skin treatment of 0.75 mg GTI/g API.

For the more challenging case of Beta, (Fig. 5.12) when the process takes place at 25 °C there is a good recovery of the API around 98 %, but 43 % of the GTI remains in solution reaching a final ratio of 4.33 mg GTI/g Beta, which is a value far from the 0.6 mg GTI/g API limit required. However, when the process takes place at 55 °C, it is possible, using the solvent washing step to recover about 79 % of the initial 13% of API bound to **PBI-adenine**, with 96 % removal of the GTI, leading to an overall loss of about 3.5 % of API. Since only 4 % of the GTI remains in solution, a final ratio of 0.50 mg GTI/g Beta is reached, which is a value within the limit imposed by legislation of 0.6 mg GTI/g API.

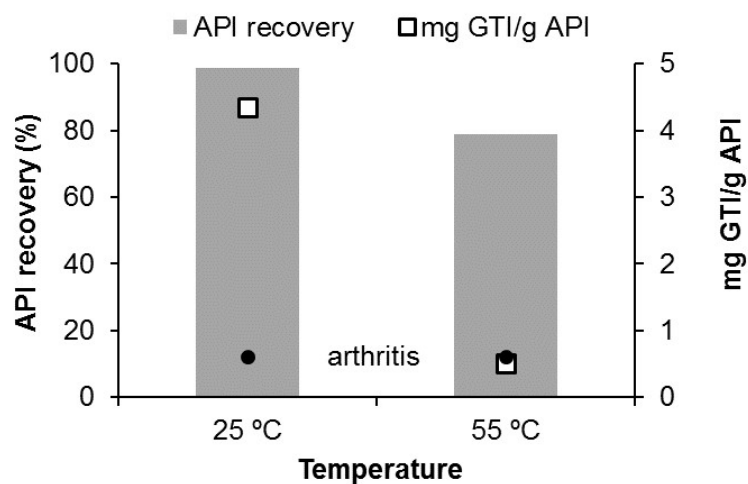


Fig. 5.12. Performance of a single step process concerning API recovery and level of degenotoxification of MPTS to Beta as a function of temperature (white squares). Dots represent the limit for arthritis treatment of 0.6 mg GTI/g API.

Overall, for both APIs the best GTI to API ratio is always achieved when the binding process takes place at 55 °C, which contributes to a faster GTI removal and prevented API inhibition of GTI binding, leading to a final GTI to API ratio that is within the limits imposed by strict regulatory authorities, with virtually no losses of API for the case of Meta and about 3.5 % loss in the case of Beta.

5.5. Conclusions

The potential development of a versatile material able to scavenge a broad range of DNA alkylating agents from organic solvent based solutions was investigated. Adsorption of GTIs from different chemical families, on an adenine modified PBI polymer, was found to be effective (> 80 %) at room temperature. Our results show that in a typical industrial scenario, where the GTI is present in low concentration compared to the API, the efficiency and GTI removal rate can be improved with temperature increase. Furthermore, a simple solvent washing step was implemented to recover the API trapped in **PBI-adenine** polymer without GTI back contamination, exploring the fact that, the GTI is not easily retrieved from the adsorbing platform. Based on these achievements, a strategy is proposed for the efficient removal of a DNA alkylating GTI from an API solution in an organic solvent, leading to GTI to API ratios within the limits imposed by legislation, as low as 0.6 mg GTI/g API with only a 3.5 % loss of API for the worst-case scenario considered. From the point of view of an industrial application this is a major advantage, since with one simple washing step it could be possible to recover the API, minimizing its loss, addressing the economic impact for the pharmaceutical companies associated with API losses in time consuming and material demanding elaborated purification strategies.

5.6. References

- [1] EMEA Guidelines on “Limits on Genotoxic Impurities”, EMEA/CHMP/QWP/251344/2006, 2006.
- [2] Guidance for Industry Genotoxic and Carcinogenic Impurities in Drug Substances and Products: Recommended Approaches; U.S. Department of Health and Human Services; Food and Drug Administration; Center for Drug Evaluation and Research (CDER); December 2008.
- [3] Zhou, L., et al, Impurity profile tracking for active pharmaceutical ingredients: case reports, *J. Pharm. Biomed. Anal.* 44, 2007, 421-429.
- [4] Székely, G., et al, Genotoxic impurities in pharmaceutical manufacturing: sources, regulations, and mitigation, *Chem. Rev.*, 16, 2015, 8182-8229.
- [5] Székely, G., et al, Environmental and economic analysis for selection and engineering sustainable API degenotoxification processes, *Green Chem.*, 15, 2013, 210-225.
- [6] Székely, G., et al, Organic solvent nanofiltration: a platform for removal of genotoxins from active pharmaceutical ingredients, *J. Membrane Sci.*, 381, 2011, 21-33.
- [7] Omerod, D., et al, Demonstration of purification of a pharmaceutical intermediate via organic solvent nanofiltration in the presence of acid, *Sep. Purif. Technol.*, 115, 2013, 158-162.
- [8] Peeva, L., et al, Continuous purification of active pharmaceutical ingredients using multistage organic solvent nanofiltration membrane cascade, *Chem. Eng. Sci.*, 116, 2014, 183-194.
- [9] Buonomenna M. G., Bae J., Organic solvent nanofiltration in pharmaceutical industry, *Sep. Purif. Rev.* 44, 2015, 157-182.

- [10] Székely, G., et al, Removal of potentially genotoxic acetamide and arylsulfonate impurities from crude drugs by molecular imprinting, *J. Chromatogr. A*, 1240, 2012, 52-58.
- [11] Sellergren, B., et al, Polymers for drug purification, WO 2012172075 A1, 2012.
- [12] Székely, G., et al, Design, preparation and characterization of novel molecularly imprinted polymers for removal of potentially genotoxic 1,3-diisopropylurea from API solutions, *Sep. Purif. Technol.*, 86, 2012, 190-198.
- [13] Esteves, T., et al, Molecularly imprinted polymer strategies for removal of a genotoxic impurity, 4-dimethylaminopyridine, from an active pharmaceutical ingredient post-reaction stream, *Sep. Purif. Technol.*, 163, 2016, 206-214.
- [14] Székely, G., et al, A hybrid approach to reach stringent low genotoxic impurity contents in active pharmaceutical ingredients: Combining molecularly imprinted polymers and organic solvent nanofiltration for removal of 1,3-diisopropylurea, *Sep. Purif. Technol.*, 86, 2012, 79-87.
- [15] Székely, G., et al, Molecularly imprinted organic solvent nanofiltration membranes – Revealing molecular recognition and solute rejection behavior, *React. Funct. Polym.*, 86, 2015, 215-224.
- [16] Humbert, H., et al, Performance of selected anion exchange resins for the treatment of a high DOC content surface water, *Water Res.*, 39, 2005, 1699-1708.
- [17] Mohan, D., Pittman Jr. C. U., Arsenic removal from water/wastewater using adsorbents – A critical review, *J. Hazard. Mater.*, 142, 2007, 1-53.
- [18] Lin, S. H., Juang, R. S., Adsorption of phenol and its derivatives from water using synthetic resins and low-cost natural adsorbents: A review, *J. Environ. Manage*, 90, 2009, 1336-1349.

- [19] Elwakeel, K. Z., Environmental application of chitosan resins for the treatment of water and wastewater: a review, *J. Disper. Sci. Technol.*, 31, 2010, 273-288.
- [20] Smith, K. M., et al, Sewage sludge-based adsorbents: a review of their production, properties and use in water treatment applications, *Water Res.* 43, 2009, 2569-2594.
- [21] Adams, C., et al, Removal of antibiotics from surface and distilled water in conventional water treatment processes, *J. Environ. Eng.*, 128, 2002, 253-360.
- [22] Kecili, R., et al, Selective scavenging of the genotoxic impurity *p*-toluenesulfonate from pharmaceutical formulations, *Sep. Purif. Technol.*, 103, 2013, 173-179.
- [23] Lee, C., et al, Removal of potential genotoxic impurities using nucleophilic reactive resins, *Org. Process Res. Dev.*, 14, 2010, 1021-1026.
- [24] Kondo, N., et al, DNA damage induced by alkylating agents and repair pathways, *J. Nucleic Acids*, 2010, DOI: 10.4061/2010/543531.
- [25] Hoffmann, G. R., Genetic effects of dimethyl sulfate, diethyl sulfate, and related compounds, *Mutat. Res.-Rev. Genet.*, 75, 1980, 63-129.
- [26] Kim, Y. S., et al, *Methods in Molecular Biology*, volume 323, ed. J. Salinas, J. J. Sanchez-Serrano and Humana Press, Totowa, New Jersey, 2006, pp. 101-103.
- [27] Gocke, E., et al, Literature review on the genotoxicity, reproductive toxicity, and carcinogenicity of ethyl methanesulfonate, *Toxicol. Lett.* 190, 2009, 254-265.
- [28] Vicente, A. I., et al, Solvent compatible polymer functionalized with adenine, a DNA base, for API degenotoxification: preparation and characterization, *Sep. Purif. Technol.*, 179, 2017, 438-448.
- [29] Qiu, H., et al, Critical review in adsorption kinetic models, *J. Zhejiang Univ. Sci. A* 10, 2009, 716-724.
- [30] Foo, K. Y., Hameed, B. H, Insights into the modeling of adsorption isotherm systems, *Chem. Eng. J.*, 156, 2010, 2-10.

[31] Heggie, W., Bandarra, J., Process for the preparation of Mometasone furoate, US 6177560 B1, 2001.

[32] Salem, I. I., et al, LC-MS/MS determination of betamethasone and its phosphate and acetate esters in human plasma after sample stabilization, J. Pharmaceut. Biomed., 56, 2011, 983-991.

Chapter VI

**API recovery from methanolic mother liquors using adsorbers:
Screening commercially available resins and application for
simultaneous removal of two potential genotoxins**

Article *in* Separation Science and Technology · December 2018

DOI: 10.1080/01496395.2018.1556304 by Teresa Esteves, Flávio A. Ferreira, Mariana Pina, João Bandarra and Frederico Castelo Ferreira, with the title: “Screening commercial available resins for simultaneous removal of two potential genotoxins from API methanolic streams”

6.1 Outline

This chapter explores potential API loss mitigation during purification in recrystallization mother liquors, by including a resin adsorption step, to remove potential genotoxin impurities (PGTIs). Mometasone furoate (Meta) is used as model active pharmaceutical ingredient (API) in the presence of 4-dimethylaminopyridine (DMAP) and methyl *p*-toluenesulfonate (MPTS) as two model PGTIs. The first results section (Section 6.4.1) describes typical recrystallization operation and yields obtained at laboratory scale. Then, sections 6.4.2 and 6.4.3 are dedicated to assessing the use of several readily available commercial resins for the removal of DMAP and MPTS from organic solvent solutions, discussing the effect of solvent matrix and pH on binding properties and establishing the kinetics and isotherms behaviour for the adsorption processes. AG 50W-X2 and IRA68 resins efficiently removed DMAP and MPTS from methanol solutions, respectively, with adsorptions higher than 93% and Meta binding below 2%. In section 6.4.5 removal of GTIs using these resins sequentially, or combining them in a single step, was also assessed, with superior results for the later approach. In section 6.4.6, different approaches are assessed to use the resins for API reclaiming from the mother liquor by (i) direct API reclaiming from the mother liquor; or (ii) recycling an API rich stream, obtained after resin treatment of the mother liquor, to the recrystallization feed. Combination of recrystallization and resin adsorption unit operations efficiency is also theoretically analyzed assuming different API losses in the recrystallization mother liquor and through binding to the resin. Finally, in section 6.4.7 is presented a brief economic evaluation.

Keywords: Potential genotoxin impurity; Resin adsorbents; 4-Dimethylaminopyridine; Methyl *p*-toluenesulfonate; Active pharmaceutical ingredient purification.

6.2 Introduction

In this chapter, the removal of two PGTIs, 4-dimethylaminopyridine (DMAP) and methyl *p*-toluenesulfonate (MPTS), from Mometasone furoate (Meta) post reaction stream in dichloromethane (DCM), is used as a model study (Figure 6.1). Meta, a glucocorticoid used in inflammatory diseases treatment [1], synthesis involves a sulfonylation reaction in DCM in the presence of a base. DMAP may be used as catalyst in this methodology [2] and has two genotoxic structural alerting functional groups: aromatic and alkyl amine [3,4]. Alkyl and benzyl sulfate acids are widely used as counterions in API salt formation [5]. However, in the presence of alcohols, such as methanol (MeOH), they originate the corresponding sulfonate esters [6], known to be DNA alkylating agents [7]. One of such cases is well documented in the literature for the API Viracept [8].

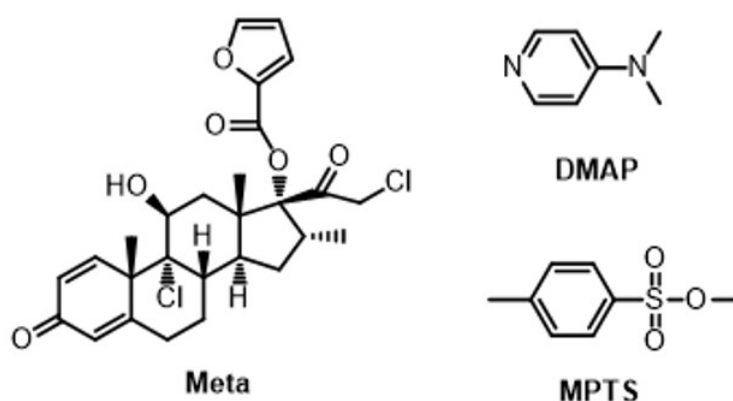


Figure 6.1. Structures of Meta, DMAP and MPTS.

The motivation to perform the studies on this chapter lays on the fact that it is common knowledge that recrystallization is still the most common technique to purify/isolate APIs in pharmaceutical industry due to its simplicity, including removal of GTIs from Meta, [9], with the advantage to isolate Meta as a solid ready to be put in

storage or further processed into the final formulation. However, a large fraction of the API is often lost in recrystallization mother liquors [10]. Additionally, this chapter also details further information concerning possible side reactions taking place between DMAP and MPTS.

While previous chapters have been dedicated to enhance the adsorption capabilities of PBI in DCM, to provide a solvent stable scavenger able to remove GTIs, this chapter targets removal of GTIs from methanol exploring available adsorbers. Methanol is often used in recrystallizations, but contrary to many solvents used on API or API intermediates synthesis has lower ability to dissolve or swell many polymers. Therefore, the overall aim of the current chapter is to discuss the possibility to reclaim the API lost in recrystallization mother liquor using inexpensive resins, which is not trivial considering the intricate relations between solute ionic states, resins and solvent matrix. To reclaim API, otherwise lost in the recrystallization methanolic mother liquor, while respecting TTC limits, two routes are envisaged using the selected resins: i) Direct API reclaiming approach: removal of GTIs from methanolic mother liquor to values at which GTI/API ratio in such solution complies with the TTC value; ii) Recycle stream approach: to decrease GTI concentrations down to levels meeting the GTI/API ratio of the initial post-synthetic API crude stream, allowing recycling the API back into the next batch recrystallization cycle.

6.3 Materials and Methods

6.3.1 Model compounds and solvents

4-Dimethylaminopyridine (DMAP), methyl *p*-toluenesulfonate (MPTS) and *p*-toluenesulfonic acid monohydrate (PTSA) were purchased from Acros (Belgium). Mometasone furoate (Meta) was kindly provided by Hovione PharmaScience Ltd (Portugal). Dichloromethane (DCM), methanol (MeOH) and acetonitrile (MeCN) HPLC grade were purchased from Fisher Chemicals (USA). Formic acid (FA) was purchased from Panreac (Spain). All chemicals were of reagent grade or higher and were used as received.

6.3.2 Resins and Adsorbents

Amberlite resins (CG400, IRA458, IRA68, IRC50, IRC86, XAD16 and XAD7) were purchased from Aldrich (Switzerland). Dowex resin AG 50W-X2 was purchased from BioRad (USA). Activated charcoal powder was purchase from Merck (Germany). The chemical nature of several resins used in this study is described in Table 6.1 and provides a variety of ionic resins with acidic or basic groups, as well as non-ionic resins with useful chemical functionalities to interact with DMAP and MPTS.

Table 6.1. Chemical nature of the resins used in this study.

Resin	Functional group	Characteristic
AG 50W-X2	Sulfonic acid	Strong acid cation exchange
IRC50	Carboxylic acid	Weak acid cation exchange
IRC86	Carboxylic acid	Weak acid cation exchange
XAD16	Hydrophobic polyaromatic	Adsorption
XAD7	Acrylic ester	Adsorption
CG400	Quaternary amine	Strong base anion exchange
IRA458	Quaternary amine	Strong base anion exchange
IRA68	Tertiary amine	Weak base anion exchange

Purification processes using adsorbing or ionic exchange resins are well developed at the industrial scale and can be easily implemented for Meta purification that is lost in recrystallization mother liquor. However, the solvent in question is MeOH and most of the commercially available resins are designed to perform in aqueous solutions. Therefore, assessing DMAP and MPTS removal using different resins from MeOH is not without challenge. The strategy followed started by assessing removal of DMAP from water, then from a water:MeOH (1:1) mixture, to assess organic solvent versus water interference in binding process. Afterwards, only for the resins yielding higher DMAP binding in 1:1 mixture, its removal from pure MeOH was tested. Activated charcoal was also considered in these studies for performance comparison.

6.3.3 HPLC analyses

Measurements were performed on a Merck Hitachi pump coupled to a L-2400 tunable UV detector using an analytic Macherey-Nagel C18 reversed-phase column Nucleosil 100-10, 250 x 4.6 mm with eluents, A: 0.1% FA aqueous solution, B: 0.1% FA, MeCN solution. For Meta and DMAP a flow rate of 1 mL·min⁻¹ was used with UV detection at 280 nm; method: 0-3 min, 60% to 20% A; 3-4 min, 20% A; 4-8 min, 20% to 60% A; 8-15 min 60% A. For MPTS a flow rate of 2 mL·min⁻¹ was used with UV detection at 230 nm; method: 0-15 min, 70% A-30% B. For PTSA a flow rate of 1.5 mL·min⁻¹ was used with UV detection at 230 nm; method: 0-10 min, 90% A-10% B.

6.3.4 Recrystallization process

To simulate a post reaction stream, a solution containing 1 g/L DMAP, 1 g/L MPTS and 10 g/L Meta was prepared in DCM, referred as crude solution. **Solvent exchange step protocol:** The initial DCM solution (50 mL) was concentrated to 10% of its initial crude volume (10%V₀, 5 mL) in a rotary evaporator (Buchi, Switzerland). Followed by addition of fresh MeOH (20% V₀, 10 mL), the solution was heated at about 50 °C until the volume was reduced (10%V₀, 5 mL) in the rotary evaporator. In this process crystals started to appear. This procedure was repeated twice. **Recrystallization step protocol:** The slurry obtained was allowed to cool to 20 °C for about 1 h, then to 10 °C for over 1 h, with a Haake D1 immersion circulator water bath, with stirring at 220 rpm and finally, left at 10 °C for 2 additional h. At this stage, Meta was filtered with a qualitative filter paper (Filter-Lab, Spain) with 2-4 µm pores and washed twice with 2 mL of cold MeOH (10 °C). The crystals were collected and dried in an oven for 24 h at

70 °C. The recrystallization mother liquor (about 10 mL) was analysed for DMAP, MPTS and Meta quantification.

6.3.5 Resin assessment for solute adsorption

Adsorption of DMAP and MPTS, unless otherwise stated, was assayed at a concentration of 1 g/L in 4 mL solution of water, MeOH or 1:1 of water:MeOH mixtures using 20 mg of resin and left at 220 rpm on a stirring plate (IKA, Germany) for 24 h at room temperature, after which the supernatant was filtered and analysed by HPLC for solute quantification and binding percentage determination. Experimental triplicates and controls without resin addition were carried out. pH was adjusted using 1M aqueous solutions of HCl and NaOH and measured using a 702 MS Titrino (Metrohm, Switzerland). The three different temperatures, 25 °C, 35 °C and 45 °C assessed, were controlled in an incubation chamber (J. P. Selecta, Spain). Adsorption isotherm studies were established by, at a fixed temperature and pH: (i) different amounts of resin (10, 20, 40, 80, 100, 200 or 400 mg) added to 4 mL solutions with an initial GTI concentration of 1 g/L; (ii) or 20 mg of resin added to 4 mL of GTI solutions with concentrations of 0.1, 0.25, 0.5, 0.75 or 1 g/L. For kinetic studies, identical solutions were prepared and the supernatant collected and filtered at 2, 4, 6, 10, 15, 30, 60, 120, 240, 480 and 1440 min. The amount of GTI bound to the resins was calculated from Equation 6.1.

$$q_{\text{eq}} = \frac{V[C_0 - C_{\text{eq}}]}{M} \quad (\text{Eq. 6.1})$$

where q_{eq} (mg/g) is the amount of GTI bound to the resin, C_0 (mg/L) is the initial GTI (DMAP or MPTS) concentration, C_{eq} (mg/L) is the equilibrium concentration of GTIs in

solution, V (L) is the volume of solution used and M (g) is the resin mass. The assays were carried out in duplicates.

The adsorption models considered were:

$$\text{Langmuir: } \frac{q_{\text{eq}}}{q_m} = \frac{K_L \cdot C_{\text{eq}}}{1 + K_L \cdot C_{\text{eq}}}$$

$$\text{Freundlich: } q_{\text{eq}} = K_F \cdot C_{\text{eq}}^{\frac{1}{n}}$$

where q_m (mg/g) is the maximum amount of GTI bound to the resin in a monolayer for the Langmuir model, whereas K_L and K_F are equilibrium constants (L/mg) for the Langmuir and Freundlich models, respectively, and are related with the energy taken for adsorption. n is a parameter related with the surface layer heterogeneity [11-13].

Experimental data, obtained from kinetic experiments, were fitted to pseudo-first (Eq. 6.2) and pseudo-second (Eq. 6.3) order kinetic models [14].

$$\ln(q_{\text{eq}} - q_t) = \ln(q_{\text{eq}}) - k_1 \cdot t \quad (\text{Eq. 6.2})$$

$$\frac{t}{q_t} = \frac{1}{k_2 \cdot q_{\text{eq}}^2} + \frac{t}{q_{\text{eq}}} \quad (\text{Eq. 6.3})$$

where q_{eq} and q_t (mg/g) are adsorption capacities at equilibrium and time t (min), respectively. k_1 (min^{-1}) and k_2 ($\text{g}/(\text{mg} \cdot \text{min})$) are pseudo- first and second order rate constants for the models.

The same batch binding experiments described above, were performed for 4 mL of MeOH solutions with 10 g/L of Meta and 1 g/L of the GTI (DMAP or MPTS) with AG 50W-X2 or IRA68 resins. After 24 h in contact with 25 mg of each resin at 200 rpm and at room temperature, the mixtures were filtered and analysed by HPLC for solute quantification and binding percentage determination. Experimental triplicates and controls without resin addition were carried out.

6.3.6 Mother liquor purification

Adsorption experiments for the mother liquor solution in MeOH, with 6 g/L Meta, 5 g/L DMAP and 5 g/L MPTS, were assayed with AG 50W-X2 and IRA68 resins using 25 mg of resin for 1 mL of solution left stirring at 220 rpm for 24 h at room temperature, for each adsorption stage. In the combined strategy, 25 mg of each resin (50 mg in total) were loaded on 1 mL of solution. After incubation time, the supernatant was filtered and analysed by HPLC for solute quantification and binding percentage determination. The assays were carried out in duplicates.

6.4 Results and Discussion

Different types of studies are presented and discussed. The first sections report experimental studies for individual operations, recrystallization and screening of different resins for GTI adsorption. Then, selected resins following specific adsorption strategies are experimentally assessed, concerning GTIs and API removal from recrystallization synthetic mother liquors. Finally, the impact of the two suggested process approaches (direct API reclaiming or recycling stream) are theoretically assessed for different cases and a brief economic assessment is presented.

6.4.1 Recrystallization

For Meta, recrystallization is the purification process usually performed for removal of GTIs from the post reactional stream. DCM is the solvent usually used in Meta synthesis and a disclosed purification process comprises two recrystallizations from MeOH, an intermediate activated charcoal adsorption step from DCM and the required

solvent exchange steps [9]. This process was assessed in a previous study [10] in which, the overall purification allowed to decrease a GTI to API mass ratio from 200 mgGTI/gAPI (100 mgGTI/gAPI for each GTI) present in the initial solution, to a value of 3.1 mgGTI/gAPI in solid API, representing a total GTI removal of 98.7%, which fulfils the TTC for a case study of a maximum dosage of 200 µg/day for airways administration. The largest fraction of API loss was observed in the first recrystallization, accounting for about half of total API lost over the 3 steps, whereas GTI removal was not preferentially assigned to any stage. Nevertheless, DMAP removal tends to occur in the first recrystallization and activated charcoal adsorption steps, while the sulfonate ester (methyl methanesulfonate) removal was driven by recrystallization, with a higher efficiency in the second one, when DMAP was present at lower concentrations.

The specific allocation of API losses and GTI removals during a recrystallization process vary widely, mainly according to the scale used that impacts in losses through the washing and filtration operations. In this study, 10 g/L API and 1 g/L of each GTI in DCM were used, following the previous study with Meta [10], but focusing only in the first recrystallization step, which accounts for about half of the total API lost in the entire purification process. In this report, the recrystallization was performed at a scale 10 times lower than previously. Still, the results obtained are consistent concerning API yield [(91.1±0.4)% vs. (91.4±0.5)% [10]], API concentration in the mother liquor [(5.3±0.7) g/L vs (4.8±0.3) g/L [10]] as well as sulfonate ester removal [(26.2 ±8.5)% for MPTS vs 36.8% [10] for methyl methanesulfonate] achieved in the first recrystallization. However, DMAP removal was higher in the current study than in the previous one [(81.9±0.9)% vs 53.9% [10]] implying higher concentrations for DMAP than for MPTS in the mother liquor, (5.1±0.7) g/l and (1.4±0.4) g/L, respectively. An additional recrystallization of Meta from a Meta/MPTS solution (in the absence of DMAP), was performed, simulating

the second recrystallization that targets sulfonate esters removal, after elimination of a larger DMAP fraction. In this recrystallization, API loss and concentration in the mother liquor were similar to values previously observed, but MPTS removal increased to 95.7%, corresponding to a 4.8 g/L MPTS concentration in the mother liquor.

The values described above allowed us to establish reference concentrations of API and GTIs in MeOH that should be loaded to a resin purification step, corresponding to about 6 g/L of API and 5 g/L for each GTI, i.e. a ratio of 1666.7 mgGTIs/gAPI (833.3 mgGTI/gAPI for each GTI) that is about 8 times higher than the initial post-synthetic API crude stream (200 mgGTI/gAPI, considering both GTIs).

6.4.2 Screening scavengers for DMAP adsorption

The results obtained in water (Figure 6.2A) showed that resins with acidic groups (AG 50W-X2, IRC50, IRC86), and also the activated charcoal were efficient for DMAP adsorption with removals above 80% for 1g/L solutions. Intermediate DMAP bindings were obtained using non-ionic resins (XAD7 and XAD16), and a low performance was observed for amine based resins assessed. As MeOH was included in the solvent matrix, DMAP removal by non-ionic and amine based resins became negligible and activated charcoal ability also decreased, probably by possible MeOH adsorption, being a competitive factor in DMAP adsorption. The three resins with acidic groups (AG 50W-X2, IRC50, IRC86), showed a decrease in their performance in MeOH (Figure 6.2A), but still reached acceptable values higher than 80% for AG 50W-X2 and about 60% for the IRC resins. This decrease in performance, can possibly be attributed to resin swelling and competition of the solvent. These results prove that the use of this technology with such organic solvent is challenging.

DMAP binding is lower for the resins in all solvent matrices at pH 6-8 (Figure S6.1), i.e., when DMAP is on its conjugated protonated acid form. However, the resins performance was improved for pH values around 10 (Figure 6.2B), whereas for a value close to 12 the possible formation of competing ionic species (sodium ions towards sulfonic and carboxyl groups) can take place and the adsorption was low in all cases. The difference in response for the acidic groups (i.e. cationic resins) resins compared to non-ionic or amine based (i.e. anionic) resins, suggested that the ionic interaction between DMAP and resin sulfonate and carboxyl groups is maintained in MeOH, whereas the solvent competes with the solute by non-ionic interactions with the adsorbent.

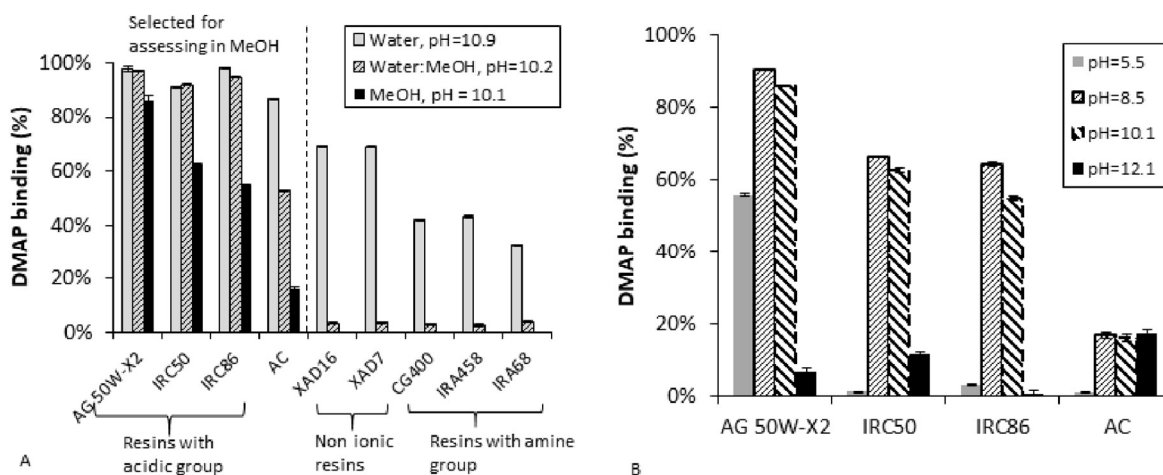


Figure 6.2. DMAP binding for different resins tested: A) without pH adjustment for different solvent matrices; B) Influence of pH on DMAP adsorption in MeOH. AC – activated charcoal.

DMAP is a Brønsted base with a pKa of 9.7 with different inductions of charge distribution in the molecule according to solution pH. HCl or NaOH 1M solutions were used to adjust pH to values lower or higher than pKa, respectively. The activity of MeOH affects equilibrium constants of resins and solutes (i.e. pKa), as well as pH electrode readings scale. Moreover, the addition of HCl and NaOH may influence both DMAP and

ionic exchange resins ionic states [15]. The ionic exchange resins with acidic groups are cationic resins, which are supplied in hydrogen form, i.e. protonated, and they are usually converted to their anionic form through a preconditioning step using NaOH for resin deprotonation and conjugation with sodium ions. These results are not of trivial reasoning, but it should be noted that, in this work, these cationic resins were used on the hydrogen form, which could sustain an explanation based on the action of DMAP as a base, and electrostatic interactions between the resins and DMAP, mediated by hydrogen bonding.

Considering the results previously discussed, a pH value around 10 was chosen to study the effect of temperature, adsorption kinetics, and establish binding isotherms with AG 50W-X2 resin in MeOH. Solvent effect in adsorption kinetics showed to be significant. The adsorption process was very fast in water and in water:MeOH mixture, with approximately 1-5 min being necessary for the resin to reach adsorption equilibrium (Figure S6.2). On the other hand, in MeOH, the lower DMAP adsorption comprehends a slower adsorption process, and in this case about 15 minutes are needed for the system to reach the same equilibrium (Figure 6.3). Furthermore, in MeOH, the temperature proved to have no effect in DMAP adsorption in the range (25-45) °C (Figure 6.3).

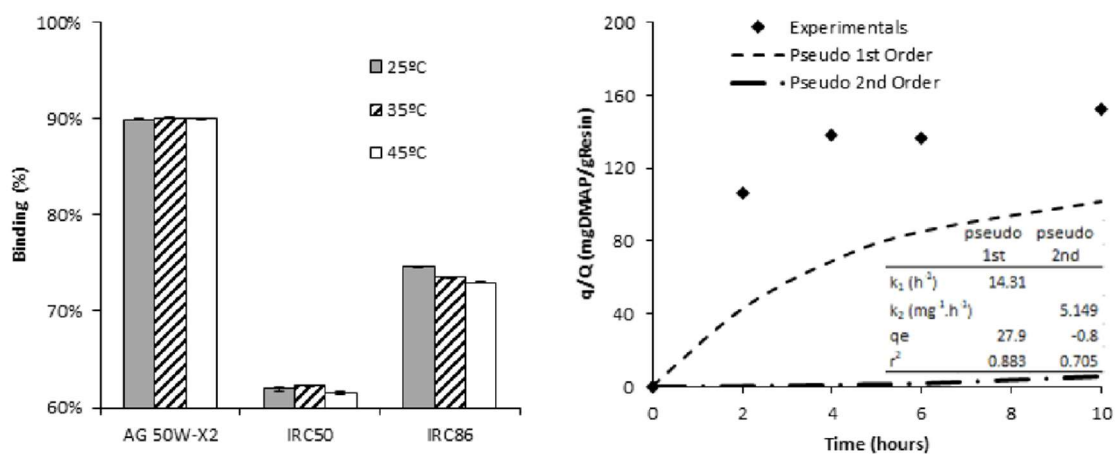


Figure 6.3. Left: Temperature influence in DMAP adsorption from MeOH. Right: DMAP binding capacity in AG 50W-X2 resin for a 1 g/L solution in MeOH along time at 25 °C.

The isotherm binding model behaviour for each scavenger in MeOH at 25 °C contributes to provide additional information on equilibrium between DMAP and the scavenger, with the results presented in Figure 6.4. The physical parameters determined for the theoretical models are included in Supporting Information (Table S5.1). AG 50W-X2 and IRC 50 resins follow the Freundlich isotherm model that assumes that the amount of DMAP adsorbed tends to infinity and that multilayers of adsorbed GTI molecules are formed. IRC 86 resin follows the Langmuir isotherm model suggesting the formation of a monolayer in a homogeneous surface.

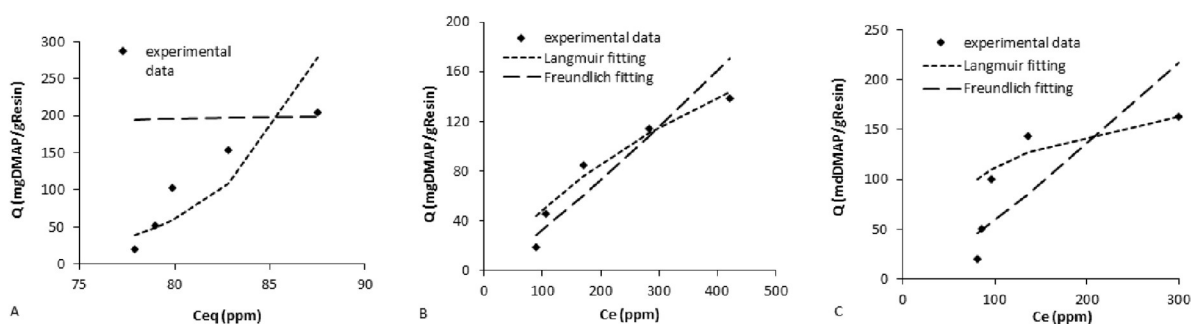


Figure 6.4. Adsorption isotherm models for DMAP in MeOH for several resins at 25 °C: A) AG 50W-X2; B) IRC50; C) IRC86. A good correlation of the Langmuir fitting with AG 50W-X2 resin could not be determined.

From the studies for DMAP, and based on the results presented in Figure 6.2A, AG 50W-X2 and IRC50 resins were selected to be assessed towards API binding in following sections, since these were the resins with higher DMAP adsorption in MeOH.

6.4.3 Screening scavengers for MPTS adsorption

MPTS removal from a MeOH solution was assessed at acidic and alkaline pH, following the same approach described in the previous section for DMAP (Figure 6.5A). As expected, for the acidic resins, the absence of nucleophilic sites for sulfonate interaction, prevented any affinity towards the resins and almost no adsorption was observed. The activated charcoal also showed a low performance, with only 22% of binding, not affected by pH value. MPTS adsorption on IRA458 resin is pH dependent, being favoured at lower pH values. However, from the several scavengers assessed, the IRA68 resin, the only tertiary amine, showed a higher performance, regardless solution pH. The nucleophilic amine groups of this resin are prone to interact with the electrophilic MPTS groups with improved binding performance. Therefore, this resin ability for MPTS adsorption was further characterized concerning temperature effect, kinetics and equilibria isotherm models. Figure 6.5C shows a slow kinetic with only 67% and 90% of maximum resin capacity for MPTS reached after 4 and 8 h, respectively, which implies longer operation times. Moreover, MPTS removal over time is better described by a pseudo first order kinetic model ($r^2 = 0.993$) and the equilibrium isotherm is better described by the Langmuir adsorption model (Figure 6.5D). Both kinetic and isotherm equilibrium data were obtained at 25 °C, but the results of assays at different temperatures (Figure 6.5B) show that MPTS removal can be improved by increasing temperature.

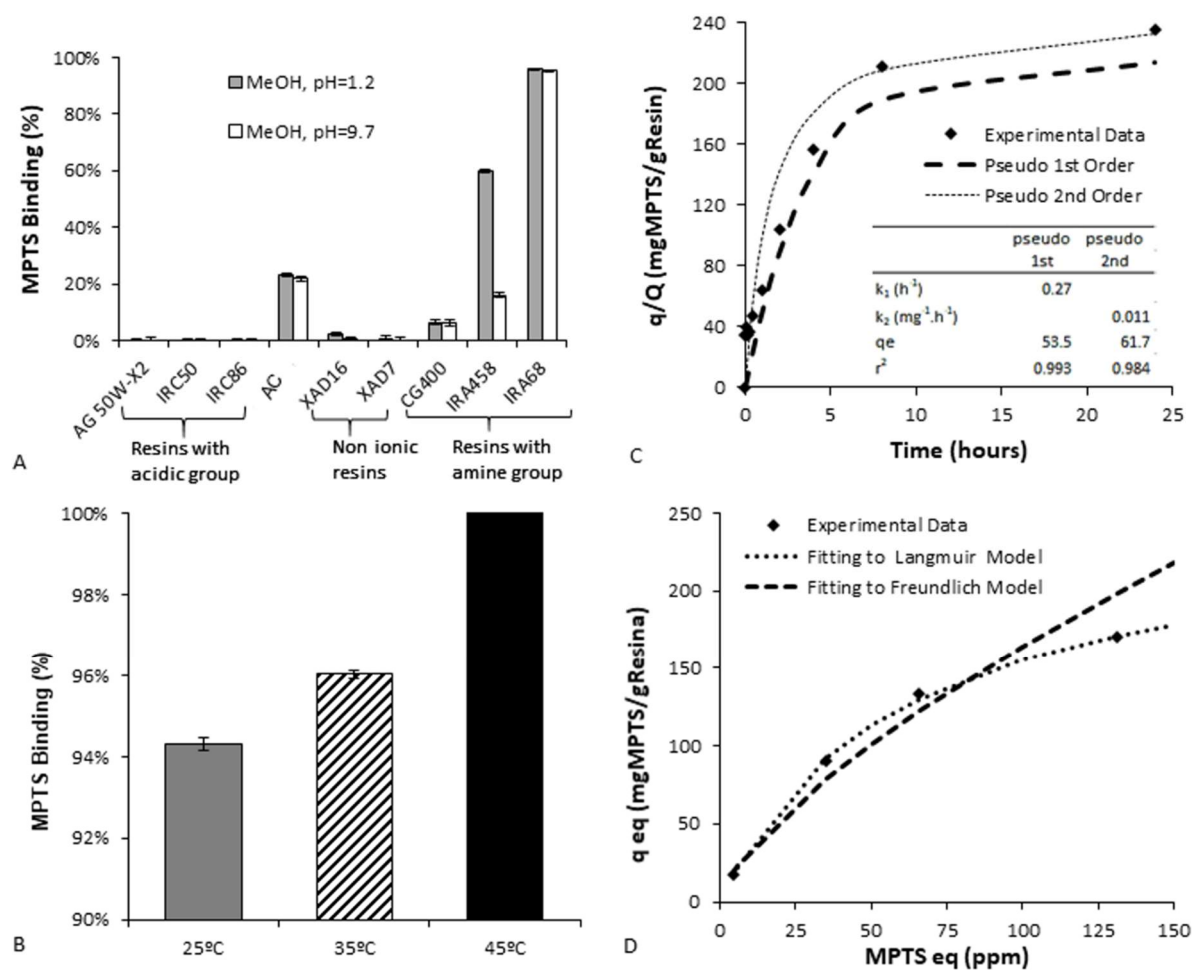


Figure 6.5. A) MPTS equilibrium binding percentage for several scavengers from a 1 g/L solution in MeOH at different pH values at 25 °C; B) MPTS equilibrium binding percentage to IRA68 resin for a 1 g/L solution in MeOH at different temperatures; C) MPTS binding capacity in IRA68 resin for a 1 g/L solution in MeOH along time; fitting trends to pseudo 1st and 2nd order kinetic models and respective parameters; D) MPTS equilibria isotherm in IRA68 resin and fitting trends to Langmuir and Freundlich models and respective parameters at 25 °C. AC – Activated charcoal.

6.4.4 Screening scavengers for low Meta adsorption

From the studies in MeOH, the resins selected for potential use in removal of GTIs from recrystallization mother liquor were either AG 50W-X2 or IRC50 for DMAP, and IRA68 for MPTS. To establish at which extent Meta is adsorbed on these resins, a test solution with 10 g/L API and 1 g/L GTI was subjected to these resins: AG 50W-X2 and IRC50 resins were assessed with DMAP while IRA68 was assessed with MPTS. The

results presented in Figure 6.6 show that AG 50W-X2 resin was able to remove about 93% of DMAP with only about 2% of Meta loss reaching a final ratio of 7.14 mgDMAP/gMeta. For IRC50 resin, DMAP removal was lower (about 63%), without Meta loss, reaching a final ratio of 37 mgDMAP/gMeta. From these results, the AG 50W-X2 resin is the scavenger providing a lower mgDMAP/gMeta ratio, which may enable recycling the API lost in recrystallization mother liquor into the recrystallization process.

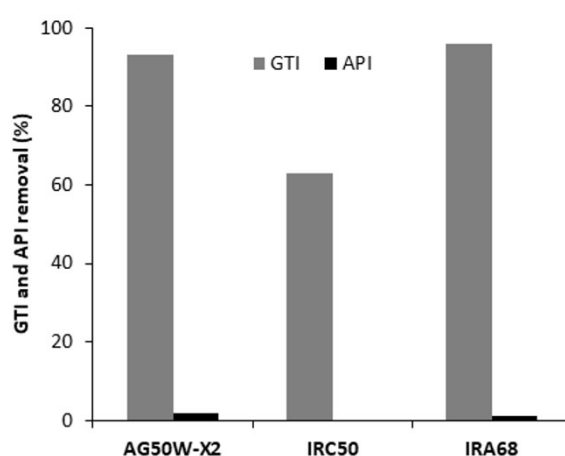


Figure 6.6. Amount of API and GTI removed in MeOH for Meta and DMAP mixture with AG 50W-X2 and IRC50 resins, and for Meta and MPTS mixture with IRA68 resin.

As shown in Figure 6.6, IRA68 resin was able to remove about 96% of MPTS with only about 1% of Meta loss reaching a final ratio of 4.04 mgMPTS/gMeta. This value is of the same order of magnitude to the one obtained for DMAP with the AG 50W-X2 resin (7.14 mgDMAP/Meta) and accordingly, IRA68 resin may allow to recycle the API lost in recrystallization mother liquor.

6.4.5 Mother liquor purification using resins: assessing strategies to combine different resins

6.4.5.1 ML purification with AG 50W-X2 and IRA68 resins in MeOH

AG 50W-X2 and IRA68 resins were selected for the removal of DMAP and MPTS from Meta recrystallization mother liquor and evaluate possible API recovery. A synthetic mother liquor solution was prepared in MeOH with API and GTI concentrations based on recrystallization assays: 6 g/L for Meta and 5 g/L for each GTI (DMAP and MPTS). As a single resin able to remove both GTIs efficiently was not identified, different adsorption strategies were assessed. In strategies 1 and 2, two sequential adsorption steps were considered, i.e. after the mother liquor is treated in a first adsorption step (using IRA68 or AG 50W-X2, for strategy 1 or 2 respectively), the treated solution is then submitted to further treatment with the second resin (AG 50W-X2 or IRA68, for strategy 1 or 2 respectively). In strategy 3, the mother liquor is treated with both resins simultaneously in one single step.

Table 6.2. Strategies for ML purification with AG 50W-X2 and IRA68 resins in MeOH.

Strategy	GTI removal (%)			Meta loss (%)	[GTI] after resin		mgGTI/gMeta [#]
	DMAP	MPTS	Total		DMAP (ppm)	MPTS (ppm)	
1 (IRA/AG)	85.2 ± 0.2	> 99.8	92.5 ± 0.2	11.6 ± 1.9	636.8 ± 8.3	< 5.0	102.4*
2 (AG/IRA)	89.9 ± 0.1	> 99.8	94.9 ± 0.1	13.1 ± 1.2	455.6 ± 7.1	< 5.0	74.7**
3 (AG+IRA)	99.9 ± 0.1	> 99.8	99.8 ± 0.1	9.6 ± 2.7	2.5 ± 1.1	< 5.0	1.2

Note: [#]The mgGTI/gMeta ratio considers the sum of the 2 GTI species and Meta detected in solution after adsorption resin step(s); *101.6 mgDMAP/gAPI and < 0.8 mgMPTS/gAPI; **73.9 mgDMAP/gAPI and < 0.8 mgMPTS/gAPI.

Table 6.2 shows the results obtained, including the final ratios of GTI/API achieved. The presence of both GTIs (DMAP and MPTS) in solution, has effect in API adsorption, being as high as 13% (Table 6.2) compared with only (1-2)% for the same resins when only one of the GTIs and Meta were present in the solution (Figure 6.6). Furthermore, in the case of two sequential adsorption steps, API loss is slightly higher (11-13%) than when GTI removal is carried out in one single step (9.6%), however the difference is not statistically significant ($p > 0.10$). With two sequential steps, the final ratios vary between (74.7-102.4) mgGTI/gMeta. These values are lower than the initial 200 mgGTI/gMeta present in Meta crude solution, allowing to use these strategies to recycle this API from the mother liquor to the next batch recrystallization.

The highest GTI removal and lowest API loss values were obtained for the one single adsorption step strategy 3, showing a synergistic effect of using both resins together. The final ratio of 1.2 mgGTI/gMeta, reached when using strategy 3, is considerably lower than the initial 200 mgGTI/gMeta present in the crude Meta solution. This promising pathway allows to recover 90% (5.4 g/L) of Meta present in the mother liquor. Note that, in the previous study, assessing Meta purification by recrystallization, from a total API loss of 15.6%, only 3.3% were lost through adsorption to activated charcoal, while the remaining 12.4% were lost through recrystallization mother liquor [10].

6.4.5.2. ML purification with AGW-X2 and IRA68 resins in MeOH in presence of secondary species

MPTS resin adsorption studies confirmed the electrophilic interaction of sulfonate groups from MPTS with nucleophilic amine groups of IRA68 resin in MeOH, and that this reaction is favoured with temperature. During Meta recrystallization, temperature is used to promote solvent exchange from DCM to MeOH. Considering DMAP and MPTS

in solution, this same interaction can take place between both GTIs. In fact, after the recrystallization, the appearance of two secondary products could be observed in HPLC spectra of the mother liquor. One of the products was identified as *p*-toluenesulfonic acid (PTSA) in its ionic form, by co-elution of the mother liquor test solution and PTSA commercially available. By ¹H NMR studies (Figures S6.4-S6.6), it was postulated that the other species corresponded to methylated DMAP (DMAP-Me), which is formed based on the reaction depicted in Figure 6.7. Accordingly, the mechanism previously proposed for binding between MPTS and amine-based nucleophilic scavengers involves the methylation of the resin amine group and formation of PTSA [16].

The results suggest that recrystallization of the model system used in this study yields a mother liquor with the API and, instead of two, four species that should be removed to acceptable levels, which is an interesting challenge. The three strategies presented in Table 6.2 were explored to answer this new and interesting challenge (Table 6.3). In each situation, the species DMAP, DMAP-Me, MPTS and PTSA were considered as impurities and a stringent case of a ML with 6 g/L Meta, 5 g/L (DMAP+DMAP-Me) and 5 g/L (MPTS+PTSA) was explored.

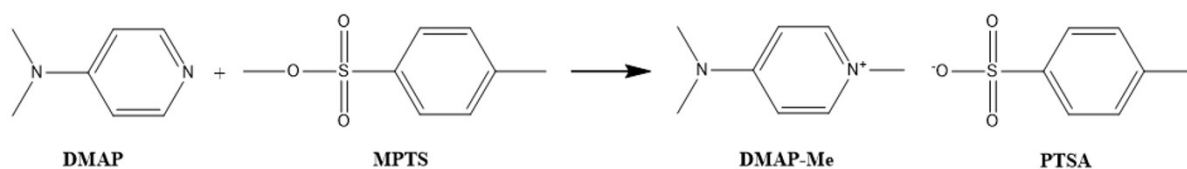


Figure 6.7. Proposed formation of DMAP-Me and PTSA in recrystallization mother liquor.

Table 6.3. Strategies for ML purification with AG 50W-X2 and IRA68 resins in MeOH in the presence of secondary species.

Strategy	GTI Removal (%)			Meta loss (%)	[GTI] after resin		mgGTI/gMeta [#]
	DMAP DMAP-Me	MPTS PTSA	Total		MPTS (ppm)	PTSA (ppm)	
1A (IRA/AG)	87.0 ± 0.7	55.4 ± 1.1	71.2 ± 1.3	28.3 ± 0.8	< 5.0	2232.32	670.0*
2A (AG/IRA)	92.5 ± 0.1	87.5 ± 1.3	90.0 ± 1.3	33.2 ± 0.3	< 5.0	626.26	249.9**
3A (AG+IRA)	99.8 ± 0.3	100	99.9 ± 0.3	19.0 ± 3.8	< 5.0	< 2.5	2.1

Note: [#]The mgGTI/gMeta ratio considers the sum of all the 4 GTI species and Meta detected in solution after adsorption resin step(s); *151.1 mgGTI/gAPI for DMAP/DMAP-Me and 518.9 mgGTI/gAPI for MPTS/PTSA; **93.6 mgGTI/gAPI for DMAP/DMAP-Me and 156.3 mgGTI/gAPI for MPTS/PTSA.

The results presented in Table 6.3 confirm that, the simultaneous presence of the several GTIs in solution, leads to a higher API adsorption (19-33%). The lowest API losses (19%) are observed for strategy 3, when GTIs removal is carried out in one single step using both resins together. For strategy 1 and 2, when two sequential adsorption steps are used, the final ratios vary between 249.9-670.0 mgGTI/gMeta. These values, are higher than the 200 mgGTI/gMeta ratio of the post-reaction stream initially fed to the recrystallization, making challenging to explore these adsorption strategies to recycle the mother liquor back to the process.

A synergistic effect was again observed in strategy 3A (Table 6.3), with the highest GTI removal, when both resins are used together, reaching a final ratio of 2.1 mgGTI/gMeta and 81% (4.9 g/L) of Meta recovery from the recrystallization mother liquor. Therefore strategy 3 is a promising pathway for API reclaiming from the mother liquor, allowing significant removal of GTIs and secondary species.

6.4.6 API reclaiming: assessment of different process approaches

This section presents theoretical calculations for generic GTI removal and API reclaiming considering, not only the results obtained, but several possible cases, following the two approaches illustrated in Figure 6.8. Therefore, calculations include: (i) Direct API reclaiming from the mother liquor, by using the resins to remove GTIs to ultra-low concentrations; or (ii) Recycle API rich stream obtained after resin treatment of the mother liquor to the recrystallization feed, where the resin separation reduces the GTI/API ratio from high values of the mother liquor to lower values present in the initial post-synthetic API crude stream. The higher the API loss, the higher the impact on the introduction of the resin reclaiming step. Therefore, the examples considered 25%, 20%, 15% and 10% API loss in the original recrystallization/activated charcoal adsorption (i.e. losses for the recrystallization mother liquor of 21.7%, 16.7%, 11.7% and 6.7%, considering a 3.3% API loss through adsorption to activated charcoal which, by using the resin API reclaiming approach, can be decreased to 7.6%, 6.6%, 5.6% and 4.6%). These cases are illustrated in Figure 6.9A. Considering a 20% API binding to the resin and a stringent case where the methanolic mother liquor contains 6 g/L API and 10 g/L GTI (5 g/L of each GTI), a GTI removal higher than 99.6% (Table 6.3, strategy 3A) would ensure a value lower than 7.5 mgGTI/gMeta for the stream directly processed through the resins (e.g. for 99.9% GTI removal observed in strategy 3A of Table 6.3, a 2.1 mgGTI/gAPI is attained). This result complies with the TTC of 7.5 mgGTI/gAPI for the case study of maximum dosages of 200 µg/day for airways delivery.

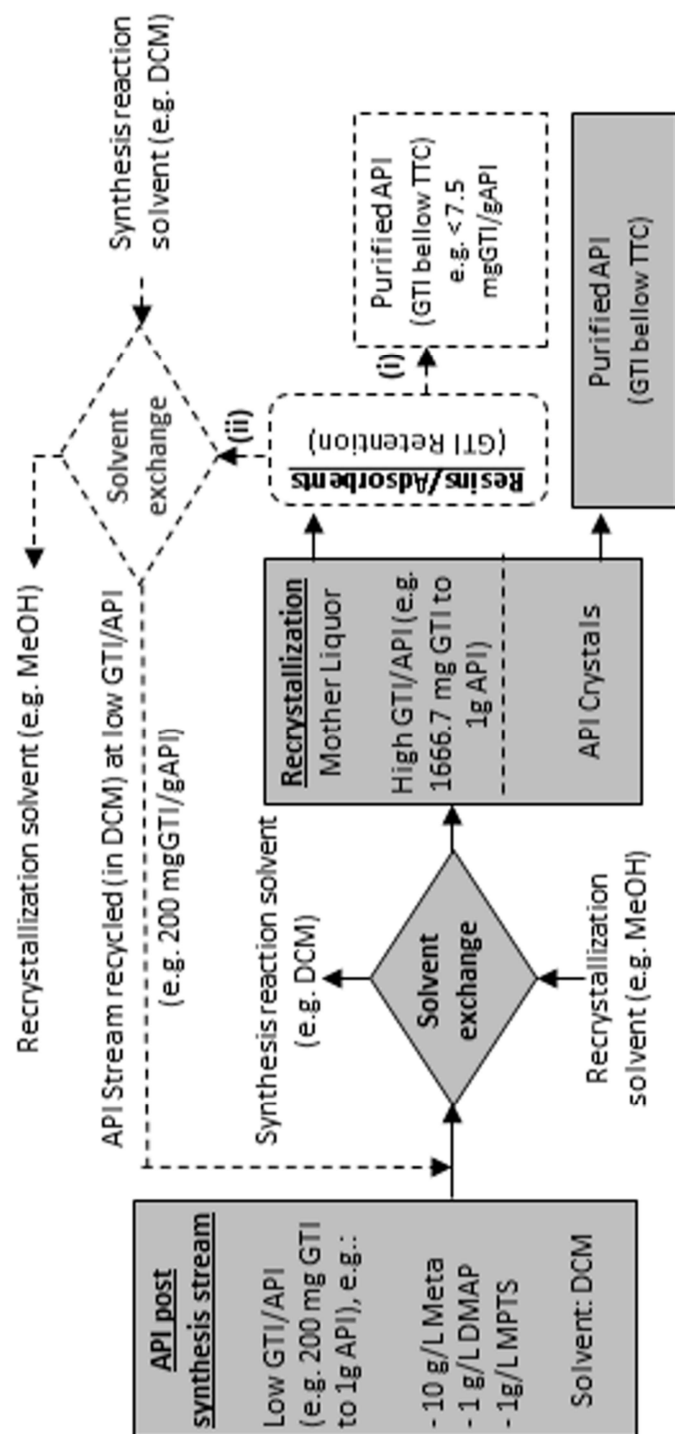
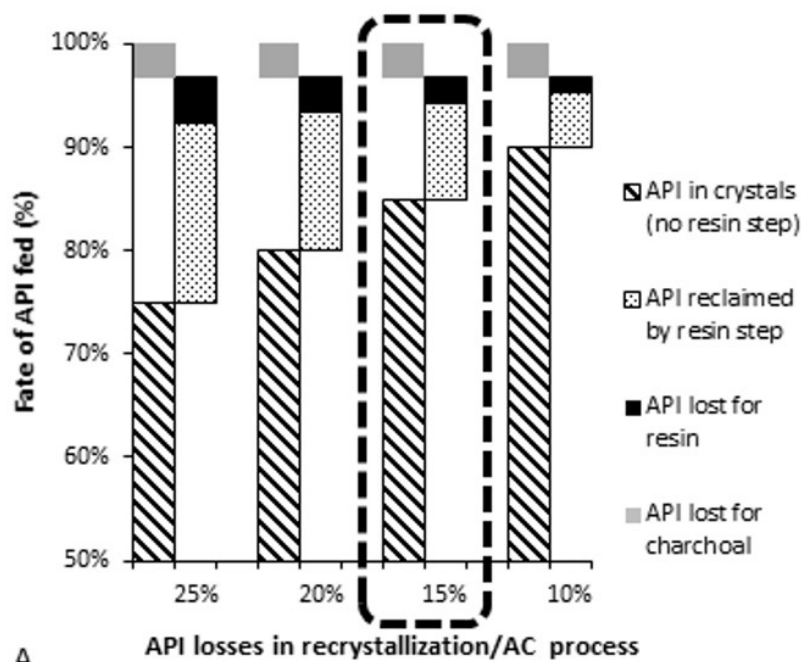
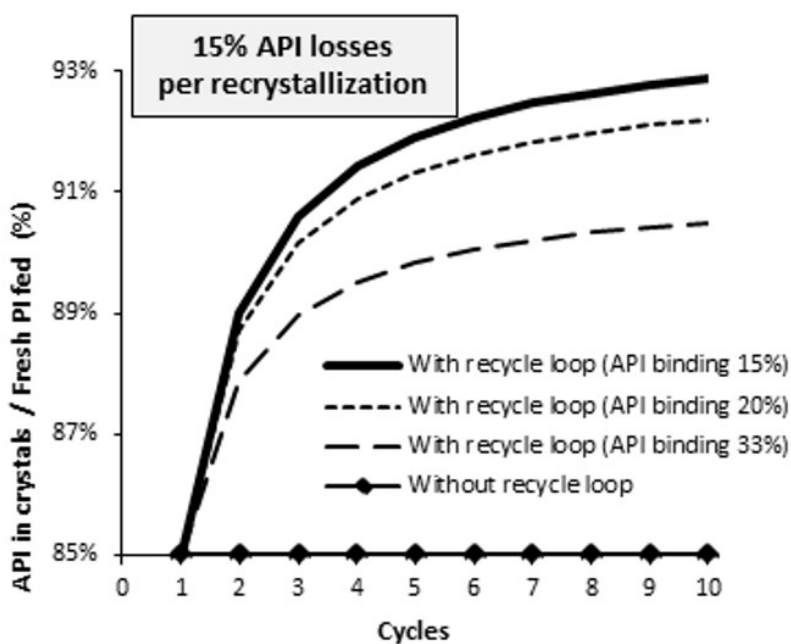


Figure 6.8. Schematic illustration of the role of a resin based step, in two different approaches, to: (i) remove GTI from recrystallization mother liquor to an ultra-low level, allowing direct reclaim of API from mother liquor; or (ii) remove GTI from recrystallization mother liquor to an intermediate low level, decreasing the GTI/API ratio allowing mother liquor recycling to initial post-synthetic API crude stream fed into recrystallization. Grey filled boxes and solid black lines represent recrystallization process alone; black dotted lines and empty boxes represent steps for mother liquor subjected to resin treatment for API loss mitigation.



A



B

Figure 6.9. Potential to improve API yields in recrystallization/activated charcoal process by API reclaiming directly from the mother liquor or recycling feedback loop of mother liquor after resin treatment: A) Calculations for potential direct API reclaim as function of API losses in recrystallization/activated charcoal process (assuming a 20% API binding to the resins), or after steady state is reached through successive recycling of resin treated mother liquor; B) Transient profile of API isolated as crystals when resin treated mother liquor streams are recycled into next batch recrystallization/activated charcoal cycle (assuming a case of an initial recrystallization/activated charcoal process with 15% API losses and several percentages of API binding to the resins).

For removal of potential GTIs from other API post reaction streams, the use of resins may not reach so high GTI removals and thus, the stream processed by the resins may not comply with TTC values. For example, considering the same 6 g/L API to 10 g/L GTI (5 g/L of each GTI), i.e. 1667 mgGTI/gAPI, GTI removals (about 71% or 90%) and API losses (28% or 33%), did result on GTI/API ratios of 670 or 250 mgGTI/API for strategies 1A and 2A (Table 6.3), respectively. These values are considerably higher than 7.5 mgGTI/gAPI. For such cases, the resin step can be used to decrease the high GTI to API ratio observed in mother liquor to the initial post-synthetic API crude stream level, allowing recycle back the mother liquor stream in the next batch recrystallization (after solvent exchange from MeOH to DCM). The 250 mgGTI/gAPI ratio obtained in strategy 2A (Table 6.3) is already quite close to the GTI/API ratio of the initial post-synthetic API crude stream fed into the recrystallization process at a value of 200 mgGTI/gAPI. Hypothetical cases able to meet such 200 mgGTI/gAPI ratio include resins performances for API bindings of 33%, 20% or 15% and GTI removals of 92%, 90.5% or 90%, respectively.

The calculation of the transition profile, in increase of API isolated in the crystals, as API in the mother liquor is recycled into the next batch recrystallization/activated charcoal cycle, is illustrated in Figure 6.9A, showing the effect of three levels of API binding to resins for a recrystallization/activated charcoal process with an initial API loss of 15%. Calculations taken for Figure 6.9B consider that the overall API fed to each new successive recrystallization is increasing over time since, the API in resin treated mother liquor of the previous recrystallization is added to the constant value of “fresh API” stream. Therefore, increase in percentage of “API in the crystals/fresh API fed” during the transition profile is not driven by an increase in recrystallization yield, but higher

amount of API fed into each recrystallization, until convergence of this value, when resin treated mother liquor is recycled.

6.4.7 Economic Assessment

The approaches suggested in this work to mitigate API losses are (i) to recover the API directly from the mother liquor using a resin step or, (ii) to recycle the API from recrystallization mother liquor, after the resin adsorption step that re-establishes the GTI to API mass ratio found in Meta crude solution, into a next API purification by batch recrystallization. The economic impact involved in these proposed API recovery strategies is here briefly considered. For example, in the central case scenario, in which 15% of API is lost to the mother liquor at a concentration of 6 g/L, the possibility to recover 80% of such API represents a gain in API yield of 12% (from 85% to 97%). The cost of introducing an additional resin adsorption step is preliminary assessed.

The major costs in adsorption processes is often related with infrastructure (Figure 6.10), especially in the case of two sequential resin steps (70%) (Figure 6.10, right). This cost analysis follows a previous work [10] considering batch operations of 1 m³ featuring 10 kg of API, and an annual production of 10 batches. The current analysis considers only incremental capital and operation cost required to introduce the resin operation unit at total values of 66 k€ and 118 k€ per year, corresponding to 6.6 k€ and 11.8 k€ per batch, for direct API reclaiming from mother liquor or API recirculation, respectively.

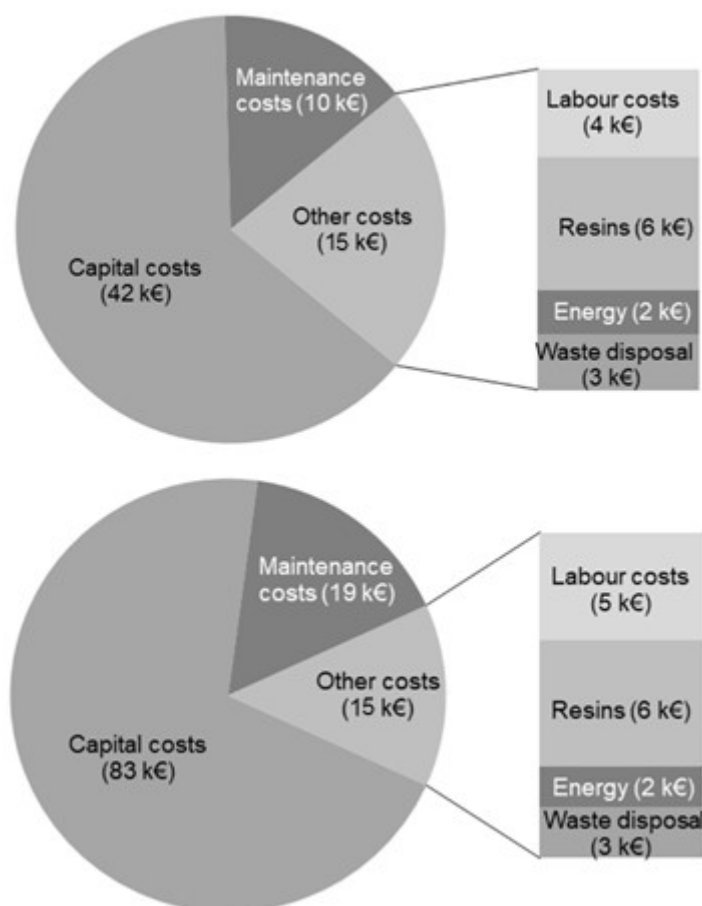


Figure 6.10. Costs associated to API resin adsorption step for: top - API reclaiming directly from mother liquor; bottom - recycling feedback loop of mother liquor after resin treatment. Assumptions: the resin is not recycled; no fresh solvent is added; solvent disposal is not considered; additional equipment concerns pumps, fluidized bed reactors for adsorption and extended period of oven and dryer usage, with the later two already included in the recrystallization process.

For the central scenario, the capital cost was calculated assuming the use of non-depreciated equipment, linear depreciation over 10 years and infrastructure and respective costs were calculated considering equipment allocation according with operation times. Facility maintenance was assumed to be 10 k€ and 19 k€, per year, which is significant.

Operation costs consider labour, energy requirements, resins and solid waste disposal. The analysis follows a conservative view in which resins are not recycled and the correspondent solid waste generated is sent to disposal. In these case scenarios the resins correspond to about (5-10)% of total cost with solid waste disposal being evaluated

in 3 k€ corresponding to (2-3)% of total adsorption cost. Labour and energy is estimated considering operations carried out. The mother liquor on the original recrystallization process requires to be distilled for solvent recycle or disposed, therefore we consider that the introduction of a resin step does not imply additional costs with solvent treatment or disposal.

Figure 6.10 represents central case scenarios in which an API cost of 6 k€/Kg was stipulated [17]. In the case of direct API reclaiming from the mother liquor, the API savings cover the costs associated with the additional adsorption step considering 80% recovery of the 6 g/L API (i.e. 15% API is initially present in the mother liquor and would be otherwise lost) (Figure 6.11).

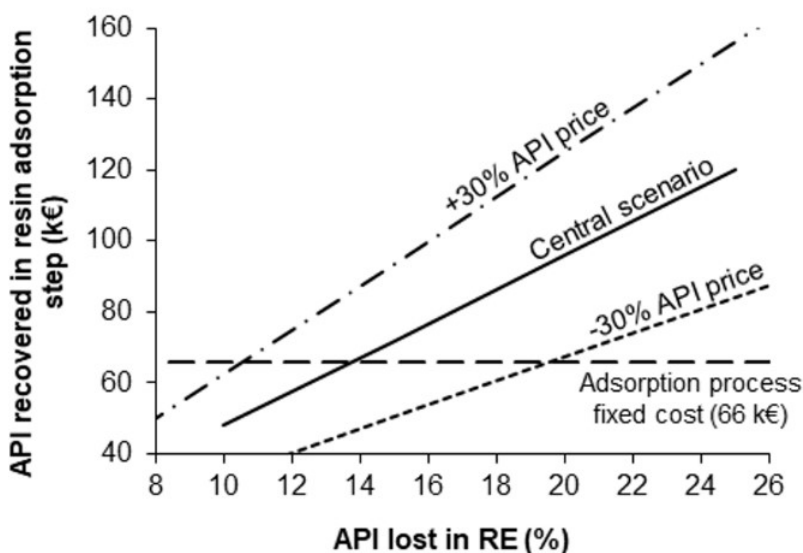


Figure 6.11. Potential gain in API reclaiming directly from the mother liquor with a resin adsorption step for several percentages (10 – 25)% of API loss in mother liquor (assuming a non-optimized case scenario considering the use of 50 kg of selective agent per 1 m³ of mother liquor and a constant recovery of 80% of API) and considering several scenarios for API price in €/Kg.

Figure 6.11 shows yearly API savings for different scenarios of API lost in the mother liquor, assuming a constant API reclaiming of 80%. The horizontal dashed line shows the yearly cost of introducing the resin step. For example, for the central case scenario, with an API price of 6 k€/Kg, the cost associated to the adsorption step is offset

for an API loss of 14%. For an API that is 30% more expensive, the adsorption cost is offset for a 11% API loss. On the other hand, for an API that is 30% cheaper, the cost of adsorption is only offset at a higher API loss of 20%. Since APIs have an associated high production cost, these results show that the introduction of an additional adsorption step, after a recrystallization, is economically feasible for API recovery from mother liquor, that would be otherwise lost.

6.5. Conclusions

Several commercially available resins were screened for DMAP and MPTS, indicating that AG 50W-X2 and IRA68 resins were the ones able to efficiently remove these products, in MeOH in one single step, with adsorption of 99.8% of DMAP and its methylated conjugate (DMAP-Me) and the full removal of PTSA and MPTS from the mother liquor with an API loss of about 19%, reaching a final ratio of 2.1 mgGTI/gMeta, enabling the reintroduction of this enriched Meta solution to the process. The potential for improving the recrystallization economics, through mitigation of API losses is suggested based on: (i) direct reclaiming of API from a recrystallization mother liquor, when resin step is able to bring down GTI to ultra-low levels, and so GTI to API ratio in the mother liquor is able to comply with TTC or; (ii) through recycling recrystallization resin treated mother liquor into the next batch recrystallization/activated charcoal cycle, where such mother liquor has GTI/API ratio that meets the value of the initial post-synthetic API crude stream. Recycling the mother liquor may be a more challenging strategy to implement, since the recrystallization step in many processes is also used to purge, through the mother liquor, additional impurities driven from the previous API synthetic steps and, recycling of this stream may require process requalification.

6.6. References

- [1] a) Bousquet, J., Mometasone furoate: an effective anti-inflammatory with a well-defined safety and tolerability profile in the treatment of asthma, *Int. J. Clinical Practice*, 63, 2009, 806-819; b) Heggie, W.; Bandarra, J. Process for the preparation of mometasone furoate. US 6177560 B1, 2001.
- [2] Draper R. W., et al, Unusual hydroxy- γ -sultone byproducts of steroid 21-methanesulfonylation. An efficient synthesis of mometasone 17-furoate (Sch 32088), *Tetrahedron*, 55, 1999, 3355-3364.
- [3] Sawatari, K., et al, Relationships between chemical structures and mutagenicity: A preliminary survey for a database of mutagenicity test results of new work place chemicals, *Ind. Health*, 39, 2001, 341-345.
- [4] Müller, L., et al, A rationale for determining, testing, and controlling specific impurities in pharmaceuticals that possess potential for genotoxicity, *Regul. Toxicol. Pharmacol*, 44, 2006, 198-211.
- [5] Szekely, G., et al, Genotoxic impurities in pharmaceutical manufacturing: Sources, regulations, and mitigation. *Chem. Rev.* 16, 2015, 8182-8229.
- [6] Zweifel G. S, et al, *Modern Organic Synthesis: An Introduction*; Wiley: Hoboken, 2017.
- [7] Vicente A. I., et al, Solvent compatible polymer functionalization with adenine, a DNA base, for API degenotoxification: Preparation and characterization, *Sep. Purif. Technol.*, 179, 2017, 438–448.
- [8] Gerber C.; Toelle H., What happened: The chemistry side of the incident with EMS contamination in Viracept tablets, *Toxicol. Lett.*, 190, 2009, 248–253.
- [9] Fu, X., et al, Process for the Preparation of 17-esters of 9 α ,21-dihalo-pregnane-11 β ,17 α -diol-20-ones, WO1998000437 A1, 1998.

- [10] Székely, G., et al Environmental and economic analysis for selection and engineering sustainable API degenotoxification processes, *Green Chem.*, 15, 2013, 210-225.
- [11] Li, C., et al, Chemical modification of Amberlite XAD-4 by carbonyl groups for phenol adsorption from wastewater, *Chem. Eng. J.*, 229, 2013, 20-26.
- [12] Belhachemi, M.; Addoun, F., Comparative adsorption isotherms and modeling of methylene blue onto activated carbons, *Appl. Water Sci.*, 1, 2011, 111-117.
- [13] Tosun, I., Ammonium removal from aqueous solutions by clinoptilolite: Determination of isotherm and thermodynamic parameters and comparison of kinetics by the double exponential model and conventional kinetic models, *Int. J. Environ. Res. Public Health*, 9, 2012, 970-984.
- [14] Qiu, H., et al, Critical review in adsorption kinetic models, *J. Zhejiang Univ. Sci. A*, 10, 2009, 716-724.
- [15] Scudder, P. H. *Electron flow in organic chemistry: a decision-based guide to organic mechanisms*; Wiley: Hoboken, N.J., 2013.
- [16] Kecili, R., et al, Selective scavenging of the genotoxic impurity methyl p-toluenesulfonate from pharmaceutical formulations, *Sep. Purif. Technol.*, 103, 2013, 173–179.
- [17] <https://www.pharmacompass.com/active-pharmaceutical-ingredients/mometasone-furoate> (assessed in June 2018).

Chapter VII

**Optimization of organic dnanofiltration with adsorption
recycle loop for product reclaiming: application to genotoxics
removal from active pharmaceutical compounds**

Paper will be submitted to Journal of Membrane Science

7.1. Outline

This is the last experimental chapter and, as Chapter VI is dedicated to process improvement, using a hybrid approach to recover the API lost in the main unit operation. But in this chapter, a mathematic model to help in the decision among which process is most suitable for API purification was created (section 7.3), and the decision framework depending on the type of membrane or adsorber available in a wide range is presented in section 7.5, as a function of parameters intrinsic to each unit operation (OSN in section 7.5.2 or adsorption in section 7.5.3), verifying the loss of API and classifying it as acceptable, worrying or prohibitive. As an alternative to processes whose API loss is considered worrying or prohibitive, a hybrid process was developed (section 7.5.4) combining the two unit operations. Membrane solute rejection was used as parameter for OSN. In the case of adsorption, two adsorption isotherm models were considered (Langmuir and Freundlich fitting models). For the hybrid process, the effect of recirculation volume were investigated as the amount of adsorber used (sections 7.5.4.2 and 7.5.4.3). One case of each model was experimentally validated in section 7.5.5, and in the case of hybrid process, a drastic reduction of the API loss was achieved (4.8%), for the study case presented. When using the isolated unit operations, the API loss would be 27.7 % for OSN and more than 99% in the case of adsorption. An economic and environmental analysis were assessed comparing OSN and hybrid process (section 7.5.6) showing that the later approach to be the most environmentally friend.

Keywords: Hybrid process, Adsorption, OSN, API purification,

7.2. Introduction

Active pharmaceutical ingredients (APIs) available in the market are mostly synthesized in organic solvent media, using highly reactive molecules, and usually, low levels of reagents, fractions of catalysts, or by-products are present in the final API or drug product as impurities. Some of these impurities have unwanted toxicities, including genotoxicity and carcinogenicity. Therefore, related API administration risks for patient's health caused by the genotoxic impurities (GTIs) has become an increasing concern from pharmaceutical companies and regulatory authorities [1]. Although it is desirable to avoid the use of GTIs in the manufacture of APIs, this is not always possible. Thus, it is mandatory to produce APIs with low GTI content, controlled below the Threshold of Toxicological Concern (TTC) established by regulatory authorities (1.5 µg/day) [2].

In order to attain product purity thresholds a possible practice is the use of organic solvent nanofiltration (OSN), since this technique allows solute separation ranging from 200 to 2000 Da, being an alternative with rapid isolation of a target, and high yields using low energy compared with conventional methods, such as chromatography and distillation [3,4]. OSN in diafiltration mode can remove the impurity, usually smaller molecules, through the permeate, based in the difference of membrane rejection for product and impurities. However, this approach requires a rejection of the product near 100%, otherwise, as diavolumes increase product losses through OSN permeate become significant, and an increase in rejection of impurity also implies an increase in diavolumes. Moreover, solvent intensity is high and solvent recycle is translated in high energy use.

Approaches to address this issue can include the use of membrane cascades or solvent recycling, both for minimization of product losses and use of less solvent [5-7].

A stringent case, where product is very expensive is API purification, where GTIs have to be present in a very low impurity threshold defined by TTC, make the purification step challenging. Since, to achieve ultralow levels of contamination, significant API losses take place, the development of new processes becomes necessary for the purification to be reached with minimal API losses.

In the previous chapters the use of adsorbers to remove GTIs from solvent matrices was discussed. Previously, using different adsorbers, and according to GTI and API, different efficiencies on GTI removal and API losses could be obtained. In some cases, the adsorber shows to be extremely effective at high GTI concentrations, well above the values usually found in API and API intermediates post reaction streams, which can be useful when designing processes combining two separation operation units, in which API lost in the first operation unit (e.g. recrystallization in Chapter VI or OSN in diafiltration mode in this chapter) is fed to a second operation unit (e.g. resin adsorption in Chapter VI, or enhanced PBI in this chapter) to decrease the ratio of GTI/API to a value that allows to recycle back such upgraded stream into the first operation unit.

Importantly, in this chapter, we aim to discuss and provide guidelines for GTI removals at minimal API losses. Specifically, we aim to discuss when it makes sense to use OSN in diafiltration mode alone, adsorption alone, or OSN in diafiltration combined with an adsorption step. Therefore, the specific objectives of this chapter are:

1. Establish a framework to guide when it is reasonable to use OSN in diafiltration mode.
2. Establish a framework to guide when it is reasonable to use adsorption.

3. Identify in which cases recycling of product from OSN to adsorption is necessary.
4. Show the use of a hybrid process for GTI removal from API, combining organic solvent nanofiltration with polybenzimidazole adsorbents.
5. Perform economic and environmental analysis evaluating OSN and hybrid process using green metrics.

7.3. Mathematical approach: Modeling section

7.3.1. Set-up and boundaries

Three mathematical models were established using as objective function the value for the GTI/API ratio on the final outlet stream, i.e, the concentrations obtained in the end ($C_{out,GTI}$ and $C_{out,API}$) of the operation from the retentate, in case of OSN, or the eluate in the case of adsorption. The calculations were performed to reach a target objective of a maximum contamination ($MaxC$) allowed of 7.5 mgGTI/gAPI (equation 7.1), corresponding to the less stringent case of Meta application, with administrations of 200 $\mu\text{g/day}$ for airways treatment (e.g. allergic rhinitis and asthma).

$$MaxC = \frac{C_{out,GTI} (\frac{mg}{L})}{C_{out,API} (\frac{g}{L})} = 7.5 (\frac{mgGTI}{gAPI}) \quad (7.1)$$

The calculations were performed considering as input a post-reaction solution of 10 g/L of API and 1000 mg/L of GTI. All the calculations were based on a processing fix volume of post reaction stream.

The main operating parameters that the model will calculate to reach the target objective will be

- Diavolumes (D) for OSN

- Amount of adsorber (m).

The models uses a discrete number of values for the main parameters within a given range (described below), which were selected taking into account the values obtained from the previous chapters and from the literature. The main parameters considered, for each solute (API and GTI) were:

-Membrane Rejection for OSN, and

-Isotherm adsorption constants.

Solution flux and adsorption kinetics were then considered on economic analysis to define operation times and membrane areas.

7.3.2. Organic solvent nano diafiltrations (OSNd)

Membrane Rejections to the solutes, the main intrinsic parameter ruling organic solvent nanodiafiltration (OSNd), were computed as a constant parameter along the OSN filtrations according with equation 7.2:

$$R_{x,i}(\%) = \left(1 - \frac{C_{P,x,i}}{C_{F,x,i}}\right) \cdot 100\% \quad (7.2)$$

where x is GTI or API, $C_{P,x,i}$ and $C_{F,x,i}$ are concentration of GTI or API in the Permeate and in the Feed, which are variable over diavolume “i” used. $C_{F,x, \text{when } i=0}$ is the concentrations of GTI or API fed at the beginning of the diafiltration. Rejections are assumed to be maintained constant over the diafiltrations. The feed volume (V_F) and retentate volume (V_R) are maintained constant over diafiltrations and permeate volume ($V_{P,i}$) and the fresh volume of solvent added ($V_{Add,i}$) is assumed to be equal.

Diavolumes, the main operating parameter to be adjusted, are defined as the Volume added per the initial Volume

$$D_i = \frac{V_{Add,i}}{V_F} = \frac{V_{P,i}}{V_F} \quad (7.3)$$

The following mass balance can be established

$$V_F C_F = V_R C_{R,x,i} + V_{P,i} C_{P,x,i} \quad (7.4)$$

Based on the assumptions above, the $C_{R,x,i}$ and mass balance equations can be calculated for each diavolume (D_i) [8] from Eq. 7.5

$$\frac{C_{R,x}}{C_{F,x}} = e^{-D_i(1-R_x)} \quad (7.5)$$

Applying Equation 7.5 to GTI and API and considering the established value of maximum contamination allowed (eq. 7.1), the diavolumes needed to API purification will be given by equations 7.6a-c.

$$D = \frac{\ln\left(\frac{C_{R,GTI}/C_{R,API}}{C_{F,GTI}/C_{F,API}}\right)}{Rej_{GTI} - Rej_{API}} \quad (7.6a)$$

Note that while $C_{R,GTI}/C_{R,API}$ is our objective function, with $C_{F,GTI}$ the post reaction GTI concentration and $C_{F,API}$ the post reaction API concentration. Therefore Diavolumes used can be calculated as:

$$D = \frac{\ln\left(\frac{MaxC_{GTIin}^{API}}{C_{GTIin}}\right)}{R_{GTI} - R_{API}} \quad (7.6b)$$

Considering that, our case study is set to values of 7.5 mgGTI/gAPI and initial concentrations of 1000 mg/L of GTI and 10 g/L of API , the Diavolumes required to fulfill the TTC, , can be analytically calculated according to the membrane rejections and the equation below:

$$D = \frac{\ln\left(7.5 \frac{10}{1000}\right)}{R_{GTI} - R_{API}} = \frac{-2.59}{R_{GTI} - R_{API}} \quad (7.6c)$$

Membrane Rejection ranges considered: Again, the main parameter to describe OSN is Membrane Rejection and thus, the following range of membrane rejections were considered:

-0 to 70% for GTI (8 values)

-80% to 99.99% for API (7 values)

Therefore, 56 membrane selective behaviours were considered.

API Losses: The model was used to compute both diavolumes required to reach our target objective of 7.5 mgGTI/gAPI as well as the API losses according to (eq. 7.8), calculated by rearrangement of equation 7.5 for each Diavolume and R_{API} :

$$API \text{ loss } (\%) = \{1 - e^{[-D(1-R_{API})]}\}. 100\% \quad (7.8)$$

Operation times: Solution flux through the membrane (J_i) was also considered as an important parameter for process economics and to define operation times (t_i) and membrane area required, as presented in Eq. 7.9:

$$J_i = \frac{V_{P,i}}{A_m t_i} \quad (7.9)$$

where t_i is filtration time and A_m is the area of the membrane.

Solution flux through the membrane depends of applied pressure and solution properties that will condition solution permeability through the membrane, such as solvent used, solutes properties and concentration, solution viscosity and resulting osmotic pressure.

7.3.3. Adsorption

The adsorption processes are usually described using isotherm equations. In this model, we only considered two isotherm fitting models, namely Langmuir and Freundlich. Additionally, we did also considered that for a specific adsorber, both GTI and API follow the same adsorption isotherm behavior and, in the particular case of the Freundlich model, mainly chemisorption was considered with $1/n$ parameter equal or less than 1. Also, we did not consider here the use of adsorber columns, but only simple batches with adsorber beds fed with API post reaction stream, and unload after the adsorption equilibrium is reached. Taken into account these limitations of the models, the classic equations for Langmuir and Freundlich isotherm models [8] were considered, Eq. (7.10) and (7.11), respectively.

$$q_{e,x,i} = \frac{Q_{max,x,i} k_{L,x,i} C_{e,x,i}}{(1 + k_{L,x,i} C_{e,x,i})} \quad (7.10)$$

$$q_{e,x,i} = k_{F,x,i} C_{e,x,i}^{\frac{1}{n}} \quad (7.11)$$

$q_{e,x,i}$ is the adsorber adsorption capacity (mg/g for GTI, g/g for API), Q_{\max} (mg/g) is the maximum amount of GTI bound to the adsorber in a monolayer for the Langmuir model, whereas k_L and k_F are equilibrium constants (L/mg) for the Langmuir and Freundlich models, respectively, and are related with the energy taken for adsorption, n is a parameter related with the surface layer heterogeneity.

Isotherms parameters are the main intrinsic parameter ruling adsorption:

The adsorber mass is the main operating parameter to be adjusted in an adsorption process. The adsorber mass can be calculated analytically considering our target objective, considering the isotherms equations and the following mass balance can be established in terms of mg for GTI and g for API:

$$V \cdot C_{in,x,i} = V \cdot C_{e,x,i} + q_{e,x,i} \cdot m \quad (7.12)$$

where V is the volume of the post-reaction stream submitted to the batch adsorption. Again, equation 7.1 can be used as an objective function. Therefore, to calculate the adsorber mass, analytical equations for the $C_{e,GTI,i}$ and $C_{e,API,i}$ are necessary to be defined first.

For **Langmuir isotherms**, by replacing equation 7.12 on 7.10, it is possible to obtain, the analytical concentration for the equilibrium, given by equation 7.13.

$$C_{e,x,i} = \frac{-V - m \cdot Q_{\max} \cdot k_{L,x,i} + k_{L,x,i} \cdot C_{in,x,i} \cdot V}{2k_{L,x,i} \cdot V} + \frac{\sqrt{V^2 + 2m \cdot Q_{\max} \cdot k_{L,x,i} \cdot V + 2C_{in,x,i} \cdot k_{L,x,i} \cdot V^2 - 2m \cdot Q_{\max} \cdot C_{in,x,i} \cdot k_{L,x,i} \cdot V + k_{L,x,i}^2 \cdot C_{in,x,i}^2 \cdot V^2 + m^2 \cdot Q_{\max}^2 \cdot k_{L,x,i}^2}}{2k_{L,x,i} \cdot V} \quad (7.13)$$

For **Freundlich isotherms**, by replacing equation 7.12 on 7.11 and considering n to be 1, 2 or 3, it is possible to obtain the analytical concentration for the equilibrium, given by equations 7.14 a-c:

For n=1:

$$C_{e,x,i} = \frac{V \cdot C_{in,x,i}}{k_{F,x,i} \cdot m + V} \quad (7.14a)$$

Having the analytical solution for adsorber mass calculation:

$$m = V \left(\frac{MaxC \cdot C_{in,API,i} - C_{in,GTI,i}}{C_{in,GTI,i} \cdot k_{F,API,i} - MaxC \cdot C_{in,API,i} \cdot k_{F,GTI,i}} \right) \quad (7.14a')$$

For n=2:

$$C_{e,x,i} = \frac{2C_{in,x,i} \cdot V^2 + m^2 \cdot k_{F,x,i}^2 - \sqrt{4C_{in,x,i} \cdot m^2 \cdot k_{F,x,i}^2 \cdot V^2 + m^4 \cdot k_{F,x,i}^4}}{2V^2} \quad (7.14b)$$

For n=3:

$$C_{e,x,i} = \sqrt[3]{\frac{-C_{in,x,i} \cdot m^3 \cdot k_{F,x,i}^3}{2V^3} + \sqrt{\frac{C_{in,x,i}^2 \cdot m^6 \cdot k_{F,x,i}^6}{4V^6} + \frac{m^9 \cdot k_{F,x,i}^9}{27V^9}}} + \sqrt[3]{\frac{-C_{in,x,i} \cdot m^3 \cdot k_{F,x,i}^3}{2V^3} - \sqrt{\frac{C_{in,x,i}^2 \cdot m^6 \cdot k_{F,x,i}^6}{4V^6} + \frac{m^9 \cdot k_{F,x,i}^9}{27V^9}}} + C_{in,x,i} \quad (7.14c)$$

Note that to meet the objective (MaxC), the variable $C_{e,x,i} \in \mathbb{R}_+^*$. Since polynomial equations, such as quadratic and cubic, assumes imaginary numbers as possible solutions, the equations 7.14 b and 7.14 c are the ones that satisfy at the same time the existence conditions to API and GTI. (more information in Appendix C).

Isotherms parameters ranges considered: Again, the main parameter to describe adsorption are the isotherms parameters. However, while OSN only has one main parameter, membrane rejection per solute, to be considered on the equations

solutions, each isotherm has two parameters. Therefore, the following approaches and ranges of parameters were assessed:

For the adsorbers that follow **Langmuir's model**, the strategy is to consider different ranges of parameters corresponding first to adsorbers with different $Q_{\max, x, i}$ (i.e different capacities) as:

- $Q_{m, x, i}$ values were set as 4 values within the ranges:

1 to 1000 mg/g for $Q_{\max, GTI, i}$

0.0085 to 8.5 g/g for $Q_{\max, API, i}$

Then for each adsorbent capacity $Q_{\max, x, i}$ we set different solute affinities k_L as:

- $k_{L, x, i}$ values were set as four values within the ranges:

0.0081-8.1 L/mg for $k_{L, GTI, i}$

0.0021-1.1 L/g for $k_{L, API, i}$

The values considered were combined to generate 16 Langmuir isotherms for GTI removal and other 16 Langmuir isotherms for API binding (See table 7.3), resulting in 256 possible combinations of adsorbers with Langmuir isotherms behavior.

For the **Frendlich model**:

-n parameter was set for three values: 1, 2 or 3 for both API and GTI

- k_F values were set within the ranges

0.05-30 L/mg for $k_{F, GTI}$ (11 different values)

0.001-0.5 L/mg for $k_{F, API}$ (6 different values)

Therefore, a total combination of $i = n \times k_{L,GTI} \times k_{L,API} = 3 \times 11 \times 6 = 198$ different adsorbers were considered using Freundlich isotherm model.

Model calculations and API Losses:

An analytical solution was not obtained for all adsorption models to calculate the adsorber mass. Instead, the solver mathematical function from Excel, version 2013, was used to generate aleatory values for adsorber mass (m), and perform multiple calculations of $C_{e,GTI,i}$ and $C_{e,API,i}$ until their ratio met our target value of 7.5 mgGTI/gAPI. $C_{e,GTI,i}$ and $C_{e,API,i}$ were calculated according to equations 7.13 and 7.14 a-c, with different parameters assumed (see range of parameters on isotherms considered), and our case study values set to 1000 mg/L and 10 g/L of GTI and API initial concentrations. The model was used to compute adsorber amount required to reach our target objective of 7.5 mgGTI/gAPI as well as API losses as:

$$API \text{ loss } (\%) = \left[1 - \frac{C_{R,API,i}}{C_{in,API}} \right] \cdot 100\% \quad (7.15)$$

where $C_{R,API,i}$ was calculated by equations 7.13 to 7.14 for each adsorber mass considered and isotherm constants assumed.

Operation times: Adsorption kinetics must be considered as an important parameter for process economics to define operation times. The operation time must be equal to the time needed to reach the equilibrium concentration, (note that, to determine the time of contact between the stream and adsorber, laboratory assay is needed).

7.3.4 Hybrid Process

A hybrid process combining OSN and adsorption was designed to address the cases when OSN or adsorption as single steps are unable to reach TTC value with acceptable API loss.

The process is illustrated on Figure 7.1 composed by three stages:

- (i) Diafiltration using an OSN membrane with recovery of purified API in retentate (R)
- (ii) Distillation to reduce volume of permeate (P), and
- (iii) Adsorption to remove GTIs, i.e, decrease the ratio of C_{GTI}/C_{API} for further recirculation of the stream back to feed the next batch OSN cycle.

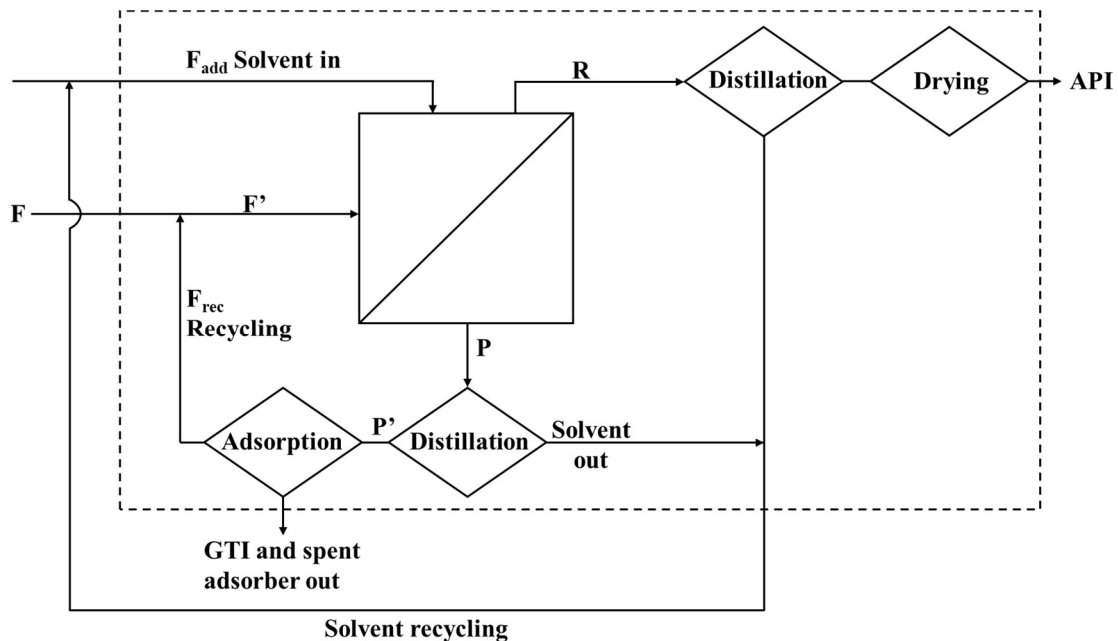


Figure 7.1. Schematic representation of Hybrid process OSN-Adsorption, the dashed line indicates the volume of control for mass balance.

Importantly the calculations for the hybrid process assume that there are several cycles (indicated by j) and calculations will be made for consecutive cycles. The set-up of the model and boundaries used are maintained. In other words:

(i) 7.5 mgGTI/gAPI (equation 1) in the OSN retentate (R) stream is used as target objective; and, (ii) 10 g/L API and 1000 mg/L of GTI were used, respectively as $C_{F,API,i,j}$ and $C_{F,GTI,i,j}$ input concentrations for the Feed (F) stream for all cycles j .

Note that, the initial ratio of GTI/API of 100 mgGTI/gAPI, should decrease to 7.5 mgGTI/gAPI on the retentate, and consequently will increase to values higher than 100 mgGTI/gAPI on the permeate. Therefore, the role of the adsorption step is to reduce such ratio to a value at the level of the feed stream, or reduce GTI content with minimum API loss, allowing recycling.

The same volume of feed stream $V_{F,i,j}$ was used for all cycles, from here onwards referred as V_F .

This model is a simplified approach that does not take into account factors like hydrodynamic interactions between species.

The main intrinsic parameters considered to rule the process efficiencies are still, for each solute (API and GTI):

(i) **Membrane Rejection** for OSN,

(ii) **Isotherm constants** for isotherms considered, $k_{L,x,i}$, $Q_{\max,x,i}$, $k_{F,x,i}$, n_i ,

which are assumed constant over several cycles for a given system i , (i.e. using a given membrane and adsorber).

The main operating parameters are still

(i) **Diavolumes** ($D_{i,j}$) for OSN, calculated for each cycle j by equation 7.16

$$D_{i,j} = \frac{V_{Add,i,j}}{V_F} = \frac{V_{P,i,j}}{V_{F',i,j}} \quad (7.16)$$

(ii) **Amounts of adsorber** ($m_{i,j}$), which was actually maintained constant over the several cycles j , and thus from here onwards is referred as m_i .

However, an additional operation parameter has to be considered, by taking into account the distillation of the permeate:

(iii) **Ratio Recirculation/Feed streams:**

$$\frac{F_{Rec,i,j}}{F} = \frac{V_{Rec,i,j}}{V_F} = \frac{V_{F',i,j} - V_F}{V_F} \quad (7.17)$$

Importantly, the following **mass balances** and **equations** were considered to build the model:

-Considering Volumes for each cycle

$$V_{F',i,j} = V_{F,i} + V_{Rec,i,j-1} \quad (7.18)$$

$$V_{Rec,i,j} = V_{P',i,j} \quad (7.19)$$

To the operation was impose to the operation the volume relations which imply that diafiltration operated assuming no change of volume (equation 7.20 and 7.21) inside the membrane set-up and with diavolumes calculated in relation to feed of OSN (7.22). The ratio of recirculation, $R_{Rec/F}$, is fixed (equation 7.23) and the concentration ratio $V_{P',i,j}/V_{P,i,j}$ performed by distillation before the adsorption step is calculated according with $R_{Rec/F}$, and mass balance equation 7.19.

$$V_{F',i,j} = V_{R,i,j} \quad (7.20)$$

$$V_{Add,i,j} = V_{P,i,j} \quad (7.21)$$

$$D_{i,j} = \frac{V_{add,i,j}}{V_{F',i,j}} = \frac{V_{P,i,j}}{V_{F',i,j}} \quad (7.22)$$

$$R_{Rec/F} = \frac{V_{Rec,i,j-1}}{V_{F',i,j}} = \frac{(V_{F',i,j} - V_F)}{V_F} \quad (7.23)$$

For the solutes $x = \text{API}$ or GTI , it is assumed no losses of solute by adsorption when mixing the feed and the recirculation stream (equation 7.24), on the membrane operation (equation 7.25), and over the distillation (equation 7.26) the following mass balances equations are established:

$$V_{F',i,j} C_{F',x,i,j} = V_F C_{F,x,i} + V_{Rec,i,j-1} C_{Rec,x,i,j-1} \quad (7.24)$$

$$V_{F',i,j} C_{F',x,i,j} = V_{R,x,i,j} C_{R,x,i,j} + V_{P,x,i,j} C_{P,x,i,j} \quad (7.25)$$

$$V_{P,i,j} C_{P,x,i,j} = V_{P',i,j} C_{P',x,i,j} \quad (7.26)$$

The concentrations on the retentate are as previously calculated according with diavolume and rejection of the membrane for each species:

$$\frac{C_{R,x,i,j}}{C_{F',x,i,j}} = e^{[-D_{i,j}(1-R_{x,i})]} \quad (7.27)$$

The concentrations of the solutes obtained after the adsorption step in the recirculation $C_{Rec,x,i,j}$ can be calculated using $V_{P',i,j}$, the $C_{P',x,i,j}$ and the Langmuir parameters (equation 7.28, adapted from equation 7.13) or Freundlich parameters (equations 7.29a, b, c adapted from 7.14a, b, c).

For Langmuir:

$$C_{Rec,x,i,j} = \frac{-V_{P'} - m \cdot Q_{max} \cdot k_{L,x,i} + k_{L,x,i} \cdot C_{P',x,i,j} \cdot V_{P'}}{2k_{L,x,i} \cdot V_{P'}} +$$

$$\frac{\sqrt{V_{P',x,i,j}^2 + 2m \cdot Q_{max} \cdot k_{L,x,i} \cdot V_{P'} + 2C_{P',x,i,j} \cdot k_{L,x,i} \cdot V_{P'}^2 - 2m \cdot Q_{max} \cdot C_{P',x,i,j} \cdot k_{L,x,i} \cdot V_{P'} + k_{L,x,i}^2 \cdot C_{P',x,i,j}^2 \cdot V_{P'}^2 + m^2 \cdot Q_{max}^2 \cdot k_{L,x,i}^2}}{2k_{L,x,i} \cdot V_{P'}}$$

(7.28)

$$\text{For Freundlich, with } n = 1: C_{Rec,x,i,j} = \frac{V_{P'} \cdot C_{P',x,i,j}}{k_{F,x,i} m + V_{P'}} \quad (7.29a)$$

For Freundlich, with $n = 2$:

$$C_{Rec,x,i,j} = \frac{2C_{P',x,i,j} \cdot V_{P',x,i,j}^2 + m_i^2 \cdot k_{F,x,i}^2 - \sqrt{4C_{P',x,i,j} \cdot m^2 \cdot k_{F,x,i}^2 \cdot V_{P',x,i,j}^2 + m^4 \cdot k_{F,x,i}^4}}{2V_{P',x,i,j}^2} \quad (7.29b)$$

For Freundlich, with $n = 3$:

$$C_{Rec,x,i,j} = \sqrt[3]{\frac{-C_{P',x,i,j} \cdot m^3 \cdot k_{F,x,i}^3}{2V^3} + \sqrt{\frac{C_{P',x,i,j}^2 \cdot m^6 \cdot k_{F,x,i}^6}{4V^6} + \frac{m^9 \cdot k_{F,x,i}^9}{27V^9}}} +$$

$$\sqrt[3]{\frac{-C_{P',x,i,j} \cdot m^3 \cdot k_{F,x,i}^3}{2V^3} - \sqrt{\frac{C_{P',x,i,j}^2 \cdot m^6 \cdot k_{F,x,i}^6}{4V^6} + \frac{m^9 \cdot k_{F,x,i}^9}{27V^9}}} + C_{P',x,i,j} \quad (7.29c)$$

Intrinsic parameters ranges considered: We maintained the script i to identify the system of membrane and adsorption parameters. Contrary to the previous models with a quite large range of different intrinsic parameters, for the hybrid process it was selected a particular case where the Adsorption and OSNd would have losses of API of 99% and 27%, respectively. The parameters selected for calculations were:

For OSNd stage:

-10% for membrane rejections to GTI

-90% for membrane rejections to API

For Adsorption stage:

For Langmuir case study

-100 mg/g for $Q_{\max, GTI, i}$

-0.085 g/g for $Q_{\max, API, i}$

-0.0081 L/mg for $k_{L, GTI, i}$

-2.1 L/g for $k_{L, API, i}$

For Freundlich case study

-adsorber following Freundlich model considering $n = 2$ for both API and GTI

-0.1857 L/mg for $k_{F, GTI, i}$

-0.0078 L/g for $k_{F, API, i}$

Calculations and API Losses: The amount of adsorber was kept constant for all cycles. Values of 20 g/L and 40g/L were selected for the Langmuir and 20 g/L and 40g/L were selected for Freundlich case studies. The $R_{Rec/F}$ (and consequently the concentration factor $V_{P',i,j} / V_{P,i,j}$) was assessed in a range of 0.05 to 1, considering both the isotherm behavior and the API loss to be no high than 10%.

The diavolumes required and the API loss for each cycle were calculated by equations 7.30 and 7.31.

$$D_{i,j} = \frac{\ln\left(\frac{MaxC_{API, i,j}}{C_{GTI, i,j}}\right)}{R_{GTI} - R_{API}} \quad (7.30)$$

$$API \text{ loss } (\%) = \left(1 - \frac{C_{R, API, i,j}}{C_{F, API}}\right) \cdot 100\% \quad (7.31)$$

7.4. Materials and methods: Experimental Section

7.4.1. Materials

4-Dimethylaminopyridine (DMAP) and methyl *p*-toluenesulfonate (MPTS) were purchased from Acros (Belgium). Both reagents were used as supplied, without further purification. Polybenzimidazole adsorbers PBI-TA and PBI-TB, were obtained as described in Chapter III. Dichloromethane (DCM), methanol (MeOH) and acetonitrile (MeCN) HPLC grade solvents were purchased from Fisher Chemicals (USA). Formic acid (FA) was purchased from Panreac (Spain). Mometasone furoate (Meta) and betamethasone acetate (Beta) were kindly provided by Hovione PharmaScience Ltd (Portugal). GMT-oNF-2 membrane was purchased from Borsig Membrane Technology GmbH (Germany).

7.4.2. Apparatus and analysis

HPLC measurements were performed on a Merck Hitachi pump coupled to a L-2400 tunable UV detector, using an analytic Macherey-Nagel C18 reversed-phase column Nucleosil 100-10, 250 x 4.6 mm, an injection volume of 10 μ L and the eluents, A: aqueous 0.1% formic acid solution, B: MeCN 0.1% FA solution. For MPTS a flow rate of 2 mL \cdot min⁻¹ and UV detection at 230 nm was used; method: 0-12 min., 70%A-30%B. For DMAP, Meta and Beta UV detection at 280 nm and flow rate of 1 mL \cdot min⁻¹ was used with the method: 0-3 min, 60%-20% A; 3-4 min, 20% A; 4-8 min, 20%-60% A; 8-15 min 60% A.

Distillation was performed at atmospheric pressure and 40°C using a Rotavapor R-3 Büchi Labortechnik AG.

7.4.3. Organic solvent nanofiltration (OSN) experiments

A dead-end Sterlitech HP 4750 Stirred Cell was used to carry out filtrations of API/GTIs solutions. A pressure of 20 bar was applied using nitrogen, providing the driving force for the filtrations. All experiments were performed under magnetic stirring of 300 rpm. The membrane Borsig GMT oNF-2 ($A_m = 14.6 \text{ cm}^2$) was preconditioned by filtering pure DCM solvent, until a constant solvent flux was obtained. An HPLC pump Series I, Scientific Systems Inc. was coupled to OSN apparatus and was adjusted to pump fresh DCM at constant flux during the experiment to perform diafiltration. Membrane rejections were estimated using single solute feed solutions of APIs and GTIs at concentrations of 10 g/L and 1000 mg/L, respectively, and solutions of an API contaminated with GTI (ratio 100 mgGTI/g API). Rejection values (R_x) were calculated from equation 7.2 on the basis of solute concentration in feed ($C_{F,x}$) and permeate ($C_{P,x}$).

7.3.3. Adsorption experiments

Batch binding experiments were performed by placing 50 mg of adsorber in 2 ml Eppendorf vials and addition of 1 mL of 10 g/L of API contaminated with 1000 mg/L of GTI. The suspensions were stirred for 24 h at 200 rpm. After this time the samples were centrifuged and the supernatant was filtered and analyzed by HPLC for GTI and API quantification. These assays were performed with duplicate samples. (note that the values of adsorber mass and concentration of solutions may vary depending on model response).

The percentage of GTI or API bound to the adsorber was calculated from equation 7.32, where C_{in} (mg/L) is the initial concentration of GTI or API, and C_e (mg/L) is the final concentration of GTI or API in solution.

$$\text{Binding (\%)} = \left[\frac{C_{in} - C_e}{C_{in}} \right] \cdot 100\% \quad (7.32)$$

7.3.4. Binding adsorption isotherm experiments

For the adsorption isotherm experiments at room temperature, 1 mL of DMAP or MPTS solutions prepared in DCM, with different initial concentrations (100, 500, 1000, 2000, 3000, 4000 and 5000 ppm) were added to 50 mg of the adsorbers. The mixtures were stirred at 200 rpm for 24 h. After that time, the suspensions were centrifuged and the supernatants were filtered and analyzed by HPLC. All experiments were carried out in duplicate. For Meta, solutions with different initial concentrations (100, 500, 1000, 2000, 5000 and 10000 ppm) were submitted to the same procedure. The percentage and the amount of GTI or API bound to the adsorbers was calculated from equations 7.32 and 7.33.

$$Q = \frac{V \times [C_{in} - C_e]}{m} \quad (7.33)$$

where Q (mg/g) is the amount of GTI or API bound to the adsorber, C_{in} (mg/L) is the initial concentration of GTI or API, C_e (mg/L) is the final concentration of GTI or API in solution, V (L) is the volume of solution used and m (g) is the adsorber mass. (note that the values of adsorber mass and concentration of solutions may vary depending on model response).

The experimental data were fitted to the Langmuir and Freundlich isotherm models [9] according to equations 7.10 and 7.11.

7.5. Results and discussion

7.5.1 Model results: decision making framework

To make an efficient API purification, the processes must respect the TTC value and take into account factors like API loss and operation costs. This model was proposed to help to make a decision between the use of diafiltration, adsorption or a hybrid process combining both. To validate the models, solutions of 10 g/L of an API (Meta or Beta) containing 1000 mg/L of a GTI (MPTS or DMAP) are prepared, simulating four different post-reaction streams. These were tested using PBI-TA or PBI-TB as adsorbers for the adsorption process, a GMT-oNF-2 membrane for the OSN process, and a combination of membrane-adsorber for the hybrid process. For this work, a TTC value corresponding to a maximum contamination (MaxC) of $7.5 \text{ mg}_{\text{GTI}}/\text{g}_{\text{API}}$ was used to validate the model.

7.5.2 OSN Diafiltration: Thresholds

Purification by OSN can reach ultralow levels of contamination, but it costs a great volume of solvent and high API losses depending on rejection of the species.

For this model, the number of diavolumes needed to reach the TTC value was calculated based on different values for rejection of both API (80 to 100%) and GTI (0 to 99.99%), meaning each combination is one different kind of membrane.

The number of diavolumes for each combination is shown in Table 7.1.

Table 7.1. Diavolume required for different combination of API and GTI rejections.

		Diavolumes						
		API Rejection						
		80%	85%	90%	95%	97.5%	99%	99.99%
GTI rejection	0%	3.2	3.0	2.9	2.7	2.7	2.6	2.6
	10%	3.7	3.5	3.2	3.0	3.0	2.9	2.9
	20%	4.3	4.0	3.7	3.5	3.3	3.3	3.2
	30%	5.2	4.7	4.3	4.0	3.8	3.8	3.7
	40%	6.5	5.8	5.2	4.7	4.5	4.4	4.3
	50%	8.6	7.4	6.5	5.8	5.5	5.3	5.2
	60%	13.0	10.4	8.6	7.4	3.9	6.6	6.5
	70%	25.9	17.3	13.0	10.4	9.4	8.9	8.6

When diafiltration is used to purify the API, as the number of diavolumes is increasing, API losses also increase, so a careful comparison between the number of diavolumes and API loss presented in Tables 7.1 and 7.2 is needed to avoid sacrificing too much API to reach a higher purity.

Table 7.2. API loss in diafiltration mode for different combinations of API and GTI rejections.

		API loss (%)						
		API Rejection						
		80%	85%	90%	95%	97.5%	99%	99.99%
GTI rejection	0%	47.7	36.7	25.0	12.7	6.4	2.6	0.0
	10%	52.3	40.4	27.7	14.1	7.1	2.9	0.0
	20%	57.8	45.0	30.9	15.9	8.0	3.2	0.0
	30%	64.5	50.7	35.1	18.1	9.1	3.7	0.0
	40%	72.6	57.8	40.4	21.0	10.7	4.3	0.0
	50%	82.2	67.0	47.7	25.0	12.7	5.1	0.0
	60%	92.5	78.9	57.8	30.9	15.9	6.4	0.0
	70%	99.4	92.5	72.6	40.4	21.0	8.5	0.0

API losses in Table 7.2 are divided in three ranks:

Values lower than 10% (no color) are considered acceptable values to use diafiltration as a single step purification. values of API losses between 10 and 30% (light grey) were considered not acceptable, but such conditions are good candidates to a hybrid process, where API is further recovered from the permeate. For API losses higher than 30% (dark grey) it was considered that the use of diafiltration alone or in combination with other unit operation would not be acceptable and alternatives using entirely different purification steps should be sought.

Acceptable API losses are achieved only for membranes with higher API rejections, which means that for the case considered, with a 100mg GTI/gAPI ratio used in the feed solution, membranes with API rejections higher than 97.5% should be used, regarding GTI rejections. Another factor that must be evaluated is the number of diavolumes required. Even if the API loss is low, using higher numbers of diavolumes implies intensive solvent consumption, which can turn the process impractical from an operation, cost and environmental perspectives.

7.5.3 Adsorption: Thresholds

Adsorption is a process commonly used for purification and it can also be used to remove GTI content from an API. To describe and forecast the performance of an adsorption process, it must be determined which model of isotherm, for both API and GTI, is to be followed by the adsorber to be explored. Then, it is possible to estimate how much adsorber is needed to reach the TTC value.

The tables presented in this section were calculated by simulating that both compounds have the same isotherm behavior (Langmuir or Freundlich). In the cases of Freundlich, the same value for “n” was considered. Other combinations between different

behaviors are possible but were not calculated in this work (e.g. API follows Langmuir and GTI Freundlich, or both follow Freundlich but with different “n” values).

The API losses presented in this section are only related to the adsorption step, and do not take into account whether the API can be recovered from the adsorber, since not all adsorbers allow the recovery of the adsorbed compound. However, when it is possible to recover the API from the adsorber (see Chapter III), one would have to consider also a balance of associated cost of such step with gains related with recovered API.

All mass values presented were calculated based on 1L of feed solution and the same rank was used for API loss in tables: values lower than 10% (no color) are considered acceptable values to use adsorption as a single step purification. For values of API losses between 10 and 30% (light grey) were considered not acceptable, but such conditions are good candidates to a hybrid process, where API is further recovered from the permeate. For API losses higher than 30% (dark grey) it was considered that the use of adsorption alone would not be acceptable and alternatives, using entirely different purification steps, should be sought. However, in some cases could work associated in a hybrid process.

7.5.3.1 Langmuir’s Isotherm behavior

When adsorption is performed to purify API, following the Langmuir’s model, both API and GTI constants must be known to calculate the adsorber mass required to reach the TTC value. The greatest problem in generalizing this case study is, each API and GTI have their own constants. So, this simulation was done using four different constants k_L and Q_{max} for API and GTI, resulting in 256 combinations. The value used

for each constant is on Table 7.3, the value of mass of adsorber required and API losses are on Tables 7.4 and 7.5, respectively.

Table 7.3. Selected Langmuir's constants for API and GTI.

	Q_{\max} (g/g for API and mg/g for GTI)		K_L (L/g for API and L/mg for GTI)	
	code	value	code	value
API	A	0.0085	1	0.0021
	B	0.085	2	0.021
	C	0.85	3	0.21
	D	8.5	4	2.1
GTI	a	1	I	0.0081
	b	10	II	0.081
	c	100	III	0.81
	d	1000	IV	8.1

Table 7.4. Required mass calculated for each Langmuir adsorber.

	Mass of adsorber (g)															
	A1	A2	A3	A4	B1	B2	B3	B4	C1	C2	C3	C4	D1	D2	D3	D4
aI	2523.49	3334.42	107051.71	526.12	3487.85	n.d.	n.d.	n.d.	n.d.	n.d.	n.d.	n.d.	n.d.	n.d.	n.d.	n.d.
aII	1081.77	1115.89	1316.20	1868.10	1122.00	n.d.	n.d.	n.d.	n.d.	n.d.	n.d.	n.d.	n.d.	n.d.	n.d.	n.d.
aIII	941.71	952.01	987.43	1044.97	953.72	n.d.	n.d.	n.d.	n.d.	n.d.	n.d.	n.d.	n.d.	n.d.	n.d.	n.d.
aIV	927.75	936.03	960.90	984.41	937.38	n.d.	n.d.	n.d.	n.d.	n.d.	n.d.	n.d.	n.d.	n.d.	n.d.	n.d.
bI	245.50	251.17	274.88	298.10	252.35	333.44	1164.49	52.60	348.78	n.d.	n.d.	n.d.	n.d.	n.d.	n.d.	n.d.
bII	107.77	108.11	109.27	110.00	108.18	111.59	131.62	12775.71	112.20	n.d.	n.d.	n.d.	n.d.	n.d.	n.d.	n.d.
bIII	94.04	94.15	94.52	94.73	94.17	95.20	98.74	104.50	95.37	n.d.	n.d.	n.d.	n.d.	n.d.	n.d.	n.d.
bIV	92.66	92.76	93.06	93.23	92.77	93.60	96.09	98.44	93.74	n.d.	n.d.	n.d.	n.d.	n.d.	n.d.	n.d.
cI	24.48	24.54	24.72	24.83	24.55	25.12	27.49	29.81	25.23	33.34	92.08	5.52	34.88	n.d.	n.d.	n.d.
cII	10.77	10.78	10.79	10.79	10.78	10.81	10.93	11.00	10.82	11.16	13.16	17.25	11.22	n.d.	n.d.	n.d.
cIII	9.40	9.40	9.41	9.41	9.40	9.41	9.45	9.47	9.42	9.52	9.87	10.45	9.54	n.d.	n.d.	n.d.
cIV	9.27	9.27	9.27	9.27	9.27	9.28	9.31	9.32	9.28	9.36	9.61	9.84	9.37	n.d.	n.d.	n.d.
dI	2.45	2.45	2.45	2.45	2.45	2.45	2.47	2.48	2.46	2.51	2.75	2.98	2.52	3.33	976.31	0.52
dII	1.08	1.08	1.08	1.08	1.08	1.08	1.08	1.08	1.08	1.08	1.09	1.10	1.08	1.12	1.32	1.84
dIII	0.94	0.94	0.94	0.94	0.94	0.94	0.94	0.94	0.94	0.94	0.95	0.95	0.94	0.95	0.99	1.04
dIV	0.93	0.93	0.93	0.93	0.93	0.93	0.93	0.93	0.93	0.93	0.93	0.93	0.93	0.94	0.96	0.98

Table 7.5. API loss related each Langmuir adsorber.

	API loss (%)															
	A1	A2	A3	A4	B1	B2	B3	B4	C1	C2	C3	C4	D1	D2	D3	D4
aI	4.23	34.34	99.47	41.36	38.06	n.d.										
aII	1.86	14.45	54.60	93.23	16.45	n.d.										
aIII	1.62	12.55	44.99	74.74	14.33	n.d.										
aIV	1.60	12.37	44.10	71.64	14.12	n.d.										
bI	0.43	3.59	14.98	23.85	4.23	34.34	94.95	41.35	38.06	n.d.						
bII	0.19	1.57	6.16	8.89	1.86	14.45	54.60	99.96	16.45	n.d.						
bIII	0.16	1.37	5.34	7.66	1.62	12.55	44.99	74.74	14.33	n.d.						
bIV	0.16	1.35	5.26	7.54	1.60	12.37	44.10	71.64	14.12	n.d.						
cI	0.04	0.36	1.42	2.01	0.43	3.59	14.98	23.85	4.23	34.34	93.54	43.29	38.06	n.d.	n.d.	n.d.
cII	0.02	0.16	0.62	0.88	0.19	1.57	6.16	8.89	1.86	14.45	54.60	91.99	16.45	n.d.	n.d.	n.d.
cIII	0.02	0.14	0.54	0.76	0.16	1.37	5.34	7.66	1.62	12.55	44.99	74.74	14.33	n.d.	n.d.	n.d.
cIV	0.02	0.14	0.53	0.75	0.16	1.35	5.26	7.54	1.60	12.37	44.10	71.64	14.12	n.d.	n.d.	n.d.
dI	0.01	0.04	0.14	0.20	0.04	0.36	1.42	2.01	0.43	3.59	14.98	23.85	4.23	34.34	99.94	41.27
dII	0.01	0.02	0.06	0.09	0.02	0.16	0.62	0.88	0.19	1.57	6.16	8.89	1.86	14.45	54.60	93.01
dIII	0.01	0.01	0.05	0.08	0.02	0.14	0.54	0.76	0.16	1.37	5.34	7.66	1.62	12.55	44.99	74.74
dIV	0.01	0.01	0.05	0.08	0.02	0.14	0.53	0.75	0.16	1.35	5.26	7.54	1.60	12.37	44.10	71.64

Actually, 88 of those 256 computed behaviours are not able to reach a solution that meet out target objective value, since that for some of the adsorbers with higher capacities for API, $Q_{\max,API,i}$, and lower capacities for GTI, $Q_{\max,GTI,I}$, the analytical calculation of the amount of adsorber needed may results on imaginary numbers, which should correspond to situations where either no API is left on solution or that removal of API is so stringent and GTI removal not effective enough, as such that the ratio of 7.5 mgGTI/gAPI can not be met with real values.

7.5.3.2 Freundlich's Isotherm behavior

When adsorption is performed to purify API by following the Freundlich's model both API and GTI constants must be known to calculate the mass required to reach the TTC value. For this case the constant "n" was fixed for values of 1, 2 and 3 and different values of K_F were used for API and GTI for each "n" value.

Simulation for "n=1":

Table 7.6. Required mass calculated for Freundlich n=1.

		Mass of adsorber (g)					
		0.001	0.01	0.05	0.10	0.25	0.50
K_{GTI}	K_{API}						
	0.05	336.4	n.d	n.d	n.d	n.d	n.d
	0.5	25.3	33.6	n.d	n.d	n.d	n.d
	1	12.5	14.2	37.0	n.d	n.d	n.d
	1.5	8.3	9.0	14.8	74.0	n.d	n.d
	3	4.1	4.3	5.3	7.3	n.d	n.d
	3.5	3.5	3.7	4.4	5.6	74.0	n.d
	6	2.1	2.1	2.3	2.6	4.6	n.d
	7.5	1.6	1.7	1.8	2.0	3.0	14.0
	10	1.2	1.3	1.3	1.4	1.9	3.8
	15	0.8	0.8	0.9	0.9	1.1	1.5
	30	0.4	0.4	0.4	0.4	0.5	0.5

Table 7.7. API loss related for Freundlich n=1 adsorber.

		API loss (%)					
		0.001	0.01	0.05	0.10	0.25	0.50
K _{GTI}	K _{API}						
	0.05	25.17	n.d	n.d	n.d	n.d	n.d
	0.5	2.47	25.17	n.d	n.d	n.d	n.d
	1	1.23	12.46	64.91	n.d	n.d	n.d
	1.5	0.82	8.28	42.53	88.09	n.d	n.d
	3	0.41	4.12	20.90	42.23	n.d	n.d
	3.5	0.35	3.53	17.87	36.07	94.87	n.d
	6	0.20	2.06	10.36	20.90	53.38	n.d
	7.5	0.16	1.65	8.28	16.67	42.53	87.50
	10	0.12	1.23	6.20	12.46	31.62	65.22
	15	0.08	0.82	4.12	8.28	20.90	42.53
	30	0.04	0.41	2.06	4.12	10.36	20.90

The equation 7.14a is a first degree polynomial (linear) equation and the results presented in tables 7.6 and 7.7 are not derived based on the model. In some cases API loss is not calculated by the model, probably due to the mass value result being a negative number. Alternatively, the concentration of GTI or API could have been negative and the model fails to calculate the API loss.

Simulation for “n=2”:

Table 7.8. Required mass calculated for Freundlich n=2.

		Mass of adsorber (g)					
		0.001	0.01	0.05	0.10	0.25	0.50
K _{GTI}	K _{API}						
	0.05	4250.0	n.d	n.d	n.d	n.d	n.d
	0.5	222.5	423.1	n.d	n.d	n.d	n.d
	1	109.0	135.9	n.d	n.d	n.d	n.d
	1.5	72.0	82.6	n.d	n.d	n.d	n.d
	3	35.8	38.2	58.3	n.d	n.d	n.d
	3.5	30.7	32.4	45.0	n.d	n.d	n.d
	6	17.9	18.4	21.6	29.1	n.d	n.d
	7.5	14.3	14.6	16.5	20.3	n.d	n.d
	10	10.7	10.9	11.9	13.6	36.8	n.d
	15	7.1	7.2	7.6	8.3	11.7	n.d
	30	3.6	3.6	3.7	3.8	4.3	5.8

Table 7.9. API loss related for Freundlich n=2 adsorber.

		API loss (%)					
		0.001	0.01	0.05	0.10	0.25	0.50
K _{GTI}	K _{API}						
0.05		71.61	n.d	n.d	n.d	n.d	n.d
0.5		6.79	71.47	n.d	n.d	n.d	n.d
1		3.39	34.73	n.d	n.d	n.d	n.d
1.5		2.26	22.94	n.d	n.d	n.d	n.d
3		1.13	11.36	58.99	n.d	n.d	n.d
3.5		0.97	9.72	50.22	n.d	n.d	n.d
6		0.56	5.66	28.80	58.99	n.d	n.d
7.5		0.45	4.52	22.94	46.74	n.d	n.d
10		0.34	3.39	17.12	34.73	90.35	n.d
15		0.22	2.26	11.36	22.93	58.99	n.d
30		0.11	1.13	5.66	11.36	28.80	58.99

The equation 7.14b involves a square root to calculate the mass, and as consequences some answers can be negative or imaginary numbers, making some results to be presented as not determined by the model in tables 7.8 and 7.9.

Simulation for “n=3”:

Table 7.10. Required mass calculated for Freundlich n=3.

		Mass of adsorber (g)					
		0.001	0.01	0.05	0.10	0.25	0.50
K _{GTI}	K _{API}						
0.05		3603833.0	n.d	n.d	n.d	n.d	n.d
0.5		457.1	230717.3	n.d	n.d	n.d	n.d
1		223.8	285.7	n.d	n.d	n.d	n.d
1.5		148.2	170.9	18504.5	n.d	n.d	n.d
3		73.6	78.5	144.3	n.d	n.d	n.d
3.5		63.0	66.5	100.6	n.d	n.d	n.d
6		36.7	37.8	44.9	72.1	n.d	n.d
7.5		29.3	30.0	34.2	44.3	n.d	n.d
10		22.0	22.4	24.5	28.6	n.d	n.d
15		14.6	14.8	15.7	17.1	28.9	n.d
30		7.3	7.4	7.6	7.8	9	14.4

Table 7.11. API loss related for Freundlich n=3 adsorber.

		API loss (%)					
		0.001	0.01	0.05	0.10	0.25	0.50
K _{GTI}	K _{API}	0.001	0.01	0.05	0.10	0.25	0.50
	0.05	99.99	n.d	n.d	n.d	n.d	n.d
	0.5	9.52	99.99	n.d	n.d	n.d	n.d
	1	4.74	49.14	n.d	n.d	n.d	n.d
	1.5	3.15	32.33	99.99	n.d	n.d	n.d
	3	1.58	15.96	84.13	n.d	n.d	n.d
	3.5	1.35	13.65	71.42	n.d	n.d	n.d
	6	0.79	7.93	40.67	84.13	n.d	n.d
	7.5	0.63	6.33	32.33	66.40	n.d	n.d
	10	0.47	4.74	24.09	49.14	n.d	n.d
	15	0.32	3.16	15.96	32.33	84.13	n.d
	30	0.16	1.58	7.93	15.96	40.68	84.13

The equation 7.14c involves a cubic and square roots to calculate the mass, and as consequences some answers can be negative or imaginary numbers, making some results to be presented as not determined by the model in tables 7.10 and 7.11.

Regardless the isotherm behavior, as in diafiltration, the selection of an adequate adsorber must be evaluated based on API losses and the amount of adsorber required.

7.5.4 Hybrid Process calculations

7.5.4.1 Calculation of performance over several separation cycles

A hybrid process combining OSN and adsorption can be proposed to solve the cases when OSN or adsorption as a single step are unable to reach the TTC value with acceptable API loss. In other words, the OSN-Adsorption hybrid process was designed to reach the maximum contamination value of 7.5 mgGTI /gAPI in the retentate, without sacrificing API, while maintaining API losses of less than or equal to 10%, when OSN or adsorption alone are not able to meet the contamination and API losses criteria. Note

that an association of more steps also implies increases in operation costs, being necessary to take into account whether recovery step costs (adsorber and energy to distillation and condensation of solvent) are worth it or not (section 7.5.6).

This hybrid process works with a first step composed of OSN in diafiltration mode using membranes with API losses between 10 and 30% (light grey). The OSNd will be responsible for obtaining purified final product, in spite of some of the API crossing the membrane to the permeate. The adsorption step, to which the permeate stream (after being concentrated) is fed, has the role to remove a significant part of the GTI, allowing to return API to the OSNd feed stream with a level of contamination that can be handled by the OSNd in the next cycle. As the API fed to the adsorption step is a small fraction of all the API being purified, adsorbers that would have API losses greater than 10%, when used alone (light grey and some cases dark grey where API have low adsorption), can be used in these cases.

For this model, OSN diavolumes were calculated to meet the 7.5 mgGTI/gAPI requirement.

Considering the results obtained by the diafiltration, we must verify the ratio mgGTI/gAPI of the permeate to decide if the recovery of the present API will be worth it. Since the work of the adsorber will be to reestablish this value to the initial one, high values indicate greater expense of adsorber, as well as little API to be recovered.

Table 7.12. Values of contamination in permeate for different API/GTI rejections.

		Permeate mgGTI/gAPI					
		API Rejection					
		80%	85%	90%	95%	97.5%	99%
GTI rejection	0%	201.5	259.6	377.4	733.3	1447.0	3589.3
	10%	184.4	236.3	341.9	662.0	1304.2	3232.2
	20%	167.5	213.1	306.6	590.7	1161.4	2875.1
	30%	150.9	190.1	271.3	519.5	1018.7	2518.1
	40%	134.9	167.5	236.3	448.4	876.0	2161.0
	50%	120.0	145.5	201.5	377.4	733.3	1804.0
	60%	107.5	124.8	167.5	306.5	590.7	1447.1
	70%	100.5	107.5	134.9	236.3	448.4	1090.4

As showed in the cases highlighted in the table, different membranes can achieve the same ratio of contamination in the permeate. For example, the membrane with %API /%GTI rejections of 80/20 (4.3 diavolumes and API loss 57.8%) will have a permeate with the same ratio of a membrane with rejections of 90/60 (8.6 diavolumes and API loss 57.8%).

In these cases, the work of the adsorption step will be the same, because both present the same API loss. However, it does not mean that the membrane has the same performance. The number of diavolumes is different and it is directly associated to operation time and energy to distillation and condensation of solvent (also parameters to take into account in economic and environmental analysis, in section 7.5.6).

Therefore, it is important to study which are the set of values for the other two operation parameters (mass of adsorption and ratio of recirculation to feed volumes) that minimize API loss.

7.5.4.2 Effect of recirculation to feed stream ratio, V_{Rec}/V_F

The volume of recycled stream, i.e the ratio of the volumes of recirculate to feed stream (V_{Rec}/V_F) is a crucial variable in this model, since it has a direct impact on the number of diavolumes and consequently the solvent intensity used. Different recirculation volumes were tested for a fixed adsorber mass ($m_L = 20$ g/L and $m_F = 76$ g/L) and it was verified that the higher the recirculation volume, the lower the number of diavolumes used and the higher the API loss.

A higher volume in recirculation makes the inlet stream more diluted, not requiring so many diavolumes to reach the established value for the retentate, however even with a lower number of diavolumes, the total solvent used is still greater than the cases of lower recirculation volume, dragging more API into the permeate causing higher API losses. On the other hand, if the recirculation volume is very low it may form a slurry with the adsorber, preventing recirculation.

The results of API loss and diavolume numbers in function of adsorber's mass at the end of 10 cycles for different volumes of recirculation stream are illustrated by figure 7.2.

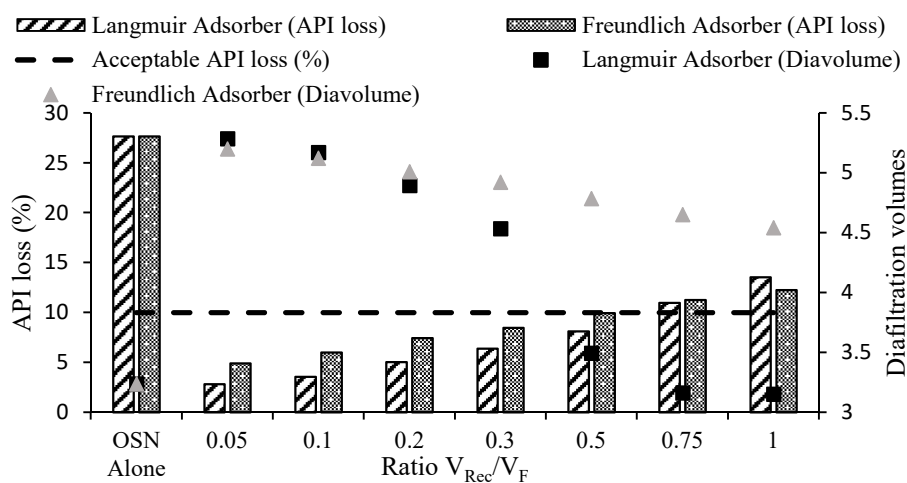


Figure 7.2. Comparison of effect of ratio recirculation/feed volume on API loss and diavolumes for hybrid process using Langmuir or Freundlich adsorber.

The simulation illustrated by figure 7.2, shows that in both cases a higher value of the recirculation volume to the feed volume ratio, requires the use of lower number of diavolumes to reach 7.5 mg/gAPI.

It is contra intuitive that API loss increases as diavolumes decrease, but the simple comparison of diavolume and API loss can be misleading, since the diavolume is a quotient of volumes (equation 7.3), e.g. if one inlet stream is 10L, 30 diavolumes will correspond to 300 L and of another inlet stream is 50 L, 10 diavolume correspond to 500 L. In this case, the first inlet will use 3 times more diafiltration volumes than the second, but in the end will use almost half of the amount of solvent used by the first one.

Following this rationale, it is reasonable the increase of API loss with the decrease of diavolumes presented in figures 7.4 and 7.5. The increase of the V_F , originates more solvent quantities and consequently more API will be dragged to the permeate.

7.5.4.3 Effect of adsorber amount

Assuming the control volume shown in figure 7.1, adsorption is the only stage where API losses can occur with these losses being related only to the mass of the adsorber used.

The use of a larger mass of adsorber will allow the recirculation stream to contain less concentration of GTI. On the other hand, more API will be adsorbed. However, even occurring a loss, this will be smaller if compared to the one coming from the OSN, if OSN worked alone.

The influence of adsorber amount was verified and the results indicate lower API loss when using lower amount of adsorber, but an increase in diavolume numbers also occurs due to the need of more solvent to wash out GTI through the permeate in the next

cycle. The simulation for mass influence in hybrid process for Langmuir model is present in figure 7.3 and for Freundlich in figure 7.4, using a ratio V_{Rec}/V_F of 0.3.

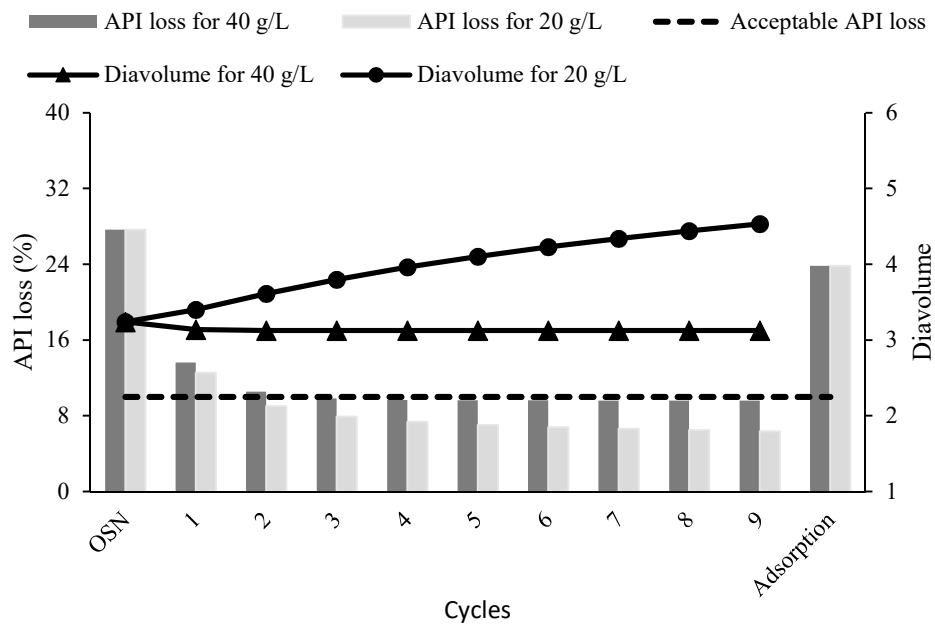


Figure 7.3. Hybrid process results by cycle comparative for 20g/L and 40g/L. Langmuir behaviour, combination B4cI, using OSN membrane with rejections of API 90% GTI 10%,).

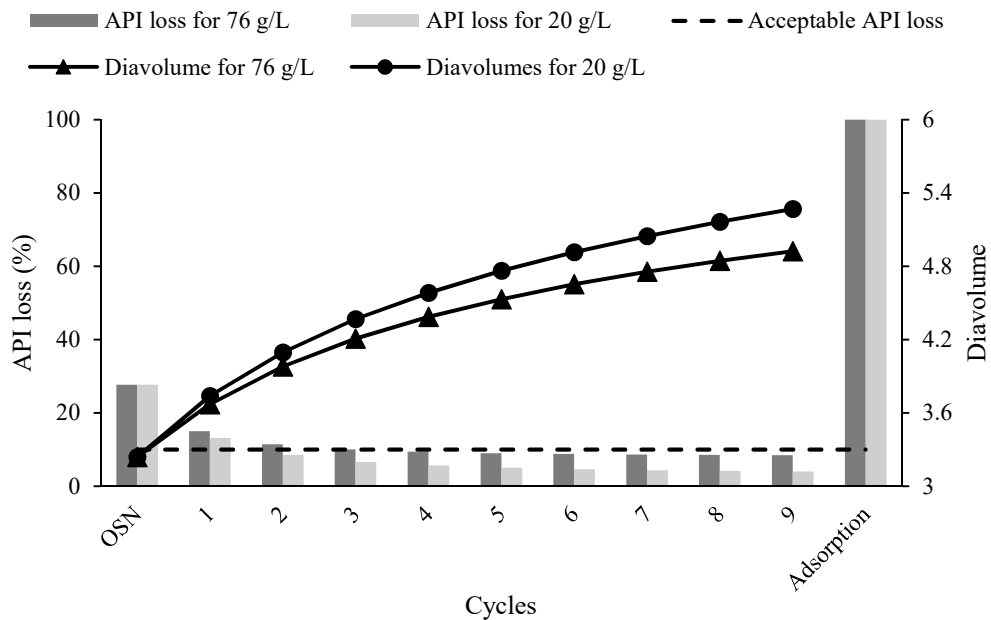


Figure 7.4. Hybrid process results by cycle comparative for 20g/L and 76g/L of PBI-TB (Freundlich behaviour using OSN membrane with rejections of API 90% GTI 10%,).

7.5.5. Experimental validation

7.5.5.1 OSN Diafiltration

The rejection of each single compound and an interaction of one API with one GTI were assessed experimentally. It was observed that the combination of API and GTI could affect the rejection of species in OSN, as illustrated in Figure 7.5. For Meta the rejection of 99% when alone in solution was reduced to 95% when contaminated with DMAP and to 90% when contaminated with MPTS. For Beta, there was no significant difference in its 90% membrane rejection, but great increases in this value were observed for GTIs.

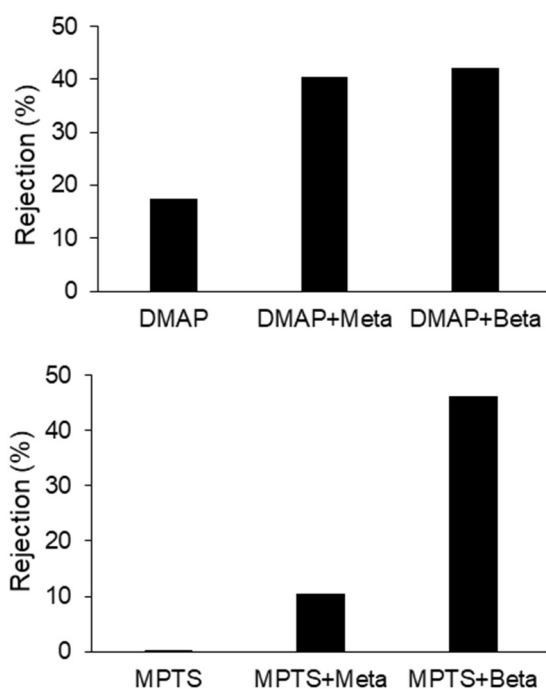


Figure 7.5. GTI rejection isolated and in presence of Meta or Beta. Top: DMAP rejection Bottom: MPTS rejection.

Reduction of API rejection implies an increase in API loss in the purification process, while increases in GTI rejection implies the need to increase the numbers of diavolumes, thus using a great amount of solvent and also pushing more API to the permeate.

Regarding the purification of the selected APIs, in the case of Beta both GTIs have higher rejections (40 to 50%), requiring 5.2 to 6.5 diavolumes to reach the TTC value with API losses higher than 40%, making OSN unable to purify Beta with reasonable losses. In the case of Meta, DMAP rejection reaches approximately 40%, with 4.7 diavolumes being necessary, with 21% of API being lost, and MPTS rejections reaches 10%, using 3.2 diavolumes with a loss of 27.7% of API.

In both cases, OSN as a single step reaches the TTC target value needed, but implies a considerable API loss, making OSN not an option for API purification in any combination of these API-GTI.

7.5.5.2 Adsorption

When performing adsorption PBI-TA follows the Langmuir adsorption behavior for Meta and DMAP (Meta: $K_L=2.2$, $Q_m= 8.2 \times 10^{-3}$ and DMAP: $k_L=8.1 \times 10^{-3}$ and DMAP $Q_m=100$, combination A4cI) and Freundlich behavior for Beta ($k_F= 1.5 \times 10^{-2}$, $n \approx 2$). PBI-TB follows Freundlich adsorption behavior for Meta and MPTS (Meta: $k_F= 7.8 \times 10^{-3}$, $n \approx 2$, MPTS: $k_F=0.1857$, $n=2$) and a multi stage for Beta (see Appendix C).

Adsorption results presented in figure 7.6, show that PBI-TA is able to remove DMAP from both Meta and Beta being suitable to perform Meta purification with a loss lower than 10%, but in case of Beta it reaches losses around 20%. For MPTS removal, adsorption with PBI-TB was not effective by itself in both cases since MPTS adsorption

is reduced almost by half when this impurity is in presence of API. One possible reason can be the stereochemical impediment caused by API molecules avoiding MPTS molecules to reach binding sites of the adsorber.

Both adsorbers allow to recover almost 100% of API bound, but for DMAP cases, the recovery step also releases minimal GTI backcontamination. (Chapter III)

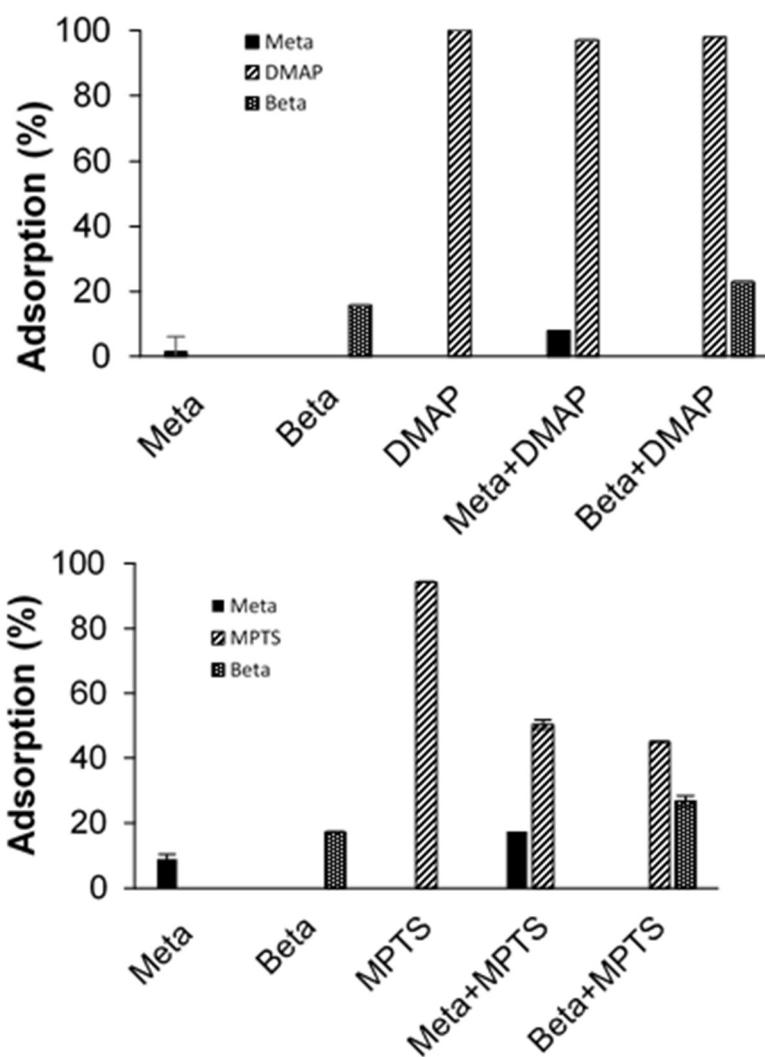


Figure 7.6. Top: Comparison of adsorption of solutions of isolated APIs, DMAP and API+DMAP in PBI-TA. Bottom: Comparison of adsorption of solutions of isolated APIs, MPTS and API+MPTS in PBI-TB.

7.5.5.3 Hybrid Process

The cases of DMAP contamination of API could be solved by adsorption, but MPTS contaminations of API would be still a challenge using the current adsorbers without further post adsorption steps to release the API bound. It has been shown in Chapter III, for PBI-TB polymer that it is possible to recover API bound to the adsorber using a DCM wash, without contamination of the GTI. However, the ability to retrieve product from the adsorber after the adsorption step is a very particular case, and therefore for illustrative reasons such step will not be considered on our hybrid process analysis. For contaminations of MPTS, in the case of Meta, OSN leads to losses of 27% being possible to use a hybrid process to reduce API loss. For the case of Beta, after using a high number of diavolume the losses are about 40 to 50%, what makes the hybrid process not recommended, since the higher loss in the first stage will make that almost half of the API will always be recycled, reducing efficiency.

Therefore, to assess experimentally the hybrid process, were considered solutions containing Meta contaminated with MPTS, an OSN membrane with rejections of 90% for Meta and 10% for MPTS and PBI-TB as adsorber (Meta: $K_F=0.0078$ $n \approx 2$, MPTS: $K_F=0.1857$ $n=2$). Again, note that it is possible for this particular adsorber to obtain an API recovery closer to 99.9% using DCM with virtually no MPTS back contamination. Still neither OSNd nor adsorption process could practically be used to meet the 7.5 mgGTI/gAPI. OSN in diafiltration mode alone will lead to the unacceptable API loss of around 28% and adsorption alone requires 1203.4g of PBI per liter (which is unpractical) and will lead to 91.59% of API loss, when the DCM additional recovery step was not considered.

The model was then used to estimate the conditions at which the hybrid process, combining OSNd and adsorption, estimating the need of 3.2 diavolumes to meet the target value of 7.5mgGTI/gAPI in the retentate stream, when the permeate stream was distilled to have a volume of 30% of the initial feed volume and 76 g of adsorber per L.

Using these estimations, the process was operated at laboratory scale for three cycles, being the first cycle loaded with 50 mL of feed and the others with 65 mL (50mL of fresh solution and 15 mL recycled, ratio $V_{Rec}/V_F = 0.3$). The adsorber amount was fixed to 76 mg per milliliter of solution. The calculated and experimentally obtained API losses and the ratio of mgGTI/gAPI at the retentate are presented in table 7.13.

Table 7.13. Comparison between predicted and experimental values of hybrid process.

Cycles	API loss (%)		mg GTI/ g API	
	Model	Experimental	Model	Experimental
1	27.66	24.73	7.5	7.25
2	14.96	16.03	7.5	7.08
3	11.38	9.76	7.5	6.62

The observed differences between the values predicted by the model and the obtained experimentally are not statistically significant ($p = 0.43$ for API loss and $p = 0.11$ for GTI/API ration) and can be attributed to rounding values of diavolumes and or adsorption constants.

7.5.6. Economic and environmental analysis of process scale-up

An economic and environmental analysis was performed for the API purification processes comparing OSN and the hybrid processes for the case study considered. The API selected for purification is Meta and MPTS as GTI. For the case of OSN, the selected membrane had a rejection of 90% for Meta and 10% MPTS. For the adsorption step of

the hybrid process, the adsorber selected is PBI-TB (see Chapter III) following a Freundlich isotherm with $n = 2$, and constants $k_F = 0.0078$ L/g for Meta and $k_F = 0.1857$ L/mg for MPTS.

7.5.6.1. Process design and scale-up factors

While the data used were obtained at laboratory scale, the economic and environmental analyses make sense to be made at a larger scale. As such, the scale-up factor for volume (V_F) of each batch to be purified was set at 1000 times (i.e. 1 m^3) for the three processes, while maintaining API and GTI concentrations constant. In terms of adsorber quantity, a factor of 1000 was equally used for the hybrid process, so that the adsorber to solvent ratio would be maintained. For the (dia)nanofiltration, flux was kept constant and diavolumes were kept proportional to solvent use, while the scale up factor for membrane area was 10000, and considering a spiral wound membrane module.

Annual API purification was established at 450 kg of API, resulting from 90 batches taking place each year. To achieve more environmentally and economically sustainable processes, solvent recycling was considered in both cases. Through distillation and condensation steps, a solvent recovery efficiency of 95% was assumed.

Process flow diagrams designed for the two processes are represented in Figure 7.7. Storage 1/S1 represents an auxiliary storage tank in both processes, for the contaminated API stream coming from the upstream process. Storage 2/S2 works as an auxiliary storage tank for permeate after a (dia)nanofiltration step, containing low API

and high GTI concentrations (Figure 7.7). Common to all processes, Storage 3/S3 is an auxiliary storage tank for recycled solvent after distillation; Mixing/MX1 represents a valve that works as a mixing knot for recycled and make-up solvent streams; Distillation 1/D1 and Distillation 2/D2 represent distillation columns for solvent evaporation for recycling; and Condenser 1/C1 and Condenser 2/C2 are heat exchangers for condensation of the recycled solvent.

In Figure 7.7 right, the equipment called Adsorption/A1 is a chromatographic column used for separation of GTI and API, letting most GTI be adsorbed and API to be eluted with the solvent. Diafiltration/DF1 operation units in Figure 7.7 A and B represent organic solvent (dia)nanofiltration equipment, including a tank for diavolume solvent. The Tray Drying/TD1 operation unit is a tray drying equipment used for the remaining solvent removal from purified API. For all processes, Pump 1/P1 to Pump 8/P8 are centrifugal pumps used for transport; and S-101 to S-127 designate process streams.

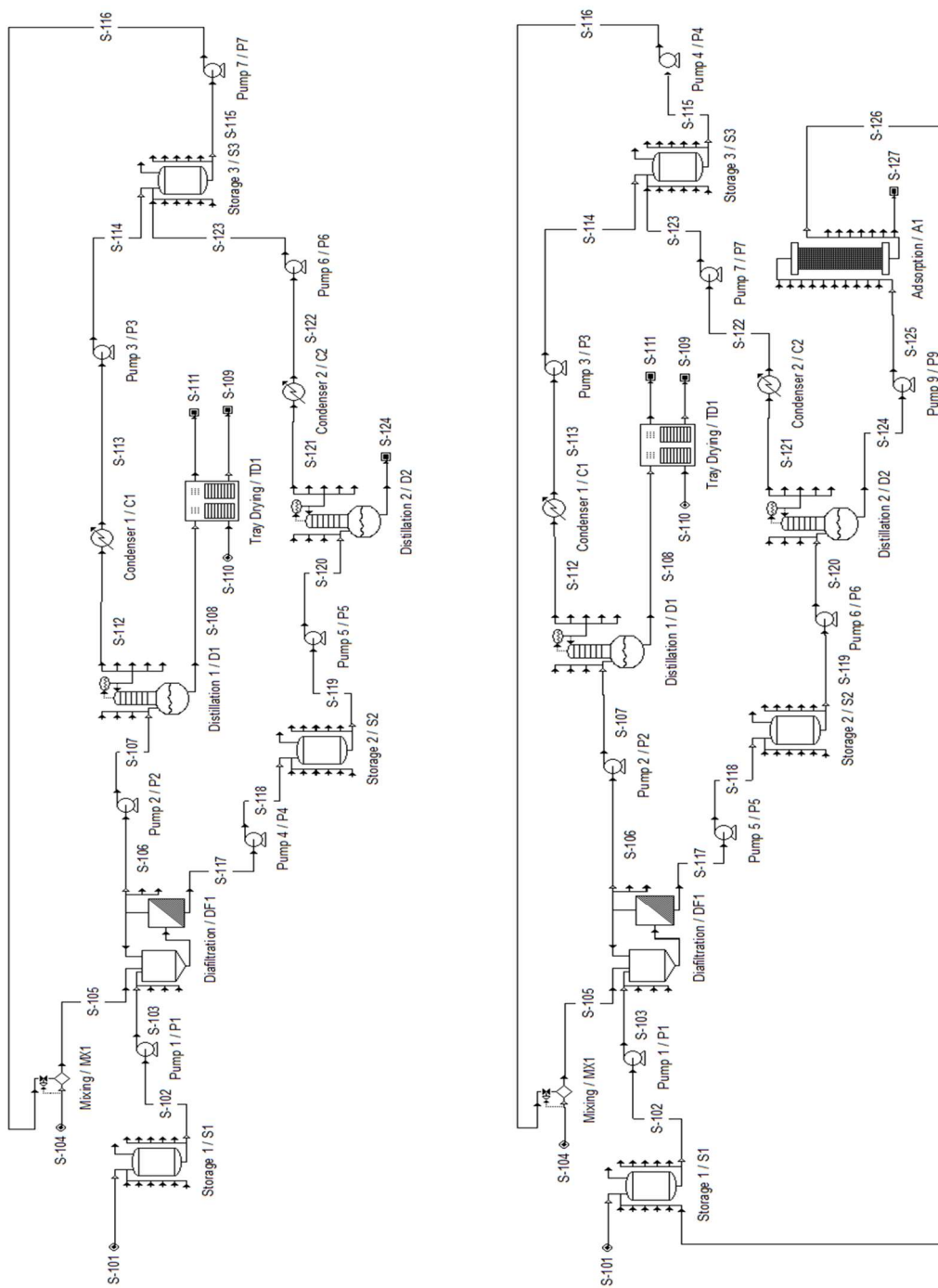


Figure 7.7. Process flow diagrams for the two processes considered for the case studies. Processes: Left) organic solvent (dia)nanofiltration process; Right) hybrid process using both organic solvent (dia)nanofiltration and column chromatography steps.

Main equipment: Storage 1/S1 – auxiliary storage tank for API stream; Storage 2/S2 –auxiliary storage tank for permeate containing low API and high GTI concentrations; Storage 3/S3 – auxiliary storage tank for recycled solvent; Adsorption/A1 – chromatographic column; Diafiltration/DF1 – organic solvent (dia)nanofiltration equipment; Distillation 1/D1 and Distillation 2/D2 – distillation columns for solvent evaporation and recycling; Condenser 1/C1 and Condenser 2/C2 – heat exchange equipment for condensation of recycled solvent; Tray Drying/TD1 – tray drying equipment for solvent removal from API; Pump 1/P1 to Pump 8/P8 – centrifugal pumps; Mixing/MX1 – valve as a mixing knot for solvent streams; S-101 to S-127 – process streams.

7.5.6.2. Economic analysis

7.5.6.2.1. Capital and operational costs

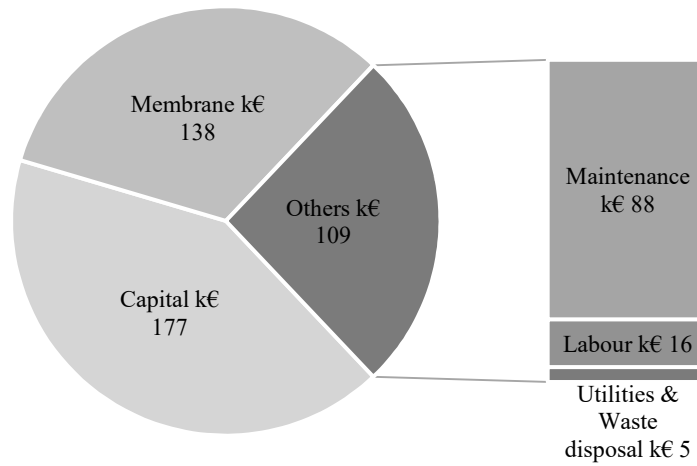
For cost analysis, it was calculated the costs associated with (i) capital costs (i.e equipment, equipment instalation), (ii) mantainance, (iii) labour costs, (iv) selective agents (i.e. membrane and adsorbent), (v) solvents, and (vi) energy and utilities.

Capital costs were estimated for both processes presented before. Direct capital costs were calculated considering equipment cost, while indirect capital costs were estimated using percentages of equipment cost for each section: 40% for equipment assembly, 70% for piping, 20% for instrumentation, 10% for electrical wiring, 15% for process building, 50% for utilities, 15% for storage, 5% for site development, 30% for design and engineering, 15% for contractors fee, and 10% for contingency [10]. Annual operational costs were obtained using percentages of the total capital costs: 5% for

maintenance, 20% for laboratory costs, 20% for supervision, 50% for plant overheads, 10% for capital charges, 1% for insurance, 2% for local taxes, and 1% for licence fees [10].

Total annual cost and corresponding cost distributions for each process are represented in Figure 7.8, considering only the most significant contributions towards yearly costs of operation, as well as capital amortization over a time period of 10 years. Figure 7.8 shows that OSN and the hybrid process have similar capital costs, since the main equipment is very similar between these processes. The most significant difference between the two is the adsorption equipment that is needed in the hybrid process, making it slightly more expensive in terms of capital cost.

A) OSN, k€ 424



B) Hybrid, k€ 1034

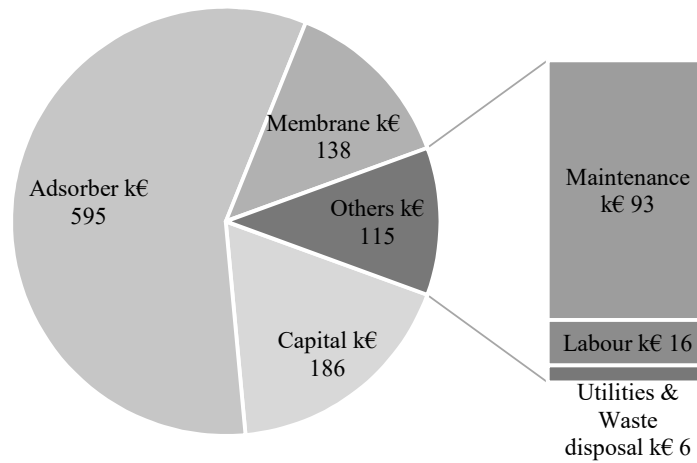


Figure 7.8. Annual cost distribution featuring the most significant contributions for the two processes: OSN (A) and hybrid (B).

Maintenance is dependent on direct capital cost, so it follows the same trend as capital amortization.

Labour cost was calculated using full time equivalent, times the number of work days per year, multiplying by the number of batches per year and the wages. Similar values between processes means that labour cost does not vary significantly between processes.

Selective Agents: Membrane cost is the most substantial section of the annual cost of the OSN process at 138 k€/year (Figure 7.8 A), which would be expected as it is the main consumable for this process. Given that the hybrid process shares a diafiltration operation in its configuration, (Figure 7.8 B) includes a membrane cost section at the same value, since both OSN and hybrid configuration process the same volume in this operation. For the hybrid process, the most relevant contributor towards yearly cost is the adsorber (Figure 7.8 B) at a cost of 595 k€/year. This was to be expected as the chromatographic column was set up to not include regeneration of the adsorber, meaning that each time the column is operated the adsorber will be discarded along with adsorbed GTI after the purification step is finished.

Solvents: Fresh dichloromethane used for 5% solvent make-up was determined to cost 0.9975 €/L. The amount of solvent needed is the same for OSN and the hybrid process, since these processes require 3.2 diavolumes of dichloromethane for the diafiltration unit operation. Figure 7.9 accounts for these solvent needs per batch, and the amount of adsorber required per batch for the hybrid process. The price of the adsorber was estimated to be 580 €/kg, membrane price was 2098.5 €/m², while waste disposal was set at 0.5 €/kg or 0.5 €/m².

Energy and utilities: Cost of utilities was determined using the power multiplied by the working time of equipment (pumping); heating and cooling were determined through mass and energy balances. Energy requirements per batch for the processes are represented in figure 7.10 showcasing that energy needs in terms of steam are equal for OSN and the hybrid process. Since most steam in the processes is used for solvent distillation for recycling, it would be expected that having the same volume of solvent to distillate would lead to similar needs in steam for the boiler that is coupled to the distillation column. The same trend is followed by the cooling requirements. Energy

requirements for pumping are due to input pressure to the filtration process. Therefore, energy and waste disposal showed similar values for OSN and the hybrid process, since recycling the same amount of solvent corresponding to the diavolumes for the diafiltration operation, lead to an increase in utilities' cost coming from steam and cooling.

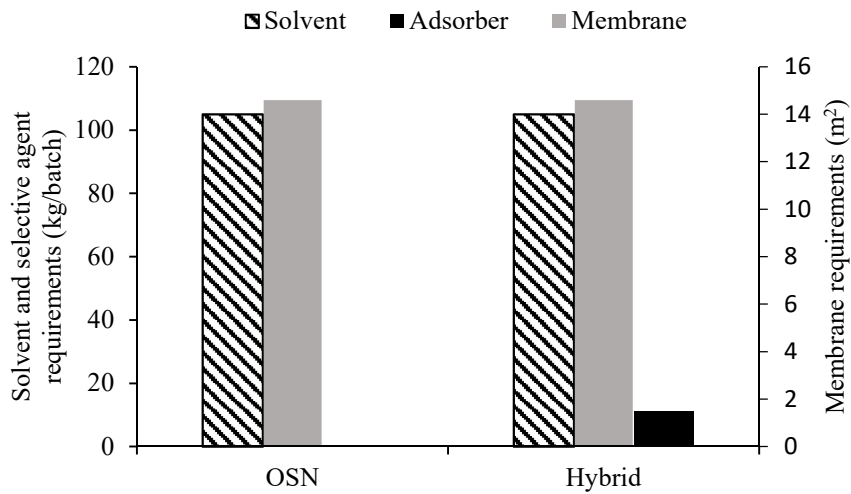


Figure 7.9. Comparison of solvent and selective agent (adsorber) requirements for OSN and hybrid processes, in a batch basis.

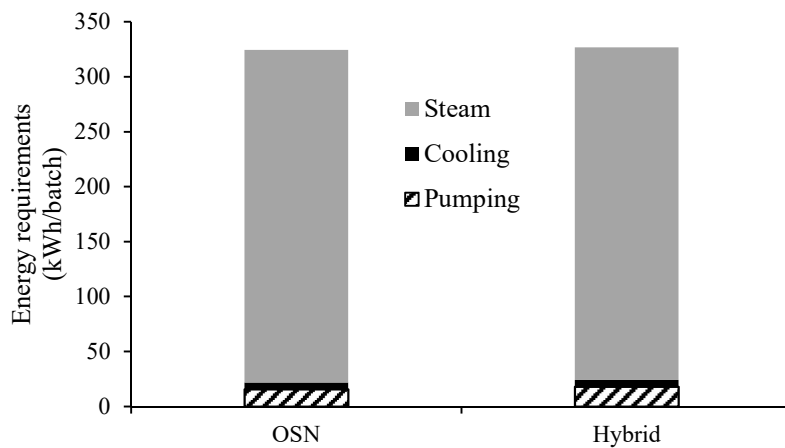


Figure 7.10. Comparison of energy requirements per batch in terms of steam, cooling and pumping, for OSN and hybrid processes.

In terms of total annual costs, the hybrid process is costlier than OSN, at 1034 k€/year and 424 k€/year, respectively. This difference is probably caused by the cost of replacing the adsorber every new batch for the former, when compared to membrane replacement every 20 batches for the latter.

Cost of API purification treatment is a relevant measure of process viability as it will set the point at which the process becomes profitable or not. However, profitability is also dependent on the efficiency of the process at recovering API, as API losses can become significant. Figure 7.11 aims to showcase the importance of these measures in the loss of revenue in the case studies, assuming the target API production and an API value of 7.52 €/g. When considering both costs associated with the purification process and API losses, both processes have similar revenue losses. However, OSN shows the lowest percentage in terms of costs associated to the treatment. On the other hand, the amount of API not being recovered in OSN is very significant, when compared to the hybrid process.

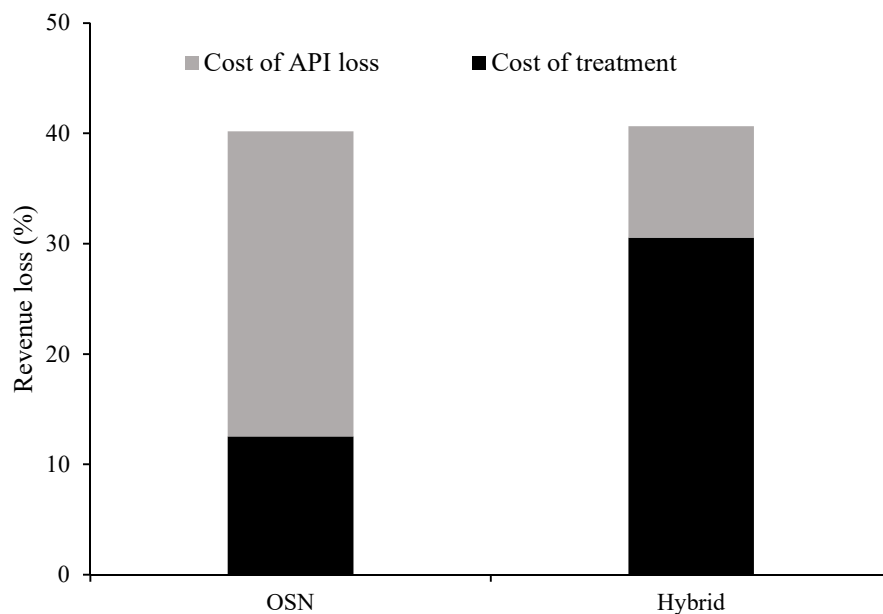


Figure 7.11. Comparison on percentage of revenue loss in terms of cost of purification treatment and cost of API loss in each purification process (OSN and hybrid).

7.5.3.3. Environmental analysis

Notwithstanding the importance of an economic analysis, other parameters should be considered when designing a process. An environmental analysis would provide another measure of process impact by using green metrics.

Mass intensity was calculated considering the mass of solvent used per kg of purified API [10]. The approach for energy intensity was similar, considering the energy requirements in steam, cooling and pumping per kg of API produced. These two green metrics were plotted in Figure 7.12 (top), where OSN has a higher impact than the hybrid process in terms of mass and energy. These observations were expected as solvent and energy requirements presented in Figure 7.9 and 7.10, respectively, are very similar for OSN and hybrid, as previously discussed, but API recovery is different. The hybrid process has lower losses of Meta, meaning that the similar amount of mass and similar

energy requirements divided by a higher amount of API recovered, translates into lower green metrics.

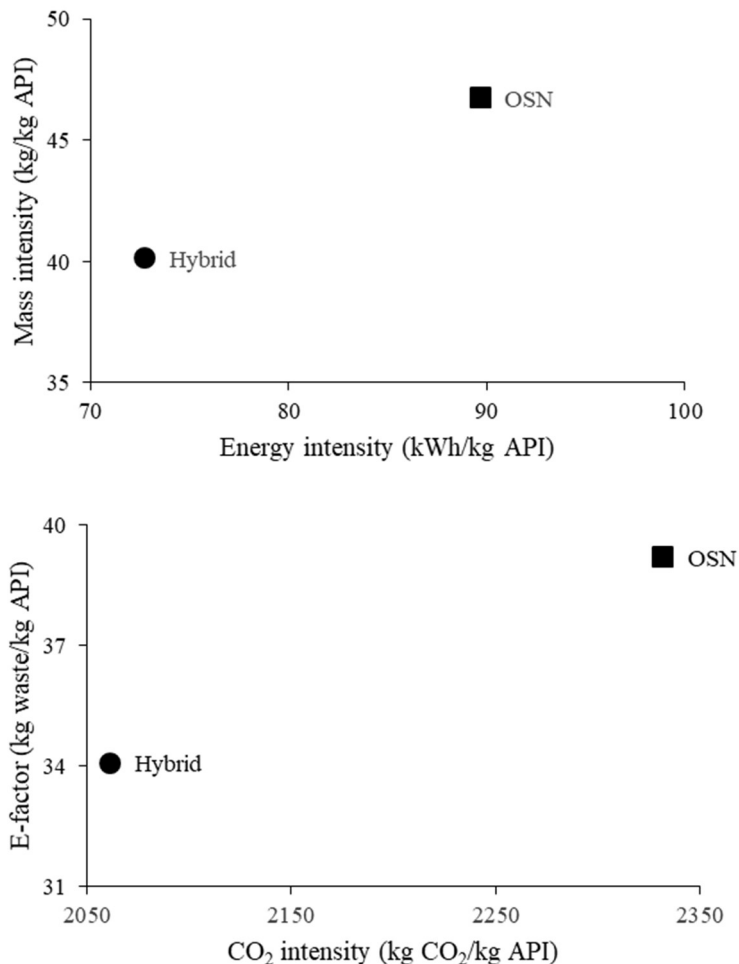


Figure 7.12. Top: Mass intensity and energy intensity metrics. Bottom: Environmental (E) factor and carbon dioxide intensity metrics.

The green metrics E-factor and carbon dioxide intensity are represented in Figure 7.12 (bottom). The Environmental factor, or E-factor, was determined by taking into account solid and liquid waste generated in each process per kg of API recovered [11].

The metric hereby called carbon dioxide intensity was obtained by adding all sources of carbon dioxide generated by the process (e.g., solvent waste that is not recycled

and goes into incineration, carbon dioxide associated with generation of electricity, steam and cooling used in the process), divided by the mass of purified API [12].

Generation of CO₂ in the hybrid process is lower than that generated by OSN. In terms of waste generated per kg of API, the hybrid process has the least environmental impact. Even though the adsorption step of the hybrid process generates waste in the form of used adsorber every batch it operates, increasing the waste generated when compared to OSN, the E-factor is lower due to the higher amount of API recovered. The same happens with the CO₂ generated.

7.6. Conclusions

Through the characteristics of API and GTI as rejection and adsorption constants it was possible to create a model that assists in the decision between purification by OSN or adsorption, as well as the possibility of associating them in a hybrid process, when the performance of both as unitary operation is not satisfactory. The hybrid process proposed in the case study had a gain higher than 30% when compared to OSN, recovering API almost in its totality and reducing the level of contamination of the final product to levels lower than the limit set by regulatory agencies.

Regarding the cost of implementation of the processes, the hybrid process requires a bigger investment than OSN, given the higher number of equipment needed. In the other hand, API losses in the hybrid process are lower, making this process more profitable.

The hybrid process is the most environmentally friendly, as it is the one with the best performance in all of the green metrics discussed.

7.7. References

- [1] Teasdale A.; Elder D.; Chang S. J.; Wang S.; Thompson R.; Benz N.; Flores I. H. S., *Org. Process Res. Dev.* 17, 2013, 221-230.
- [2] EMEA Guidelines on the “Limits on Genotoxic Impurities”, EMEA/CHMP/QWP/251344/2006, 2006.
- [3] Boam, A. & Nozari, A., *Filtration + Separation*, 2006, April, 46-48.
- [4] Rundquist, E. M., et al, *Green Chem.*, 2012, 14, 2197-2205.
- [5] Kim, F. J. et al, *Separation and Purification Technology*, 2013, 116, 277-286.
- [6] Kim, F. J. et al, *Green Chem.*, 2014, 16, 133-145.
- [7] Schaepertoens, M. et al, *Journal of Membrane Science*, 2016, 514, 646-658.
- [8] Mulder, M., *Basic Principles of Membrane Technology*, Springer, 2nd edition, 1996.
- [9] Mehdi, V., et al, *J. Modern Drug Discovery and Drug Delivery Res.*, 2014, V113.
- [10] Sinnott, R.K.; *Chemical Engineering Design*, Butterworth-Heinenmann, 4th edition, v 6, 2005.
- [11] Jimenez-Gonzalez, C.; Constable, D.J.C. and Ponder, C.S.; Evaluating the “Greenness” of chemical processes and products in pharmaceutical industry – a green metrics primer, *Chem. Soc. Rev.*, 2012, 41, 1485-1498.
- [12] SZÉKELY, G., et al, Environmental and economic analysis for selection and engineering sustainable API degenotoxication processes, *Green Chem.*, 15, 2013, 210 - 225.

Chapter VIII

Conclusions and future perspectives

8.1 Conclusions

The aim of this thesis was the development of cost efficient and sustainable strategies for API purification, with API losses below than 10%, achieving GTI removal to levels that decrease patients risk to values below the limits imposed by regulatory agencies.

Several research questions were highlighted in Chapter I, regarding polymer physico-chemical features that could be improved for genotoxic compounds removal in API new purification processes in organic solvent media. Moreover, different process configurations were explored, evaluating hybrid configurations against isolated unit operations to minimize API losses, always respecting TTC imposed limits for genotoxic impurities. These questions have been addressed along chapters III to VII.

8.2 Work summary

New adsorbers, derived from polybenzimidazole (PBI) polymer were obtained through physico-chemical alterations or by chemical functionalization. The new obtained materials, presented high genotoxic removal (more than 95%) with minimal API losses (less than 5% and virtually null after recovery step), in DCM solutions, showing to be good platforms for API purification in organic solvent media.

Enhanced PBI: Different GTI could be removed by this polymer depending on the pH conditioning. **PBI-TA** has high efficiency on aromatic amine removal (higher than 90%) even at high concentrations (5000 ppm) with fast adsorption kinetics (less than 30 min) with API loss virtually null after recovery step, having the possibility of be reused after GTI elution. **PBI-TB** has high efficiency on alkylating agent removal (higher than 90%), with slow kinetics at room temperature being necessary an increase of temperature

to decrease the adsorption time required, having also API loss virtually null after recovery step. The advantage of these polymers, regardless the pH conditioning, is the versatility of applications of both polymers due the different morphologies (beads or electrospun fibers) in which they can be obtained, allowing their use in applications such as adsorption column (beads) and membrane (fibers). No change in adsorption performance of the polymers obtained in chapter III was observed due to the difference in morphology between beads or fibers.

PBI-COOH, was effective for removal of DMAP (more than 95%) from DCM solutions at high GTI concentrations, with faster adsorption kinetics (under 30 min). with API losses lower than 8% regardless the size of spacer chain, being in accordance with the limits imposed by TTC. Beside DMAP, 9 aromatic amines were assessed, showing lower or no removal giving rise to a hypothesis of efficiency removal may be dependent on pKa of adsorbate needing further studies.

PBI-Adenine, was effective for the removal of 5 different families of DNA alkylating agents. Removals above 96% with minimum losses of 4% of API, respecting the limits imposed by TTC. With the increase of temperature, the same results can be achieved at shorter time of contact with adsorber. The adsorbed API can be recovered almost in its totality, rendering the loss due to purification virtually null. The advantage of this polymer is biomimicking approach, allowing this polymer to simulate the double helix of DNA and also be effective for removal of intercalating agents of DNA.

Commercial resins: They were evaluated in MeOH and it was possible to propose a purification methodology using two commercial resins to recover API present in mother liquor, which otherwise would be lost. The use of the resins was evaluated

sequentially and together, being this last configuration the most adequate, leading to higher API recovery. This methodology, also showed greater versatility when the resins were also efficient in removal of by-products obtained from the reaction between two impurities in the API solution. Optimization of the purification efficiency by recrystallization was achieved by inserting an adsorption step to recover the API lost in the mother liquor.

Evaluation of process configuration for API purification with lowest possible loss: A decision make framework was mathematically obtained by modelling adsorption (taking in account adsorption isotherm constants of Langmuir or Freundlich) and OSN (taking in account membrane solute rejections) purification processes, showing cases where each process could achieve TTC value with acceptable API losses. For the cases where neither adsorption or OSN were able to perform API purification as a single step unit operation, and for the cases where the single step would not meet the requirements, a hybrid process was proposed. The hybrid approach considers an adsorption step to reduce the GTI content in the permeate stream (after distillation), allowing the API that would be lost, to recycling being added to next feed stream. The advantages of hybrid approach were allow to use of materials (membranes or adsorbers), that if used as single, would not reach the values imposed by the TTC for the considered impurities. The economic and environmental analysis between OSN and Hybrid were assessed, showing that hybrid proved to be the most sustainable and environmental friendly purification process.

8.3 Future perspectives

Although the ability of the new PBI derived adsorbers and new process configurations, to perform an API purification, was demonstrated, further improvements of these platforms are required to make these strategies economically sound, when developed at industrial scale.

- Sustainable adsorbers

The versatility of morphology in which the novel PBI adsorbers presented in Chapter III could be explored in a wide range of separation processes because they can be obtained as beads or fibers (different 3D configurations) to be used as a single unit operation or in hybrid processes. Be used as scavengers for impurities and by-products originating in solutions containing API. The regeneration and reuse capacity could be further assessed and improved making these polymers even more industrial attractive and economically sustainable.

- Conductive polymers as GTI sensors

The use of PBI doped with acids is reported in literature to enhance PBI's conductivity fuel cell membranes, following this idea, the conductivity of these polymers could be explored, assessing whether the polymer conductivity is whether or not affected by GTI presence, allowing their use as sensor to controlling GTI conten at real time.

- Polymer biomimetics

PBI-adenine can be used targeting DNA intercalators.

The coupling of complementary basis can also be explored enabling the synthesis of a PBI-DNA that are similar to a DNA chain, it can be formulated as a membrane or fibers and be designed as a membrane responsive to the presence of GTI, opening the pores to passage of this solute, retaining the API.

The regeneration could be explored.

- Process configuration and improvements

The process configuration for API purification proposed in chapter VII following a hybrid approach can be further optimized in terms of assessment of recyclability and reuse of the adsorber or OSN in concentration mode can be considered. Other solvents or different pH could be assessed.

The manufacturing of membranes with the polymers presented in Chapters III, IV and V could be explored to verify the influency of different conditioning or functional group has in PBI membrane rejection for GTI and API. Solutions API and GTI with similar molecular weight could be assessed in order to observe if the separation could be possible took advantage of the specific bonds on different states of protonation of polymer and solutes.

Appendix

Appendix A - Supporting Information for chapter V

“Mimicking DNA alkylation: Removing genotoxin impurities from API streams with a solvent stable polybenzimidazole-adenine polymer”

Contents:

- Kinetic parameters for MPTS and MMS in DCM at 25 °C and 55 °C.
- Adsorption isotherm parameters for MPTS and MMS in DCM at 25 °C and 55 °C.
- Swelling ratio of PBI and PBI-adenine polymers.

- Kinetic parameters for MPTS and MMS in DCM at 25 °C and 55 °C.

Table S5.1. Kinetic parameters for MPTS and MMS in DCM at 25 °C and 55 °C.

			Pseudo first order			Pseudo second order	
GTI	T (°C)	$q_{e(\text{exp})}$ (mg/g)	q_e (mg/g)	$k_1 \times 10^{-3}$ (min ⁻¹)	q_e (mg/g)	$k_2 \times 10^{-3}$ (g/(mg min))	
DCM	MPTS	25	2.17 ± 0.04	2.07 ± 0.08	3.22 ± 0.16	2.43 ± 0.15	2.03 ± 0.46
	MMS		2.22 ± 0.03	2.38 ± 0.05	3.45 ± 0.09	2.68 ± 0.16	1.17 ± 0.17
	MPTS	55	2.49 ± 0.01	2.40 ± 0.09	5.07 ± 0.23	3.14 ± 0.58	20.00 ± 5.00
	MMS		1.86 ± 0.04	2.09 ± 0.12	37.10 ± 1.00	1.87 ± 0.02	49.80 ± 31.20

- Adsorption isotherm parameters for MPTS and MMS in DCM at 25 °C and 55 °C.

Table S5.2. Adsorption isotherm parameters for MPTS and MMS in DCM at 25 °C and 55 °C.

			Langmuir		Freundlich	
GTI	T (°C)	q_m (mg/g)	$k_L \times 10^{-1}$ (L/mg)	n	$k_F \times 10^{-1}$ (L/mg)	
DCM	MPTS	25	66.23 ± 0.05	0.06 ± 0.01	1.44 ± 0.01	6.82 ± 0.76
	MMS		12.03 ± 5.76	0.53 ± 0.26	1.72 ± 0.11	7.16 ± 0.39
	MPTS	55	22.47 ± 1.23	0.16 ± 0.03	1.69 ± 0.23	7.63 ± 1.00
	MMS		20.62 ± 0.16	0.96 ± 0.26	1.82 ± 0.31	1.85 ± 0.18

- Swelling ratio of PBI and PBI-adenine polymers.

Swelling studies of the PBI raw and PBI-adenine polymers were carried out in two different solvents: DCM and MeOH. The weighed amount of the dried beads (0.050 g) was immersed in 1 mL of the swelling solvent at room temperature for 24 h. After this time, the polymers were separated from the solvent, and weighed until a constant value. The swelling ratio (S) of the polymers was calculated according to the following equation:

$$S(\%) = (w_s - w_d) / w_d \times 100$$

where w_s is the weight of swollen polymer and w_d is the weight of dry polymer.

Table S5.3. Swelling ratio of PBI raw and PBI-adenine polymers in DCM and MeOH.

	MeOH	DCM	DCM/MeOH
PBI raw	12	4	0.3
PBI-adenine	3	1	0.3

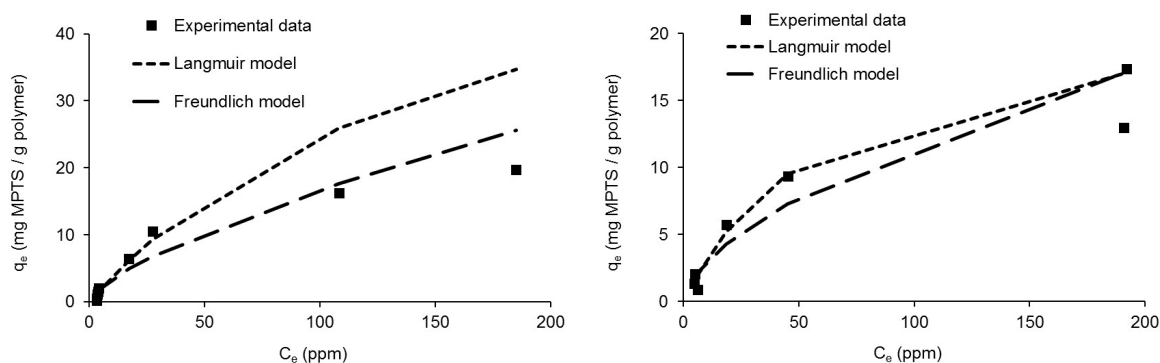


Figure S5.1. Adsorption isotherms for MPTS in DCM at 25 °C (left) and 55 °C (right).

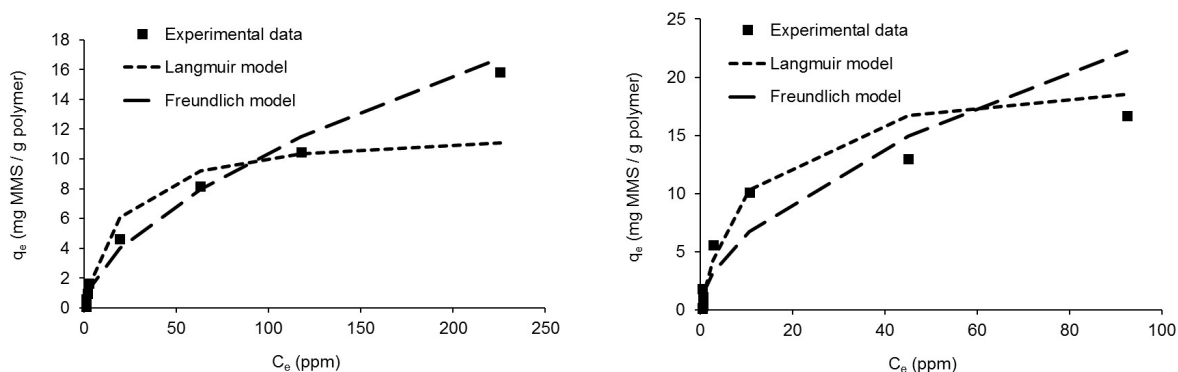


Figure S5.2. Adsorption isotherms for MMS in DCM at 25 °C (left) and 55 °C (right).

Appendix B - Supporting information for Chapter VI

“Screening commercial available resins for simultaneous removal of two potential genotoxins from API methanolic streams”

Contents:

- Influence of pH on DMAP binding for different resins tested: A) in water; B) in water:MeOH (1:1) mixture.
- DMAP binding capacity in AG 50W-X2 resin for a 1 g/L solution in water along time at 25 °C.
- Adsorption isotherm parameters for DMAP in MeOH with AG 50W-X2, IRC50 and IRC86 resins.
- ¹H NMR experiments for proposed formation of DMAP-Me and PTSA in recrystallization ML.

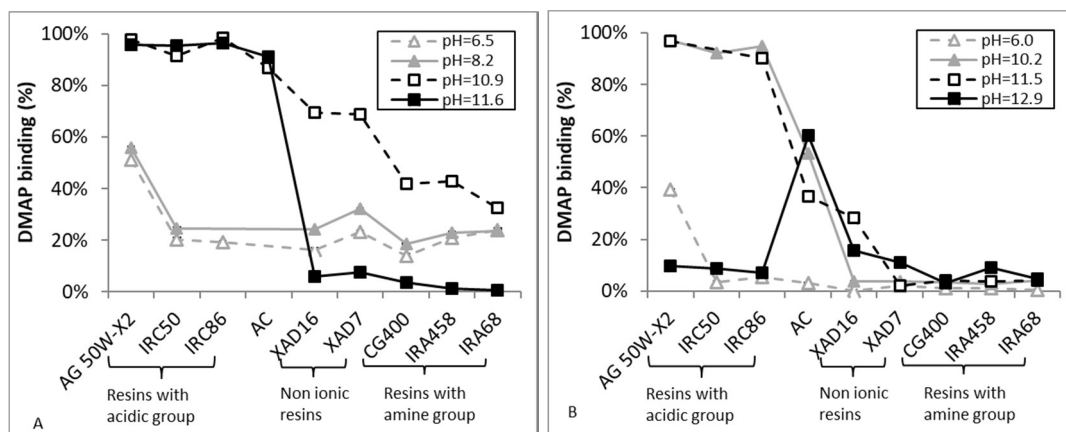


Figure S6.1. Influence of pH on DMAP binding for different resins tested: A) in water; B) in water:MeOH (1:1) mixture.

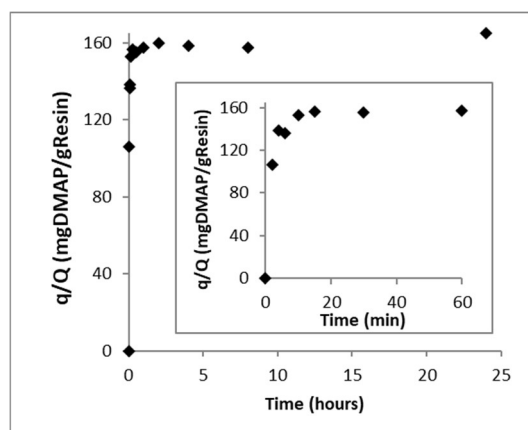


Figure S6.2. DMAP binding capacity in AG 50W-X2 resin for a 1 g/L solution in water along time at 25 °C.

Table S6.1. Adsorption isotherm parameters for DMAP in MeOH with AG 50W-X2, IRC50 and IRC86 resins.

Resin	Langmuir			Freundlich		
	R ²	K _L (L/mg)	q _m (mg/g)	R ²	K _F (L/mg)	n
AG 50W-X2	NA	4.5 x 10 ⁻²	250.00	0.7325	3.0 x 10 ⁻³¹	0.059
IRC50	0.7553	1.5 x 10 ⁻³	370.37	0.8425	1.7 x 10 ⁻¹	0.87
IRC86	0.9586	1.1 x 10 ⁻²	212.77	0.5460	2.5 x 10 ⁻¹	0.84

NA – a good correlation for the data could not be determined.

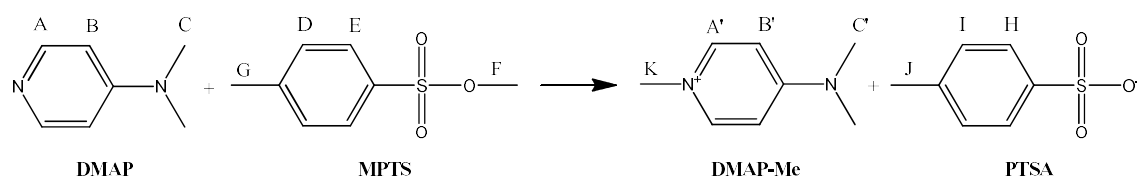


Figure S6.3. Proposed formation of DMAP-Me and PTSA in recrystallization ML.

¹H NMR experiments

¹H NMR spectra were obtained in MeOH-d₄ (99.8%) purchased from Cambridge Isotope Laboratories, Inc. (USA) and were recorded on a Bruker spectrometer MX300 operating at 300 MHz.

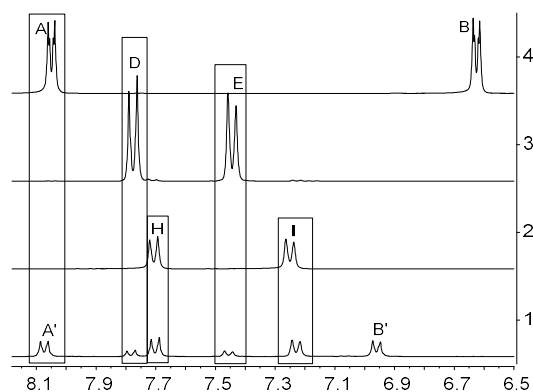


Figure S6.4. ¹H NMR spectra in MeOH-d₄ (8.1-6.5 ppm) for: 1) ML with DMAP, MPTS, DMAP-Me and PTSA; 2) PTSA; 3) MPTS; 4) DMAP.

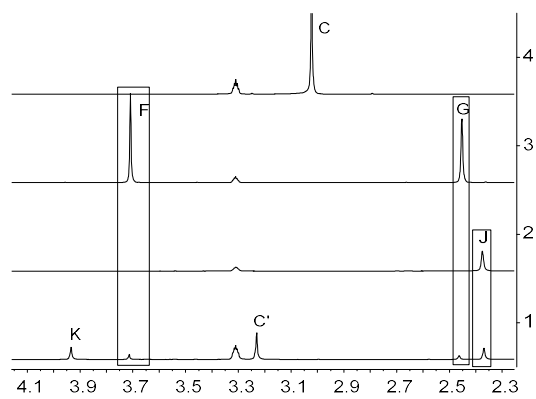


Figure S6.5. ^1H NMR spectra in MeOH-d_4 (4.1-2.3 ppm) for: 1) ML with DMAP, MPTS, DMAP-Me and PTSA; 2) PTSA; 3) MPTS; 4) DMAP.

Appendix C - Supporting Information for chapter VII

“Optimization of organic dianonofiltration with adsorption recycle loop for product reclaiming: application to genotoxic removal from active pharmaceutical compounds”

Contents:

- Considerations about the equations obtained for the models.
- Beta adsorption isotherm profile.

Considerations about the equations obtained for the models

Since $C_{e,x,i} \in \mathbb{R}_+^*$, the conditions of existence imposed to the equations obtained for the models are:

For Langmuir

$$C_{e,x,i} = \frac{-V - m \cdot Q_{max} \cdot k_{L,x,i} + k_{L,x,i} \cdot C_{in,x,i} \cdot V}{2k_{L,x,i} \cdot V} \pm \frac{\sqrt{V^2 + 2m \cdot Q_{max} \cdot k_{L,x,i} \cdot V + 2C_{in,x,i} \cdot k_{L,x,i} \cdot V^2 - 2m \cdot Q_{max} \cdot C_{in,x,i} \cdot k_{L,x,i} \cdot V + k_{L,x,i}^2 \cdot C_{in,x,i}^2 \cdot V^2 + m^2 \cdot Q_{max}^2 \cdot k_{L,x,i}^2}}{2k_{L,x,i} \cdot V}$$

$$1. \quad V^2 + 2m \cdot Q_{max} \cdot k_{L,x,i} \cdot V + 2C_{in,x,i} \cdot k_{L,x,i} \cdot V^2 - 2m \cdot Q_{max} \cdot C_{in,x,i} \cdot k_{L,x,i} \cdot V + k_{L,x,i}^2 \cdot C_{in,x,i}^2 \cdot V^2 + m^2 \cdot Q_{max}^2 \cdot k_{L,x,i}^2 \geq 0,$$

to not have an imaginary number as answer.

2. The signal \pm implies two values as answer for square root, being necessary, for the case of sum:

$$\frac{\sqrt{V^2 + 2m \cdot Q_{max} \cdot k_{L,x,i} \cdot V + 2C_{in,x,i} \cdot k_{L,x,i} \cdot V^2 - 2m \cdot Q_{max} \cdot C_{in,x,i} \cdot k_{L,x,i} \cdot V + k_{L,x,i}^2 \cdot C_{in,x,i}^2 \cdot V^2 + m^2 \cdot Q_{max}^2 \cdot k_{L,x,i}^2}}{2k_{L,x,i} \cdot V} > \frac{-V - m \cdot Q_{max} \cdot k_{L,x,i} + k_{L,x,i} \cdot C_{in,x,i} \cdot V}{2k_{L,x,i} \cdot V} \quad \text{if} \quad \frac{-V - m \cdot Q_{max} \cdot k_{L,x,i} + k_{L,x,i} \cdot C_{in,x,i} \cdot V}{2k_{L,x,i} \cdot V} < 0$$

and in the case of subtraction:

$$\frac{\sqrt{V^2 + 2m \cdot Q_{max} \cdot k_{L,x,i} \cdot V + 2C_{in,x,i} \cdot k_{L,x,i} \cdot V^2 - 2m \cdot Q_{max} \cdot C_{in,x,i} \cdot k_{L,x,i} \cdot V + k_{L,x,i}^2 \cdot C_{in,x,i}^2 \cdot V^2 + m^2 \cdot Q_{max}^2 \cdot k_{L,x,i}^2}}{2k_{L,x,i} \cdot V} < \frac{-V - m \cdot Q_{max} \cdot k_{L,x,i} + k_{L,x,i} \cdot C_{in,x,i} \cdot V}{2k_{L,x,i} \cdot V} \quad \text{if} \quad \frac{-V - m \cdot Q_{max} \cdot k_{L,x,i} + k_{L,x,i} \cdot C_{in,x,i} \cdot V}{2k_{L,x,i} \cdot V} > 0 \quad \text{and if} \quad \frac{-V - m \cdot Q_{max} \cdot k_{L,x,i} + k_{L,x,i} \cdot C_{in,x,i} \cdot V}{2k_{L,x,i} \cdot V} < 0 \quad \text{the solution is not possible for that domain.}$$

For Freundlich

n=2:

$$C_{e,x,i} = \frac{2C_{in,x,i} \cdot V^2 + m^2 \cdot k_{F,x,i}^2 \pm \sqrt{4C_{in,x,i} \cdot m^2 \cdot k_{F,x,i}^2 \cdot V^2 + m^4 \cdot k_{F,x,i}^4}}{2V^2}$$

In this case the square root does not impose a condition for existence because all variables are positive and there are no subtractions involved, but the signal \pm implies in two values as answers for square root, being necessary, for the case of subtraction:

$$2C_{in,x,i} \cdot V^2 + m^2 \cdot k_{F,x,i}^2 > \sqrt{4C_{in,x,i} \cdot m^2 \cdot k_{F,x,i}^2 \cdot V^2 + m^4 \cdot k_{F,x,i}^4}$$

n=3:

$$C_{e,x,i} = \sqrt[3]{\frac{-C_{in,x,i} \cdot m^3 \cdot k_{F,x,i}^3}{2V^3} + \sqrt{\frac{C_{in,x,i}^2 \cdot m^6 \cdot k_{F,x,i}^6}{4V^6} + \frac{m^9 \cdot k_{F,x,i}^9}{27V^9}}} + \sqrt[3]{\frac{-C_{in,x,i} \cdot m^3 \cdot k_{F,x,i}^3}{2V^3} - \sqrt{\frac{C_{in,x,i}^2 \cdot m^6 \cdot k_{F,x,i}^6}{4V^6} + \frac{m^9 \cdot k_{F,x,i}^9}{27V^9}}} + C_{in,x,i}$$

In this case the cubic root can result in a negative number to satisfy the domain imposed to $C_{e,x,i}$:

For the first cubic square, if it results in negative value:

$$\begin{aligned} & \sqrt[3]{\frac{-C_{in,x,i} \cdot m^3 \cdot k_{F,x,i}^3}{2V^3} - \sqrt{\frac{C_{in,x,i}^2 \cdot m^6 \cdot k_{F,x,i}^6}{4V^6} + \frac{m^9 \cdot k_{F,x,i}^9}{27V^9}}} + C_{in,x,i} \\ & > \sqrt[3]{\frac{-C_{in,x,i} \cdot m^3 \cdot k_{F,x,i}^3}{2V^3} + \sqrt{\frac{C_{in,x,i}^2 \cdot m^6 \cdot k_{F,x,i}^6}{4V^6} + \frac{m^9 \cdot k_{F,x,i}^9}{27V^9}}} \end{aligned}$$

And if the second cubic root results are negative values:

$$\sqrt[3]{\frac{-C_{in,x,i} \cdot m^3 \cdot k_{F,x,i}^3}{2V^3} + \sqrt{\frac{C_{in,x,i}^2 \cdot m^6 \cdot k_{F,x,i}^6}{4V^6} + \frac{m^9 \cdot k_{F,x,i}^9}{27V^9}} + C_{in,x,i}}$$

$$> \sqrt[3]{\frac{-C_{in,x,i} \cdot m^3 \cdot k_{F,x,i}^3}{2V^3} - \sqrt{\frac{C_{in,x,i}^2 \cdot m^6 \cdot k_{F,x,i}^6}{4V^6} + \frac{m^9 \cdot k_{F,x,i}^9}{27V^9}}}$$

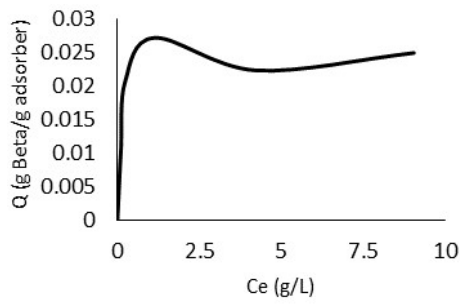


Figure S7.1: Beta adsorption isotherm profile.